



Instituto de Parasitología y Biomedicina “Lopez-Neyra” Consejo Superior de
Investigaciones científicas

Departamento de Bioquímica y Biología Molecular
Universidad de Granada

Structural determinants for SNARE-mediated neurosecretion

Elena Fernandez Fernandez

Tesis Doctoral

Septiembre 2009

Editor: Editorial de la Universidad de Granada
Autor: Elena Fernández Fernández
D.L.: GR. 3954-2009
ISBN: 978-84-692-7837-6

D.^a: Sabine Nicole Navarro Hilfiker, Investigadora científica del Departamento de Biología Molecular del Instituto de Parasitología y Biomedicina “ Lopez-Neyra” del CSIC en Granada:

CERTIFICA que D.^a Elena Fernández Fernández, Licenciada en Bioquímica, ha realizado bajo su dirección y en el Departamento de Biología Molecular del Instituto de Parasitología y Biomedicina “ Lopez-Neyra” del CSIC en Granada, el trabajo titulado: Structural determinants for SNARE-mediated neurosecretion, reuniendo el mismo las condiciones necesarias para optar el grado de Doctor Europeo por la Universidad de Granada.

En Granada, a 09 de Octubre del 2009-09-23

Vº Bº Directora

La interesada

Sabine N. Navarro Hilfiker

Elena Fernández Fernández

Cover by Elena Fdez 2008.

Overlay of the ab initio beads model of the novel wing shaped soluble SNARE complex dimer structure obtained by Small Angle X-ray Scattering and a confocal image of a PC12 cell overexpressing VAMP2-GFP, labelled in pink. Cells were coostained with anti synaptotagmin antibody, labelled in cyan.

Portada por Elena Fdez 2008.

Superposición del modelo de esferas ab initio de la estructura abierta de dos alas obtenida por dispersión de rayos-X en ángulo pequeño y una imagen de microscopia confocal de una célula PC12 sobrepresando VAMP2-GFP, coloreada en rosa. Las células se marcaron con un anticuerpo anti-synaptotagmin, coloreado en cian.

ACKNOWLEDGMENTS / AGRADECIMIENTOS:

Quiero agradecer profundamente a mi supervisora la Dra. Sabine Hilfiker por la oportunidad única de hacer la tesis en su laboratorio, donde sin duda he disfrutado de la ciencia y superado los objetivos profesionales que me había propuesto. Gracias por apoyarme y animarme a asistir a congresos y estancias en el extranjero, experiencias que considero fundamentales para mi formación. Quiero agradecer la confianza y complicidad, tanto profesional como personal, que has tenido conmigo desde un principio. Muchas gracias por tu saber escuchar, por tu paciencia y por tus consejos.

I want to thank Dr. Philip Woodman for his support during my stay in his lab where I have learned many novel biochemical and biophysical approaches which so well complement my scientific expertise. I really appreciate your help and enjoyed very much living in Manchester. I also want to thank my co-workers in the lab, especially to Eduard, Connie and Aurelie for their kind help.

Quiero agradecer a todos los miembros del Instituto de Parasitología y Biomedicina “Lopez-Neyra” incluyendo al personal técnico, investigadores y, por supuesto, a mis compis los becarios. Por su compañerismo y profesionalidad que hacen posible la formación científica de nosotros los estudiantes.

Quiero agradecer a mis niñas del laboratorio 114, en especial a Elena y a Irene por la ayuda y la amistad que me han dado durante los últimos años. He disfrutado muchísimo de vuestra compañía. Ya echo de menos esas risas matinales!!

También quiero agradecer a mis chicas/os del laboratorio 109-110, Miguel, Marta, Noemí y como no, a mi querida amiga Beatriz de Blanco. Agradeceros esos buenos momentos dentro y fuera del IPB. He disfrutado muchísimo de las tertulias en las comidas y las risas en el café. Gracias por vuestro apoyo en los momentos difíciles, sobre todo el tuyo, Bea. Te voy a echar muchísimo de menos!!

Por último y más importante, quiero agradecer a mi familia el cariño y el apoyo incondicional que me han dado. A mis padres, Rafael y M^a del Carmen, por haberme apoyado y permitido estudiar para hoy ser quien soy. Por el ejemplo y los principios que me habéis enseñado. Por celebrar conmigo los momentos buenos y animarme (soportarme...) en los malos. A mis hermanas, Belén, Chiqui y Ángela, por su cariño, risas y confianzas que alegran mi vida. Porque me habéis apoyado y animado allí donde he estado y lo he necesitado. A Sergio por el amor y el apoyo que me das todos los días. Por confiar en mis posibilidades más que yo misma. Por tu optimismo, cariño, paciencia y ayuda que tanto he necesitado estos últimos meses. A Diego, nuestro futuro hijo, porque me has dado la fuerza para escribir esta tesis.

Gracias a todos!!

INDEX

| | | |
|-------------|--|-----------|
| I. | SUMMARY: | 1 |
| II. | ABBREVIATIONS /ABREVIATURAS: | 2 |
| III. | INTRODUCTION: | 9 |
| | 1. SNARE-MEDIATED MEMBRANE TRAFFICKING:..... | 9 |
| | 2. NEUROSECRETION:..... | 12 |
| | 3. NEURNAL SNAREs:..... | 16 |
| | 3.1 STRUCTURE OF INDIVIDUAL SNAREs..... | 16 |
| | 3.2 SNARE COMPLEXES..... | 19 |
| | 3.2.1 BINARY COMPLEXES..... | 19 |
| | 3.2.2 TERNARY COMPLEXES..... | 20 |
| | 3.2.3 CIS AND TRANS SNARE COMPLEXES..... | 26 |
| | 4. PHARMACOLOGICAL EVIDENCE..... | 29 |
| | 5. GENETIC EVIDENCE..... | 33 |
| | 5.1 VAMP2..... | 33 |
| | 5.2 SNAP-25..... | 33 |
| | 5.3 Syntaxin1A..... | 34 |
| | 6. BIOCHEMICAL EVIDENCE:..... | 34 |
| | 7. OLIGOMERIZATION AND COOPERATIVITY:..... | 36 |
| | 8. TRANSMEMBRANE DOMAINS:..... | 40 |
| | 9. SNARE REGULATORS:..... | 48 |
| | 9.1 COMPLEXIN..... | 48 |
| | 9.2 SYNAPTOTAGMIN..... | 51 |
| | 9.3 LIPIDS..... | 54 |
| IV. | SPECIFIC AIMS: | 59 |
| V. | RESULTS: | 61 |
| | 1. A Role for soluble N-Ethylmaleimide-Sensitive Factor Attachment Protein Receptor Complex Dimerization During Neurosecretion..... | 61 |
| | 2. Transmembrane Domains Determinants for SNARE-mediated Membrane Fusion..... | 103 |
| | 3. Vesicle pools and synapsins: New insights into old enigmas..... | 153 |
| | 4. Sensing the Difference: Neuronal Calcium Sensor-1 and its role in vesicle biogenesis, trafficking and fusion..... | 165 |

| | | |
|--------------|--|------------|
| VI. | ANNEXES: | 195 |
| | 1. ANNEX I: Detection of endogenous SNARE complexes in PC12 cells..... | 195 |
| | 2. ANNEX II: Detection of overexpressed GFP tagged VAMP2 proteins..... | 198 |
| | 3. ANNEX III: Determination of tryptophan solvent accessibility in inherent tryptophan fluorescent experiment..... | 202 |
| | 4. ANNEX IV: Peptidergic approach to interfere with SNARE-complex Dimerization in vitro..... | 204 |
| | 5. ANNEX V: Measuring cooperativity of SNARE dependent neurosecretion..... | 207 |
| | 6. ANNEX VI: Additional insights into detecting VAMP2 interactions by Bimolecular Fluorescence Complementation approach..... | 209 |
| | 7. ANNEX VII: Primer sequences..... | 215 |
| VII. | DISCUSSION: | 223 |
| | 1. Structure of SNARE complex oligomers in solution..... | 223 |
| | 2. Mapping of the dimer interface..... | 226 |
| | 3. Effects of VAMP2 dimerization mutants on neurosecretion..... | 227 |
| | 4. Visualization of SNARE protein interactions by BiFC in vivo..... | 229 |
| | 5. Characterization of VAMP2 TMD-mediated dimerization..... | 230 |
| | 6. N- and C-terminal regions of VAMP2 TMD differentially affect neurosecretion..... | 233 |
| VIII. | CONCLUSIONS: | 237 |
| IX. | REFERENCES: | 241 |

SUMMARY

I. SUMMARY:

A major goal of neuroscience is to understand the molecular mechanisms underlying brain function. A complicated network of neurons communicate with each other by releasing neurotransmitters at synapses. Such neurotransmitter release requires the fusion of synaptic vesicles with the plasma membrane. A crucial step in membrane fusion is the interaction between a synaptic vesicle protein (VAMP2) and two plasma membrane proteins (syntaxin1A and SNAP-25) through their specialized cytoplasmic motifs termed “SNARE motifs”, leading to the formation of an energetically favourable core complex that brings both membranes into apposition to allow membrane fusion.

Multiple SNARE complexes cooperate to bring about an individual vesicular fusion event, but the exact molecular mechanism(s) responsible for SNARE complex multimerization remain unclear. Here, we report the molecular identification and characterization of a dimer formed between the cytoplasmic portions of neuronal SNARE complexes *in vitro*. Dimerization generates a novel two-winged open structure where the two complexes interact through their C-terminal ends, involving three residues (R86, W89 and W90) from VAMP2. Mutations on these residues significantly reduces the stability of SNARE complex dimers *in vitro* and lead to a corresponding decrease in neurosecretion *in vivo*. The reported findings are consistent with an important role for such SNARE complex dimerization in neurotransmitter release.

In addition to the cytoplasmic domains of the SNARE proteins, their transmembrane domains (TMDs) clearly contribute to membrane fusion as well. However, the precise structural and functional requirements remain largely unknown. Here we have used a bimolecular fluorescence complementation approach (BiFC) to provide *in vivo* evidence for individual VAMP2 molecule interactions mediated by the TMDs and involving a glycine residue (G100). Replacing the glycine residue with amino acids of increasing molecular volume abolishes such VAMP2 dimerization without affecting neurosecretion. These results suggest that dimerization of the TMDs of VAMP2 does not play an important functional role. In contrast, deleting or inserting residues within the C-terminal half of the VAMP2 TMD causes a severe inhibition of exocytosis, while

similar alterations within the N-terminal half do not result in secretory deficits. Our results indicate that distinct structural requirements exist between the N- and C-terminal halves of the VAMP2 TMD, with the C-terminal part being essential for SNARE-mediated neurotransmitter release.

ABBREVIATIONS / ABREVIATURAS

II. ABBREVIATIONS / ABREVIATURAS:

AAA: ATPase Associated with diverse cellular Activities
ADP: adenosine diphosphate / adenosín bifosfato
ATP: adenosine triphosphate / adenosín trifosfato
ATPase: adenosine triphosphatase / adenosín trifosfatasa
BiFC: bimolecular fluorescence complementation / complementación de fluorescencia bimolecular
BoNT: botulinum neurotoxins / neurotoxina botulínica
Ca²⁺: calcium ions / iones de calcio
CaCl₂: calcium chloride / cloruro de calcio
CD: circular dichroism / dicroísmo circular
CNT: clostridial neurotoxina / neurotoxina clostridial
CV: coated vesicles / vesículas con cubierta
DAG: diacylglycerol / diacilglicerol
EE: early endosomes / endosomas tempranos
EM: electron microscopy / microscopía electrónica
EPR: electron paramagnetic resonance / resonancia paramagnética electrónica
ER: endoplasmic reticulum / retículo endoplasmático
FRET: fluorescence resonance energy transfer / transferencia de energía de resonancia de fluorescencia
GFP: green fluorescent protein / proteína verde fluorescente
GPI: glycosylphosphatidylinositol / glicosil fosfatidil inositol
GTPase: guanosine triphosphatase / guanosina trifosfatasa
HC: heavy chain / cadena pesada
hGH: human growth hormone / hormona de crecimiento humana
IR: infrared spectroscopy / espectroscopía de infrarrojos
ISG: immature secretory granule / gránulo secretor inmaduro
LC: light chain / cadena ligera
LE: late endosomes / endosomas tardíos
MALLS: Multi Angle Laser Light Scattering / dispersión de luz láser multiángulo
Mg²⁺: magnesium ions / iones de magnesio
MgATP: magnesium-ATP / magnesio-ATP

NMR: nuclear magnetic resonance / resonancia magnética nuclear
NSF: N-ethylmaleimide-sensitive factor
PLA: phospholipase A / fosfolipasa A
PLC: phospholipase C / fosfolipasa C
PKA: protein kinase A / proteína quinasa A
RE: recycling endosomes / endosomas de reciclaje
RRP: readily-releasable pool / reserva de vesículas listas para secretar
SAXS: small angle X-ray scattering / dispersión de rayos X en ángulo pequeño
SDS-PAGE: sodium dodecyl sulphate polyacrylamide gel electrophoresis /
electroforesis en gel de poliacrilamida con dodecilsulfato
SG: secretory granules / gránulos secretores
SNAP: synaptosome-associated protein / proteína asociada al sinaptosoma
SNAREs: soluble N-ethylmaleimide-sensitive factor attachment protein receptors
SV: synaptic vesicles / vesículas sinápticas
TEM: transmission electron microscopy / microscopía electrónica de transmisión
TeNT: tetanus neurotoxin / neurotoxina tetánica
TfR: transferrin receptor / receptor de la transferrina
TGN: trans Golgi network / red del trans golgi
TMD: transmembrane domain / dominio transmembrana
VAMP: vesicle-associated membrane protein/ proteína asociada a la vesícula
WT: wild type

INTRODUCTION

III. INTRODUCTION:

1. SNARE-MEDIATED MEMBRANE TRAFFICKING:

Membrane fusion plays crucial roles in a wide range of biological processes such as cell growth and division by membrane addition, cell to cell communication by delivering signalling molecules to the plasma membrane, and viral infection. In eukaryotic cells, intracellular membrane fusion distributes proteins and lipids that need to be transported and reach their proper intracellular organelles without disrupting structural integrity of cellular compartments. This membrane trafficking involves budding of a vesicle from a donor membrane, which is then transported and docked to its specific target membrane. After priming events, the vesicle is prepared for fusion with the destined acceptor membrane compartment (for reviews see [1-4]). The series of coordinated steps inherent to vesicle trafficking are accomplished by multi-protein complexes consisting of a compartment-specific superfamily of small proteins called SNAREs (soluble N-ethylmaleimide-sensitive factor attachment protein receptors) that are highly conserved throughout eukaryotic evolution [3, 5] with 25 members in *Saccharomyces cerevisiae*, 36 members in *Homo sapiens* and 54 members in *Arabidopsis thaliana* [6].

Apart from extracellular membrane, mitochondrial and peroxisomal fusion events, which involve unrelated proteins [7-9], SNARE proteins are considered the basic molecular machinery mediating membrane fusion in all intracellular membrane trafficking events studied so far. According to their function, they have been classified as v- and t-SNAREs, because they operate in opposing membranes: vesicle and target membrane (Figure 1). The mechanistic molecular model for SNARE-mediated membrane fusion postulates that specific interactions occur between the v- and t-SNAREs that bring the lipid bilayers into close proximity and drive membrane fusion by using the free energy that is released during such SNARE complex formation.

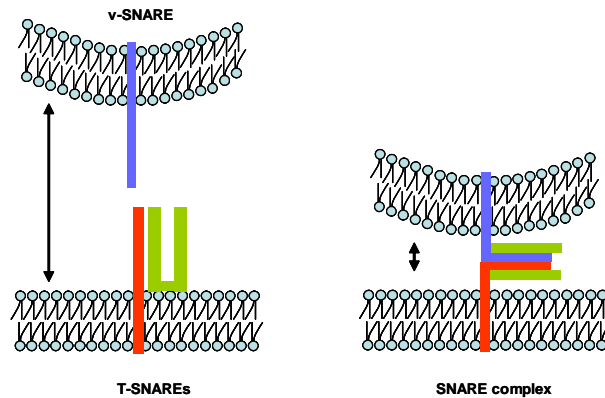


Figure 1. A general model for SNARE assembly. A v-SNARE (blue) assembles with its target membrane t-SNARE partners (red and green) to bring opposing membranes into close proximity.

The different intracellular membrane trafficking steps employ different sets of partner v-/t-SNAREs, resulting in a wide distribution of SNAREs along the membrane-trafficking pathways in eukaryotic cells (Figure 2). Based on sequence homology and domain structure, the mammalian SNAREs are classified as members of syntaxin and SNAP (synaptosome-associated protein) families (t-SNAREs), or VAMP families (v-SNAREs). It was initially believed that specificity of organelle trafficking resides at the membrane fusion stage mediated by specific interactions between VAMP and its cognates syntaxin and SNAP [10]. However, a certain degree of promiscuity is observed in SNARE core complex assembly of artificial combinations of SNAREs *in vitro* with similar biophysical and biochemical properties [11, 12]. Furthermore, liposome fusion assays *in vitro* either display specificity with respect to SNARE partners resembling the compartmental localization of intracellular trafficking in the case of yeast [13-16], or promiscuity in the case of mammalian endosomal and exocytic SNAREs [17]. Finally, *in vivo*, some SNAREs such as VAMP2 and cellubrevin can functionally substitute for each other in regulated exocytosis to a certain extent [18, 19]. Individual SNAREs can also operate in more than one fusion step involving different SNARE partners, for example VAMP8 (also called endobrevin), which

functions in late-endosome fusion as well as in exocytosis in the exocrine pancreas [20, 21]. The currently available evidence thus indicates that SNAREs by themselves contribute to the specificity of membrane fusion events, whilst on their own they are not being entirely sufficient for such specificity.

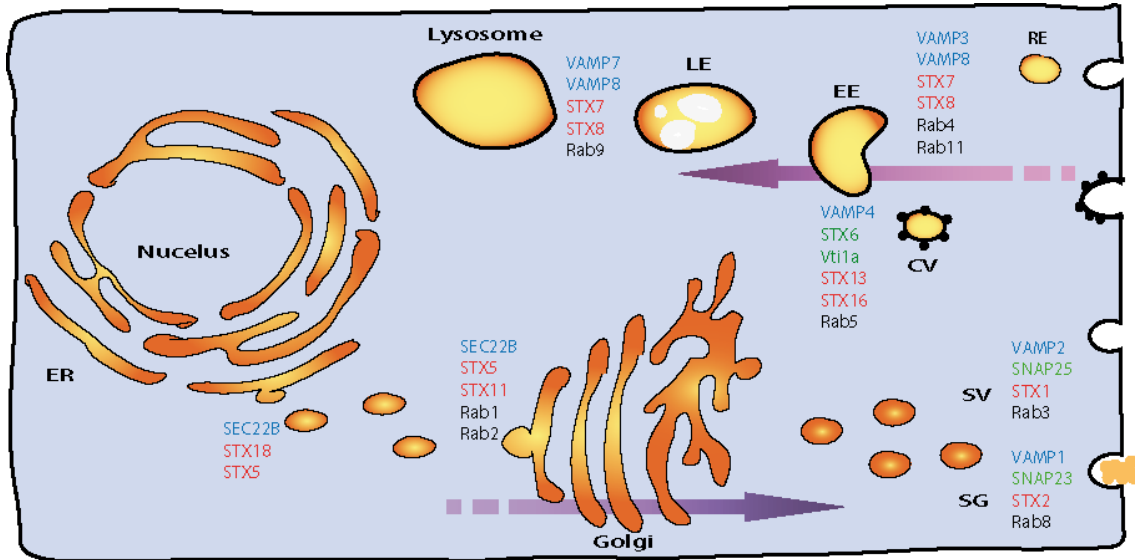


Figure 2. A general overview of intracellular localization of SNARE and Rab proteins in mammalian cells. A summary of intracellular membrane trafficking pathways including the secretory pathway from the endoplasmic reticulum (ER) to the Golgi apparatus, and secretory granules (SG) or secretory vesicles (SV) which then fuse with the plasma membrane; and the endocytic pathway from recycling endosomes (RE) or coated vesicles (CV) to early endosomes (EE) and late endosomes (LE). Each trafficking step is carried out by a set of SNARE (Vamp family is labelled in blue, SNAP in green and syntaxin in red) and Rab (black) partners.

The precise mechanism by which the cell can select one set of SNAREs for an upcoming fusion event, while silencing others that might be present in the same membrane, is still unknown. Several studies support the hypothesis that specificity of membrane trafficking may occur upstream of SNARE-mediated membrane fusion by Rab proteins and tethering factors [22-24]. In particular, it has been suggested that specificity takes place at the vesicle targeting and docking

stages, due to the tethering of the transport vesicle by long extended proteins in the target membrane consisting of GTPases of the Rab family, which are also localized to many different cellular compartments (Figure 2). In this manner, a sequential combination of Rab and SNARE protein action seems to make specificity within the system more reliable (see also reviews [6, 25, 26]).

2. NEUROSECRETION:

Neurons have long processes that make close contact (10-30 nm) with the target cell at specialized compartments called synapses. Signals between neurons are transmitted chemically, whereby specialized secretory organelles called synaptic vesicles fuse with the synaptic plasma membrane to release their content. Synaptic vesicles store concentrations of neurotransmitter which can exceed 0.1 M [27]. In resting nerve terminals, these synaptic vesicles are located in clusters where they are not freely diffusible but are tethered in place by a meshwork of filaments and cytoskeletal components. At least two distinct vesicle pools can be observed in such vesicle clusters based on morphological and physiological properties [28-30]. Morphologically, we can distinguish between vesicles that are docked at the plasma membrane and those further away from the plasma membrane. Physiologically, a distinction can be made based on the vesicle's ability to be released. In that manner we can distinguish between vesicles that are ready to fuse (readily-releasable pool, RRP), a recycling pool of vesicles that after exocytosis is endocytosed and locally recycled to undergo another round of secretion, and a reserve pool of vesicles (Figure 3). Whilst there is currently no direct correlation between morphologically and physiologically defined vesicle pools, it is clear that the presence of a large number of vesicles allows the nerve terminal to faithfully transmit signals over a large firing range.

Synaptic transmission is initiated when an action potential arrives at the presynaptic nerve terminal [31]. This action potential depolarizes the plasma membrane and induces the opening of voltage-dependent Ca^{2+} channels which results in a local Ca^{2+} influx that triggers synaptic vesicle exocytosis and thus neurotransmitter release into the synaptic cleft [32-35]. After stimulation, vesicle mobility increases, thus making more vesicles available for fusion. The

responsible players for this Ca^{2+} stimulus-dependent tethering and release of synaptic vesicles from vesicle clusters are the synapsins [36-39]. This protein family seems to specifically interact with synaptic vesicles and actin filaments in a manner regulated by Ca^{2+} -dependent phosphorylation [40-43].

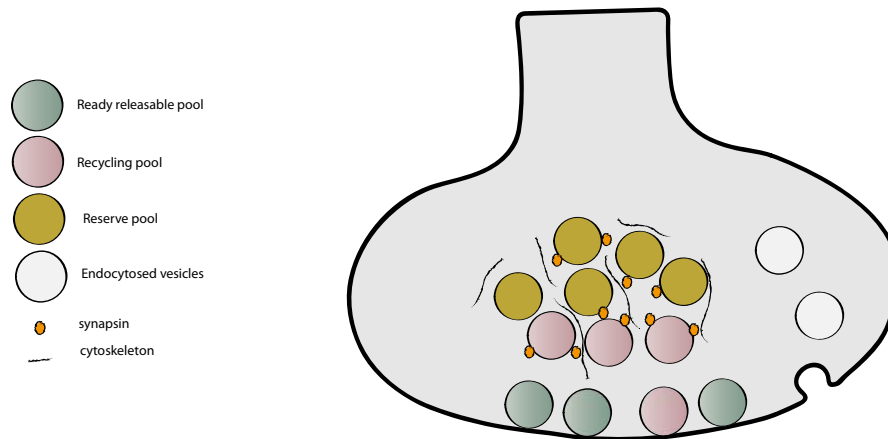


Figure 3. Schematic diagram of distinct vesicle pools at the synapse: the readily releasable pool (labelled in grey), the recycling pool (labelled in pink) and the reserve pool (labelled in brown). These pools are functionally distinguishable, even though their position with respect to the plasma membrane can be partially overlapping. Vesicles from the readily releasable pool are thought to be docked at the plasma membrane and thought to be preferentially released upon basal stimulation. The recycling pool can be docked or proximate to the cell membrane, and tends to be recycled upon moderate stimulation. The reserve pool constitutes the vast majority of vesicles in the nerve terminal, is proximal to the plasma membrane, and may be required to faithfully transmit signals during times of prolonged, high synaptic activity. Some vesicles are endocytosed (labelled in white) after exocytosis to undergo a new secretion event. Vesicles are trapped in clusters by cytoskeletal filaments (black lines) and synapsins (orange circles).

Vesicles undergo membrane fusion in a SNARE-dependent manner. The neuronal SNAREs include the synaptic vesicle protein VAMP2 (also called

synaptobrevin2) and the synaptic plasma membrane proteins syntaxin1A and SNAP-25 [44-47]. A molecular model of SNARE-mediated vesicle exocytosis has emerged within the last 30 years [2, 48] (Figure 4). This model of regulated exocytosis consists of a series of transition steps that are controlled by additional late regulatory proteins including synaptotagmin, complexin, tomosyn, Munc-13, syntaphilin and snapin [49-55]. The process begins when syntaxin1A and SNAP-25, which are organized in clusters at the plasma membrane [56, 57], assemble together to form a binary complex called acceptor complex [58-60]. The acceptor complex provides a binding interface for the vesicular SNARE VAMP2, thus forming a ternary complex.

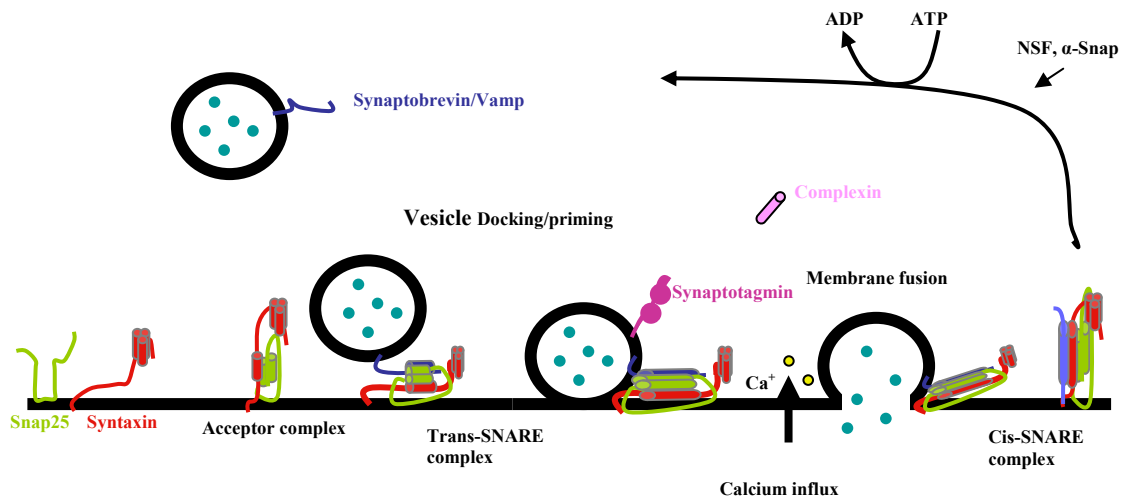


Figure 4. Model for SNARE-mediated neuronal exocytosis. The neuronal t-SNAREs SNAP-25 and syntaxin1A (labelled in green and red, respectively), assemble together to form the acceptor complex followed by binding of the v-SNARE partner VAMP2 (in blue). The three SNARE proteins form the trans-SNARE complex that brings opposing membranes into close proximity awaiting a Ca^{2+} signal. Additional proteins such as synaptotagmin (purple) and complexin (pink) bind to this trans-SNARE complex with possibly distinct outcomes. Ca^{2+} entry triggers membrane fusion, followed by the generation of cis-SNARE complexes, which are disassembled by NSF and α -SNAP upon ATP-hydrolysis

This ternary complex proceeds from a loose state (in which only the N-terminal part is assembled) as studied *in vivo* [61-63] and *in vitro* [64] to a tight

state in which the v- and t-SNAREs zipper up from the N- to the C-terminal end [63, 65]. The zippering up of the natively unfolded cytosolic domains of SNARE proteins into a highly stable four helix-bundle complex pulls the two membranes tight together against the lipid repulsion forces [66-68]. Once the SNARE complex is formed, the primed vesicle is ready to fuse. This last stage, the triggering of release, is Ca^{2+} -dependent and coordinated by a calcium sensor [69, 70], most likely synaptotagmin I [71]. Synaptotagmin I is also localized to synaptic vesicles, binds Ca^{2+} and is considered the receiver of the Ca^{2+} signal in neurons [71, 72]. The late steps of membrane fusion are also regulated by complexin [50, 73], which does not have an apparent Ca^{2+} binding site, but binds to the SNARE complex [50, 73], preventing spontaneous fusion in the absence of a Ca^{2+} signal by acting as a fusion clamp [74-77]. When Ca^{2+} enters, Ca^{2+} binding to synaptotagmin is thought to relieve this clamp such that the vesicle can fuse (see for review [78]).

After membrane fusion, the SNARE complex remains assembled in the acceptor membrane, the plasma membrane, and is called a cis-SNARE complex [79]. Such cis-SNARE complexes are disassembled by N-ethylmaleimide sensitive factor (NSF) [80] and soluble co-factor NSF attachment protein (α -SNAP) [81, 82] upon ATP hydrolysis, re-setting the individual SNAREs for another round of membrane docking and fusion [83-88]. NSF belongs to the AAA+ protein family which often operate as “unfoldases” that disassemble protein complexes (see review [89]). Binding of three α -SNAP molecules to the center of the SNARE complex [90, 91] is followed by binding and activation of the hexameric NSF, forming a 20S supramolecular complex. Whilst the exact mechanism of disassembly remains unknown, this last step is crucial for maintaining fusion competence in the secretory pathway [92, 93].

3. NEURONAL SNAREs:

3.1 STRUCTURE OF INDIVIDUAL SNAREs.

As mentioned above, the first SNARE proteins to be biochemically characterized were the neuronal SNAREs syntaxin1A, SNAP-25 and VAMP2 (Figure 5).

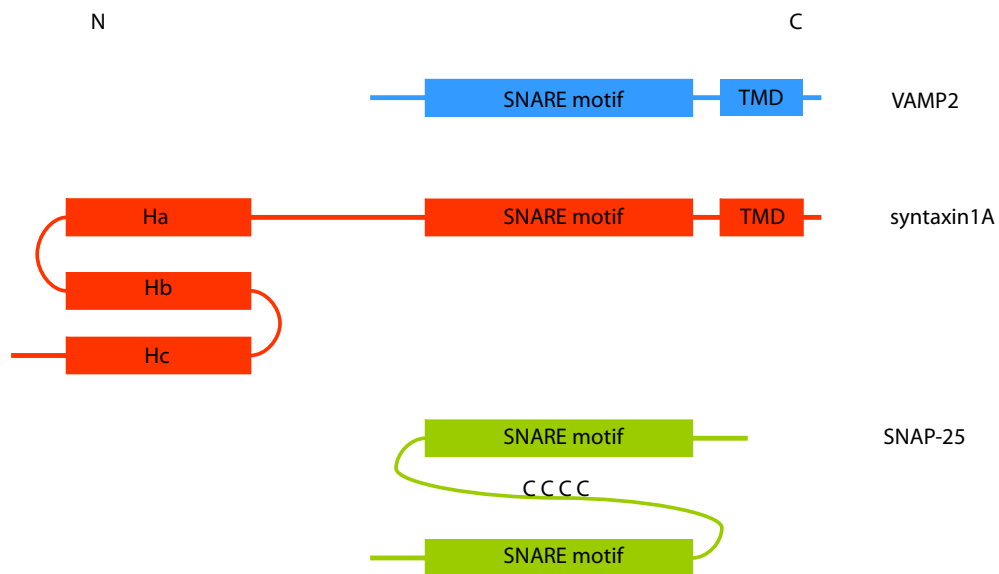


Figure 5. Schematic domain representation of individual neuronal SNAREs. VAMP2 (blue) and syntaxin1A (red) are composed of a C-terminal TMD connected to the SNARE motif by a short linker. Additionally, syntaxin1A has an N-terminal domain natively folded that forms a three α -helix (Ha, Hb and Hc) bundle. SNAP-25 (green) contains two SNARE motifs connected by a central long linker which is anchored to the plasma membrane by palmitoylation of four cysteine residues.

VAMP2, also called synaptobrevin2, is a 12kDa vesicle-associated protein with a C-terminal transmembrane domain (TMD) [44, 47, 94]. Similarly, syntaxin1A (a 35kDa protein) is C-terminally anchored to the plasma membrane through a single pass TMD [45, 95]. SNAP-25A is a 25kDa protein attached to

the plasma membrane via posttranslational palmitoylation of four cysteines residues [96]. When not incorporated into SNARE complexes, the cytoplasmic domains of the neuronal SNARE proteins are unstructured in the case of VAMP2 and SNAP-25, and partially unstructured in the case of syntaxin1A [58, 97-99]. These unstructured proteins have a high propensity to interact with each other through a domain called SNARE motif or core domain, which consists of 60-70 residues highly evolutionarily conserved that assemble together either in binary or ternary complexes [99, 100] .

Syntaxin1A contains a long N-terminal domain (Habc domain), connected to the SNARE core domain by a flexible linker [101] (Figure 5). The Habc domain forms a three helix-bundle which competes with VAMP2 and SNAP-25 coils for binding to its own C-terminal coil (also called H3), forming the so-called closed conformation of syntaxin [102, 103] (Figure 6).

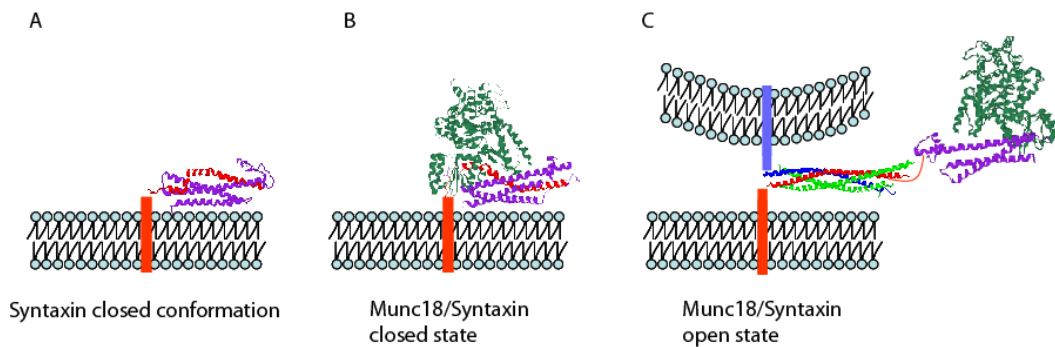


Figure 6. Model for switch of syntaxin1A from a closed to an open conformation. A) Syntaxin1A closed conformation was obtained by removal of Munc18 sequence from Munc18-syntaxin1A PDB file (3C98). Syntaxin TMD (schematically depicted) and the SNARE motif are shown in red. Three α -helices from the N-terminal domain (purple) interact with the SNARE motif α -helix (red). B) Prevention of SNARE core complex formation by binding of Munc18 (greenblue) to the syntaxin1A closed conformation. C) Munc18-syntaxin1A PDB file (3C98) was modified in order to remove syntaxin1A SNARE motif (residues 190-262). A conformational change mediates the transition between Munc18-syntaxin1A complex to the core complex (PDB 1SFC) where VAMP2 is labelled in blue and SNAP-25 in green.

The closed conformation of syntaxin1A has been shown to interact with the chaperone Munc-18, which after a conformational change, seems to open it up to facilitate SNARE complex formation [98, 104-107] (Figure 6). While such scenario would suggest a negative role for Munc18 in membrane fusion, recent studies indicate that Munc18 performs a positive role in regulating SNARE-dependent membrane fusion, by binding and stabilizing the assembled SNARE complex [108].

Many SNARE proteins are susceptible to posttranslational modifications such as palmitoylation or phosphorylation [109-111]. Protein phosphorylation is a common mechanism for regulating a variety of cellular processes, including synaptic transmission mediated by SNAREs [112]. Several SNARE proteins and their regulators have been shown to be phosphorylated *in vitro* [113-115]. In some cases, SNARE phosphorylation can modulate interactions with regulatory proteins. Most SNAREs and SNARE regulators are substrates for multiple kinases, indicating a redundancy in regulatory mechanisms, and most phosphorylation events seem to be inhibitory, suggesting that the role of phosphorylation may be to decrease unwanted SNARE interactions (see for review [116]).

SNAP-25 [96, 117-119], as well as some yeast SNAREs [120] are palmitoylated at cysteine residues *in vivo* and *in vitro* close to the membrane region. As palmitoylation increases hydrophobicity, this posttranslational modification facilitates membrane interactions. Indeed, palmitoylation of SNAP-25 seems to be required for its proper targeting to the plasma membrane [121, 122].

Proper membrane targeting of syntaxins seems to depend on the length of the TMDs as well as of proximal amino acids [123]. For example, the TMDs of the plasma membrane-localized syntaxin3 and 4 fused to GFP, target the proteins to the plasma membrane, whilst shortening those TMDs causes their accumulation in the Golgi compartment [124]. However, the TMDs on their own are not sufficient for proper targeting, as chimeras containing the cytosolic domain of syntaxin1A and the TMD of endosomal syntaxins (6, 7 and 8) lead to plasma membrane localization [123] (see for review [125]). Finally, vesicular targeting of VAMP2 requires specific sequences within its core domain [126, 127].

Apart from their specific destinations, SNAREs can also be found, under certain conditions, in other intracellular localizations. For example, small amounts of VAMP2 can be found at the plasma membrane during high-frequency stimulation [128], which is in accordance with the speed of exocytosis exceeding that of endocytosis. Additional ultrastructural studies have shown the presence of synaptic vesicle proteins, including VAMP2, on the surface of resting synapses [129], which may form a large surface reservoir during recycling [130]. Finally, small amounts of syntaxin1A have been found in recycling vesicles [131-134], a finding that can be explained if NSF action proceeds after vesicular membrane has been endocytosed. In either case, the segregation of SNAREs in intracellular compartments according to their mode of action is largely preserved, even under conditions of high synaptic activity.

3.2 SNARE COMPLEXES.

As the cytoplasmic SNARE domains are unfolded in solution, complex formation is associated with conformational and free-energy changes. When the appropriate set of SNAREs are combined, the SNARE motifs spontaneously associate to form helical core complexes of extraordinary stability, as evidenced by their resistance to SDS denaturation, protease digestion and clostridial neurotoxin cleavage [79, 135-137]. Upon complex formation, major structural changes occur for the ternary complex [58, 99, 138] and for some of the binary combinations of syntaxin1A and SNAP-25 [100]. Such free energy transition from a disordered to an ordered state is conserved among the other members of the SNARE superfamily [58].

3.2.1 BINARY COMPLEXES.

Several biochemical data indicate that neuronal SNARE motifs assemble in different binary combinations. For example, site-directed spin label electron paramagnetic resonance (EPR) spectroscopy studies have shown that the binary 2:1 syntaxin1A/SNAP-25 complexes consist of a parallel four helix bundle [139-

141] which may be a dead-end intermediate state. Indeed, the crucial acceptor complex for VAMP2 binding is a transient 1:1 binary complex of syntaxin1A/SNAP-25 [59].

In addition, NMR studies have shown a weak interaction between VAMP2 and syntaxin1A, implying a small increase in α -helicity [97, 100]. This is supported by some *in vitro* liposome fusion assays that could be accomplished with just VAMP2 and syntaxin1A in opposing membranes, in the absence of SNAP-25 [142-144]. This phenomenon may underlie the finding that SNAP-25 knockout mice can support spontaneous neurotransmitter release, whilst Ca^{2+} triggered release is abolished [145].

3.2.2 TERNARY COMPLEXES.

As SNARE complex formation involves the cytosolic core domains of the individual SNAREs, the vast majority of biochemical, biophysical and structural studies have used recombinant SNAREs devoid of transmembrane domains purified by chromatography [100, 146]. Such ternary SNARE complexes consist of a parallel, four-helix bundle contributed by one coil of VAMP2 and syntaxin1A, respectively, and two coils of SNAP-25 which are separated by the central cysteine palmitoylated region.

A minimal core complex, consisting only of the assembled recombinant core domains of syntaxin1A, SNAP-25 and VAMP2 was further obtained by partial proteolysis [147]. This minimal core complex displays biophysical properties similar to the full-length complex [136, 147]. The minimal core complex has an apparent molecular mass of 60-97 kDa as studied by Multi Angle Laser Light Scattering (MALLS) (compared to a calculated monomeric molecular mass of 41 kDa), indicating that oligomerization (apparently dimers) may occur in solution [147]. On the other hand, analytical equilibrium ultracentrifugation data suggest that the core complex may exist in a monomer-trimer equilibrium [147].

The minimal core complex has been subjected to crystallographic studies. A 2.4Å resolution structure of the neuronal SNARE core complex shows that one coil of VAMP2 (residues 1-96) and syntaxin1A (residues 180-262), and two coils

of SNAP-25 (residues 1-83 and 120-206) assemble together to form a parallel four helix-bundle of 120Å length [148] (Figure 7A).

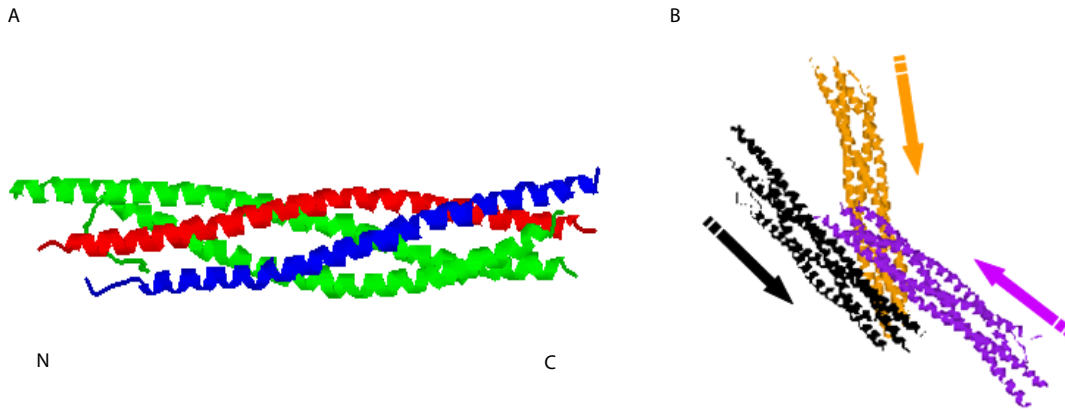


Figure 7. General topology of the synaptic SNARE complex. A) Ribbon drawing of the crystal structure obtained with the minimal SNARE complex (PDB 1SFC). Neuronal SNAREs: one coil of VAMP2 (in blue), one coil of syntaxin1A (in red) and two coils of SNAP-25 (in green) assemble into the core complex forming a parallel four helix bundle. B) Three synaptic fusion complexes (black and orange in a parallel orientation, purple in an antiparallel orientation) obtained in the asymmetric unit of the crystal. Arrows indicate N- to C- terminal.

Three independent SNARE complexes were observed in the crystal unit, two of which displayed a parallel orientation with their C-termini in close proximity, with the third one in an antiparallel orientation (Figure 7B). Whilst in agreement with studies reporting a monomer/trimer mixture of SNARE complexes in solution [147], such trimeric nature, as depicted by crystal lattice interactions, contrasts with the apparent molecular mass of SNARE complexes (indicating dimers) reported by other studies [100, 140, 149].

The crystal structure reveals that the SNARE core complex is composed of 15 hydrophobic layers and one central ionic layer (0-layer) formed by interacting sidechains from each of the four α -helices (Figure 8A). These interactions are perpendicular to the axis of the core complex and their radius varies depending on the side chain packing volumes [148]. The conserved ionic layer is present at the center of the core complex (0 layer) consisting of an arginine (VAMP2 R56) and

three glutamine residues (SNAP-25 Q53 and Q174, and syntaxin1A Q226) (Figure 8B).

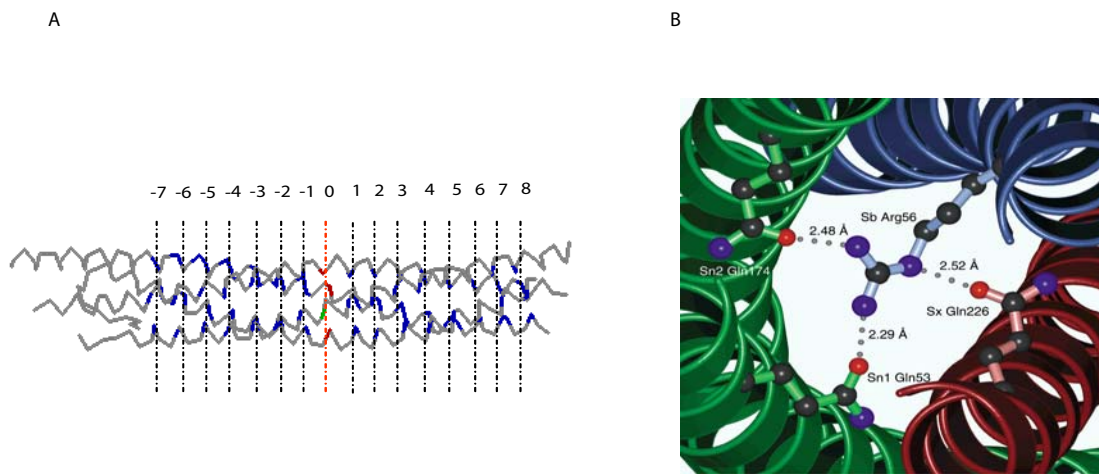


Figure 8. General topology of the synaptic SNARE complex. A) Backbone drawing of the hydrophobic layers (black dotted lines) contributed by highly conserved heptad aminoacid repeats (in blue) and the central ionic layer (red dotted line) formed by one arginine (in green) and three glutamines (in red). B) The central ionic layer of the synaptic fusion complex represented as ribbon diagram (Image from [148]). Crucial side chain interactions are shown as balls and sticks.

On the basis of the conservation of this ionic layer, SNARE proteins are nowadays classified into Q-SNAREs (containing glutamine in the ionic layer: Qa, Qb and Qc) and R-SNAREs (containing arginine) (Figure 9 and Table 1) [150, 151]. The precise role of the Q and R residues is still uncertain. Mutations in these residues may reduce complex stability and cause defects in membrane trafficking [150, 152], suggesting that fusion-competent SNARE complexes require three Q-SNAREs and one R-SNARE [153-155] (see also review [156]). However, *in vivo* mutational studies in chromaffin and PC12 cells where Q residues were mutated to L or R residues ruled out an essential role for the 3Q:1R configuration in at least the final stages of membrane fusion [10, 157, 158].

R-SNAREs

endobrevin (vamp8) (12) LVRNLQSEVEGVKNIMTQNVERILARGENLEHLRNKTEDLEATSEHFKTTSQKVA
vamp4 (52) KIKHVQNQVDEVIDVMQENITKVIERGERLDELQKSESLSDNATAFSNRSKQLR
synaptobrevin (vamp2) (31) RLQQTQAQVDEVVDIMRVNVDKVLERDQKLSLDDRADALQAGASQFETSAAKIK

Qa-SNAREs

STX7 (174) SIRQLEADIMDINEIFKDLGMMIHEOGDVIDSIEANVENAEVHVQQANQQLSRAA
STX13 (187) AIRQLEADILDVNQIFKDLAMMIHDOGDLIDSIEANVESSEVHVERATEQLQRAA
STX1A (201) EIIKLENSIRELHDMFMDMAMLVESOGEMIDRIEYNVEHAVDYVERAVSDTKKAV

Qb-SNAREs

vti1b (144) SIERSHRIATETDQIGSEIIEELGEORDQLERTKSRLVNTSENLKSRKILRSMS
vti1a (130) RLEAGYQIAVETEIQIGQEMLENLSHDREKIQRARERIRETDANLGSRSRILTGML
Snap25 N (27) STRMQLVVEESKDAGIRTLVMLDEQGEQLERIEEGMDQINKDMKEAEKNLTDLG

Qc-SNAREs

STX8 (154) GLDALSSIISRQKQMGQEIIGNELDEQNEIIDDLANLVENIDEKLRNETRVMNV
STX6 (172) QLELVSGSIGVLKNMSQRIGGELEEQAVMLEDFSHLESTQSRIDNVMKKLAQVS
snap25 C (39) NLEQVSGIIGNLRHMALDMGNEIDTONRQIDRIMEKADSNKTRIDEANQRATKML

Figure 9. SNARE core domain sequence alignment from different sets of SNAREs. Mammalian late endosomal SNAREs (top lines), early endosomal SNAREs (middle lines) and neuronal SNAREs (bottom lines) share highly conserved residues (in red). Alignment shows heptad aminoacid repeats participating in hydrophobic layers (yellow boxes) and the central ionic layers of the R- and Q- SNAREs (green boxes).

Table 1

| Mammalian | Yeast | Structural | |
|-----------------|----------|------------|--|
| SNARE | ortholog | role | Mammalian localization; functional role; notes; alternate names |
| Syntaxin 1a, 1b | Sso1, 2p | Q-A | PM; neurotransmission; enriched in neurons (<i>syntaxin 1a</i> , <i>SNAP-25</i> , <i>VAMP2</i>) |
| Syntaxin 2 | | Q-A | PM; varied functions, e.g., sperm acrosomal reaction and platelet dense core granule exocyt. (w/SNAP-23); splice isoforms w/ different PM domain and tissue distributions |
| Syntaxin 3 | | Q-A | PM; varied functions, e.g., apical delivery in intestinal epith. and exocyt. in ribbon synapses |
| Syntaxin 4 | | Q-A | PM; varied functions, e.g., GLUT4 translocation in muscle/fat and mast cell granule exocyt. and platelet a-granule exocyt.; binds synip |
| Syntaxin 5 | Sed5p | Q-A | ER, VTCs, throughout Golgi; ER 3 Golgi, intra-Golgi, endosome 3 Golgi?; partic. in multiple. SNARE complexes (<i>syntaxin 5</i> , <i>membrin</i> , <i>rbet1</i> , <i>sec22b</i>) |
| Syntaxin 7 | Vam3p | Q-A | Endosomal compartments; LE 3 L, homotypic LE and L fusion, PM 3 EE? (<i>syntaxin 7</i> , <i>vti1b</i> , <i>syntaxin 8</i> , <i>VAMP 8</i>) |
| Syntaxin 11 | | Q-A | LE, TGN; enriched in immune system; no TMD; palmitoylated? |
| Syntaxin 13 | Pep12p | Q-A | EE, RE; EE and RE fusion and neural axon extension; binds pallid |
| Syntaxin 16 | Tlg2p | Q-A | Golgi; ubiquitous expression; cytosolic splice variant lacks SNARE motif and TMD |
| Syntaxin 17 | | Q-A | Smooth ER; enriched in steroidogenic cells; two TMDs; bound to sec22b and rbet1 |
| Syntaxin 18 | Ufe1p | Q-A | ER; homotypic ER fusion? ER 3 Golgi? G 3 ER? |
| vti1a | Vti1p | Q-B | Golgi; intra-Golgi?, endosome 3 Golgi; SV variant vti1a- \diamond involved in SV biogenesis? |
| vti1b | | Q-B | Endosomes, Golgi; homotypic LE fusion, intra-Golgi?; E in middle of TMD |
| vti1c | | Q-B | Not characterized; no TMD |
| vti1d | | Q-B | Not characterized; no TMD |
| GOS-28 | Gos1p | Q-B | Golgi; intra-Golgi, late ER 3 Golgi?; binds GATE-16/aut7 |
| Membrin | Bos1p | Q-B | VTCs and throughout Golgi; ER 3 Golgi and perhaps intra-Golgi |
| Syntaxin 6 | Tlg1p | Q-C | TGN, endosomes, ISGs, neutrophil PM; TGN 3 endosome, ISG 3 endosome, neutrophil exocyt.; binds FIG and EEA1 |
| Syntaxin 8 | Vam7p | Q-C | EE, LE; homotypic LE fusion, EE 3 LE? |
| Syntaxin 10 | | Q-C | Golgi, TGN |
| rbet1 | Bet1p | Q-C | ER, VTCs; early ER 3 Golgi, Golgi 3 ER? |
| gs15 | Sft1p | Q-C | Golgi; intra-Golgi? |
| SNAP-23 | Sec9p | Q-BC | PM of most cell types, basolateral PM in acinar cells, pool in RE; GLUT4 transloc., platelet L and a-granule exocyt. and dense granule exocyt., TR cycling, mast cell compound exocyt.; no TMD |
| SNAP-25 | | Q-BC | PM; regulated exocyt.; neuron-specific; C-terminus binds synaptotagmin; no TMD |
| SNAP-29 | Spo20p | Q-BC | Several organelles; enriched in Golgi; many cell types; no TMD |
| VAMP1, 2 | Snc1, 2p | R | SVs, SGs, REs; regulated exocyt.; enriched in neurons; multiple splice isoforms; also called synaptobrevin 1 and 2 |
| VAMP3 | | R | constitutive REs; RE 3 PM, e.g., TR, possibly GLUT4 translocation; most cell types; also called cellubrevin |
| VAMP 4 | | R | TGN, ISGs; TGN 3 LE?; binds syntaxin 6 and synaptophysin |
| VAMP 5 | | R | PM, peripheral vesicles; induced in differentiating myotubes; expressed in skeletal muscle and heart, not in brain; also called myobrevin |
| VAMP 7 | Nyv1p | R | LE, lysosomes, TGN, novel compartment involved in neurite extension; endosome 3 L, homotypic L fusion, neurite extension and apical exocyt. in polarized epithelia; also called TI-VAMP |
| VAMP 8 | | R | EE, LE, apical RE in polarized epithelia; homotypic EE and LE fusion; also called endobrevin |
| sec22b | Sec22p | R | ER, VTCs, COPII buds; early ER 3 G, G 3 ER?, COPII homotypic vesicle fusion? |
| ykt6 | Ykt6p | R | Golgi?; Late ER 3 Golgi?; no TMD, prenylated, .50% cytosolic |
| Tomosyn | | R | Nerve terminals; neurotransmission, mast cell exocyt.; enriched in brain; binds syntaxin 1 and SNAP-23/25; regulator or SNARE? |

Table 1: Summary of mammalian SNAREs. Table modified from review [156]. For each mammalian SNARE, subcellular localization, functional data, and tissue distribution are summarized. Where applicable, a yeast ortholog is suggested, although it is not known whether a direct functional correspondence exists in all cases. Members of well characterized mammalian SNARE complexes are listed in parentheses in the appropriate QA-SNARE row. Structural roles indicate which position in a four-helix bundle each SNARE is predicted to occupy, based upon protein profiling by Bock *et al.* [151]. N-terminal domains that have been well-characterized are indicated. Although the structure of the Habc domains has not been determined for all syntaxins, their conservation is assumed. Those SNAREs for which an independent N-terminal domain is unlikely (because the protein is too small) are marked “no,” and those that are likely to contain one (by protein size and secondary structure predictions) but whose nature is unknown are marked “?”. EE, early endosome; ISG, immature secretory granule; LE, late endosome; L, lysosome; PM, plasma membrane; RE recycling endosome; SG, secretory granule; SV, synaptic vesicle; TMD, transmembrane domain; TGN, trans-Golgi network; TR, transferrin receptor; VTC, vesicular tubular cluster.

Alternatively, other authors proposed that the shielding provided by the adjacent hydrophobic layers is thought to create a sealed zone at the central ionic layer (zero layer) [148], which has been proposed to be required for efficient α -SNAP and NSF-mediated dissociation of the complex [91]. However, such scenario has recently been questioned as well [159], and the precise role for this layer, if any, remains to be determined.

A slight truncation of the minimal core complex, resulting in the removal of approximately one α -helical turn at the C-terminal ends of syntaxin1A and VAMP2, was used to obtain a higher resolution structure at 1.4Å [149]. This truncated micro complex is formed by one coil of VAMP2 (residues 28-89), one coil of syntaxin1A (residues 191-256) and two coils of SNAP-25 (residues 7-83 and residues 141-204). It lacks residues involved in phospholipid binding [160,

161] and denatures at a lower temperature than the minimal complex as determined by SDS and CD thermal melts.

Interestingly, this C-terminally truncated micro complex has an apparent molecular mass of 32 kDa as determined by MALLS, compared to a calculated molecular mass of 32 kDa [149]. Thus, the micro complex seems to be monomeric and monodisperse, in contrast to the various oligomeric states (monomer/trimer or dimer) of the minimal neuronal SNARE complex measured in solution [147]. These results are consistent with the observation that C-terminal truncations of VAMP2 by botulinum neurotoxin B or tetanus toxin [140] result in a monomeric complex, and that C-terminal truncations of endobrevin in the endosomal SNARE complex also produce a monodisperse sample [20]. In addition, the micro complex is still able to bind the Ca^{2+} sensor synaptotagmin I in the presence and absence of Ca^{2+} as determined by GST pull-downs [149].

The structure of the neuronal SNARE core complex is highly conserved, as evidenced by its comparison to the structure of the early endosomal and late endosomal SNARE complexes, respectively [162, 163]. In contrast, the yeast exocytosis SNARE complex structure reveals slight differences, mainly helix bending near the ionic layer and water-filled cavities in the center of the complex [164]. These differences are consistent with the reduced thermal stability of the yeast as compared to the mammalian SNARE complexes. Interestingly, while three SNARE complexes per asymmetric unit were obtained for mammalian and yeast exocytosis SNARE complex crystal structures, only one copy was observed for the late and early endosomal mammalian SNARE complexes. The possible functional significance of this finding, if any, remains to be determined.

3.2.3 CIS AND TRANS SNARE COMPLEXES.

The largely accepted molecular model for SNARE complex assembly is the zippering model [84, 165-167] (reviewed in [66, 168]). This model states that complex assembly starts at the N-terminal regions in a trans configuration, with the SNAREs residing in opposing membranes. In that manner, the vesicle is thought to be pulled closer to the target membrane. The zippering up from the N- to the C-terminal ends leads to full complex assembly and eventually the final

membrane fusion event. The process ends with the formation of a cis-SNARE complex, whereby both SNARE proteins reside on the same membrane (Figure 10).

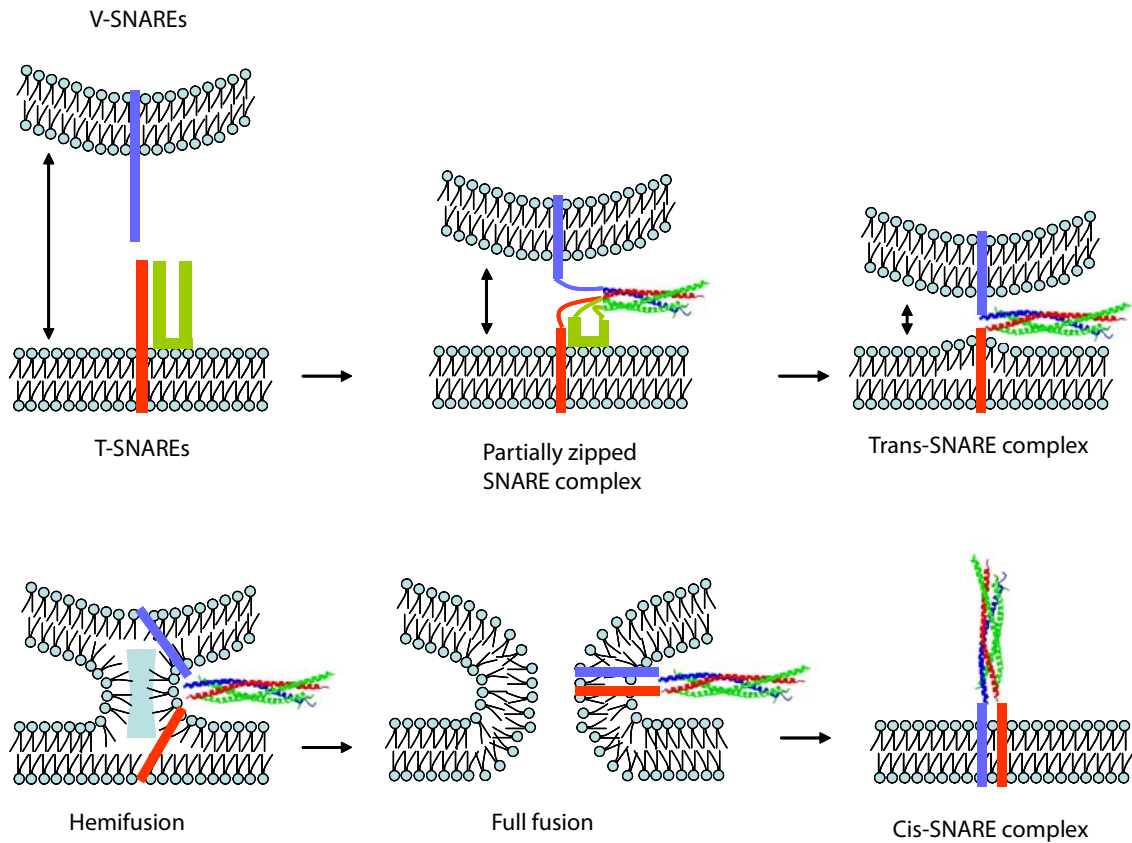


Figure 10. Model for SNARE-mediated lipid fusion. V- and t-SNAREs are in opposing membranes that make close contact by forming the SNARE complex which zippers up from the N- to the C-terminus, thereby drawing the two membranes further towards each other. SNARE assembly exerts a mechanical force on membranes which causes fusion through an intermediate hemifusion stage. At the hemifusion stage, the outer monolayers are merged, forming a bent stalk and generating hydrophobic voids (light blue box). This step is followed by the formation of a fusion pore (full fusion) which subsequently expands.

The directional folding of the unstructured SNARE coils into a highly stable parallel four-helix bundle is thought to provide the energy required to drive membrane fusion [58, 66, 99, 169, 170]. The free energy released upon complex formation further has to be transferred to the transmembrane domains, which may also participate in later stages of fusion [171, 172]. However, the specific transitions that lipids experience as two membranes become merged into a single bilayer are still unclear [173]. In general, it is believed that phospholipid membrane fusion proceeds through an intermediate called stalk or hemifusion state, before the formation of a fusion pore [172, 174-176]. In the hemifusion state, the two outer lipid monolayers are connected by a highly bent stalk, generating hydrophobic void spaces which may stabilize this state depending on the lipid composition. On the other hand, the inner monolayers retain their original integrity whilst being pulled towards each other, forming a dimple [177-179] (Figure 10). It is envisioned that straining of the rigid linkers between the SNARE motifs and the TMDs may transmit the energy to the membranes [178, 180, 181], bending them or disturbing the lipid environment which thus would facilitate the hemifusion state. The energy required for bending a monolayer also depends on lipid composition, with cone inverted phospholipids (such as lysophospholipids) favouring a positive curvature, and regular cone phospholipids (such as phosphatidylethanolamine) favouring a negative curvature [182-184].

Albeit less attractive at present, another model proposes that formation of SNARE complexes connects two preformed proteinaceous pores, either made of the TMDs of the individual SNAREs [95], or of distinct pore-forming proteins [185].

It seems that the hemifusion state mentioned above can be easily reached upon membrane apposition, indicating that the repulsive forces between opposing bilayers as well as the energy required for local lipid mixing would not exhibit a major barrier in the fusion pathway [174, 186]. It is thus possible that the energy released during trans-SNARE complex formation suffices to induce outer leaflet mixing. However, whilst trans-SNARE complexes are widely thought to be essential intermediates in the fusion pathway, no direct evidence has been obtained [187]. Furthermore, some *in vivo* and *in vitro* studies have shown that partially assembled, loose SNARE complexes exist before the Ca^{2+} signal arrives [25, 62-64]. In this state, the SNAREs are still susceptible to cleavage by a set of

clostridial neurotoxins (CNTs) [188-190]. Thus, it is also possible that partially zippered SNARE complexes are the molecular machines bringing membranes close together and holding them in a state ready for fusion upon an appropriate signal.

Whatever the precise assembled state of the trans SNARE complexes before membrane fusion, they are subject to regulation by other proteins such as synaptotagmin and complexin [50, 191]. *In vitro* studies indicate that complexin inhibits lipid mixing and may differentially affect outer- and inner- leaflet mixing, resulting in a hemifusion state arrest, which may then be relieved by synaptotagmin upon an appropriate Ca^{2+} signal [77].

4. PHARMACOLOGICAL EVIDENCE:

Pharmacological evidence for the crucial role of SNAREs in exocytosis has come from studies with bacterial neurotoxins (see reviews [192-195]). Specifically, two species of clostridial bacteria, *Clostridium botulinum* and *Clostridium tetani*, produce botulinum neurotoxins (BoNTs) and tetanus neurotoxins (TeNT), respectively. These clostridial neurotoxins (CNTs) are the agents that cause the neuromuscular diseases botulism and tetanus [196, 197] and are considered potential agents for bioterror attacks [198]. They are released from bacteria as single-chain polypeptides (~150kDa). Immediately, they are activated by proteases which generate two-chain toxins composed of a heavy chain (HC) and a light chain (LC), linked by a single disulfide bond which is reduced while delivering the LC into the cytosol (Figure 11) [199].

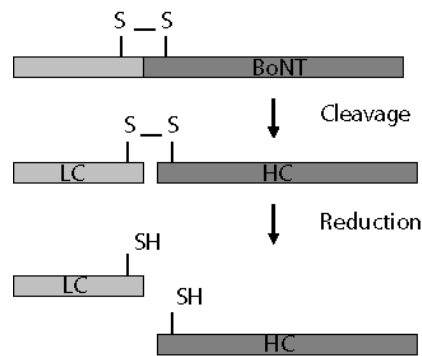


Figure 11. Botulism neurotoxin heavy and light chain. The single polypeptide chain of BoNT is cleaved by proteases, generating a toxin light chain (LC) (light gray) and heavy chain (HC) (dark gray), which are covalently linked by a disulfide bond.

These toxins bind very specifically to the presynaptic cell surface of motorneuron nerve endings. Binding is thought to require the presence of gangliosides, even though additional receptors have to exist as well. Once bound to the surface, the toxins become internalized into endocytic compartments, likely by receptor-mediated endocytosis (Figure 12). A pH-dependent structural rearrangement of the toxin inside the acidic endocytic compartment seems to trigger a structural change, leading to greater hydrophobicity of the molecule and facilitating penetration of the lipid bilayer. It has been shown that some toxins form ion channels in phospholipid bilayers. Whilst the C-terminal half of the HC seems to be responsible for the binding to ganglioside receptors, the N-terminal half of the HC is implicated in membrane translocation by forming membrane pores (reviewed in [194]).

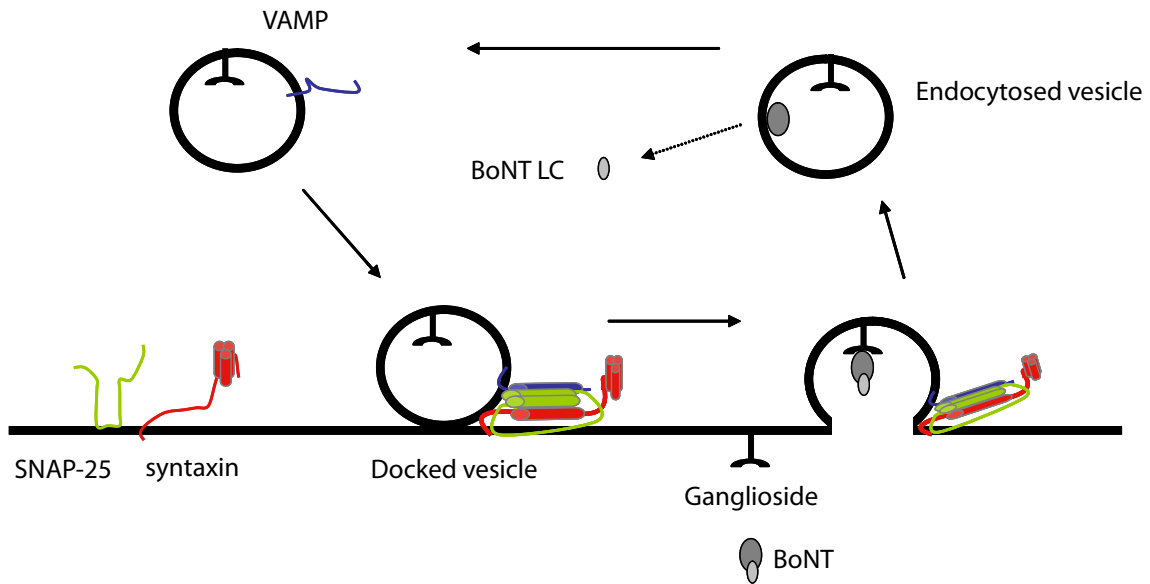


Figure 12. Internalization and mechanism of action of clostridial toxins in neurons. Internalization of BoNT seems to occur via a ganglioside receptor. The acidic pH in intraluminal endocytic compartments triggers a conformational change, somehow allowing the HC to act as a pore through which the LC can be released into the cytosol. BoNT LC then cleaves its SNARE target(s), thus inhibiting exocytosis.

Finally, the active LC is translocated to the cytosol, where it exerts its toxic activity by cleaving SNAREs. BoNTs act locally by blocking the release of acetylcholine thus causing a flaccid paralysis. On the contrary, TeNT is transported retrogradely and reaches the spinal cord, blocking the release of inhibitory neurotransmitters [200, 201] which impairs the neuronal circuits responsible for voluntary muscle contraction, thus causing a spastic paralysis [202, 203]. The discovery that SNARE proteins are targets of CNTs clearly elucidated the important role of SNAREs in neurotransmission [204]. Despite being extremely dangerous poisons, CNTs are also widely used for medical purposes [205]. In addition, CNTs have become useful tools in dissecting the specific aspects of SNARE function in intact and permeabilized cells.

CNTs usually cleave only one of the SNARE proteins, with the exception of BotNT/C, which cleaves both syntaxin1A and SNAP-25 [206] (Figure 13). On the other hand, CNTs cleave SNAREs in a sequence-specific manner, such that the observed sites tend to be distinct for the distinct CNTs. An exception is

BotNT/B and TeNT, which cleave at the exact same site within VAMP2 (Figure 13).

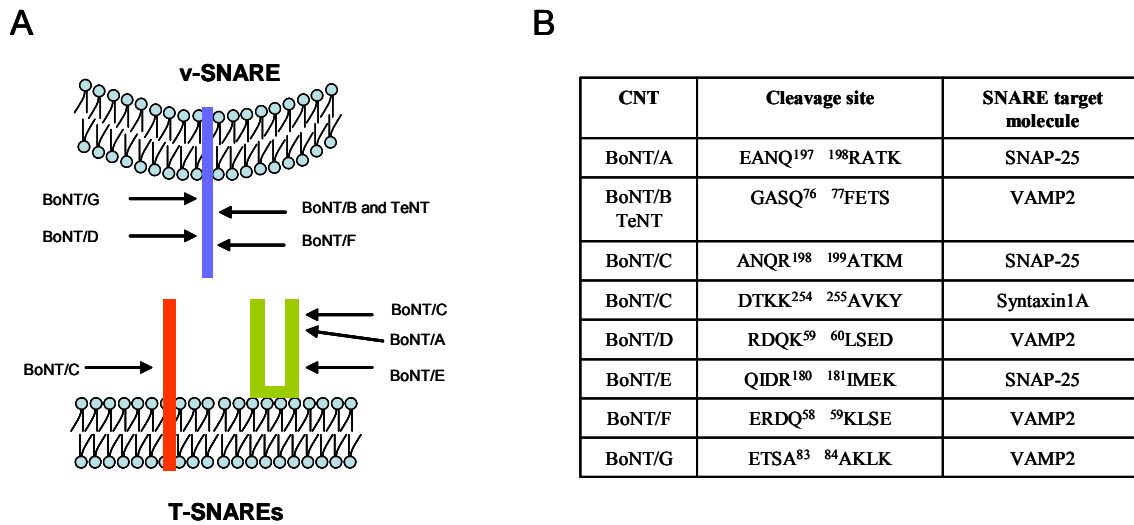


Figure 13. Cleavage sites of clostridial neurotoxins. A) Schematic representation of cleavage sites of botulinum toxin serotypes (A, B, C, D, E, F and G) and tetanus toxin (TeNT). VAMP2 (blue), SNAP-25 (green) and syntaxin1A (red). B) Table indicating the sequence specificity of the cleavage sites of clostridial neurotoxins in rat neuronal SNARE molecules (reviewed in [207]).

Finally, some CNTs can also cleave other SNAREs not classically involved in neuronal exocytosis, as long as the cleavage site is conserved (e.g. Table 2).

| Sequence cleavage site | SNARE target molecule | BoNT/B cleavage |
|------------------------|-----------------------|-----------------|
| GASV-FESS | VAMP1 | Not |
| GASQ-FETS | VAMP2 | Yes |
| GASQ-FETS | VAMP3 | Yes |
| NATA-FSNR | VAMP4 | Not |
| MSSA-FSKT | VAMP5 | Not |
| SSVT-FKTT | VAMP7 | Not |
| TSEH-FKTT | VAMP8 | Not |

Table 2. BoNT/B sequence cleavage site conservation amongst rat VAMP family members.

5. GENETIC EVIDENCE:

Several genetic studies have further expanded our knowledge of how SNARE proteins mediate vesicle trafficking and exocytosis, as animal models have become available.

5.1 VAMP2

The v-SNARE (VAMP2) knockout mice show a deficit in both spontaneous as well as evoked neurotransmission, the latter being much more pronounced [208]. This phenotype can be partially rescued by cellubrevin (VAMP3), a VAMP2 homolog [209]. Mice deficient in both VAMP2 and cellubrevin display a complete inhibition of spontaneous release [18]. Together, these findings indicate that VAMP2 is essential for evoked release, and cooperates together with cellubrevin in maintaining spontaneous release.

VAMP2 also seems to be essential for fast synaptic vesicle endocytosis, as in VAMP2 deficient synapses, an aberrant size of synaptic vesicles and delayed stimulus-dependent endocytosis was observed [210]. An important role for VAMP2 in transmitter release has also been observed in *Drosophila*, where mutants defective in VAMP2 display an inhibition of release without changes in vesicle docking [211], as well as in *C. elegans*, where *snb-1* mutants display a general defect in the efficacy of synaptic transmission [212].

5.2 SNAP-25

Studies in knockout mice lacking SNAP-25 show that Ca^{2+} triggered release is abolished [145], and over-expression of a SNAP-25 homolog rescues Ca^{2+} dependent fusion [19]. Heterozygous mice display spontaneous locomotor activity [96, 213] which is rescued by introducing a SNAP-25 transgene [214]. Studies in other animal model systems, such as in *C. elegans*, also indicate the importance of SNAP-25 in presynaptic function.

5.3 Syntaxin1A

Syntaxin1A knockout mice show normal synaptic transmission, probably compensated by other syntaxin proteins [215]. However, these mice exhibit impaired long term potentiation in the hippocampus, and impaired memory consolidation, indicating that syntaxin1A is closely associated with neuronal plasticity [215]. The syntaxin1A homologue in *Drosophila* shares 70% identity with its vertebrate counterpart, but is not neuron-specific. As a result, syntaxin-deficient *Drosophila* mutants not only display deficits in neurosecretion, but also in a wide variety of non-neuronal secretion events [216]. Analysis of the synaptic boutons in *Drosophila* syntaxin1A deficient mutants reveals an increase in the number of docked vesicles, suggesting that syntaxin functions downstream of vesicle docking [217]. In addition, a temperature sensitive paralytic mutation in *Drosophila* has been described [218]. This syntaxin mutant is unable to interact with SNAP-25 and VAMP2, and exposure to 38°C causes paralysis within seconds, suggesting an impairment of synaptic transmission. *C.elegans* mutants have been described as well, with the most severe phenotype associated with loss of syntaxin function [219, 220]. Syntaxin-deficient animals die as paralysed larvae just after completing embryogenesis [220].

Finally, mutations in the three yeast SNARE equivalents which promote secretory vesicle fusion with the plasma membrane display defects in secretion and an accumulation of secretory vesicles [221]. In sum, data obtained from a variety of animal models are consistent with the crucial role for SNARE proteins in mediating neurosecretion.

6. BIOCHEMICAL EVIDENCE:

When separately reconstituted into synthetic liposomes or ectopically expressed on the surface of cells, neuronal v- and t-SNAREs are sufficient to drive liposome docking and lipid mixing/fusion *in vitro* through their assembly into the SNARE complex, leading to the conclusion that SNAREs are the minimal molecular machinery for intracellular membrane fusion [75, 166, 222, 223]. However, the *in vitro* fusion assays generally suffer from several deficiencies as

compared to *in vivo* fusion events [166], the most important one being the minute time scale of the *in vitro* fusion assay [15, 170, 224], which contrasts to the submillisecond time scale in the case of synaptic neurotransmission [225, 226]. In addition, protein density in liposomes is generally too high as compared to physiological conditions (for example an estimated 750 VAMP2 molecules per 50 nm liposome [166], compared to an estimated 70 molecules per synaptic vesicle [227]). Finally, classical liposome fusion assays also suffer from the impossibility to measure kinetics of individual liposome fusion events. Although a well accepted measure of kinetics involves determining rounds of fusion, it is necessary to measure both lipid mixing and content mixing to obtain a detailed kinetic model of the fusion process [228, 229] and to distinguish fusion events from liposome leaking effects [230].

To solve these problems, another set of liposome fusion assays have subsequently been carried out using physiological protein: lipid ratios. However, the time scale was still over a minute, and content mixing was not determined [224]. Such kinetic differences may be due to the absence of the Ca^{2+} sensor synaptotagmin, or the lack of preformation of the binary acceptor complex of SNAP-25 and syntaxin1A. Indeed, preformation of such binary complex was found to significantly enhance the kinetics of fusion in this *in vitro* system [223]. Finally, recent single-molecule microscopy and spectroscopy experiments have been employed to observe individual membrane fusion events (reviewed in [231]). Individual membrane fusion events between VAMP2 reconstituted liposomes and syntaxin1A-SNAP-25 reconstituted bilayers are much faster, on a millisecond timescale, and are Ca^{2+} independent [142, 143].

Whilst the Ca^{2+} dependency of neuronal secretion is clearly due to synaptotagmin action, additional Ca^{2+} -dependent effects have been proposed based on liposome fusion assays. For example, *in vitro* fusion assays can be enhanced by adding divalent cations (Ca^{2+} and Mg^{2+}) in the absence of synaptotagmin [232]. In addition, the SNARE complex displays several putative cation binding sites of relatively low affinity [150, 233], suggesting that Ca^{2+} binding to the SNARE complex may have direct downstream effects on SNARE-mediated membrane fusion. However, these liposome fusion assays again were carried out at very high protein concentrations, and subsequent studies at physiological protein concentrations indicated that SNARE-mediated fusion

events are not dependent on Ca^{2+} in the absence of synaptotagmin [142, 143]. Thus, the relevance of Ca^{2+} binding to the SNARE complex, if any, remains to be determined.

Despite some controversial data, many results from liposome fusion assays are consistent with known structural features of SNAREs and SNARE complexes, and such fusion assays have also yielded additional insights into membrane fusion not evident from mere biochemical studies. For example, lipid fusion is prevented by replacement of VAMP2 and syntaxin TMDs with covalently attached lipids [234, 235], revealing the importance of SNARE membrane anchors. In addition, insertion of large flexible linkers between the TMD and the SNARE motif interferes with membrane fusion, indicating that the energy released by SNARE complex formation can only be transferred to the membrane anchors/lipid bilayer when those are in close proximity [236].

Finally, biochemical studies have also employed permeabilized cells. In such permeabilized cells, cleavage of endogenous SNAREs by recombinant TeNT or BotNT inhibits secretion. Neurosecretion can be restored by previously transfecting cells with toxin-resistant SNAREs [160, 237, 238], and such toxin rescue assays have been successfully used to analyse the importance of specific amino acid residues within SNAREs for secretion in the absence of endogenous, wild type protein.

7. OLIGOMERIZATION AND COOPERATIVITY:

Whilst SNAREs have clearly been shown to be essential for membrane fusion, it is unclear how many SNARE complexes are necessary for a single fusion event (reviewed in [239]) (Figure 14). In cells, Ca^{2+} triggered membrane fusion seems to involve the cooperative action of multiple SNARE complexes [240-242]. For example, in permeabilized PC12 cells, introduction of the cytosolic domain of VAMP2 (which forms a non-productive SNARE complex, thus acting as a dominant-negative) inhibits exocytosis, and the concentration-dependent inhibition has been used to estimate that at least three SNARE complexes are required for a vesicle fusion event [243]. Other experiments have been used to calculate that around five to eight [95] or ten to fifteen [239, 244,

245] SNARE complexes cooperate to accomplish membrane fusion (Figure 14). Such different estimates probably reflect the distinct technologies applied and/or the types of secretory organelles studied. Higher order multimers of SNARE complexes may be required for fast exocytosis of small synaptic vesicles, whereas lower order multimers may be sufficient for slower exocytosis of large-dense core granules from chromaffin and neuroendocrine PC12 cells [239].

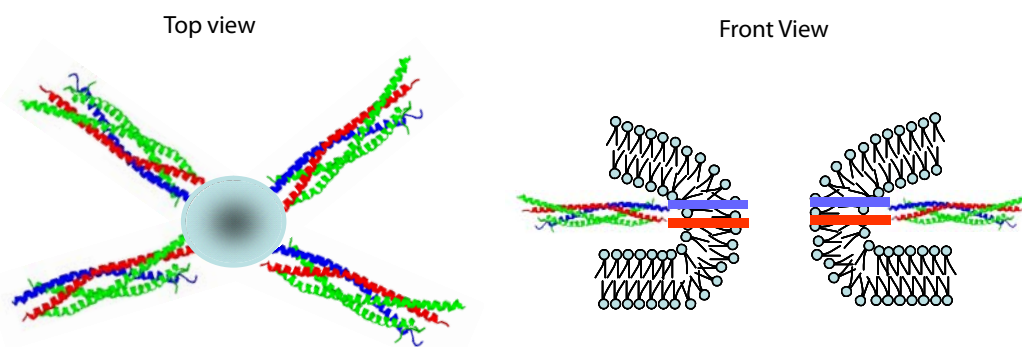


Figure 14. Model for SNARE complex oligomerization around the fusion pore. Model based on the SNARE complex crystal structure (PDB 1SFC). Top and front side section view (respectively) of the fusion pore surrounded by multimeric SNARE complexes which may cooperate to drive membrane fusion. The number of SNARE complexes around a fusion site has been arbitrarily set to 4.

In vitro biochemical studies also indicate the presence of higher order multimeric SNARE complexes [20, 136, 147, 246]. However, the molecular mechanism(s) responsible for SNARE complex multimerization remains controversial. Initial studies suggested that multimerization of synaptic SNARE complexes could be obtained via domain swapping, whereby one of the two SNAP-25 helices could be substituted by the equivalent helix from a neighboring complex (Figure 15A) [247]. Alternative models proposed the involvement of accessory proteins, such as synaptotagmin (Figure 15B) [248] or complexin (Figure 15C) [249], in synaptic SNARE complex multimerization. In addition, as SNARE complexes assembled from recombinant coils and lacking

transmembrane domains are able to associate with each other [99, 140, 147, 149], at least some of the interactions that support multimerization seem to require neither accessory proteins nor the TMDs of SNAREs.

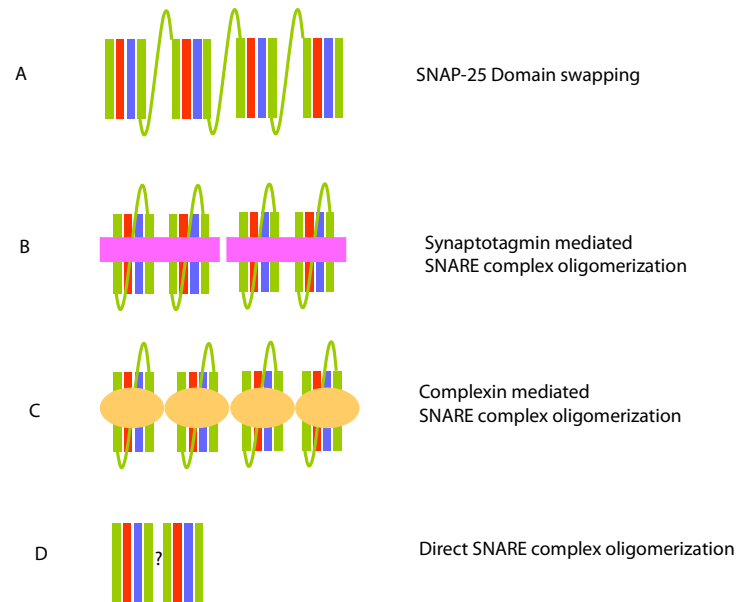


Figure 15. Different proposed models for SNARE complex oligomerization. A) SNARE complexes formed by one coil of VAMP2 (blue), one coil of syntaxin1A (red) and two coils of SNAP-25 (green) oligomerize by one SNAP-25 coil domain swapping over to the adjacent SNARE complex. B) Ca^{2+} binding to synaptotagmin (pink) promotes its oligomerization and clustering of two SNARE complexes bound per synaptotagmin molecule. C) Complexin (light orange)-mediated SNARE complex oligomerization by cross-linking the complexes via SNAP-25 hinges. D) SNARE complexes directly interact in the absence of regulatory proteins, either in a TMD or non-TMD-mediated fashion.

The TMDs of SNAREs may play an important role in SNARE complex oligomerization as well. For example, self-interactions of the syntaxin1A TMDs have been proposed to play a scaffolding role for the subsequent formation of a supramolecular SNARE complex at the fusion site [250], or to be implicated in mediating the transition from a hemifusion to a full fusion state [251]. Whilst TMD-mediated SNARE complex oligomerization constitutes an attractive model,

it is confounded by other observations which indicate that TMD interactions of SNARE proteins not incorporated into complexes occur as well. For example, individual VAMP2 or syntaxin1A molecules have been reported to form TMD-mediated homodimers and heterodimers in a sequence-specific manner [252-257]. However, the relative affinity of such interactions has been controversial [258, 259], and their *in vivo* relevance remains unclear, given that all studies have been performed *in vitro*, that is, in detergent solution or in liposomes. Similarly, the observation that native oligomers of SNARE complexes, isolated from brain extracts, are assembled into star-shaped particles containing 3 to 4 bundles as analyzed by electron microscopy (EM) [260], may be, at least in part, due to TMD interactions upon detergent solubilization (Figure 16).

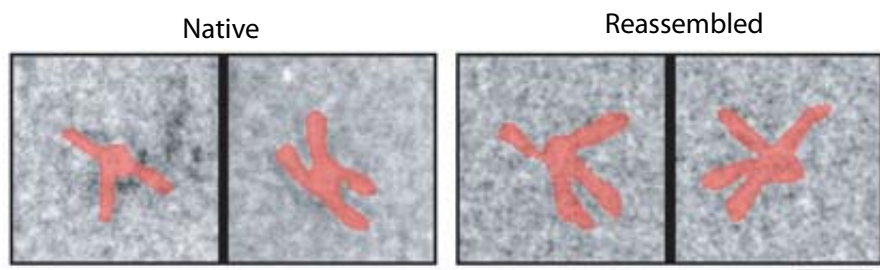


Figure 16. Native and reconstituted SNARE complexes form star-shaped oligomers (Figure from [260]). All SNARE complexes isolated from brain appear as oligomeric particles which predominantly contain three to four SNARE complexes. Reassembling highly purified individual SNAREs reconstitute identical star-shaped particles. The SNAREs are false-coloured in red.

Furthermore, a recently solved X-ray structure of the neuronal SNARE complex containing VAMP2 and syntaxin1A TMDs, reveals a similar X-shape assembly of four SNARE complexes where the four VAMP2 TMDs build the internal core of this multimer, surrounded by the four syntaxin1A TMDs [261] (Figure 17). In sum, although the crucial importance of the TMDs of SNAREs for membrane fusion events is recognized [262], the precise structural and functional requirements for the TMDs, especially in intact cells, are largely unknown.

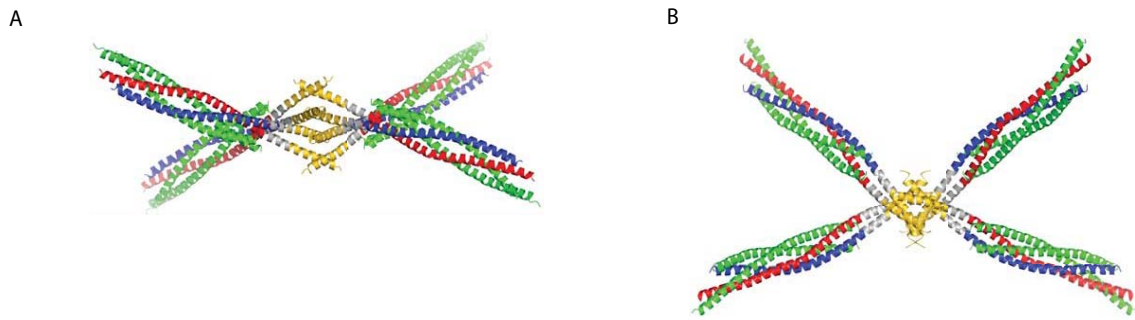


Figure 17. Ribbon scheme of the X-shape assembly of four synaptic SNARE complexes in a side view (A) and front view (B) (Figure modified from [261]). SNARE coils are represented using the same colour code as in previous figures. TMDs are shown as yellow ribbons.

8. TRANSMEMBRANE DOMAINS:

SNARE-mediated membrane fusion bears important mechanistic resemblance to viral membrane fusion events (see for reviews [263, 264]). Both membrane fusion processes are driven by a sequential cascade of protein binding and folding reactions and both share a number of basic architectural features. For example, both involve integral membrane proteins with a single-span TMD, both involve complex assembly via formation of soluble coiled-coil domains, and in both cases these complexes form supramolecular multimers (see for reviews [168, 239, 264]).

While SNARE proteins are essential for intracellular membrane fusion along the secretory and endocytic pathways, various viral fusogenic peptides mediate infection of eukaryotic cells by enveloped viruses (see for reviews [6, 265]). Viruses bind to the cell surface through interactions between their envelope proteins and specific receptors in the host cell (Figure 18) [266, 267]. Such interactions are followed by conformational changes in the N-terminally TMD-anchored fusion proteins, which thereupon insert their C-terminal hydrophobic segment (fusion peptide) into the target membrane. Subsequently, the fusion proteins undergo an additional conformational change, by rearrangement and

protein folding, of three fusion proteins (in the case of virus class I) into a coiled-coil structure that brings viral and host membranes into close proximity and results in membrane fusion (see for review [268]).

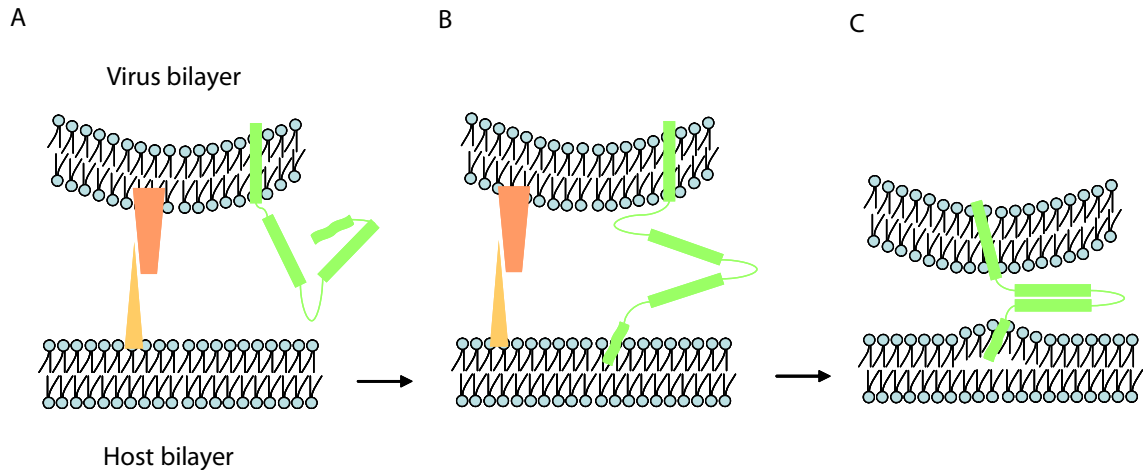


Figure 18. Simplistic model for viral fusion. A) Viral envelope protein (dark orange) interacts with specific receptors (light orange) of the host cell. B) Insertion of the fusion peptide from the viral fusion protein (green) into the target membrane. C) Reassembly of the TMD-anchored fusion protein into a coiled-coil structure brings opposing membranes into close proximity, deforming the local lipid environment around the TMD and the fusion peptide, which then ends up in membrane fusion. For simplicity, only one single viral fusion protein is depicted.

For both SNARE-mediated or viral-mediated membrane fusion events, it has become clear that the TMDs act as more than just membrane anchors (see examples in Table 3 and Table 4, reviewed in [262]). Specifically, the TMDs seem to be involved in the transition from the hemifusion to the full fusion state. For example, mutating, shortening or replacing viral TMDs by GPI anchors results in a hemifusion arrest [269-271]. Similarly, SNAREs whose TMDs have been replaced by GPI-anchors pronouncedly inhibit outer leaflet mixing [175]. Finally, *in vivo*, mutations in the syntaxin or VAMP2 TMDs lead to impaired neurotransmission in *C.elegans* [212, 220].

In vitro, TMD peptides display fusogenic activity on their own. For example, peptides which mimic synaptic or yeast vacuolar SNARE TMDs, as well as viral peptides, drive liposome fusion in a sequence-specific manner [171, 251, 272, 273]. Such fusogenic activity does not seem to be due to the inherent hydrophobicity of the TMD peptides, as for example oligo-leucine peptides are not fusogenic [171]. Rather, the fusogenic activity of the TMD peptides may be related to the stability of their α -helical conformations, combined with helix flexibility contributed by the presence of β -sheet-promoting residues such as isoleucine and valine in SNAREs TMDs [171], or helix breaking residues such as glycine in viral peptides [171, 274].

Table 3

| Protein | Type of TMD alteration | Functional defect | Reference |
|--|--|---|-----------|
| Caenorhabditis elegans Snb-1 | Frame shift within TMD of naturally occurring mutant | Reduced neurotransmission | [212] |
| Caenorhabditis elegans Unc-64 | Truncated TMD | Reduced neurotransmission | [220] |
| Synaptobrevin II and syntaxin 1A | Replacement by phosphatidyl-ethanolamine anchor | Reduced liposome-liposome fusion | [14] |
| Yeast exocytotic Snc1p and Sso2p | Replacement by isoprenoid anchor | Reduced exocytosis, rescue by lysolipid addition to distal leaflet | [178] |
| Synaptobrevin II TMD peptide | Multiple point mutations | Reduced liposome-liposome fusion | [171] |
| Yeast vacuolar Vam3p | Replacement by isoprenoid anchor | Reduced vacuole-vacuole fusion | [275] |
| Yeast exocytotic Snc1p | Truncation of TMD to half of its original length | Reduced inner leaflet mixing in liposome-liposome fusion | [172] |
| Synaptobrevin II and syntaxin 1A | Replacement by GPI anchor | Abolished inner leaflet mixing in cell-cell fusion (“flipped” SNAREs) | [175] |
| Yeast vacuolar Vam3p (full-length protein and TMD peptide) | Multiple point mutations | Reduced vacuole-vacuole fusion reduced inner leaflet mixing in liposome-liposome fusion | [251] |

Table 3. Functional defects displayed by altered or replaced SNARE TMDs. For more details see review [262].

Table 4

| Protein | Type of TMD alteration | Functional defect |
|--|---|--|
| Influenza hemagglutinin | Replacement by GPI anchor | Abolished contents mixing but retained outer leaflet mixing |
| Influenza hemagglutinin | Replacement by GPI anchor | Abolished contents mixing that is partially rescued by chlorpromazine |
| Influenza hemagglutinin | Replacement by GPI anchor | Inefficient fusion pore formation and growth |
| Influenza hemagglutinin | Replacement by unrelated TMDs | Fusion retained |
| Influenza hemagglutinin | TMD G520L mutation (Japan strain) | Abolished contents and reduced inner leaflet mixing, absence of fusion pores, fusion rescued by chlorpromazine |
| Influenza hemagglutinin | Shortening of TMD by 12 residues | Abolished contents mixing but retained outer leaflet mixing, partially rescued by chlorpromazine |
| VSV G-protein | Replacement by GPI anchor | Abolished fusion |
| VSV G-protein | Deletion of TMD residues or mutation of a GxxxG motif | Abolished contents mixing but retained outer leaflet mixing |
| VSV G-protein | Replacement by unrelated TMDs | Fusion retained |
| HIV gp120 | Replacement by GPI anchor | Reduced syncytia formation |
| HIV gp120 | Different truncations and mutations | Reduced syncytia formation |
| HIV gp120 | Replacement by CD22 TMD or R696I mutation | Viral particle release maintained |
| HIV gp120 | Replacement by glycoporphin A or VSV G-protein TMD | Reduced outer and inner leaflet mixing |
| HIV gp120 | Mutation of GGxxG motif | Reduced cell-cell fusion |
| Measles virus Fprotein | Cysteine residues mutated | Reduced palmitoylation and cell-cell fusion |
| HN protein of Newcastle disease virus | Mutation of leucine zipper repeat | Reduced fusion-promoting activity |
| Moloney murine leukemia virus envelope protein | Mutation of Pro617 | Reduced fusion and infectious particle formation |
| Reovirus fusion associated small transmembrane protein | Mutation of tri-glycine motif | Reduced syncytia formation |
| p10 Herpes simplex virus type 1 glycoprotein gD | Replacement by GPI anchor | Reduced cell-cell fusion |
| Herpes simplex virus type 1 glycoprotein gH | Various point mutations | Reduced cell-cell fusion |
| VSV TMD peptide | Mutating GxxxG motif and other point mutations | Reduced liposome-liposome fusion |
| VSV TMD peptide | Mutating GxxxG motif | Reduced liposome-liposome fusion |
| Semliki forest virus E1 protein | Mutation of conserved Gly residues | Reduced cell-cell fusion and increased dependence of liposome fusion on cholesterol |

Table 4. Functional defects displayed by altered or replaced viral fusion peptides. For more details see review [262].

The fusogenic activity of the SNARE TMDs has been proposed to involve sequence-specific TMD interactions to promote oligomerization and bilayer mixing [26]. For example, SNARE TMD-TMD interactions may mediate the transition from hemifusion to full fusion by forming a ring around the hemifusion diaphragm [174]. Likewise, viral proteins seem to cooperate by TMD-mediated multimerization [276, 277].

Assessing TMD-mediated interactions between assembled trans SNARE complexes is confounded by the observation that individual SNAREs, not incorporated into complexes, can interact via their TMDs as well. Indeed, VAMP2 homodimers have been detected in neuronal membranes [259, 278-281], and the synaptic SNAREs VAMP2 and syntaxin1A can assemble in homo- and hetero-dimers *in vitro* through a conserved motif within their TMDs [253-256]. This interaction interface has been mapped by an alanine scanning mutagenesis approach [254], and in the case of VAMP2 involves at least six residues (L99, I102, C103, L107, I110 and I111) (Figure 19).

```

VAMP2      ...97  IILGVICAIILIIIIIV  112...
syntaxin1A ...265  KIMIIICCVILGIIIA  280...

```

Figure 19. Sequence alignment of the proposed dimerization interface of SNARE TMDs. Residues involved in VAMP2 homodimerization are shaded. Note the high homology between both TMDs, suggesting a similar dimerization interface for the syntaxin1A TMD.

When this motif is reconstituted onto a polyalanine sequence, two additional residues (I98 and I106) seem to be necessary to restore homodimerization (Figure 19) [255]. Molecular modelling further suggests that this motif within the VAMP2 TMD forms a tightly packed interface, whereby the predicted alpha-helices pack against each other with a negative crossing angle of -38°, and whereby C103 is the residue closest to this interaction interface (Figure 20) [252]. However, other studies have questioned the affinity of the VAMP2

TMD interactions, and the *in vitro* detection of such interactions seems to be protocol-dependent [258].

The VAMP2 homodimerization motif is highly conserved amongst the syntaxin1A TMD except for a single aminoacid substitution (Figure 19) [255], which indicates that analogous TMD interactions may occur between syntaxin1A molecules, or between VAMP2 and syntaxin1A molecules. Indeed, syntaxin1A-VAMP2 heterodimers and syntaxin1A homodimers have been detected by *in vitro* crosslinking assays [255, 256, 259]. However, additional studies indicate alternate interfaces mediating homo- and heterodimeric syntaxin1A and VAMP2 TMD interactions *in vitro* [253]. In the heterodimeric scenario, a negative crossing angle would contrast with the positive angle of the cytosolic SNARE complex, necessitating an unstructured linker region between the SNARE coil and the TMD [255].

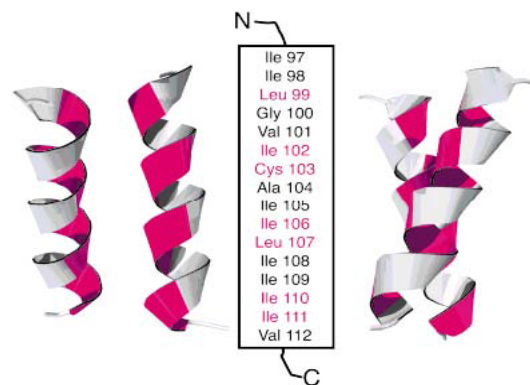


Figure 20. Computational modelling of VAMP2 homodimer. The interacting residues are shown in magenta. Left: View illustrating the symmetric nature of the interaction. Right: Rotated 90° revealing the negative crossing angle between the two helices, with the closest interaction occurring at C103. Figure from [252].

The precise role and structure of the linker region between the SNARE coiled-coil domain and the TMDs has been highly controversial as well. It is clear that the linker region is important for coupling the energy released during SNARE complex assembly onto the TMDs, allowing hemifusion to occur. However, exactly how such mechanical coupling would occur remains unclear. One model proposes alpha-helical continuity between the SNARE domains and the TMDs,

assuming a certain flexibility in short amino acid stretches at the membrane-proximal region [148]. However, insertions in the linker region can profoundly inhibit SNARE-mediated membrane fusion, indicating that mere alpha-helical continuity, with a kink at the membrane-proximal region, is not structurally sufficient to drive membrane merger [236, 282].

Further insight into the linker region has come from EPR studies, which showed that the linker region of syntaxin1A is unstructured, but laterally inserted into the membrane, tightly coupling the coiled-coil to the membrane but tolerating helix-disrupting mutations [247, 283]. On the other hand, EPR studies of VAMP2 indicate that its linker region is inserted into the membrane, with two tryptophan residues (W89 and W90) buried in the hydrophobic part of the bilayer [284]. Interestingly, such tryptophan residues near the transmembrane domains are found in many v-SNAREs [285]. The EPR studies also suggest that residues K85 to N92 form an alpha-helix, which is inserted into the membrane with a tilted orientation of -33° with respect to the axis perpendicular to the membrane plane [286]. The study further implies a perpendicular orientation of the alpha-helical TMD, tolerated by a short unstructured linker (residues 93-95) (Figure 21).

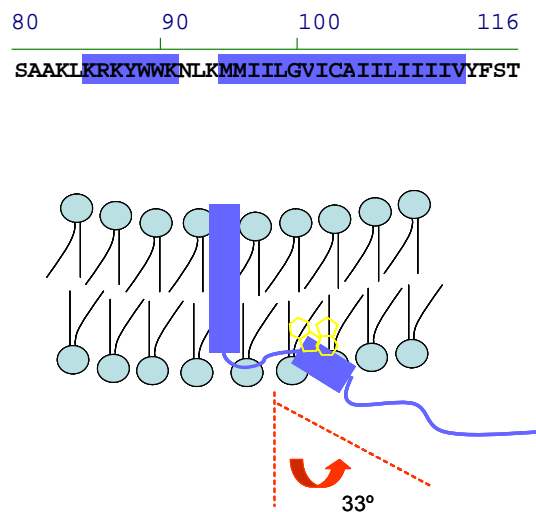


Figure 21. Model for structural arrangement of C-terminal part of VAMP2 with respect to membrane bilayer. Upper panel shows rat VAMP2 sequence from residues 80 to 116. Residues with α -helical structure are indicated in blue, and are divided by a short unstructured linker (NLK). Lower panel depicts the tilted orientation of the C-terminal part of VAMP2, with W89 and W90 in yellow.

Apart from the tryptophan residues, the membrane-proximal region of VAMP2 is enriched in basic amino acid residues (lysines and arginines), a common feature of all SNARE linker regions [285]. These positively charged residues have been proposed to interact with negatively charged phospholipid headgroups, thereby stabilizing a TMD/lipid interaction as observed in other membrane proteins [287]. In addition, insertion of the short alpha-helical region proximal to the TMD into the membrane has been suggested to prevent VAMP2 from forming the SNARE complex by acting as a negative regulatory domain [286, 288, 289].

Studies employing circular dichroism (CD) and infrared spectroscopy (IR) techniques have reached different conclusions as to the conformation of the membrane-proximal domain of VAMP2, indicating full alpha-helical continuity between the TMD and the polybasic region, with a tilted orientation of -35° relative to the bilayer normal (Figure 22) [290]. Interestingly, viral fusion peptides are also found to be inserted with oblique angles into membranes, such as $30-55^\circ$ in the case of influenza virus [291], and an oblique insertion has been suggested to correlate with fusogenic activity [292].

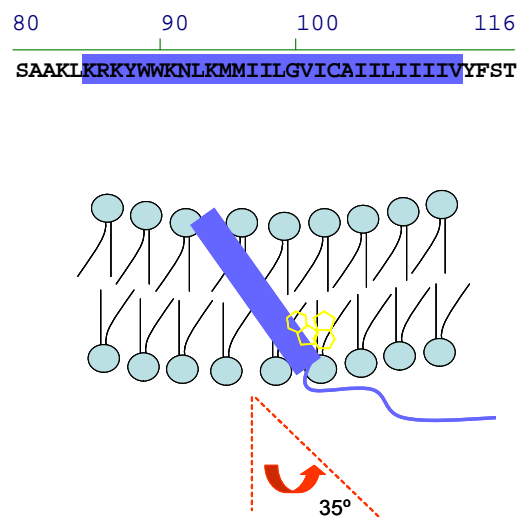


Figure 22. Alternative model for VAMP2 TMD conformation. Helical continuity from the TMD to the polybasic region as represented in the upper panel (residues shaded in blue). Lower panel shows oblique insertion of the TMD into the membrane, including the two tryptophan residues W89 and W90 (yellow).

Finally, a recent study suggests that the TMDs of VAMP2 are inserted at an oblique angle, but change this orientation in the presence of cholesterol to one perpendicular to the membrane normal [257]. However, it is hard to imagine how the unusually large predicted TMD sequences would be accommodated in a fully perpendicular fashion without unnecessarily exposing hydrophobic residues to an aqueous environment.

In sum, it becomes clear that the precise structure of the membrane-proximal domain and TMD of VAMP2 remains to be established, especially in an intact cell environment, without disturbing membrane lipid composition. However, the functional significance of this region is clearly evidenced by toxin rescue studies in PC12 cells, where mutating W89-W90 residues of VAMP2 was found to profoundly reduce secretion [160, 161, 289].

9. SNARE REGULATORS:

9.1 COMPLEXIN

Complexins, also named synaphins, are evolutionary conserved small proteins of approximately 15 kDa that are mainly found in the presynaptic part of neuronal cells [50, 73]. Complexin contains two unstructured regions at the N- and C-terminus, and a central alpha helix responsible for binding to the SNARE complex in a Ca^{2+} independent manner which contains two contiguous domains termed central helix and the accessory helix located proximal to the membrane where the final stages of SNARE complex zippering take place [293] (Figure 23A,B).

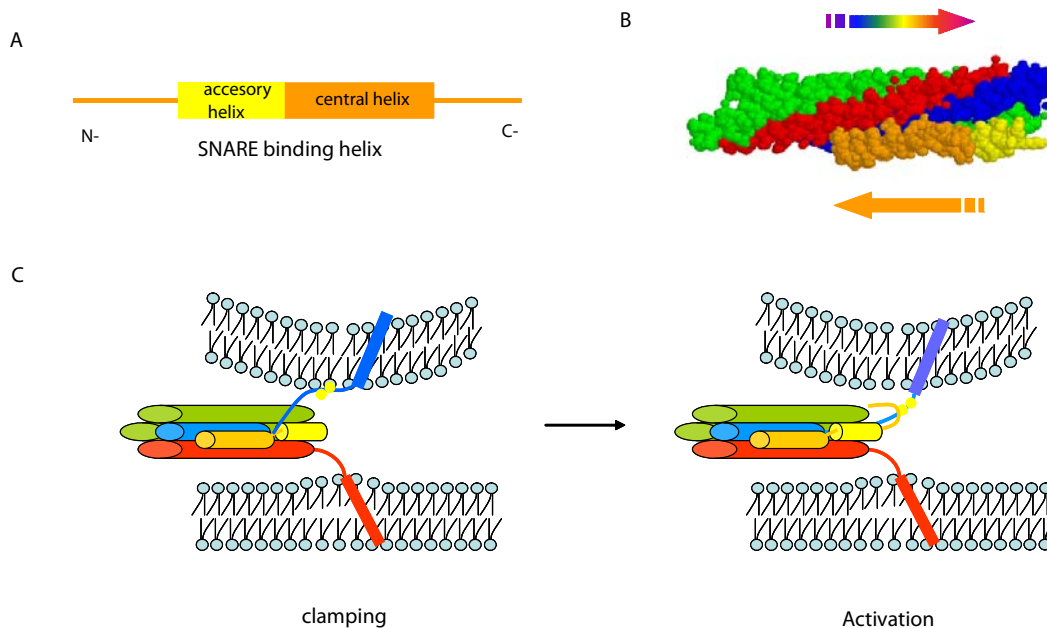


Figure 23. Complexin-SNARE interactions. A) Schematic diagram representing the accessory (residues 26-47) and central (residues 48-70) helices of complexin binding region to the SNARE complex and two unstructured regions at the N- and C-terminus. B) Spacefill representation of the crystal structure (PDB 1KIL) of complexin bound to the SNARE complex in an antiparallel fashion. Arrows indicate the N- to C-terminal orientation of the SNARE complex (multicolor) and of complexin (orange-yellow). C) Proposed model of mutual clamping and activation functions of complexin. Schematic drawing indicates how the central helix binds to the partially zippered SNARE complex while the accessory helix prevents the C-terminal region of VAMP2 (tryptophans are shown as yellow spheres) from completing full zippering, thus clamping fusion and suppressing spontaneous release. Activation of the fusion machinery is then thought to be mediated by the unstructured N-terminal domain of complexin which somehow releases the membrane proximal region of VAMP2 from vesicle membrane, allowing full SNARE complex zippering.

Two complexin isoforms exist (complexin I and II), and depletion studies indicate that complexins play an important role in regulating SNARE-mediated neurotransmitter release. For example, complexins have been proposed to act as a

negative clamp, causing a block of SNARE-dependent fusion in *in vitro* fusion assays [77]. Alternative studies indicate that deletion of complexin selectively impairs fast synchronous neurotransmitter release without affecting spontaneous release, indicating that complexin plays a positive role in bringing about membrane fusion events [294, 295]. Recent studies may reconcile such contradictory models, and suggest that complexins play both positive and negative roles in regulating SNARE-mediated fusion events [296]. These knockdown studies indicate that complexins seem to activate fast, calcium-evoked fusion, and simultaneously suppress spontaneous fusion. In this model, SNARE binding by the central helix of complexin and its accessory helix are required for activation and clamping of fusion, whilst the N-terminal unstructured region is required for activation but not clamping [296] (see for review [78]). It is envisioned that the accessory helix clamps fusion by forming an alternative four-helix bundle with the membrane-proximal portion of the trans SNARE complex, thereby preventing VAMP2 from completing its zippering and triggering fusion [297]. On the other hand, the unstructured N-terminal helix which activates fusion may independently interact with the trans SNARE complex close to the membrane, because a point mutation in VAMP2 (W89AW90A) mimicks the complexin knockout phenotype [296]. However, such data do not prove causal relationship, and further studies will be necessary to determine the function of the N-terminal sequence of complexin and its relation to the C-terminus of VAMP2. In either case, the present model for complexin function is attractive, as it reconciles currently available data, whereby complexin may suppress spontaneous fusion by inserting into the assembling trans SNARE complex, and whereby complexin may activate evoked fusion by directly or indirectly interacting with the membrane-insertion sequence of SNARE proteins in the trans SNARE complex.

9.2 SYNAPTOTAGMIN

Several isoforms of synaptotagmin have been characterized in neurons and non-neuronal cells [298]. However, the best characterized member of the family is synaptotagmin I, a Ca^{2+} binding protein. Reducing the Ca^{2+} binding affinity of synaptotagmin in mice causes a corresponding reduction in the Ca^{2+} sensitivity of fusion, thus formally proving that synaptotagmin I is the calcium sensor for fusion [71].

Structurally, synaptotagmin I is a synaptic vesicle protein composed of a short intraluminal N-terminal domain, a single TMD, and a large cytoplasmic domain harbouring two tandem C2 domains (C2A and C2B) [299] (Figure 24A). The C2 domains interact in a Ca^{2+} dependent fashion with acidic lipids such as phosphatidylserine [72, 300-304]. X-ray structure of the C2A domain revealed a β -sandwich fold with three top Ca^{2+} binding loops (1, 2 and 3), whereby loops 1 and 3 contribute the conserved acidic residues for cation coordination (Figure 24B) [305]. The C2B domain is structurally similar to the C2A domain (Figure 24B), and also displays a Ca^{2+} response upon binding of two Ca^{2+} ions [306]. In addition, the C2B domain may promote Ca^{2+} -triggered dimerization of synaptotagmin [307]. Both C2 domains have low intrinsic affinity for Ca^{2+} ; however, the apparent Ca^{2+} affinity increases in the presence of phospholipid membranes [308].

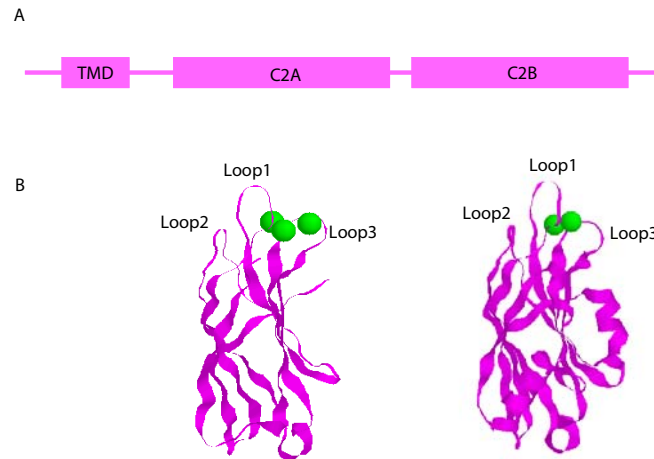


Figure 24. Overall topology of synaptotagmin I. A) Schematic domain representation of synaptotagmin I, composed of an N-terminal TMD and two cytoplasmic C2 domains (C2A and C2B). B) Ribbon diagram of the crystal structures of the C2A (left, PDB 1BYN) and C2B (right, PDB 1OUW) domains with bound Ca^{2+} ions (green spheres).

In addition, upon Ca^{2+} binding, hydrophobic and positively charged residues on the top of loops 1 and 3 embed both C2 domains in the membrane through interaction with lipids [302, 304, 309-312]. Decreasing or increasing the apparent Ca^{2+} affinity in the presence of phospholipids leads to parallel changes in the Ca^{2+} sensitivity of release, indicating that Ca^{2+} dependent phospholipid binding is crucial for synaptotagmin function [71, 313], and that the Ca^{2+} -dependent synaptotagmin-phospholipid complex might be the driving force behind the Ca^{2+} triggering of neurotransmitter release, involving a cooperative action of both C2 domains [71, 314]. This is further supported by a reduction of exocytosis in PC12 cells when the linker between the C2 domains is lengthened, suggesting that the C2A and C2B domains cooperate [315]. Finally, synaptotagmin binding to lipids has been proposed to induce a positive curvature in the target membrane which, in conjunction with the zippering of SNAREs, may promote membrane fusion [316].

Apart from binding to lipids, synaptotagmin I has also been shown to bind to SNARE complexes. Binding *in vitro* has been suggested to be stoichiometric and to occur in the absence or presence of Ca^{2+} , depending on the ionic strength conditions employed [55]. Synaptotagmin binding to the SNARE complex seems

to take place within the C terminal part of the SNARE complex (Figure 25), forming a quaternary complex SNARE-synaptotagmin- Ca^{2+} -phospholipids [311, 317].

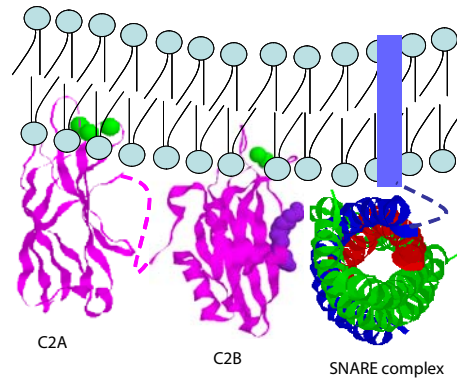


Figure 25. Schematic drawing of the proposed quaternary SNARE-synaptotagmin- Ca^{2+} -phospholipid complex. Ribbon diagram of synaptotagmin C2A and C2B soluble fragments (magenta) connected by an artificial linker (magenta dotted line), whereby binding of Ca^{2+} ions (green spheres) to the C2 domains causes the insertion of the synaptotagmin top loops into the membrane. The figure also shows a front view of the SNARE complex (same colour code as in previous figures) anchored to the vesicular membrane by VAMP2 TMD (blue). Membrane anchoring of the SNARE complex has been proposed to increase the specific affinity of its interaction with synaptotagmin through a polybasic region of C2B domain of synaptotagmin (purple spheres) [317].

Finally, synaptotagmin binding to SNARE complexes has been proposed to displace complexin from the SNARE complex, thereby releasing the clamping action of complexin on vesicles, which may be crucial to trigger membrane fusion [55, 75, 77, 317]. An alternative model proposes that synaptotagmin is recruited to the clamped complexin-SNARE complex by the C-terminal domain of complexin, without displacing complexin from the SNARE complex, and that synaptotagmin and complexin in this manner synergistically function to mediate neurotransmitter release [318]. Either way, a concerted action of complexin and synaptotagmin are necessary to bring about the final steps of membrane fusion.

9.3 LIPIDS

Whilst often neglected in the context of mechanistic aspects of vesicle fusion, it is well known that cell membranes are heterogeneous mosaics of lipids that actively participate in vesicle trafficking, signalling, protein localization and function (reviewed in [319]). For example, both plasma membrane and vesicle membranes are composed of a distinct combination of phospholipids, sphingolipids and sterols. The precise lipid composition is an important factor in the spatial regulation of membrane shape, curvature and fluidity during vesicle fusion. Distinct lipids can also interact with different proteins, regulate specific enzymatic activities and recruit proteins to different sites of exo- and endocytosis. Genetic and biochemical studies have shown that such local lipid environment, and a series of enzymes involved in such lipid metabolism, affect the synaptic vesicle cycle by direct regulation of the SNARE fusion machinery (see for review [320]). For example, Phospholipase A (PLA) produces arachidonic acid and lysophospholipids from phospholipids in membranes. While arachidonic acid diffuses out of the bilayer and seems to induce an up-regulation of secretion by allowing SNARE complex interaction with Munc18 [321], lysophospholipids tend to remain in the membrane and can facilitate membrane hemifusion due to their cone-shaped morphology [322]. Similarly, Phospholipase C (PLC) up-regulates neurosecretion by producing diacylglycerol (DAG), a substrate for DAG lipase which in turn releases arachidonic acid [323]. Other studies indicate that arachidonic acid potentiates SNARE complex formation through syntaxin activation [324, 325]. In this scenario, the flexible unsaturated fatty acid may penetrate into hydrophobic groves between the syntaxin-Munc18 complex to activate the syntaxin1A SNARE core domain, thereby allowing it to assemble into the SNARE complex [326]. Whatever the precise mechanism, it has become clear that arachidonic acid and lysophospholipids play important positive regulatory roles for neurosecretion.

In addition, sphingolipid metabolism enzymes have been shown to affect neurotransmitter release [327, 328]. A recent study indicates that sphingosine, a releasable backbone of sphingolipids, results in an up-regulation of exocytosis [329]. Sphingosine, generated from sphingolipids upon the sequential action of sphingomyelinase and ceramidase, seems to result in VAMP2 activation, possibly

by locally disrupting the electrostatic and hydrophobic interactions of the membrane-proximal region of VAMP2 with the vesicular membrane (Figure 26). Release of the C-terminal region of VAMP2 subsequently allows SNARE complex assembly. In sum, whilst further work will be necessary to dissect the precise mechanism(s) by which lipids regulate membrane fusion, a picture is emerging whereby both proteins and lipids have to work together to bring about this event.

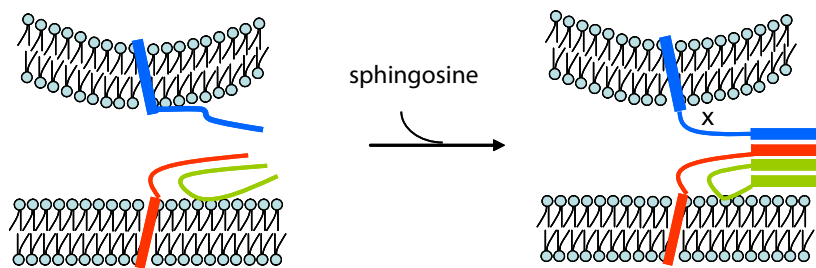


Figure 26. Schematic model for sphingosine-mediated release of the C-terminal region of VAMP2 from vesicular restriction. After VAMP2 release, the ternary SNARE complex is formed which leads to vesicle fusion with the plasma membrane. SNARE proteins (VAMP2, syntaxin1A and SNAP-25) are depicted using the same colour code as in previous figures.

SPECIFIC AIMS

IV. SPECIFIC AIMS:

- 1- Determine the existence of SNARE complex multimers *in vitro*.
- 2- Biochemically and biophysically characterize SNARE complex multimers *in vitro*.
- 3- Identify mutations which disrupt SNARE complex multimers *in vitro*.
- 4- Analyze the effects of disrupting SNARE complex multimers on neurosecretion in a toxin rescue assay system (in the absence of endogenous protein) *in vivo*.
- 5- Analyze the effects of disrupting SNARE complex multimers on neurosecretion in a dominant-negative assay system (in the presence of endogenous protein) *in vivo*.
- 6- Visualize SNARE protein interactions *in vivo* using a bimolecular fluorescence complementation (BiFC) approach.
- 7- Characterize identified interactions using a mutational approach and BiFC.
- 8- Determine the effects of interfering with such interactions on neurosecretion *in vivo*.

RESULTS

**1. A ROLE FOR SOLUBLE N-ETHYLMALEIMIDE-SENSITIVE
FACTOR ATTACHMENT PROTEIN RECEPTOR COMPLEX
DIMERIZATION DURING NEUROSECRETION.**

V. RESULTS:

1. A Role for Soluble N-Ethylmaleimide-sensitive Factor Attachment Protein Receptor Complex Dimerization During Neurosecretion.

Resumen:

Las proteínas SNARE (soluble N-ethylmaleimide-sensitive factor attachment protein receptor) juegan un papel fundamental en el proceso de neurotransmisión mediante la formación de un complejo altamente estable en el que participan una proteína vesicular (VAMP2) y dos proteínas asociadas a la membrana plasmática (SNAP-25 y syntaxin1A). Este proceso está regulado por la entrada local de Ca^{2+} y requiere la acción cooperativa de múltiples complejos de SNARE. Sin embargo, las interacciones moleculares involucradas en dicha cooperatividad aún se desconocen. En el siguiente estudio hemos identificado y caracterizado un dímero de complejos SNARE formado por los dominios citoplasmáticos de las SNAREs neuronales (VAMP2, SNAP-25 y syntaxin1A). La dimerización de los dos complejos da lugar a una estructura abierta de dos alas en la que ambos complejos SNARE se enfrentan por sus extremos carboxilo terminales. Además hemos caracterizado dicha interacción en la que al menos tres aminoácidos de VAMP2 están involucrados. Dichos aminoácidos se localizan en la región próxima a la membrana y sus mutaciones reducen la estabilidad de los dímeros de complejos SNARE *in vitro*, sin afectar la estabilidad del complejo en sí. Dichas mutaciones son incapaces de promover la neurosecreción *in vivo* en la ausencia de proteína endógena, según se observa en un sistema de células neuroendocrinas que han sido previamente tratadas con toxina botulínica. De igual manera, estos mutantes tienen un efecto dominante-negativo de la inhibición de neurosecreción en células intactas. Estos resultados nos indican la importancia de los dímeros de complejos SNARE en el proceso de neurotransmisión.

A Role for Soluble *N*-Ethylmaleimide-sensitive Factor Attachment Protein Receptor Complex Dimerization during Neurosecretion

Elena Fdez,^{*†} Thomas A. Jowitt,^{†‡} Ming-Chuan Wang,[‡] Manisha Rajebhosale,[‡] Keith Foster,[§] Jordi Bella,[‡] Clair Baldock,[‡] Philip G. Woodman,[‡] and Sabine Hilfiker^{*}

^{*}Institute of Parasitology and Biomedicine “López-Neyra,” Consejo Superior de Investigaciones Científicas, 18100 Granada, Spain; [‡]Faculty of Life Sciences, The University of Manchester, Manchester M13 9PT, United Kingdom; and [§]Syntaxin Ltd., Abingdon, Oxon OX14 3YS, United Kingdom

Submitted January 9, 2008; Revised April 30, 2008; Accepted May 21, 2008
Monitoring Editor: Thomas F. J. Martin

The interactions underlying the cooperativity of soluble *N*-ethylmaleimide-sensitive factor attachment protein receptor (SNARE) complexes during neurotransmission are not known. Here, we provide a molecular characterization of a dimer formed between the cytoplasmic portions of neuronal SNARE complexes. Dimerization generates a two-winged structure in which the C termini of cytosolic SNARE complexes are in apposition, and it involves residues from the vesicle-associated SNARE synaptobrevin 2 that lie close to the cytosol–membrane interface within the full-length protein. Mutation of these residues reduces stability of dimers formed between SNARE complexes, without affecting the stability of each individual SNARE complex. These mutations also cause a corresponding decrease in the ability of botulinum toxin-resistant synaptobrevin 2 to rescue regulated exocytosis in toxin-treated neuroendocrine cells. Moreover, such synaptobrevin 2 mutants give rise to a dominant-negative inhibition of exocytosis. These data are consistent with an important role for SNARE complex dimers in neurosecretion.

INTRODUCTION

Neurotransmitter release occurs when synaptic vesicles fuse with the plasma membrane. A crucial step in this process involves the assembly of a soluble *N*-ethylmaleimide-sensitive factor attachment protein receptor (SNARE) complex, a highly stable, parallel four-helix bundle formed between the synaptic vesicle SNARE synaptobrevin 2 (syb2) and the plasma membrane SNAREs syntaxin 1 and synaptosome-associated protein of 25 kDa (SNAP-25) (Söllner *et al.*, 1993; Hanson *et al.*, 1997; Sutton *et al.*, 1998; Südhof, 2004; Jahn and Scheller, 2006; Rizo *et al.*, 2006; Wojcik and Brose, 2007). Current data suggest that SNARE complex formation proceeds in a vectorial manner from the N-terminal, membrane-distal region toward the C-terminal, membrane-proximal end, which may draw the opposing membranes close enough together for fusion to proceed (Fiebig *et al.*, 1999; Pobbati *et al.*, 2006; Sorensen *et al.*, 2006). Consistent with this, in reconstituted assay systems, SNAREs on their own

can support membrane fusion (Weber *et al.*, 1998; Hu *et al.*, 2003; Giraudo *et al.*, 2006; Pobbati *et al.*, 2006).

In intact cells, evoked membrane fusion involves the cooperative action of multiple SNARE complexes (Cull-Candy *et al.*, 1976; Bevan and Wendon, 1984; Stewart *et al.*, 2000). The exact number of complexes required is currently unknown, and estimates vary from three (Hua and Scheller, 2001) to five to eight (Han *et al.*, 2004) to 10–15 (Keller and Neale, 2001; Keller *et al.*, 2004; Montecucco *et al.*, 2005). Such differences may reflect the distinct experimental paradigms used and/or the types of secretory organelles studied. Thus, higher order multimers of SNARE complexes may be required for fast exocytosis of synaptic vesicles, whereas lower order multimers may be sufficient for the slower exocytosis of large dense-core granules from chromaffin and neuroendocrine PC12 cells (Montecucco *et al.*, 2005).

The mechanism(s) responsible for SNARE complex multimerization remains controversial. Initial studies suggested that multimerization of synaptic SNARE complexes could be achieved via domain swapping, whereby one of the two SNAP-25 helices could be substituted by the equivalent helix from a neighboring complex (Kweon *et al.*, 2002). Alternative models proposed the involvement of accessory proteins, such as synaptotagmin (Littleton *et al.*, 2001) or complexin (Tokumaru *et al.*, 2001), or the transmembrane domains of syb2 and syntaxin 1A (Laage *et al.*, 2000), in synaptic SNARE complex multimerization. However, SNARE complexes assembled from recombinant coils and lacking transmembrane domains are able to associate with each other (Fasshauer *et al.*, 1997; Fasshauer *et al.*, 1998; Margittai *et al.*, 2001; Ernst and Brünger, 2003), arguing that at least some of the interactions that support multimerization may require neither

This article was published online ahead of print in *MBC in Press* (<http://www.molbiolcell.org/cgi/doi/10.1091/mbc.E08-01-0010>) on May 28, 2008.

[†] These authors contributed equally to this work.

Address correspondence to: Sabine Hilfiker (sabine.hilfiker@ipb.csic.es).

Abbreviations used: MALLS, multiangle laser light scattering; SAXS, small angle X-ray scattering; SNARE, soluble *N*-ethylmaleimide-sensitive factor attachment protein receptor; syb2, synaptobrevin 2; TEM, transmission electron microscopy.

accessory proteins nor transmembrane domains. The precise multimeric nature and configuration of these recombinant cytosolic SNARE complexes is ambiguous. Conflicting results have been reported, ranging from dimers involving C-terminal residues of at least one of the two monomers, to mixtures of monomers/trimers in solution (Fasshauer *et al.*, 1997, 1998; Margittai *et al.*, 2001; Ernst and Brünger, 2003). In addition, no investigations have addressed whether such interactions between SNARE complexes might contribute to their biological action.

To test whether multimerization of SNARE complexes mediated by their cytosolic domains is an important step during neurotransmitter release, we first performed a detailed characterization of how such multimers are configured. We identified amino acids within synaptobrevin 2 that contribute to a cytosolic SNARE complex dimer formed with micromolar affinity. Functional analysis of synaptobrevin 2 mutants in which these residues are replaced provides evidence for an important role for SNARE complex dimers during exocytosis.

MATERIALS AND METHODS

Plasmids and Protein Purification

Constructs encoding sequences for the “coils” that form the “minimal” SNARE complex of rat syntaxin 1a (191-262), synaptobrevin 2 (syb2) (1-96), SNAP-25 B (1-83), and SNAP-25 B (120-206), constructs encoding full-length nontagged syb2 and green fluorescent protein (GFP)-tagged syb2 and fluorescence resonance energy transfer (FRET) probes were generated using standard polymerase chain reaction (PCR) and cloning procedures (for details see Supplemental Material). Recombinant proteins were expressed as N-terminally tagged glutathione S-transferase (GST) fusion proteins and purified using standard protocols (Söllner *et al.*, 1993; also see Supplemental Material). Protein concentrations were estimated by the Bradford assay, and they ranged from 0.3 to 1 mg/ml. SNARE complexes were formed by overnight assembly of equimolar concentrations of purified components in standard buffer and concentrated to ~2 mg/ml. Complex formation was verified by SDS-polyacrylamide gel electrophoresis (PAGE). Determination of synaptotagmin 1 and complexin binding to SNARE complexes was performed as described in Supplemental Material.

Multangle Laser Light Scattering (MALLS)

SNARE complexes were purified from recombinant coils on a Superdex-200 24/30 gel filtration column (GE Healthcare, Chalfont St. Giles, United Kingdom) run in 5 mM Tris-HCl, pH 7.4, 50 mM NaCl at 0.71 ml/min using a BioLC high-performance liquid chromatography (Dionex, Camberley, United Kingdom). The SNARE complex dimer peak resolved clearly from the mixture. For SNARE complex mutants all molecular weight (MW) analysis refers to that of material within the dimer peak, although some SNARE complex monomer could also be found (data not shown). Protein passed through a Wyatt EOS 18-angle laser photometer (Wyatt Technology, Santa Barbara, CA) with the 13th detector replaced with a QELS detector (Wyatt Technology) for the simultaneous measurement of hydrodynamic radius. This was coupled to an Optilab rEX refractive index detector (Wyatt Technology), and the hydrodynamic radius, molecular weight moments, and concentration of peaks were analyzed using Astra 4.98 (Wyatt Technology).

Analytical Ultracentrifugation

SNARE complex dimers (~8 μ M) were purified by gel filtration. All experiments were performed in 5 mM Tris-HCl, pH 7.4, containing the indicated concentrations of NaCl, and using a XL-A ultracentrifuge (Beckman Coulter, Fullerton, CA) with an An50Ti 8-hole rotor fitted either with the standard two-sector open-filled centerpieces for sedimentation velocity, or with six-sector Epon-filled centerpieces for equilibrium studies, with quartz glass windows. Velocity sedimentation analysis was performed at 40,000 rpm at 20°C, with the sedimenting boundary monitored at 230 nm every 9 min. Frictional ratios for the monomer and dimer were calculated from the sedimentation coefficient. For data interpretation and solution bead modeling, see Supplemental Material.

Equilibrium sedimentation was performed at 4°C, using rotor speeds of 10, 15, and 21,000 rpm and scanning at 230 nm every 4 h until equilibrium was reached. For molecular weight analysis, data were analyzed with the fitting program HeteroAnalysis by using a single ideal model for a distribution of the mean molecular weight. Data were expressed as the average MW from this approximation (MW_{app}) relative to the theoretical MW of the monomer. Association constants were investigated using concentrations of 1, 2.5, and 5

μ M protein at the same three rotor speeds in 5 mM Tris-HCl and 0.3 M NaCl. Global analysis using Sedphat (developed by Peter Schuck, National Institutes of Health, Bethesda, MA) of a monomer-dimer association produced the best fit.

Small Angle X-Ray Scattering Data Collection

Small angle X-ray solution scattering (SAXS) was carried out using gel filtration-purified SNARE complex dimers (8 μ M) on ID02 at the European Synchrotron Radiation Facility (Grenoble, France) by using 1-m and 5-m sample to detector distances. During data collection, the sample was maintained at 10°C. The corresponding profiles were merged so as to cover the momentum transfer interval $0.0038 \text{ \AA}^{-1} < q < 0.53 \text{ \AA}^{-1}$. The modulus of the momentum transfer is defined as $q = 4\pi\sin\theta/\lambda$, where 2θ is the scattering angle, and λ is the wavelength. With a 1-m camera distance the maximum scattering angle corresponds to a Bragg resolution of 11.8 Å. SAXS patterns were recorded using an image intensified charge-coupled device (CCD) detector having single photon sensitivity and 14 bit dynamic range. The wavelength of X-rays used was 0.1 nm. For further details about data collection and analysis, see Supplemental Material.

Transmission Electron Microscopy (TEM) Single Particle Image Analysis

Gel filtration-purified SNARE complex dimers were concentrated threefold (24 μ M), and 5 μ l of sample was allowed to adsorb for 30 s onto a glow discharged (25 mA for 30 s) carbon-coated 400 mesh copper grid. The grid was washed three times with MilliQ water (Millipore, Billerica, MA) and then negatively stained with 2% (wt/vol) uranyl acetate, pH 4.7, for 20 s. Grids were observed using a Tecnai Twin TEM (FEI, Hillsboro, OR) equipped with a LaB₆ filament operating at 120 keV. Images were recorded under low dose conditions at -600-nm defocus on a 2048 × 2048 CCD camera with a pixel size of 2 Å. The level of defocus of each individual image was checked by inspecting the position of the Thon rings in the power spectra and comparing this to the calculated contrast transfer function. For details on image processing, see Supplemental Materials.

Fluorescence Spectroscopy

SNARE complexes (~5 μ M) were purified by gel filtration chromatography, and tryptophan fluorescence was measured in a 100- μ l, 1-cm path-length cell using an FP750 spectrofluorometer (Jasco, Tokyo, Japan) by excitation at 295 nm and monitoring of emission fluorescence between 300 and 450 nm.

CD Spectroscopy

The CD spectra of SNARE complexes (2–5 μ M) purified by gel filtration chromatography were monitored from 260 to 190 nm in 0.2-nm steps (with 10 averages assayed) in a 0.05-cm pathlength cuvette by using a J810 spectropolarimeter (Jasco).

Differential Scanning Calorimetry

The stability of SNARE complexes was investigated using a VP-DSC microcalorimeter (MicroCal, Northampton, MA) with a 0.52-ml total loading volume (also see Supplemental Materials).

FRET Measurements

GFP-tagged SNARE complexes (see Supplemental Materials for details) were purified by gel filtration chromatography (4 μ M), and molecular mass was analyzed by MALLS as described above, with a determined mass of 144 ± 4 kDa, close to the predicted mass of 146 kDa for GFP-tagged SNARE complex dimers. Purified C-C- or N-C-tagged SNARE complex dimers were analyzed using a J750 spectrometer (Jasco) and a 100- μ l, 1-cm pathlength cell. The excitation wavelength was 433 nm, and emission spectra were measured between 450 and 650 nm in 1-nm steps.

Determination of Localization and Expression Levels of syb2 and of SDS-resistant SNARE Complex Stability

The overexpression levels of nontagged syb2 and mutants thereof, the localization of GFP-tagged syb2 and mutants thereof, and the determination of GFP-tagged SDS-resistant SNARE complex stabilities, were determined as described in Supplemental Material.

Secretion Assays

Confluent PC12 cells were plated onto collagen-coated six-well dishes at 80% confluence, and then they were transfected the following day with 3 μ g of DNA by using 10 μ l of Lipofectamine 2000 (Invitrogen, Paisley, United Kingdom). Cells were replated into six-well dishes at a ratio of 1:2 the next day, and secretion assays performed two days after replating, with all test and control conditions carried out on the same pool of transfected cells. Controls were treated with 0.6 ml of physiological saline solution (PSS; 145 mM NaCl, 5.6 mM KCl, 2.2 mM CaCl₂, 0.5 mM MgCl₂, 5.6 mM glucose, and 15 mM HEPES-NaOH, pH 7.4), and evoked neurosecretion was triggered by a 5-min

Table 1. Comparison of experimentally derived and modelled hydrodynamic data for monomeric and dimeric SNARE complexes

| | MW ^a | Experimental hydrodynamic results | | | |
|------------|-----------------|-----------------------------------|------------------|-----------------------------|-----------------------------|
| | | S _{20,w} ⁰ | f/f ₀ | R _H ^b | R _H ^c |
| WT monomer | 44,600 | 3.05 ± 0.148 | 1.49 | 3.23 ± 0.25 | N.D. |
| WT dimer | 89,500 | 4.13 ± 0.135 | 1.75 | 5.02 ± 0.10 | 4.9 |

N.D., not determined.

^a Molecular weight derived from light scattering.

^b Hydrodynamic radius from analytical ultracentrifugation (AUC).

^c Hydrodynamic radius from light scattering.

| | Bead model hydrodynamics | | | | | |
|--------------------------------|--------------------------|------------|------|------|------|------|
| | Monomer | Dimer: 90° | 120° | 130° | 140° | 180° |
| R _H (nm) | 3.22 | 4.63 | 4.82 | 4.91 | 5.10 | 5.20 |
| S _{20,w} ⁰ | 3.26 | 4.58 | 4.40 | 4.32 | 4.16 | 4.08 |

(A) Hydrodynamic information for SNARE complex monomers and dimers was determined experimentally, by using MALLS or AUC as indicated. Predicted molecular weight for a monomeric SNARE complex, including vector-derived amino acids, is 45,768 Da. (B) Solution bead models of the SNARE complex monomer were generated using atomic coordinates of SNARE coiled-coil domains and the solution modelling software SOMO. End-end dimers, in which the monomers were oriented at the indicated angles with respect to each other, were generated using PyMOL (<http://pymol.sourceforge.net/>). Hydrodynamic parameters were generated for the monomer and for all dimer models. Note that the bead model of the SNARE complex monomer generated very similar hydrodynamic values to those observed experimentally, indicating a high level of confidence for the modelling. Comparison with the experimentally determined hydrodynamic parameters shows that the closest fit for the dimer is achieved with an end-to-end dimer oriented at ~130–140°.

incubation with high K⁺ saline solution (PSS containing 95 mM NaCl and 56 mM KCl). The amount of human growth hormone (hGH) in the medium and in cells was determined by an enzyme-linked immunosorbent assay, and the total amount of hGH and the percentage hGH secreted calculated against an hGH standard curve. Statistical analyses were performed with the paired Student's *t* test.

Toxin Rescue Assays

Release of hGH from toxin-treated, permeabilized PC12 cells transfected with botulinum neurotoxin type B (botB)-resistant syb2 (Q76V,F77W) was measured essentially as described previously (Quetglas *et al.*, 2002) in the presence of recombinantly expressed endopeptidase light chain (LC) of botB (botB/LC). BotB/LC was purified as described previously (Sutton *et al.*, 2005), was of high homogeneity as assessed by SDS-PAGE, and it showed endopeptidase activity comparable with native botulinum neurotoxin by using an *in vitro* vesicle-associated membrane protein peptide cleavage assay (Sutton *et al.*, 2005). Determination of the cleavage of endogenous syb2 upon toxin treatment, and of the levels of expressed toxin-insensitive syb2 and syb2 mutants, are described in Supplemental Material.

RESULTS

Global Solution Structure of Synaptic SNARE Complex Multimers

As an essential step toward testing whether multimerization of SNARE complexes facilitated by interactions between their cytosolic domains is important for neurotransmitter release, we first ascertained whether cytosolic portions of SNARE complexes would form multimers of defined stoichiometry and configuration in solution. SNARE complexes encompassing the cytoplasmic coiled coil-forming motifs of syb2, syntaxin 1, and SNAP-25 (Supplemental Figure 1) were purified by size exclusion chromatography to yield a single major peak containing assembled SNAREs (Supplemental Figure 2A; data not shown). When rechromatographed and analyzed by MALLS, they yielded a molecular

weight of 89,500 Da (Supplemental Figure 2B and Table 1A), twice that of a monomeric SNARE complex. Treatment with 1 M NaCl (Antonin *et al.*, 2000) reduced the molecular weight to 44,600 Da (Supplemental Figure 2B). Hence, cytosolic neuronal SNARE complexes are quantitatively incorporated into salt-sensitive dimers.

To explore how this dimer is configured, we first examined its shape in solution. Initially, purified SNARE complexes were subjected to velocity sedimentation in low or high salt. Surprisingly, the sedimentation coefficients of the dimer and monomer were relatively close, whereas the frictional ratio was appreciably different and the hydrodynamic radius of the dimer was much larger than that of the monomer (Figure 1A and Table 1A). These data suggest that the dimer is more elongated than the monomer, and they argue against it forming by extensive alignment of monomers.

The solution shape of the dimer was determined more precisely by using small angle X-ray solution scattering (SAXS). The experimental scattering profiles were modeled using an *ab initio* procedure (Svergun, 1999; Svergun *et al.*, 2001) (Supplemental Figure 3), and the averaged filtered structure resolved as a two-winged particle with each wing ~9.5 nm long and tilted at ~110° relative to each other (Figure 1B). Using transmission electron microscopy to determine the shape directly revealed a similar structure, with each wing 9–10 nm long and set at 140° to each other (Figure 1C).

To confirm that these shapes are consistent with the observed hydrodynamic properties, bead models were generated from the atomic coordinates within SNARE complexes (Sutton *et al.*, 1998) by using the program SOMO (Spotorno *et al.*, 1997), and then they were aligned in hypothetical

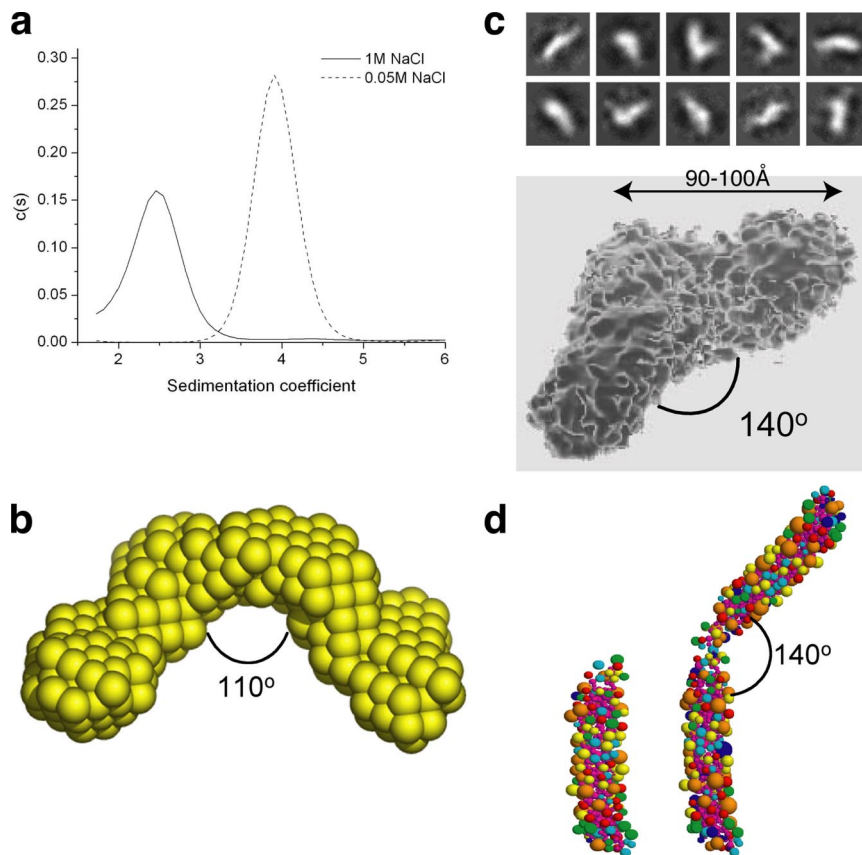


Figure 1. Neuronal SNARE complexes form a wing-shaped, end-to-end dimer. Purified SNARE complex dimers were analyzed by sedimentation in 50 mM (dashed line) or 1 M (solid line) NaCl (a); SAXS, with shapes simulated *ab initio* and the “most probable” shape represented as an array of beads (b); TEM, with the 10 most common shape classes shown above and an average refined structure below (c); and aligning SNARE complex monomer bead models (left) to generate a shape matching the observed hydrodynamic properties (right) (d).

configurations and modeled for their hydrodynamic properties. End-to-end dimers set at an angle of 130–140° generated hydrodynamic properties close to those observed experimentally (Figure 1D and Table 1B). Thus, three methods of shape analysis suggest that cytosolic SNARE complexes form uniformly configured dimers, in which the dimerization interface lies close to one end of each SNARE complex and generates an open, two-winged structure.

Orientation of the SNARE Complex Dimer

Fusion of primed vesicles requires conversion of partially assembled *trans*-SNARE complexes into fully assembled, fusion-competent SNARE bundles (Fiebig *et al.*, 1999; Pobabi *et al.*, 2006; Sorensen *et al.*, 2006). Therefore, a functionally relevant dimer should involve C-terminal SNARE complex regions that lie close to the point of membrane insertion. To address whether the C termini of SNARE complexes are close to each other within a dimer, we measured FRET in SNARE complexes assembled using a mixture of syb2-cyan fluorescent protein (CFP) and syb2-Venus, providing complexes containing either FRET donor or FRET acceptor at the C terminus (Figure 2A). For comparison, SNARE complexes were assembled using syb2-Venus and CFP-syb2. All complexes formed with similar efficiency, and they were equally stable, compared with those containing wild-type (wt) syb2 (data not shown; Supplemental Figure 4). However, only when both FRET partners were located at the C termini of syb2 molecules was a significant FRET signal observed that was sensitive to disruption of the dimer by high salt (Figure 2, B and C). Hence, the C termini of both individual, soluble SNARE complex monomers are adjacent to each other in the dimer. This would suggest that dimers

could form *in vivo* only when SNARE complex assembly is virtually complete.

Residues Involved in Forming the Dimer Interface

To test the functional significance of this dimer, we first identified amino acids that contribute to dimerization. We focused initially on neighboring tryptophan residues (W89 and W90) within syb2 that are adjacent to the cytosol-membrane interface and hence likely to be close to the point of dimerization (Figure 3A). Because these are the only tryptophans within the cytosolic SNARE complex, any changes in intrinsic tryptophan fluorescence upon conversion of dimers to monomers would indicate that these residues form part of the dimer interface. Indeed, the tryptophan fluorescence decreased with increasing [NaCl] (Figure 3B), closely matching the monomerization of SNARE complex dimers determined independently by equilibrium sedimentation (Figure 3C). The peak fluorescence emission wavelength remained unchanged (~355 nm) at all [NaCl] (Figure 3B, inset), suggesting that the tryptophan residues in both SNARE complex dimers and monomers occupy hydrophilic environments. Thus, the fluorescence decrease upon monomerization most likely results from release of rotational constraints imposed upon at least one tryptophan residue within the dimer and suggests that one or both tryptophans participate in dimerization.

Mutational analysis provided direct evidence for this. Equilibrium sedimentation of SNARE complex dimers containing syb2(W89A,W90A) showed that they were more sensitive to increasing [NaCl] than wild-type dimers (Figure 3C and Table 2A). Analysis of single mutants revealed that dimers containing syb2(W89A) displayed NaCl sensitivity

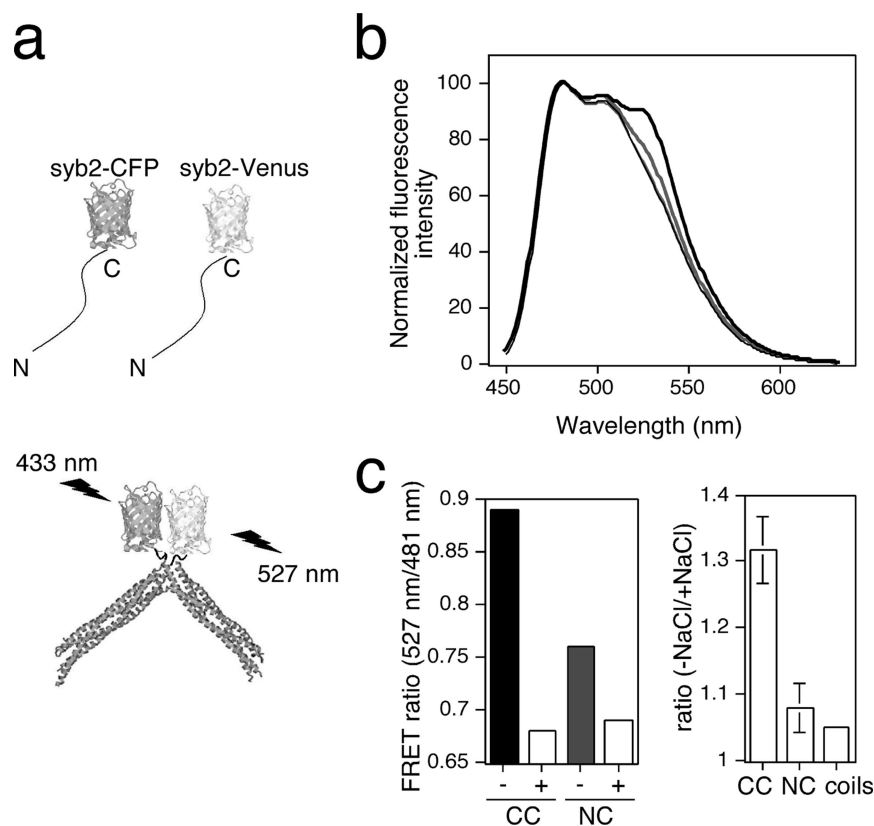


Figure 2. The C termini of both SNARE complex monomers are adjacent to each other in the dimer. (a) Schematic diagram of C-terminally tagged FRET syb2 proteins, uncomplexed or incorporated into SNARE complex dimers. (b) Emission spectra of purified dimers tagged at the C terminus with Venus as FRET acceptor, and either at the C terminus (black) or N terminus (gray) with CFP as FRET donor. Spectra are shown in the absence (thick lines) or presence (thin lines) of 1 M NaCl, and were normalized to their values at 481 nm (CFP emission peak). (c) Left, FRET ratios (emission ratio 527/481 nm) from experiments depicted in b, where – and + refer to the absence or presence of 1 M NaCl, respectively. Right, ratio of FRET ratios (–NaCl/+NaCl) obtained with SNARE complex dimers tagged at both C termini (CC) or at the C terminus and N terminus (NC), or obtained with tagged syb2 proteins only (coils). Values are mean \pm SEM (n = 5).

similar to those containing syb2(W89A,W90A), whereas those containing syb2(W90A) were slightly more stable than wild type (Figure 4A). Hence, W89 makes the greater contribution to dimer stability. However, both tryptophans seem to lie at the dimer interface, as the tryptophan fluorescence from W90 in SNARE complex dimers formed using syb2(W89A) decreased in intensity at NaCl concentrations that caused dimer disassembly (Figure 4B). This would indicate that it is W90 that is subject to rotational constraints within the dimer.

We reasoned that residues close to W89-W90 may also contribute to the dimer interface. To this end, we tested effects of mutating the conserved residue R86 within syb2 on dimer stability. Indeed, dimers formed using syb2(R86A), and syb2(R86A,W89A,W90A) were substantially more sensitive to increased [NaCl] (Figure 3C and Table 2A). To compare affinities using sedimentation analysis, SNARE complexes were analyzed after dilution in 0.3 M NaCl, a salt concentration at which wild-type and mutant SNARE complexes are all at equilibrium between monomers and dimers (Figure 3C). The association constant for each SNARE dimer species was obtained by global analysis of concentration-dependent dimerization at equilibrium (Supplemental Figure 5). The association constant was 5.43 μ M for wild-type SNARE complex dimers, compared with 11.97 and 46.23 μ M for those containing syb2(W89A,W90A) and syb2(R86A,W89A,W90A), respectively. Analysis of sedimentation experiments performed using wild-type SNARE dimers at varying salt concentrations confirmed that the association constant was linear with respect to [NaCl] (data not shown), yielding an estimated association constant of 1.23 μ M at 150 mM NaCl, close to physiological ionic strength.

The mutations that we have identified substantially reduce the affinity of SNARE complex dimerization. Importantly,

however, they do not affect the stability of each SNARE complex monomer significantly. These formed with identical helicity to wild-type SNARE complexes, assessed by the CD spectroscopy peak at 220 nm (Figure 3D). Differential scanning calorimetry was used to provide a precise estimate of the energy associated with SNARE complex formation and showed that the very high stability of the SNARE complex coiled-coil helix was essentially unaffected by the syb2 dimerization mutations; the melting temperature for all SNARE complexes was very similar and the change in enthalpy associated with this transition was not altered significantly (Figure 3E and Table 2B). Incorporation of syb2(R86A) displayed a slight effect on the stability of individual SNARE complexes (Figure 3E), but importantly, this was not observed when syb2(R86A,W89A,W90A) was used. In summary, our data indicate that three residues of syb2 (R86, W89, and W90) form part of the interaction interface of an open, wing-shaped SNARE complex dimer as observed in solution. In addition, because the two tryptophan residues are fully solvent exposed, the salt sensitivity of the dimer is likely due to salt-dependent changes in its structure, including disruption of salt bridge(s) involving R86.

Syb2 Dimerization Mutants Are Unable to Support Secretion

We next aimed to determine whether residues in syb2 found at the SNARE complex dimer interface *in vitro* may be important for supporting neurosecretion *in vivo*. For this purpose, we transfected neuroendocrine PC12 cells with a plasmid containing both syb2 and hGH (Sugita *et al.*, 1999). Cells were then permeabilized and treated with recombinant botulinum neurotoxin type B light-chain (botB/LC) (Sutton *et al.*, 2005), which cleaves and inactivates syb2 (Figure 5A).

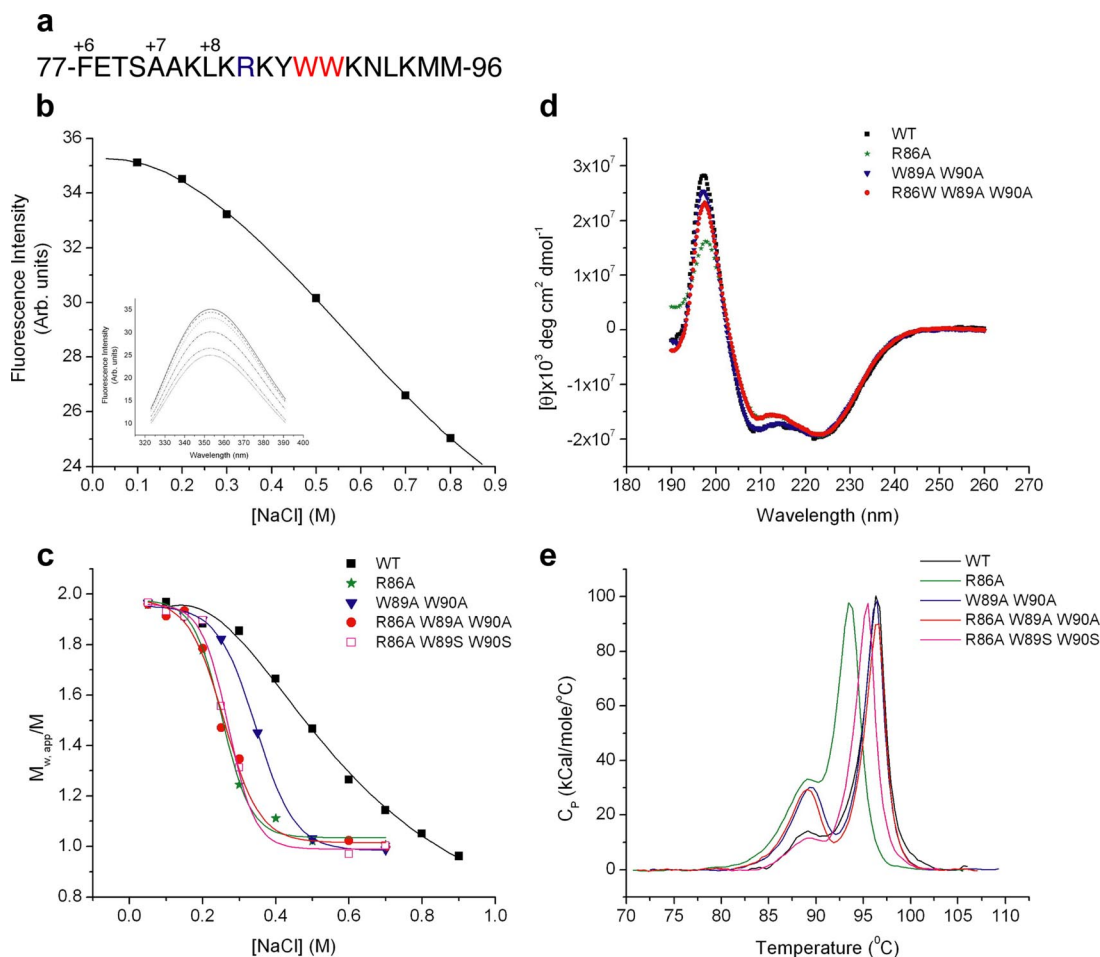


Figure 3. Three residues from syb2 form part of the dimer interface. (a) Sequence of membrane-proximal region of syb2, with amino acids important for SNARE complex dimer stability colored and the position of hydrophobic SNARE motif layers indicated above. (b) Peak intrinsic fluorescence of SNARE complex dimers at increasing [NaCl] (data not shown). Fluorescence intensity of free tryptophan remains unchanged with increasing [NaCl] (data not shown). (c) Dimers containing wild-type (black); W89A,W90A (blue); R86A,W89A,W90A (red); and R86A,W89S,W90S (magenta) syb2 were measured for their sensitivity to [NaCl] by using sedimentation equilibrium. (d) α -Helical content using CD spectroscopy (R86A,W89S,W90S mutant not determined). (e) SNARE complex melting temperature using differential scanning calorimetry.

As expected, Ca²⁺-dependent secretion of hGH was decreased (to 32% of control) by the presence of botB/LC in cells transfected with a plasmid containing wild-type syb2 (Figure 5B). Such profound, but incomplete inhibition of release has been described previously (Chilcote *et al.*, 1995; Quetglas *et al.*, 2002). The expression of botB/LC-resistant syb2(Q76V,F77W) restored secretion (104% of control) in the presence of toxin (Figure 5B). This rescue assay allowed us to measure the ability of syb2 dimerization mutants to support exocytosis in the absence of endogenous protein. Toxin-insensitive wild-type and mutant syb2 were all expressed to similar degrees (Figure 5C). However, toxin-insensitive syb2(W89A,W90A) was severely impaired in its ability to rescue secretion (17.5% of control) (Figure 5D), similar to what has been described previously (Quetglas *et al.*, 2002). Using this assay system, no further additive effects could be observed using syb2(R86A,W89A,W90A), which was equally deficient in supporting release. Interestingly, syb2(W90A) displayed a slight deficit in its ability to rescue secretion, with syb2(W89A) displaying more pronounced effects (Figure 5D). Hence, the ability of syb2 mutants to support release *in vivo* reflects the contribution of each

corresponding amino acid to the SNARE complex dimer interface. Previous studies have implicated W90 in calmodulin-dependent regulation of exocytosis (Quetglas *et al.*, 2000, 2002). However, because W90A would disrupt the calmodulin binding motif within syb2 (Rhoads and Friedberg, 1997; Chin and Means, 2000), the ability of this mutant to largely support secretion would suggest that such an interaction does not play a major role *in vivo*.

Dominant-Negative Secretory Effects of Syb2 Dimerization Mutants

To further test the importance of SNARE complex dimers during regulated exocytosis, we used a dominant-negative approach. Because PC12 cells display Ca²⁺-evoked secretion that requires cooperativity between three or more SNARE complexes (Hua and Scheller, 2001), expression of full-length syb2 mutants that are incorporated into SNARE complexes of normal stability but impaired in dimer formation should generate a dominant-negative phenotype, revealing a potential role for SNARE complex dimerization in membrane fusion.

Table 2. Syb2 mutants reduce stability of SNARE complex dimers but not monomers

| Syb2 in complex | Molecular wt (Da) | | | |
|-----------------|---------------------------------------|--|-------------------------------------|---------------------------|
| | MALLS (errors from polydispersity) | Sedimentation equilibrium (SD, n = 3) | Hydrodynamic radius (nm) (MALLS) | NaCl conc. 50% monomer |
| WT | 91,630 ± 916 | 82,546 ± 314 | 5.1 ± 0.2 | 0.52 ± 0.017 |
| W89AW90A | 92,120 ± 644 | 84,289 ± 991 | 4.8 ± 0.3 | 0.37 ± 0.008 |
| R86A-W89AW90A | 89,910 ± 225 | 84,554 ± 1978 | 4.8 ± 0.3 | 0.26 ± 0.016 |
| R86A-W89SW90S | 88,900 ± 800 | 85,167 ± 1207 | 4.9 ± 0.2 | 0.27 ± 0.01 |

| Syb2 in complex | T _m (°C) | ΔH (kCal mol ⁻¹) | ΔH _{VH} (kCal mol ⁻¹) |
|-----------------|---------------------|------------------------------|--|
| WT | 96.20 ± 0.04 | 286 ± 7.4 | 340 ± 10.9 |
| W89AW90A | 96.15 ± 0.02 | 276 ± 4.0 | 369 ± 7.9 |
| R86A-W89AW90A | 96.22 ± 0.02 | 265 ± 4.0 | 355 ± 7.1 |
| R86A-W89SW90S | 95.17 ± 0.03 | 286 ± 6.8 | 346 ± 10.0 |

(A) Dimer stability: wild-type and syb2 mutant SNARE complexes were purified by size exclusion and analyzed by MALLS or analytical ultracentrifugation. [NaCl] at which SNARE complexes are 50% monomeric is taken from Figure 4c. (B) Monomer stability: SNARE complexes were subjected to differential scanning calorimetry to obtain melting point temperatures (Figure 3e). ΔH is based on integration of the melting point transition, whereas ΔH_{VH} is based on peak width and is independent of protein concentration.

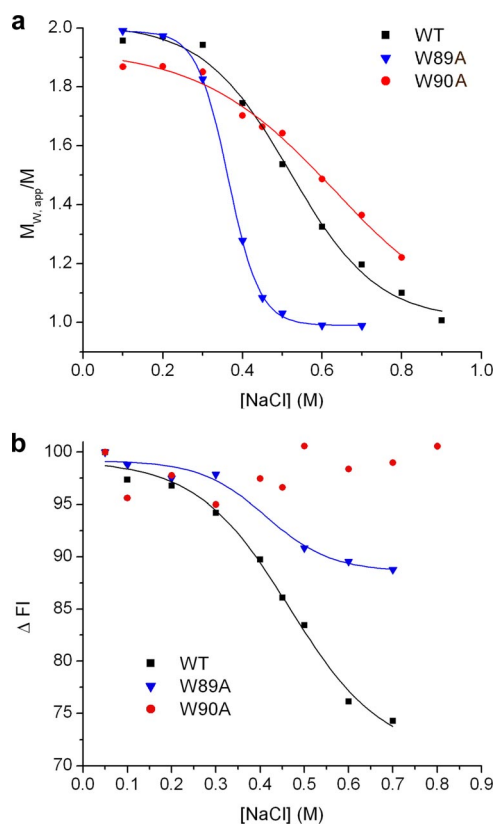
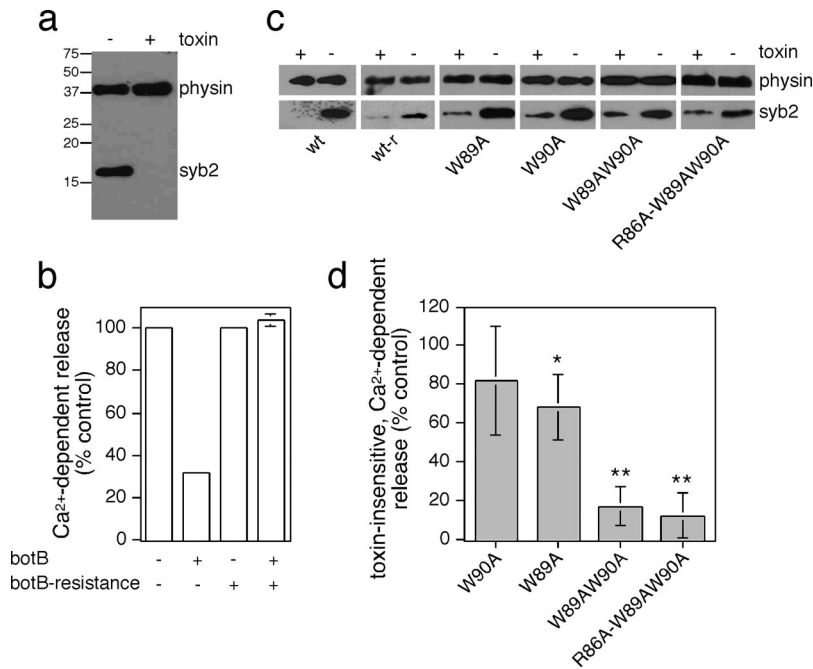


Figure 4. Relative contribution of individual tryptophan residues within syb2 to dimer interface. (a) Dimers containing wild-type (black), W89A (blue), and W90A (red) syb2 were measured for their sensitivity to [NaCl] by using sedimentation equilibrium. (b) Peak intrinsic fluorescence of SNARE complex dimers containing wild-type (black), W89A (blue), and W90A (red) syb2 at increasing [NaCl]. Fluorescence intensity is expressed relative to the emission maximum of each protein complex in 50 mM NaCl.

PC12 cells were transfected with syb2 and hGH as described above, and intact cells were assayed directly to measure constitutive and evoked exocytosis. Exogenous syb2 was expressed at ~2–3 times over endogenous levels, and all mutants analyzed were expressed to similar degrees (Figure 6A). Expression of wild-type syb2 did not affect basal or evoked secretion of hGH (data not shown). In contrast, expression of syb2 dimerization mutants reduced evoked secretion without affecting basal secretion or levels of hGH expression (Figure 6B). This inhibition was reproducible, statistically significant, and greatest for syb2(R86A,W89A,W90A), in line with the more pronounced effect of this mutant on SNARE complex dimer stability (Figure 6C). All syb2 constructs analyzed in this study localized to neuritic appendages and were efficiently incorporated with endogenous SNARE proteins into SNARE complex monomers of essentially the same stability, assessed by heating in SDS (Figure 6, E–H, and Supplemental Figures 6 and 7).

Complexins and synaptotagmin 1 bind to SNARE complexes with distinct outcomes for membrane fusion reactions (Tang *et al.*, 2006). Because such interactions may be mutually exclusive with SNARE complex dimerization, we formed SNARE complexes in the presence of complexin 1 or synaptotagmin 1, respectively, and we measured the extent of dimer formation by size exclusion chromatography. SNARE complex dimerization was not prevented by an excess of complexin 1, which coeluted with SNARE complex dimers (Supplemental Figure 8, A and B). Binding was essentially stoichiometric, as judged by the substantial change in apparent molecular weight of dimeric SNARE complexes in the presence of complexin 1. Complexin 1 bound to wild-type and syb2(R86A,W89A,W90A)-containing SNARE complexes with similar efficiency, consistent with complexin binding to a site within the SNARE complex distinct from the dimerization interface. In contrast, the C2AB domain of synaptotagmin 1 could not be detected to bind to SNARE complexes in solution (Supplemental Figure 8C). Whereas it remains formally possible that the lack of



100%, and the relative lack of rescue of secretion of test plasmids in the presence of toxin normalized to this control. Values are means \pm SEM ($n = 3-5$). The statistical significance of differences from wild-type were analyzed by a Student's *t* test (* $p < 0.05$; ** $p < 0.01$).

synaptotagmin 1 binding is a consequence of SNARE complex dimerization, this is unlikely, because no synaptotagmin 1 binding could be detected, even on overexposed blots, in fractions migrating slightly behind the SNARE complex dimer peak and containing a minor population of SNARE complex monomers (data not shown). Such lack of comigration of soluble synaptotagmin 1 with SNARE complexes during size-exclusion chromatography has been previously observed (Bowen *et al.*, 2005), indicative of a low-affinity interaction in solution. In either case, various structural and mutational data (Chen *et al.*, 2002; Rickman *et al.*, 2006; Lynch *et al.*, 2007) further indicate that residues distinct from those involved in dimerization seem to be responsible for complexin and synaptotagmin binding to SNARE complexes.

W89 and W90 of syb2 have been implicated in binding to phospholipids (Quetglas *et al.*, 2000, 2002; de Haro *et al.*, 2004). In fact, it has been suggested that the reversible insertion of these residues of syb2 into the synaptic vesicle membrane may decrease the availability of syb2 and hence the probability of SNARE complex formation (Hu *et al.*, 2002; Kweon *et al.*, 2003). We therefore also examined SNARE complex dimers formed using a syb2 mutant in which the tryptophans were replaced with hydrophilic serine residues known to support rapid SNARE complex formation (Kweon *et al.*, 2003). Expression of syb2(R86A,W89S,W90S) inhibited evoked secretion to approximately the same level as syb2(R86A,W89A,W90A) (Figure 6C). The stability of dimers formed using this mutant was virtually identical to that formed using syb2(R86A,W89A,W90A) (Figure 3C), and the stability of monomers was essentially the same as wild-type (Figure 3, D and E and Table 2B). Analogous to results obtained using the toxin rescue assay, syb2(W89A) displayed a dominant-negative effect on secretion, whereas syb2(W90A) was without effect (Figure 6D). Hence, the inhibitory effects of the mutants analyzed here are likely not due to interfering with calmodulin and/or phospholipid binding of syb2, as suggested previously (Quetglas *et al.*, 2000, 2002; de Haro *et al.*,

2004), but they are consistent with a mechanism involving impaired SNARE complex multimerization.

Figure 5. Toxin-insensitive, mutant syb2 is unable to rescue secretion from PC12 cells. (a) PC12 cells were permeabilized with 10 μ M digitonin and incubated in the presence or absence of botB/LC, followed by detection of intact syb2 coil by Western blotting. Blots were reprobated for synaptophysin (physin) to determine equal amounts of protein loading. (b) PC12 cells, transfected with a plasmid encoding for hGH as well as wild-type or botulinum toxin-resistant syb2 (Q76V,F77W) were permeabilized with 10 μ M digitonin and incubated in the presence or absence of botB/LC. Ca²⁺-dependent hGH release was evoked by 10 μ M Ca²⁺ for 10 min and compared with basal release (0 μ M Ca²⁺). The amount of hGH in the medium and in the cells was determined by an enzyme-linked immunosorbent assay, and the percentage of secreted hGH, and the total amount of hGH, were calculated against an hGH standard curve. The graph is a representative of two independent experiments with duplicate data points. Error bars are only shown if larger than bar columns. (c) Cells were transfected with wild-type or toxin-resistant wild-type syb2 (wt-r), or toxin-resistant mutant syb2 (Q76V,F77W) were permeabilized with 10 μ M digitonin and incubated in the presence or absence of botB/LC. Ca²⁺-dependent hGH release was evoked by 10 μ M Ca²⁺ for 10 min and compared with basal release (0 μ M Ca²⁺). The amount of hGH in the medium and in the cells was determined by an enzyme-linked immunosorbent assay, and the percentage of secreted hGH, and the total amount of hGH, were calculated against an hGH standard curve. The graph is a representative of two independent experiments with duplicate data points. Error bars are only shown if larger than bar columns. (d) To standardize results from repeated experiments, secretion observed in the presence of toxin-insensitive, wild-type syb2 was set to

2004), but they are consistent with a mechanism involving impaired SNARE complex multimerization.

DISCUSSION

A better understanding of the mechanistic aspects of vesicle exocytosis depends on a quantitative characterization of the elements driving this process. Functional studies have clearly indicated that multiple SNARE complexes cooperate to bring about an individual vesicular fusion event (Hua and Scheller, 2001; Keller and Neale, 2001; Han *et al.*, 2004; Keller *et al.*, 2004; Montecucco *et al.*, 2005), with the number of participating complexes possibly affecting the speed of opening, or the diameter of the fusion pore (Han *et al.*, 2004). Although oligomerization may be an inherent feature of SNARE complexes, a detailed description of how such interactions take place and their relevance for membrane fusion has been lacking. In this study, we describe and characterize a defined SNARE complex dimer that forms with micromolar affinity in solution *in vitro*, and provide evidence for its role in neurosecretion *in vivo*.

The soluble part of SNARE complexes was found to form dimers with the C termini of both monomers interacting at an obtuse angle. This novel and surprising structure is quite distinct from all lattice interactions between neuronal SNARE complex monomers displayed in the crystal structure (Sutton *et al.*, 1998) (PDB entry 1SFC). Although one such crystallographic dimer is formed toward the C termini of both SNARE complex monomers, with W89 of syb2 part of the interaction interface (Supplemental Figure 9), the alignment of monomers along their entire length make this "closed" crystal form distinct from the open, wing-shaped structure of dimers as identified in solution. Hydrodynamic bead modeling of this crystallographic dimer confirms that its hydrodynamic properties are very different from those observed experimentally. In addition, our biochemical and biophysical data strongly indicate the existence of a homogeneous population of dimers. Thus, interactions favored in

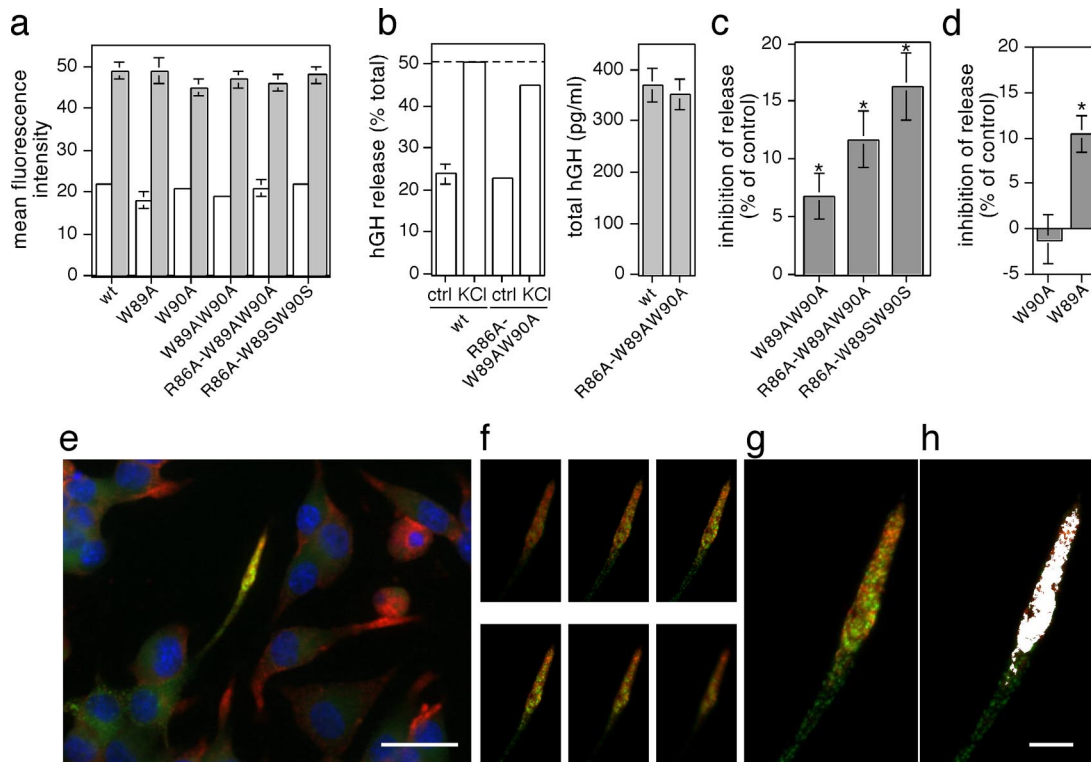


Figure 6. Syb2 mutants display dominant-negative secretory effects. (a) Expression of syb2, or syb2 mutants analyzed, relative to endogenous levels. (b) Example of hGH secretion experiment in cells transfected with wild-type or R86A-W89AW90A mutant syb2. Cells were stimulated for 5 min with physiological saline (ctrl) or high K^+ (KCl). The amount of hGH in the medium and in the cells was determined by an enzyme-linked immunosorbent assay, and the percentage of secreted hGH (left) and the total amount of hGH (right) were calculated against an hGH standard curve. Error bars are only depicted when larger than column lines. (c) To standardize results from repeated experiments, secretion observed in the presence of wild-type syb2 was set to 100%, and the relative inhibition of secretion of test plasmids normalized to control. Values are means \pm SEM ($n = 5-8$; $*p < 0.01$). (d) Secretory effects observed with the indicated individual syb2 mutants. Analysis was done as described above. Values are means \pm SEM ($n = 4$; $*p < 0.01$). (e) GFP-tagged, R86A-W89SW90S mutant syb2 is properly localized to neuritic appendages, as revealed by double staining with synaptotagmin (red). Bar, 20 μm . (f) Individual image acquisition (0.35- μm z-step sizes) of the appendage depicted in e. Maximum intensity projection of individual image stacks (g) and pseudocolored colocalization (white) (h). Bar, 5 μm .

crystal lattices may not be observed in other contexts (Vestergaard *et al.*, 2005).

Although dimerization between cytosolic domains is likely to play an important role in the multimerization of SNARE complexes, the overall oligomeric status and shape of SNARE complexes *in vivo* may be further influenced by the juxtaposition of the membrane, the presence of the transmembrane domains, and accessory factors. Indeed, previous studies have shown that native SNARE complexes purified from brain, or SNARE complexes assembled from recombinant full-length SNAREs containing transmembrane domains, assemble into star-shaped particles mostly containing three or four bundles emanating from their center (Rickman *et al.*, 2005). Such structure may be obtained when two dimers associate with each other through their transmembrane domains (Hohl *et al.*, 1998; Laage *et al.*, 2000; Bowen *et al.*, 2002; Roy *et al.*, 2004). Unfortunately, when only one of the two SNAREs carried a transmembrane domain, reassembly experiments led to the generation of large irregular aggregates (Rickman *et al.*, 2005). This makes it difficult to determine the exact contributions of the transmembrane domains and/or membrane-proximal regions of syb2 to the formation of oligomeric structures obtained with full-length SNAREs. Similarly, the need for detergent solubilization precludes analysis of whether identified SNARE complex multimers are present in their *trans*- or *cis*-forms,

and additional evidence for the existence and importance of SNARE complex oligomers may be best obtained using *in vivo* approaches.

Earlier studies using syb2(W89A,W90A) had suggested that these residues mediate the binding of syb2 to calmodulin (Quetglas *et al.*, 2002; de Haro *et al.*, 2004). However, no single mutational analysis was performed to corroborate these results. The consensus motif for Ca^{2+} -dependent calmodulin binding involves select hydrophobic residues at positions 1-5-8-14, and an overall net electrostatic charge of +2 to +6 (Rhoads and Friedberg, 1997). As such, W90 is at position 14 of this motif, and a mutation to alanine at this position would not be tolerated (Rhoads and Friedberg, 1997). We find that syb2(W90A) has no effect on secretion either in the presence or absence of endogenous syb2. Similarly, the overall net charge of the calmodulin binding motif within syb2 is +3, and the secretory effect of another mutant (syb2(K83A,K87V)) was suggested to be due to eliminating those charge requirements (Quetglas *et al.*, 2002). However, because K83 is part of the SNARE motif, the effects of this mutant may have been due to altered SNARE complex stability, which was not assessed in sufficient detail. Finally, mutating W89 and W90 to hydrophilic serines does not enhance secretion, as would be expected if the availability of syb2 would be restricted due to its interacting with the hydrophobic part of the phospholipid bilayer (Kweon *et al.*,

2003). Our analysis shows that the ability of *syb2* mutants to reduce SNARE complex dimer stability *in vitro* parallels their inhibition of secretion *in vivo*. Thus, although we cannot fully exclude compound effects, our data indicate that the secretory effects observed with the *syb2* mutants are most likely due to interfering with SNARE complex dimer stability *in vivo*.

The dimerization of neuronal SNARE complexes may generate an important intermediate during evoked secretion. This intermediate may be transient *in vivo*, formed after *trans*-SNARE complex assembly and close to the point of fusion. Although detailed electrophysiological experiments will be needed to determine the precise role of SNARE complex dimers in membrane fusion events, one can speculate from their solution structure how they might contribute toward formation of an oligomeric complex around a fusion pore, consistent with the energies required to bring about membrane fusion (Li *et al.*, 2007). It is interesting to note that the *syb2*(W89A,W90A) mutant does not seem to be defective in mediating liposomal fusion events (Siddiqui *et al.*, 2007), whereas it profoundly inhibits Ca²⁺-dependent secretion. Thus, secretory defects using the *syb2* dimerization mutants only seem to be evident in cell systems requiring cooperativity between SNARE complexes. Such SNARE complex dimerization may improve the efficiency of vesicle exocytosis by contributing to the cooperative relationship between calcium and synaptic transmission.

ACKNOWLEDGMENTS

We thank J. Zimmerberg, R. Fernandez-Chacón, and D. Thornton for critical comments. We thank S. High (University of Manchester) for the full-length *syb2* construct, G. Schiavo (Cancer Research UK) for the SNAP-25 construct, M. Carrington (University of Cambridge) for the Venus construct, H. McMahon (University of Cambridge) for the complexin constructs, A. F. Parlow (National Hormone and Pituitary Program, NIDDK) for the anti-hGH antibody, and the European Synchrotron Radiation Facility (ESRF) and T. Narayanan (ESRF) for assistance with SAXS measurements. This work was supported by the UK Medical Research Council grants G9722026 and G9901377 and Spanish Ministerio de Educación y Ciencia (MEC) grants BFU2004-02969 and BFU2007-63635. The laboratory of S. H. is member of the Network for Cooperative Research on Membrane Transport Proteins, cofunded by the MEC and the European Regional Development Fund BFU2007-30688-E/BFI). S. H. is supported by a Ramón y Cajal Fellowship. E. F. is supported by a fellowship (FPI) from the Spanish MEC.

REFERENCES

Antonin, W., Holroyd, C., Fasshauer, D., Pabst, S., Fischer von Mollard, G., and Jahn, R. (2000). A SNARE complex mediating fusion of late endosomes defines conserved properties of SNARE structure and function. *EMBO J.* *19*, 6453–6464.

Bevan, S., and Wendon, L. M. (1984). A study of the action of tetanus toxin at rat soleus neuromuscular junctions. *J. Physiol.* *348*, 1–17.

Bowen, M. E., Engelman, D. M., and Brunger, A. T. (2002). Mutational analysis of synaptobrevin transmembrane domain oligomerization. *Biochemistry* *41*, 15861–15866.

Bowen, M. E., Weninger, K., Ernst, J., Chu, S., and Brunger, A. T. (2005). Single-molecule studies of synaptotagmin and complexin binding to the SNARE complex. *Biophys. J.* *89*, 690–702.

Chen, X., Tomchick, D. R., Kovrigin, E., Arac, D., Machius, M., Südhof, T. C., and Rizo, J. (2002). Three-dimensional structure of the complexin/SNARE complex. *Neuron* *33*, 397–409.

Chilcote, T. J., Galli, T., Mundigl, O., Edelman, L., McPherson, P. S., Takei, K., and De Camilli, P. (1995). Cellubrevin and synaptobrevins: similar subcellular localization and biochemical properties in PC12 cells. *J. Cell Biol.* *129*, 219–231.

Chin, D., and Means, A. R. (2000). Calmodulin: a prototypical calcium sensor. *Trends Cell Biol.* *10*, 322.

Cull-Candy, S. G., Lundh, H., and Thesleff, S. (1976). Effects of botulinum toxin on neuromuscular transmission in the rat. *J. Physiol.* *260*, 177–203.

de Haro, L., Ferracci, G., Opi, S., Iborra, C., Quetglas, S., Miquelís, R., Leveque, C., and Seagar, M. (2004). Ca²⁺/calmodulin transfers the membrane-proximal lipid-binding domain of the v-SNARE synaptobrevin from *cis* to *trans* bilayers. *Proc. Natl. Acad. Sci. USA* *101*, 1578–1583.

Ernst, J. A., and Brünger, A. T. (2003). High resolution structure, stability, and synaptotagmin binding of a truncated neuronal SNARE complex. *J. Biol. Chem.* *278*, 8630–8636.

Fasshauer, D., Eliason, W. K., Brünger, A. T., and Jahn, R. (1998). Identification of a minimal core of the synaptic SNARE complex sufficient for reversible assembly and disassembly. *Biochemistry* *37*, 10354–10362.

Fasshauer, D., Otto, H., Eliason, W. K., Jahn, R., and Brünger, A. T. (1997). Structural changes are associated with soluble N-ethylmaleimide-sensitive fusion protein attachment protein receptor complex formation. *J. Biol. Chem.* *272*, 28036–28041.

Fiebig, K. M., Rice, L. M., Pollock, E., and Brünger, A. T. (1999). Folding intermediates of SNARE complex assembly. *Nat. Struct. Biol.* *6*, 117–123.

Giraud, C. G., Eng, W. S., Melia, T. J., and Rothman, J. E. (2006). A clamping mechanism involved in SNARE-dependent exocytosis. *Science* *313*, 676–680.

Han, X., Wang, C. T., Bai, J., Chapman, E. R., and Jackson, M. B. (2004). Transmembrane segments of syntaxin line the fusion pore of Ca²⁺-triggered exocytosis. *Science* *304*, 289–292.

Hanson, P. I., Roth, R., Morisaki, R., Jahn, R., and Heuser, J. E. (1997). Structure and conformational changes in NSF and its membrane receptor complexes visualized by quick-freeze/deep-etch electron microscopy. *Cell* *90*, 523–536.

Hohl, T. M., Parlati, F., Wimmer, C., Rothman, J. E., Söllner, T. H., and Engelhardt, H. (1998). Arrangement of subunits in 20S particles consisting of NSF, SNAPs, and SNARE complexes. *Mol. Cell* *2*, 539–548.

Hu, C., Ahmed, M., Melia, T. J., Söllner, T., Mayer, T., and Rothman, J. E. (2003). Fusion of cells by flipped SNAREs. *Science* *300*, 1745–1749.

Hu, K., Carroll, J., Fedorovich, S., Rickman, C., Sukhodub, A., and Davletov, B. (2002). Vesicular restriction of synaptobrevin suggests a role for calcium in membrane fusion. *Nature* *415*, 646–650.

Hua, Y., and Scheller, R. H. (2001). Three SNARE complexes cooperate to mediate membrane fusion. *Proc. Natl. Acad. Sci. USA* *98*, 8065–8070.

Jahn, R., and Scheller, R. H. (2006). SNAREs—engines for membrane fusion. *Nat. Rev. Mol. Cell Biol.* *7*, 631–643.

Keller, J. E., Cai, F., and Neale, E. A. (2004). Uptake of botulinum neurotoxin into cultured neurons. *Biochemistry* *43*, 526–532.

Keller, J. E., and Neale, E. A. (2001). The role of the synaptic protein SNAP-25 in the potency of botulinum neurotoxin type A. *J. Biol. Chem.* *276*, 13476–13482.

Kweon, D. H., Chen, Y., Zhang, F., Poirier, M., Kim, C. S., and Shin, Y. K. (2002). Probing domain swapping for the neuronal SNARE complex with electron paramagnetic resonance. *Biochemistry* *41*, 5449–5452.

Kweon, D.-H., Kim, C. S., and Shin, Y.-K. (2003). Regulation of neuronal SNARE assembly by the membrane. *Nat. Struct. Biol.* *10*, 440–447.

Laage, R., Rohde, J., Brosig, B., and Langosch, D. (2000). A conserved membrane-spanning amino acid motif drives homodimeric and supports heteromeric assembly of presynaptic SNARE proteins. *J. Biol. Chem.* *275*, 17481–17487.

Li, F., Pincet, F., Perez, E., Eng, W. S., Melia, T. J., Rothman, J. E., and Tareste, D. (2007). Energetics and dynamics of SNAREpin folding across lipid bilayers. *Nat. Struct. Mol. Biol.* *14*, 890–896.

Littleton, J. T., Bai, J., Vyas, B., Desai, R., Baltus, A. E., Garment, M. B., Carlson, S. D., Ganetzky, B., and Chapman, E. R. (2001). Synaptotagmin mutants reveal essential functions for the C2B domain in Ca²⁺-triggered fusion and recycling of synaptic vesicles *in vivo*. *J. Neurosci.* *21*, 1421–1433.

Lynch, K. L., Gerona, R.R.L., Larsen, E. C., Marcia, R. F., Mitchell, J. C., and Martin, T.F.J. (2007). Synaptotagmin C2A loop 2 mediates Ca²⁺-dependent SNARE interactions essential for Ca²⁺-triggered vesicle exocytosis. *Mol. Biol. Cell* *18*, 4957–4968.

Margittai, M., Fasshauer, D., Pabst, S., Jahn, R., and Langen, R. (2001). Homo- and heterooligomeric SNARE complexes studied by site-directed spin labeling. *J. Biol. Chem.* *276*, 13169–13177.

Montecucco, C., Schiavo, G., and Pantano, S. (2005). SNARE complexes and neuroexocytosis: how many, how close? *Trends Biochem. Sci.* *30*, 367.

Pobbati, A. V., Stein, A., and Fasshauer, D. (2006). N- to C-terminal SNARE complex assembly promotes rapid membrane fusion. *Science* *313*, 673–676.

- Quetglas, S., Iborra, C., Sasakawa, N., De Haro, L., Kumakura, K., Sato, K., Leveque, C., and Seagar, M. (2002). Calmodulin and lipid binding to synaptobrevin regulates calcium-dependent exocytosis. *EMBO J.* 21, 3970–3979.
- Quetglas, S., Leveque, C., Miquelis, R., Sato, K., and Seagar, M. (2000). Ca²⁺-dependent regulation of synaptic SNARE complex assembly via a calmodulin- and phospholipid-binding domain of synaptobrevin. *Proc. Natl. Acad. Sci. USA* 97, 9695–9700.
- Rhoads, A. R., and Friedberg, F. (1997). Sequence motifs for calmodulin recognition. *FASEB J.* 11, 331–340.
- Rickman, C., Hu, K., Carroll, J., and Davletov, B. (2005). Self-assembly of SNARE fusion proteins into star-shaped oligomers. *Biochem. J.* 388, 75–79.
- Rickman, C., Jiménez, J. L., Graham, M. E., Archer, D. A., Soloviev, M., Burgoyne, R. D. and Davletov, B. (2006). Conserved prefusion protein assembly in regulated exocytosis. *Mol. Biol. Cell* 17, 283–294.
- Rizo, J., Chen, X., and Arac, D. (2006). Unraveling the mechanisms of synaptotagmin and SNARE function in neurotransmitter release. *Trends Cell Biol.* 16, 339.
- Roy, R., Laage, R., and Langosch, D. (2004). Synaptobrevin transmembrane domain dimerization-revisited. *Biochemistry* 43, 4964–4970.
- Siddiqui, T. J., Vites, O., Stein, A., Heintzmann, R., Jahn, R., and Fasshauer, D. (2007). Determinants of synaptobrevin regulation in membranes. *Mol. Biol. Cell* 18, 2037–2046.
- Sorensen, J. B., Wiederhold, K., Muller, E. M., Milosevic, I., Nagy, G., de Groot, B. L., Grubmuller, H., and Fasshauer, D. (2006). Sequential N- to C-terminal SNARE complex assembly drives priming and fusion of secretory vesicles. *EMBO J.* 25, 955–966.
- Spotorno, B., Piccinini, L., Tassara, G., Ruggiero, C., Nardini, M., Molina, F., and Rocco, M. (1997). BEAMS (BEADs Modelling System): a set of computer programs for the generation, the visualization and the computation of the hydrodynamic and conformational properties of bead models of proteins. *Eur. Biophys. J.* 25, 373–384.
- Stewart, B. A., Mohtashami, M., Trimble, W. S., and Boulianne, G. L. (2000). SNARE proteins contribute to calcium cooperativity of synaptic transmission. *Proc. Natl. Acad. Sci. USA* 97, 13955–13960.
- Südhof, T. C. (2004). The synaptic vesicle cycle. *Annu. Rev. Neurosci.* 27, 509–547.
- Sugita, S., Janz, R., and Südhof, T. C. (1999). Synaptogyrins regulate Ca²⁺-dependent exocytosis in PC12 cells. *J. Biol. Chem.* 274, 18893–18901.
- Sutton, J. M., Wayne, J., Scott-Tucker, A., O'Brien, S. M., Marks, P. M., Alexander, F. C., Shone, C. C., and Chaddock, J. A. (2005). Preparation of specifically activatable endopeptidase derivatives of *Clostridium botulinum* toxins type A, B, and C and their applications. *Protein Expr. Purif.* 40, 31–41.
- Sutton, R. B., Fasshauer, D., Jahn, R., and Brünger, A. T. (1998). Crystal structure of a SNARE complex involved in synaptic exocytosis at 2.4 Å resolution. *Nature* 395, 347–353.
- Svergun, D. I. (1999). Restoring low resolution structure of biological macromolecules from solution scattering using simulated annealing. *Biophys. J.* 76, 2879–2886.
- Svergun, D. I., Petoukhov, M. V., and Koch, M. H. (2001). Determination of domain structure of proteins from X-ray solution scattering. *Biophys. J.* 80, 2946–2953.
- Söllner, T., Bennett, M. K., Whiteheart, S. W., Scheller, R. H., and Rothman, J. E. (1993). A protein assembly-disassembly pathway in vitro that may correspond to sequential steps of synaptic vesicle docking, activation, and fusion. *Cell* 75, 409–418.
- Tang, J., Maximov, A., Shin, O., Dai, H., Rizo, J., and Südhof, T. C. (2006). A complexin/synaptotagmin 1 switch controls fast synaptic vesicle exocytosis. *Cell* 126, 1175–1187.
- Tokumaru, H., Umayahara, K., Pellegrini, L., Ishizuka, T., Saisu, H., Betz, H., Augustine, G., and Abe, T. (2001). SNARE complex oligomerization by synaphin/complexin is essential for synaptic vesicle exocytosis. *Cell* 104, 421–432.
- Vestergaard, B., Sanyal, S., Roessle, M., Mora, L., Buckingham, R. H., Kastrop, J. S., Gajhede, M., Svergun, D. I., and Ehrenberg, M. (2005). The SAXS solution structure of RF1 differs from its crystal structure and is similar to its ribosome bound cryo-EM structure. *Mol. Cell* 20, 929–938.
- Weber, T., Zemelman, B. V., McNew, J. A., Westermann, B., Gmachl, M., Parlati, F., Söllner, T. H., and Rothman, J. E. (1998). SNAREpins: minimal machinery for membrane fusion. *Cell* 92, 759–772.
- Wojcik, S. M., and Brose, N. (2007). Regulation of membrane fusion in synaptic excitation-secretion coupling: speed and accuracy matter. *Neuron* 55, 11–24.

Supplementary Information: Supplementary Methods

Plasmid construction

Constructs encoding the minimal SNARE complex coil regions (Fasshauer et al., 1998) were generated by PCR from full-length SNARE constructs and subcloned into the expression plasmid pGEX-KG (Guan and Dixon, 1991) via the EcoRI/XhoI restriction sites. The coding sequence of hGH was subcloned into pCMV5 (Lawrence et al., 1994) (pCMV5-SV40-hGH), such that its expression was driven by the SV40 promoter, as previously described (Sugita et al., 1999). Full-length, non-tagged syb2 was subcloned into the polylinker of pCMV5-SV40-hGH via the EcoRI/XbaI sites such that its expression was driven by the CMV promoter. GFP-tagged syb2 was generated by subcloning full-length syb2 into pGFPemd vector (Packard) using the EcoRI/BamHI sites to generate a C-terminal GFP fusion protein. GFP-tagged syb2 constructs were also generated whereby full-length syb2 was subcloned into the EGFP-C1 vector (Clontech) using the HindIII/BamHI sites to generate an N-terminal GFP fusion protein. N-terminally and C-terminally tagged GFP-syb2 proteins showed identical localization *in vivo*. Mutant syb2 constructs were generated using the QuickChange mutagenesis kit (Stratagene).

C-terminally tagged syb2 (1-96)-CFP and syb2 (1-96)-Venus FRET constructs were generated by removing the stop codon from the pGEX-KG GST-syb2 construct, followed by addition of a GGSGGS linker at the C-terminus of syb2 using the QuickChange mutagenesis kit (Stratagene). CFP and Venus were PCR-amplified and subcloned in-frame with the linker via a HindIII site. The N-terminally tagged CFP-syb2 (1-96) construct was generated by addition of a GGSGGS linker at the N-terminus of syb2, and CFP was PCR-amplified and subcloned via an EcoRI site. The

sequences of all primers used are available upon request. All constructs were verified by DNA sequencing.

Purification of recombinant SNARE proteins

All recombinant, N-terminally tagged GST fusion proteins were purified by glutathione-Sepharose (GE, Amersham, UK) affinity chromatography using standard protocols. Proteins were eluted from the beads by thrombin cleavage overnight at 4 °C in standard buffer (50 mM NaCl, 20 mM Tris pH 7.4, 1 mM DTT). Eluted proteins were analyzed for purity by SDS-PAGE and staining with Coomassie Blue, and were determined to be around 95% pure. In most cases, proteins were further purified by ion exchange chromatography using Mono-S (for syb2) or Mono-Q (for SNAP-25 and syntaxin) columns (GE, Amersham, UK) and then dialyzed against standard buffer. Preparations of SNARE coils run on SDS-PAGE are shown in Supplementary Figure 1. For a small number of experiments, this purification step was omitted. This did not affect the efficiency of SNARE complex formation or the purity of SNARE complex dimers isolated by gel filtration.

Analytical ultracentrifugation

Velocity sedimentation data was interpreted with the model-based distribution of Lamm equation solutions $c(s)$ using the software Sedfit (Schuck, 2000), with data corrected for standard conditions of water at 20°C using a \bar{v} of 0.7311 calculated from amino acid composition.

To help describe the shape of the dimeric SNARE complexes, solution bead models were generated using atomic coordinates of monomer coiled-coil domains and oriented using PyMOL. The program Trans within the solution modelling software

SOMO (Spotorno et al., 1997) was used to build multiple bead models of SNARE complexes and SNARE complex dimers. The hydrodynamic parameters generated for these models were compared to those determined experimentally.

Small Angle X-ray Scattering Data Collection and Analysis

Multiple images were obtained of each sample tested in time frames of 0.1 sec to be able to check for radiation damage and protein aggregation between frames. After applying different detector corrections, 2-d SAXS patterns were normalized to an absolute scale and azimuthally averaged to obtain the 1-d scattering profiles (Narayanan et al., 2001). Corresponding 1-d curves for sample cell and buffer background scattering was subtracted from each sample scattering profiles. The radius of gyration, the forward scattering intensity, and the one-dimensional intra-particle distance distribution function $p(r)$ in real space were evaluated with the indirect Fourier transform program GNOM (Semenyuk and Svergun, 1991).

For *ab initio* modelling, particle shapes were restored from the experimental scattering profiles using the *ab initio* procedure based on the simulated annealing algorithm to a set of clustered spheres representing amino acid residues, GASBOR (Svergun et al., 2001) and DAMMIN (Svergun, 1999). This yields a three-dimensional distribution of spherical scattering centres that reproduces the one-dimensional profile obtained from the scattering data. Many Gasbor and Dammin simulations (~20) were performed for each protein fragment, and these generated very similar but not identical shapes in each case. An averaged filtered structure was generated using Damaver and Damfilt (Volkov and Svergun, 2003).

TEM Single Particle Image Processing

Image processing and CTF correction were carried out using the EMAN software package (Ludtke et al., 1999). 1242 particles were windowed into 24 nm x 24 nm images and centred by cross-correlation to the averaged image of the dataset. After reference free alignment, the selected particles were classified into 11 classes by multivariate statistical analysis (van Heel and Frank, 1981). Euler angles were assigned to the reference classes and an initial 3D reconstruction calculated. The 3D model was then subject to refinement by multiple iterations. The Fourier shell correlation was calculated and the resolution was determined to be 32 Å at a correlation of 0.5.

Differential Scanning Calorimetry

SNARE complexes were assembled overnight, then filtered through a 0.2 µm filter and degassed before loading at a concentration of approximately 5 µM. Data were collected between 20 and 120°C at a scan rate of 90 degrees per hr. Non-assembled coils did not produce a thermogram peak. Data were baseline subtracted and normalized to concentration before being analyzed by a non-2-state model using Microcal software. Information was taken from the major peak centered at approximately 95-96°C. Whilst the significance of the smaller peak at approximately 85-90°C remains unclear, it may represent an additional minor phase transition. The total area under the peak is the total calorimetric enthalpy (ΔH), i.e. the total energy uptake by the sample, per mol. The concentration of SNARE complexes in each reaction was estimated based on the yield of size exclusion-purified wild-type SNARE complexes from a standard reaction, and was extrapolated for other samples. A concentration-independent measurement was provided by calculating the van't

Hoff enthalpy (ΔH_{VH}), an independent estimate of the transition based on the temperature change per unit area of the peak (Dürr et al., 1999).

FRET measurements

GFP-tagged syb2 proteins were purified by affinity chromatography. SNARE complexes were formed by overnight assembly of equimolar amounts of SNARE coils, including a 1:1 mixture of C-terminally tagged syb2-Venus FRET acceptor with either C-terminally or N-terminally tagged syb2-CFP FRET donor. Complex formation was verified by SDS-PAGE. Preparations of purified GFP-tagged syb2 coils and resulting GFP-tagged SNARE complexes run on SDS-PAGE are shown in Supplementary Figure 4.

Determination of localization and expression levels of syb2

To visualize proper localization of over-expressed wild-type and mutant syb2 proteins, PC12 cells were transfected with GFP-tagged constructs, plated onto poly-L-lysine-coated coverslips the next day, and grown for 2 days in serum-reduced medium (1%) containing 50 ng/ml NGF 2.5 S (Invitrogen). Cells were fixed and processed for immunocytochemistry as described (Rajebhosale et al., 2003), using a polyclonal anti-synaptotagmin I antibody (Pieribone et al., 1995) at 1:1000 dilution, and a goat-anti-rabbit AlexaFluor-594-conjugated secondary antibody at 1:1000 (Invitrogen). Localization of GFP-tagged syb2 protein was indistinguishable from the localization of endogenous syb2 (Rajebhosale et al., 2003). Images were acquired on an Olympus microscope (Cell R IX81) using a 40x objective. Stack acquisition was performed using a 100x objective, an MT20 illumination system and an Orca CCD camera (Hamamatsu). Deconvolution of 3D images was performed using Huygens Essential

software (version 2.9; Scientific Volume Imaging). Images displayed correspond to individual deconvolved multichannel 3D image datasets. Colocalization pseudocoloring was performed using ImageJ software (version 1.37; NIH).

Over-expression levels of non-tagged wildtype and mutant syb2 were determined essentially as described before (Rajebhosale et al., 2003) with minor modifications. Non-differentiated or differentiated cells were stained with a mouse monoclonal anti-syb2 antibody (C1 69.1; Synaptic Systems) and a goat-anti-mouse AlexaFluor-488-conjugated secondary antibody at 1:1000 (Invitrogen). The anti-syb2 antibody was used at 1:5000 dilution to easily detect over-expressed syb2, but only barely detect endogenous protein. Cells were double-stained with a rabbit polyclonal anti-hGH antibody (1:100) and a goat-anti-rabbit AlexaFluor-594-conjugated secondary antibody (1:1000; Invitrogen) to unequivocally identify transfected, over-expressing cells. To quantify levels of over-expression, areas were drawn around individual, well-separated over-expressing cells from 10 random fields acquired using a 40x oil-immersion objective. The same number of cells not showing over-expression were analyzed for each field. Average pixel intensities within each area were calculated in ImageJ software (version 1.37; NIH).

Binding of synaptotagmin 1 and complexin 1 to SNARE complex dimers

The GST-fusion constructs for the C2AB domain of rat synaptotagmin 1 (96-421) (Hilfiker et al., 1999) and for complexin 1 (McMahon et al., 1995) have been previously described, and proteins were purified as described above for SNARE coils. Synaptotagmin 1 was additionally purified by size exclusion chromatography to remove high molecular weight species that might interfere with the subsequent analysis of SNARE binding (Ubach et al., 2001). SNARE complexes were formed by

overnight assembly of equimolar concentrations of purified SNARE components in standard buffer, and using a two-fold molar excess of recombinant synaptotagmin 1 or complexin 1. Samples were purified by size exclusion chromatography using a Superdex 200 column as described above, and peaks analysed by SDS-PAGE in the absence of boiling. SNARE complexes and complexin 1 were identified by Coomassie staining, whilst synaptotagmin 1 was identified by Western blotting using an affinity-purified rabbit anti-synaptotagmin antibody (Pieribone et al., 1995). For synaptotagmin 1 experiments, complex assembly and size exclusion chromatography were performed with 1 mM CaCl₂, and identical results were achieved without CaCl₂ (data not shown).

Determination of SDS-resistant SNARE complex stability

PC12 cells were transfected with N-terminally GFP-tagged wildtype and mutant syb2 constructs as described above. Three days after transfection, cells were harvested from a 100 mm dish and washed in PBS. The cell pellet was resuspended in 500 µl solubilization buffer (50 mM Tris-HCl, pH 8.0, 150 mM NaCl, 10 mM EDTA, 1% Tx-100, 1 mM PMSF) and incubated overnight at 4 °C on a rotary shaker. The lysate was cleared by centrifugation (16'000 g, 20 min, 4 °C) and protein concentration of the supernatant determined by the MicroBCA Protein Assay Kit (Pierce).

Protein extracts (40 µg) were diluted 5-fold in Laemmli buffer (final 50 mM Tris pH 6.8, 2% SDS, 4% glycerol and β-mercaptoethanol) and incubated for 5 min at different temperatures in 10 °C steps, followed by SDS-PAGE on 12.5% polyacrylamide gels without prior boiling. Proteins were transferred overnight to nitrocellulose membranes (Schleicher&Schuell), and GFP-tagged SNARE complexes

visualized using a rabbit polyclonal anti-GFP antibody (1: 1000; Abcam) followed by a polyclonal goat anti-rabbit immunoglobulin/HRP secondary antibody (1:1000; DakoCytomation), and developed using enhanced chemiluminescence detection (Lumi-Light Western Blotting Substrate; Roche) according to manufacturer's instructions.

Determination of toxin-mediated endogenous syb2 cleavage and of overexpression levels of toxin-insensitive syb2 constructs

To assess expression levels of toxin-insensitive wildtype and mutant syb2 constructs upon toxin treatment, a novel preparation of recombinant botB was employed, consisting of the light chain region of botB, an enterokinase recognition site, the N-terminal domain of the botB heavy chain and a C-terminal 6-His affinity tag (botB/HnLC). This single chain molecule preparation was of high homogeneity as assessed by SDS-PAGE, and of high specific endopeptidase activity using an *in vitro* VAMP peptide cleavage assay (data not shown; Sutton et al., 2005).

Transfected PC12 cells were washed three times with wash buffer (156 mM NaCl, 5.6 mM KCl, 5.6 mM glucose, 0.2 mM EGTA, 5 mM HEPES, pH 7.4), permeabilized for 5 min in KGEP10 buffer (10 μ M digitonin, 140 mM K-glutamate, 5 mM glucose, 5 mM EGTA, 100 μ M ZnCl₂, 20 mM PIPES, pH 6.8) and incubated in KGEP10 buffer containing 75 μ l botB/HnLC for 20 min at 37 °C. Cells were subsequently washed for 10 min with wash buffer and collected in buffer containing 50 mM Tris-HCl pH 8.0, 150 mM NaCl, 10 mM EDTA, 1% Tx-100 and 1 mM PMSF. Cell extracts were resolved on 15 % polyacrylamide gels, VAMP2 was detected with a mouse monoclonal anti-VAMP2 antibody (clone C110.1; 1:1500;

Synaptic Systems), and to confirm equal amounts of protein loading, membranes were subsequently blotted with a mouse monoclonal anti-synaptophysin antibody (clone SVP38; 1:500; Sigma).

Supplementary Information: Supplementary References

- Dürr, E., Jelesarov, I. and Bosshard, H.R. (1999) Extremely fast folding of a very stable leucine zipper with a strengthened hydrophobic core and lacking electrostatic interactions between helices. *Biochem.*, **38**, 870-880.
- Fasshauer, D., Eliason, W.K., Brünger, A.T. and Jahn, R. (1998) Identification of a minimal core of the synaptic SNARE complex sufficient for reversible assembly and disassembly. *Biochemistry*, **37**, 10354-10362.
- Guan, K.L. and Dixon, J.E. (1991) Eukaryotic proteins expressed in Escherichia coli: an improved thrombin cleavage and purification procedure of fusion proteins with glutathione S-transferase. *Anal. Biochem.*, **192**, 262-267.
- Hilfiker, S., Pieribone, V.A., Nordstedt, C., Greengard, P. and Czernik, A.J. (1999) Regulation of synaptotagmin I phosphorylation by multiple protein kinases. *J. Neurochem.*, **73**, 921-932.
- Kubista, H., Edelbauer, H. and Boehm, S. (2004) Evidence for structural and functional diversity among SDS-resistant SNARE complexes in neuroendocrine cells. *J. Cell Sci.*, **117**, 955-966.
- Lawrence, D.A., Olson, S.T., Palaniappan, S. and Ginsburg, D. (1994) Engineering plasminogen activator inhibitor 1 mutants with increased functional stability. *Biochemistry*, **33**, 3643-3649.
- Ludtke, S., Baldwin, P. and Chiu, W. (1999) EMAN: semiautomated software for high-resolution single-particle reconstructions. *J. Struct. Biol.*, **128**, 82-97.
- McMahon, H.T., Missler, M., Li, C. and Südhof, T.C. (1995) Complexins: cytosolic proteins that regulate SNAP receptor function. *Cell*, **83**, 111-119.

- Narayanan, T., Diat, O. and Bösecke, P. (2001) SAXS and USAXS on the high brilliance beamline at the ESRF. *Nucl. Instr. Meth. Phys Res. A*, **467**, 1005-1009.
- Pieribone, V.A., Shupliakov, O., Brodin, L., Hilfiker-Rothenfluh, S., Czernik, A.J. and Greengard, P. (1995) Distinct pools of synaptic vesicles in neurotransmitter release. *Nature*, **375**, 493-497.
- Rajebhosale, M., Greenwood, S., Vidugiriene, J., Jeromin, A. and Hilfiker, S. (2003) Phosphatidylinositol 4-OH Kinase Is a Downstream Target of Neuronal Calcium Sensor-1 in Enhancing Exocytosis in Neuroendocrine Cells. *J. Biol. Chem.*, **278**, 6075-6084.
- Schuck, P. (2000) Size distribution analysis of macromolecules by sedimentation velocity ultracentrifugation and Lamm equation modeling. *Biophys J*, **78**, 1606-1619.
- Semenyuk, A.V. and Svergun, D.I. (1991) GNOM - a program package for small-angle scattering data processing. *Journal of Applied Crystallography*, **24**, 537-540.
- Spotorno, B., Piccinini, L., Tassara, G., Ruggiero, C., Nardini, M., Molina, F. and Rocco, M. (1997) BEAMS (BEADs Modelling System): a set of computer programs for the generation, the visualization and the computation of the hydrodynamic and conformational properties of bead models of proteins. *European Biophysics Journal*, **25**, 373-384.
- Sugita, S., Janz, R. and Südhof, T.C. (1999) Synaptogyrins regulate Ca²⁺-dependent exocytosis in PC12 cells. *J. Biol. Chem.*, **274**, 18893-18901.
- Sutton, J.M., Wayne, J., Scott-Tucker, A., O'Brien, S.M., Marks, P.M., Alexander, F.C., Shone, C.C. and Chaddock, J.A. (2005) Preparation of specifically

- activatable endopeptidase derivatives of Clostridium botulinum toxins type A, B and C and their applications. *Protein Expr. Purif.*, **40**, 31-41.
- Svergun, D.I. (1999) Restoring Low Resolution Structure of Biological Macromolecules from Solution Scattering Using Simulated Annealing. *Biophys. J.*, **76**, 2879-2886.
- Svergun, D.I., Petoukhov, M.V. and Koch, M.H. (2001) Determination of domain structure of proteins from X-ray solution scattering. *Biophys J*, **80**, 2946-2953.
- Ubach, J., Lao, Y., Fernandez, I., Arac, D., Südhof, T.C. and Rizo, J. (2001) The C2B domain of synaptotagmin I is a Ca²⁺-binding module. *Biochemistry* **40**, 5854-5860.
- van Heel, M. and Frank, J. (1981) Use of multivariate statistics in analysing the images of biological macromolecules. *Ultramicroscopy*, **6**, 187-194.
- Volkov, V.V. and Svergun, D.I. (2003) Uniqueness of ab initio shape determination in small-angle scattering. *Journal of Applied Crystallography*, **36**, 860-864.

Supplementary Information: Supplementary Figure Legends

Supplementary Figure 1

Purification of SNARE coils and assembly of SNARE complexes.

(a) Purified SNARE coils derived from Syb2, Syb2 mutants, SNAP-25 and syntaxin were run on 15% SDS-PAGE and stained with Coomassie blue. (b) Assembled SNARE complexes were run on 15% SDS-PAGE, with and without boiling in sample buffer, and stained with Coomassie blue.

Supplementary Figure 2

Cytosolic neuronal SNARE complexes form salt-sensitive dimers in solution.

(a) SNARE coils were incubated overnight at 4 °C and subjected to gel filtration chromatography on a Superdex 200 column. Black: refractive index (indicating protein concentration). Red: light scattering (providing molecular weight information). SDS-PAGE of fractions confirmed that SNARE complexes eluted at 10-11 ml and non-complexed coils eluted at 14-16 ml (data not shown). (b) The major SNARE complex peak was re-run on a Superdex 200 column either in 0.05 M NaCl (black) or 1 M NaCl (red) and assayed for molecular weight by light scattering. The molecular weight of the SNARE complex in 0.05 M NaCl was 89,500 +/- 1,950 Da, and in 1 M NaCl was 44,600 +/- 1,000 Da (errors from polydispersity). The predicted molecular weight of the recombinant SNARE complex, including linker amino acids, is 45,768 Da.

Supplementary Figure 3

Small Angle X-ray Scattering Data.

(a) The low angle regions of the X-ray scattering data were analysed in the form of Guinier plots ($\log I$ versus q^2), from which the radius of gyration (R_g) can be extracted from the slope ($R_g^2/3$) of the straight line. The slope demonstrates the expected linearity for the values $q \leq 1/R_g$ (shown in black). (b) Pair distribution function calculated for the dataset shown in a. The curve shows with error bars the distribution of interatomic spacings, with a maximum at 17 nm. (c) Shapes were simulated ab initio using the programs DAMMIN and GASBOR. For each protein fragment the results of twenty independent simulations were averaged and filtered to give the “most probable” shape. The “most probable” GASBOR shape is represented as arrays of beads (see Figure 2b). The experimental data are plotted in grey as a function of q , and compared with a typical theoretical fit obtained with GASBOR (black).

Supplementary Figure 4

Characterization of FRET coils.

(a) FRET Syb2 coils, as indicated, were purified by affinity and ion exchange chromatography and analysed by SDS-PAGE and Coomassie staining. (b) SNARE complexes generated by mixing coils in which Syb2 was replaced by an equal concentration of Syb2-Venus and Syb2-CFP, or Syb2-Venus and CFP-Syb2, were purified by gel filtration and analysed by SDS-PAGE with or without boiling in sample buffer. The arrow indicates SDS-resistant SNARE complexes, the arrowhead indicates uncomplexed FRET Syb2 coils, and the bracket indicates the position of uncomplexed syntaxin and SNAP-25 coils.

Supplementary Figure 5

Sedimentation equilibrium of WT SNARE complexes to determine the association kinetics.

SNARE complexes generated as indicated were analysed using equilibrium sedimentation in 0.3 M NaCl at three concentrations (1, 2.5 and 5 μ M protein) and three rotor speeds (10, blue; 15, yellow; and 21,000, red, rpm), and global analysis of the data was performed using Sedphat. Best fits were achieved modelling to a monomer-dimer self-association model. This provided an apparent K_D of 5.43 μ M for SNARE complex dimers containing WT Syb2. Identical analysis provided an apparent K_D of 11.97 μ M for dimers containing Syb2 (W89A,W90A), and 46.23 μ M for dimers containing Syb2 (R86A,W89A,W90A).

Supplementary Figure 6

Localization of wildtype and mutant GFP-syb2 proteins.

PC12 cells were transfected with GFP-tagged wildtype and mutant syb2 constructs (green), and differentiated with NGF. Fixed cells were processed for immunocytochemistry using a polyclonal anti-synaptotagmin antibody (red). Bar, 20 μ m.

Supplementary Figure 7

Detection of thermostability of SDS-resistant SNARE complexes from permeabilized cells.

Cells were transfected with GFP-tagged wildtype or mutant syb2. Lysed cell extracts were diluted in Laemmli buffer and incubated for 5 min at different temperatures followed by SDS-PAGE and Western blotting with an anti-GFP antibody. Two

distinct heat-sensitive SDS-resistant SNARE complexes could be resolved, as previously described for PC12 cells (Kubista et al., 2004). The ratio of these complexes varied when the same samples were re-analyzed on SDS-PAGE, such that this behaviour was not further investigated. In either case, GFP-tagged wildtype and mutant syb2-containing complexes all melted at similar temperatures.

Supplementary Figure 8

Complexin 1 and synaptotagmin 1 binding to SNARE complexes.

(a) Wildtype (WT) SNARE complexes were assembled overnight and separated by size exclusion chromatography. Only the first 12 fractions (covering the distribution of SNARE complexes) are shown (fraction 1 = void). (b) WT SNARE complexes, or complexes containing Syb2(R86A,W89A,W90A) were assembled overnight in combination with complexin 1 and separated by size exclusion chromatography. SDS-resistant SNARE complexes (S) and complexin 1 (C) were identified by Coomassie staining. The migration of isolated complexin 1 across these fractions is shown below (note that the peak of free complexin 1 is in fraction 15). (c) WT SNARE complexes, or complexes containing Syb2(R86A,W89A,W90A) were assembled overnight in combination with synaptotagmin 1 and separated by size exclusion chromatography. Synaptotagmin was identified by Western blot. The migration of isolated synaptotagmin 1 across these fractions is shown below (note that the peak of free synaptotagmin 1 is in fraction 15).

Supplementary Figure 9

Crystal structure (left) and SOMO bead model of crystal dimer 4. The hydrodynamic properties predicted by the model show a hydrodynamic radius of 3.78 nm which

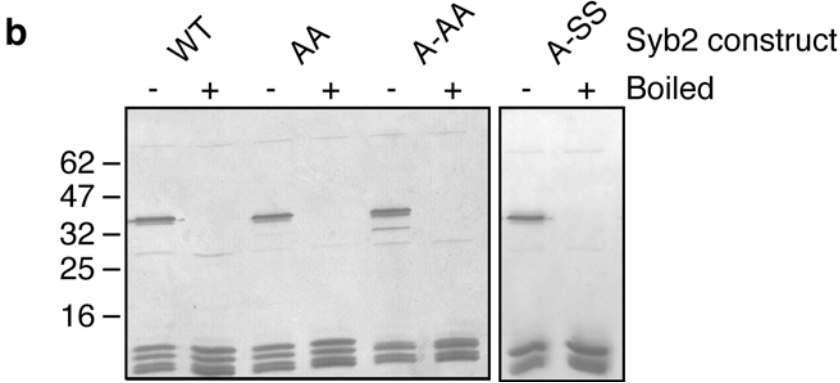
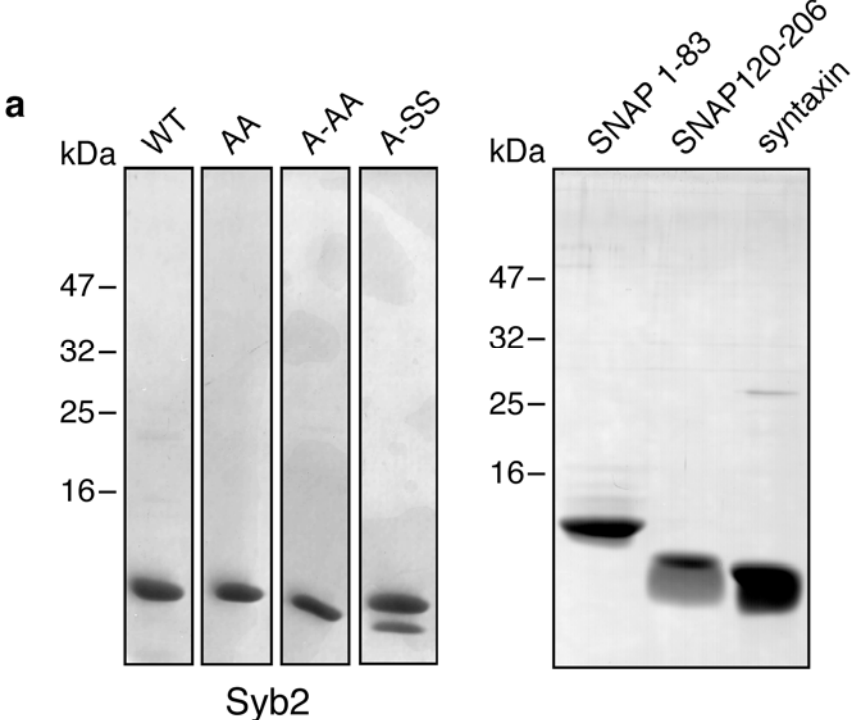
corresponds to a sedimentation coefficient of 5.56 S and a radius of gyration of 3.48 nm. This compares to measured values of 5.02 nm for the R_h and a value of 4.13 for the sedimentation coefficient (see Supplementary Table 1 for details).

Supplementary Table 1. SNARE-SNARE lattice dimers observed in the crystal structure of the SNARE complex (PDB entry 1SFC).

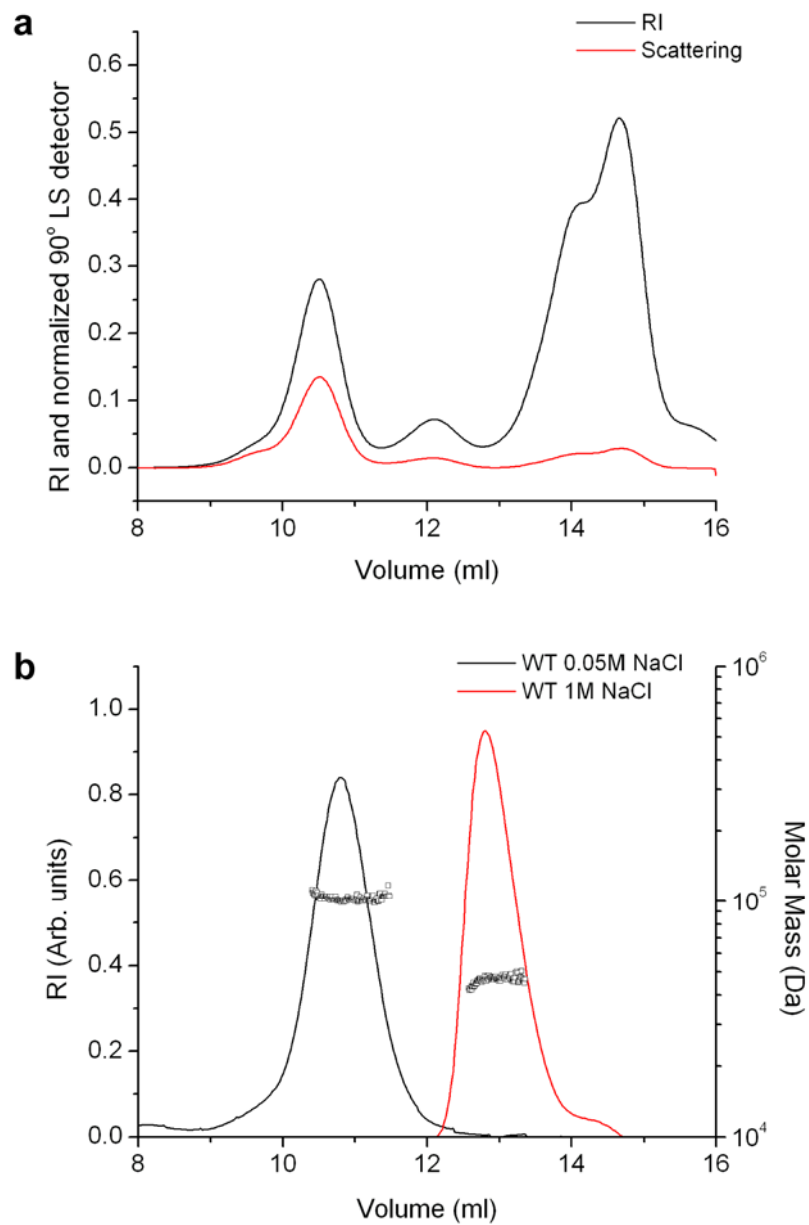
| Dimer | Complex 1 | | Complex 2 | | Parallel Antiparallel | Sr ²⁺ dependent | Buried Surface (Å ²) | Accessibility (%) | |
|-------|-----------|--------------|-----------|------------------|--------------------------|-------------------------------|-------------------------------------|-------------------|--------|
| | | <i>x,y,z</i> | | | | | | W89 | W90 |
| 1 | EFGH | <i>x,y,z</i> | EFGH | <i>x,1-y,-z</i> | A | No | 2222 | 100 | 100 |
| 2 | ABCD | <i>x,y,z</i> | IJKL | <i>x,y,z</i> | A | Yes | 2184 | 40, 37 | 58, 46 |
| 3 | IJKL | <i>x,y,z</i> | IJKL | <i>x,1-y,-z</i> | A | No | 2109 | 100 | 100 |
| 4 | ABCD | <i>x,y,z</i> | EFGH | <i>x,y,z</i> | P | No | 1714 | 0 | 69 |
| 5 | EFGH | <i>x,y,z</i> | EFGH | <i>-x,y,-z</i> | A | No | 966 | 100 | 100 |
| 6 | ABCD | <i>x,y,z</i> | ABCD | <i>-x,y,-z</i> | A | No | 937 | 100 | 100 |
| 7 | EFGH | <i>x,y,z</i> | IJKL | <i>x,y,z</i> | A | Yes | 899 | 100 | 100 |
| 8 | ABCD | <i>x,y,z</i> | ABCD | <i>-x,-y,z</i> | P | No | 881 | 100 | 100 |
| 9 | ABCD | <i>x,y,z</i> | IJKL | <i>x-,y-,z+</i> | A | No | 846 | 100 | 100 |
| 10 | IJKL | <i>x,y,z</i> | IJKL | <i>1-x,1-y,z</i> | P | No | 440 | 100 | 100 |

The 10 non-equivalent dimers with highest amount of buried surface are shown. Each SNARE monomer is in fact a four-helix bundle, with each individual chain identified as in the original PDB entry (A, B, C, D, etc.). Operations of symmetry to identify symmetry-related contacts are denoted following the convention of the *International Tables of Crystallography*. Dimers where Sr²⁺ ions are seen coordinating residues from two SNARE complexes are labelled as Sr²⁺-dependent. The percentage of accessibility is calculated for Trp side chains with respect to the values obtained in monomeric SNAREs. Note that the only instance of completely buried Trp side chains occurs at the interface of the parallel dimer 4.

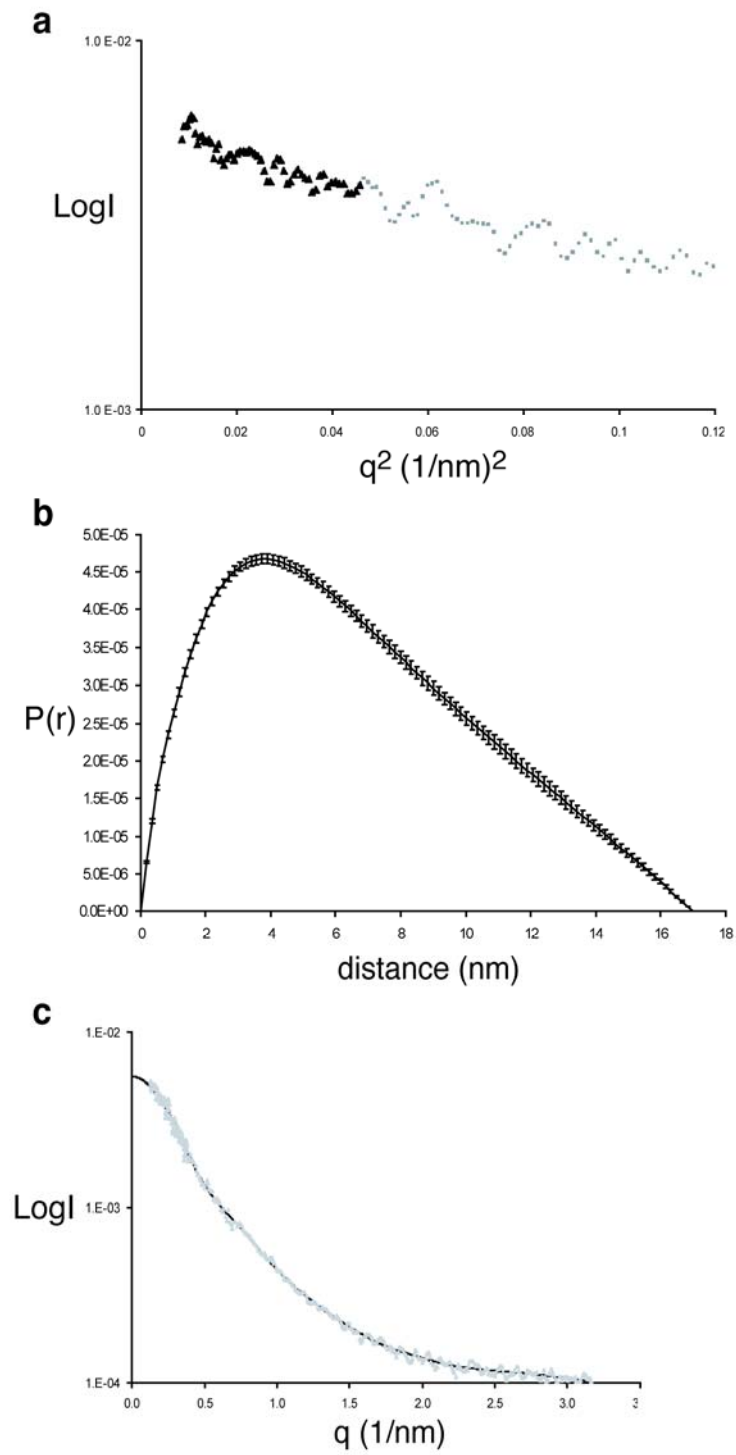
Supplementary Figure 1



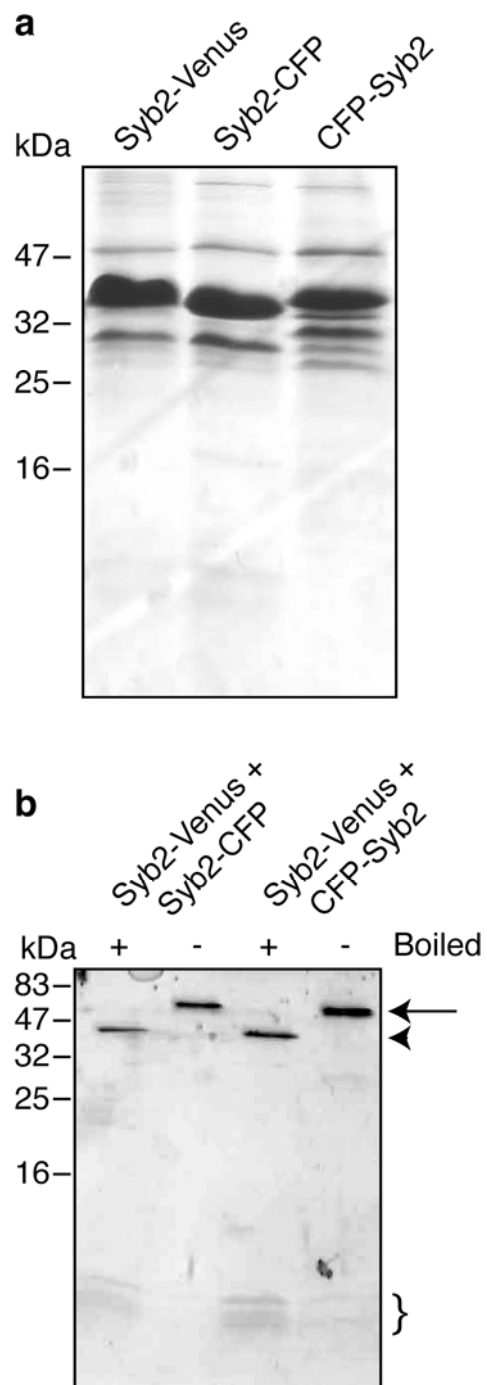
Supplementary Figure 2



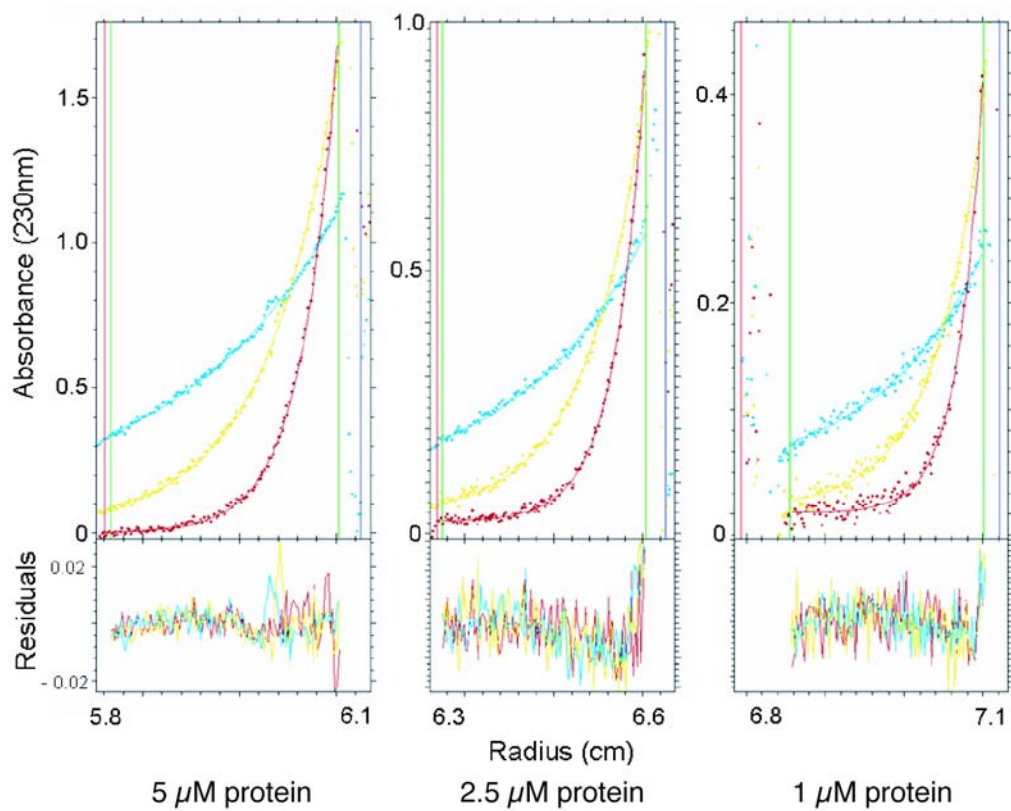
Supplementary Figure 3



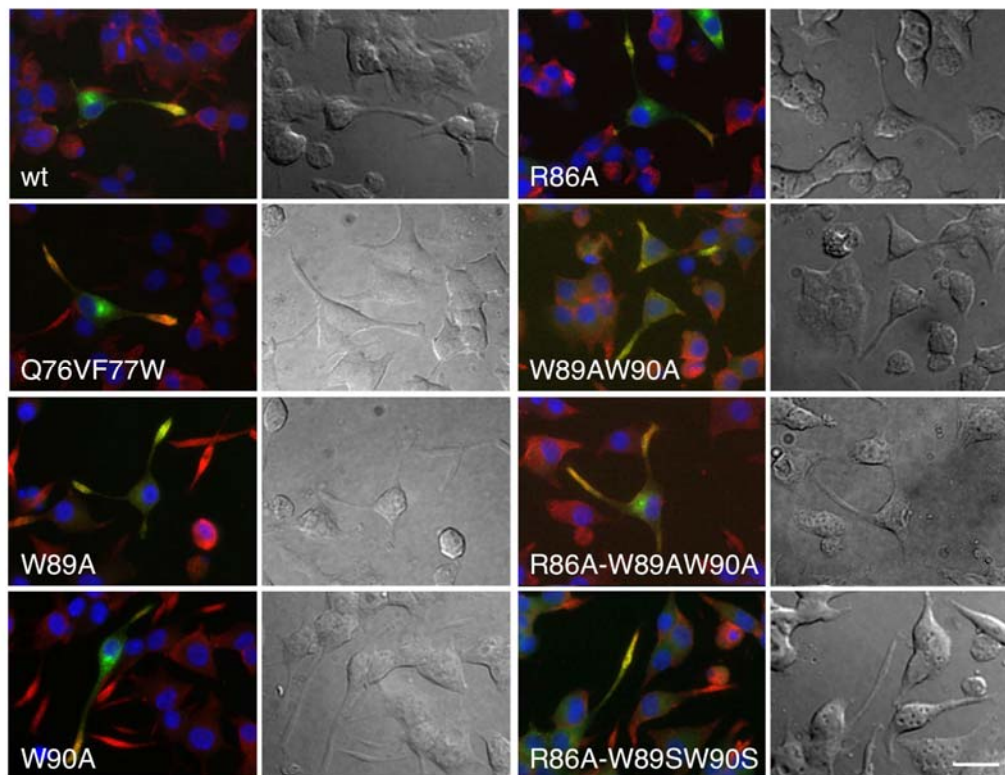
Supplementary Figure 4



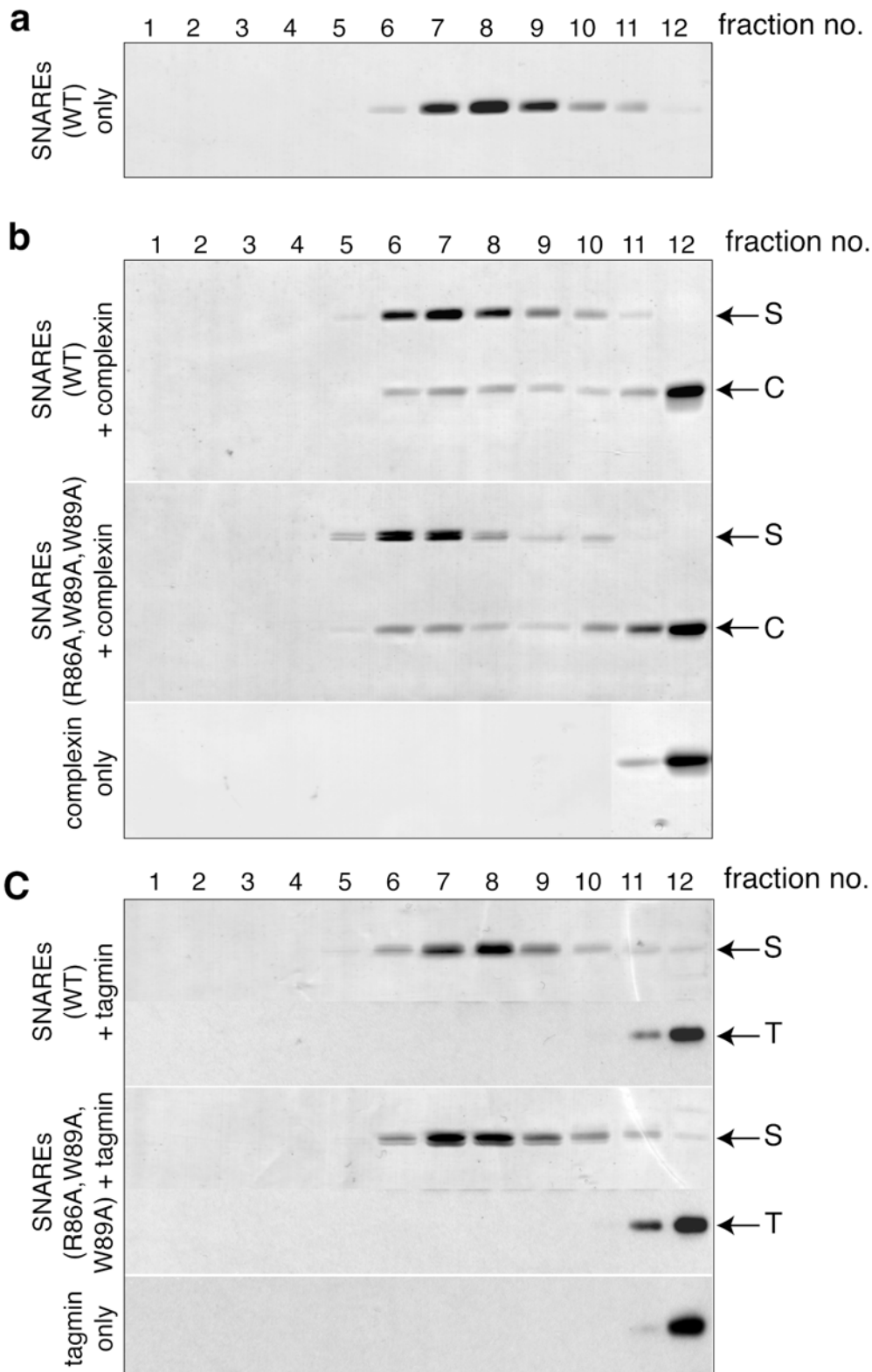
Supplementary Figure 5



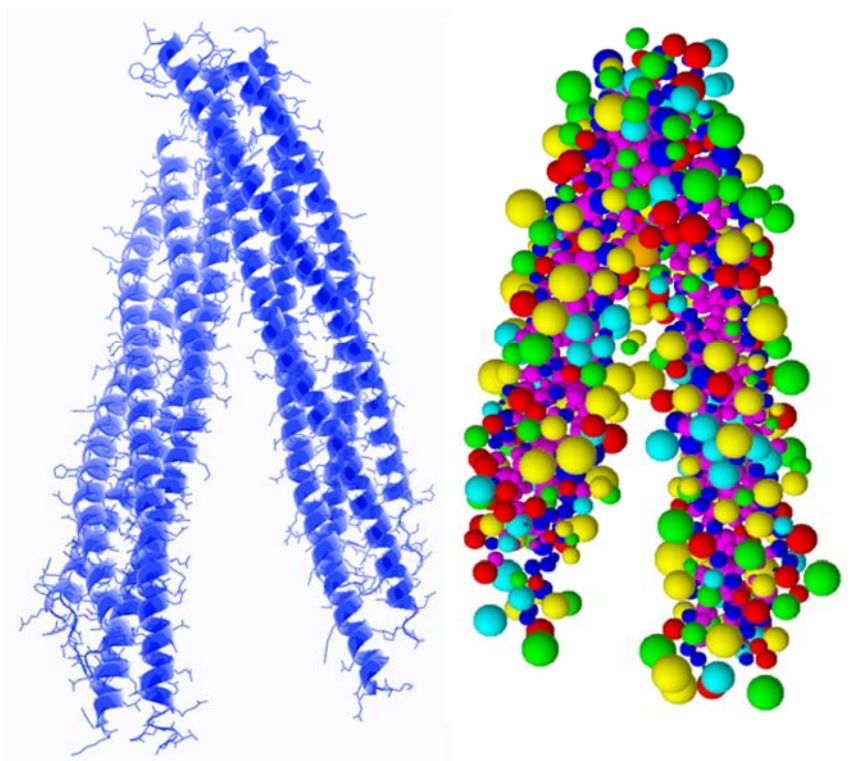
Supplementary Figure 6



Supplementary Figure 8



Supplementary Figure 9



**2. TRANSMEMBRANE DOMAIN DETERMINANTS FOR
SNARE-MEDIATED MEMBRANE FUSION.**

2. Transmembrane Domain Determinants for SNARE-mediated Membrane Fusion.

Resumen:

La liberación de los neurotransmisores contenidos en las vesículas sinápticas requiere de la aproximación de dichas vesículas a la membrana plasmática y la posterior fusión de ambas membranas. Este proceso está altamente regulado y requiere la asociación de los dominios citoplasmáticos de las proteínas SNARE neuronales VAMP2, SNAP-25 y syntaxin1A. Dos de estas proteínas (VAMP2 y syntaxin1A) contienen un dominio transmembrana claramente importante en el proceso de fusión de membranas. Sin embargo, aún se desconocen la mayoría de los requerimientos estructurales y funcionales de dichos dominios transmembrana. En el siguiente estudio hemos indagado en aquellos aspectos estructurales del dominio transmembrana de VAMP2 que afectan o no a su función. Hemos usado un ensayo de complementación de fluorescencia bimolecular (BiFC) para estudiar las interacciones mediadas por los dominios transmembrana de las proteínas SNARE *in vivo*. Aquí demostramos que moléculas de VAMP2 dimerizan mediante sus dominios transmembranas en células neuroendocrinas intactas. En dicha dimerización participa una glicina (G100) situada en el centro del dominio transmembrana cuya sustitución por aminoácidos de mayor volumen molecular como tirosina o valina impiden la dimerización de VAMP2 *in vivo*. Sin embargo, estas mutaciones son capaces de llevar a cabo el proceso de neurosecreción, lo que sugiere que la dimerización de los dominios transmembrana de VAMP2 no juegan un papel importante en la fusión de membranas. Por lo contrario, una serie de deleciones o inserciones en la región carboxilo terminal de dichos dominios causan una inhibición severa de la neurosecreción, mientras que alteraciones similares en el extremo amino terminal no tienen efectos significativos. Nuestros resultados indican que requerimientos estructurales como la longitud, principalmente de la región carboxilo terminal, del dominio transmembrana de VAMP2 son esenciales para el proceso de neurotransmisión mediado por SNAREs.

Transmembrane domain determinants for SNARE-mediated membrane fusion

Elena Fdez¹, Matthew Beard², Philip Woodman³ and Sabine Hilfiker^{1,*}

¹Institute of Parasitology and Biomedicine “López-Neyra”, Consejo Superior de Investigaciones Científicas (CSIC), Avda del Conocimiento s/n, 18100 Granada, Spain;

²Syntaxin Ltd., Abingdon, Oxon OX143YS, United Kingdom; ³Faculty of Life Sciences, University of Manchester, Oxford Road, Manchester M13 9PT, United Kingdom

*To whom correspondence should be addressed:

Sabine Hilfiker, Institute of Parasitology and Biomedicine “López-Neyra”, Consejo Superior de Investigaciones Científicas (CSIC), Avda del Conocimiento s/n, 18100 Granada, Spain; tel: +34 958 18 16 54; fax: +34 958 18 16 32; e-mail: sabine.hilfiker@ipb.csic.es.

Short title: SNARE transmembrane domain and fusion

Keywords: membrane fusion, bimolecular fluorescence complementation, synaptobrevin, transmembrane domain

Summary

Neurosecretion involves fusion of vesicles with the plasma membrane. Such membrane fusion is mediated by the SNARE complex, composed of the vesicle-associated protein synaptobrevin (VAMP2), and the plasma membrane proteins syntaxin1A and SNAP-25. Whilst clearly important at the point of membrane fusion, the precise structural and functional requirements for the transmembrane domains (TMDs) of SNAREs in bringing about neurosecretion remain largely unknown. Here, we used a bimolecular fluorescence complementation (BiFC) approach to study SNARE protein interactions involving TMDs *in vivo*. VAMP2 molecules were found to dimerize through their TMDs in intact cells. Dimerization was abolished when replacing a glycine residue in the center of the TMD with residues of increasing molecular volume. However, such mutations still were fully competent in bringing about membrane fusion events, suggesting that dimerization of the VAMP2 TMDs does not play an important functional role. In contrast, a series of deletion or insertion mutants in the C-terminal half of the TMD were largely deficient in supporting neurosecretion, whilst mutations in the N-terminal half did not display severe secretory deficits. Thus, structural length requirements, largely confined to the C-terminal half of the VAMP2 TMD, seem to be essential for SNARE-mediated membrane fusion events in cells.

Introduction

Intracellular membrane fusion events require a conserved set of proteins designated SNAREs (soluble N-ethyl maleimide-sensitive factor (NSF) attachment protein receptors) (Lin and Scheller, 2000; Jahn et al., 2003; Wickner and Schekman, 2008; Chernomordik and Kozlou, 2008). The best characterized SNAREs are those mediating neurotransmitter release, and include the C-terminally anchored integral membrane protein synaptobrevin2 (VAMP2) on the vesicular membrane, as well as two proteins on the plasma membrane, the C-terminally anchored integral membrane protein syntaxin1A and the peripherally-associated membrane protein synaptosome-associated protein of 25 kDa (SNAP-25) (Ungar and Hughson, 2003; Jahn and Scheller, 2006). These three proteins form a stable ternary *trans* SNARE complex that bridges the opposing vesicular and plasma membranes prior to the actual fusion event and mediates membrane fusion *in vitro* upon reconstitution of the proteins into liposomes (Lin and Scheller, 1997; Hanson et al., 1997; Weber et al., 1998; Poirier et al., 1998; Sutton et al., 1998; Rizo and Rosenmund, 2008).

Higher-order SNARE complex multimers seem to be required for efficient membrane fusion in intact cells (Stewart et al., 2000; Hua and Scheller, 2001; Han et al., 2004; Montecucco et al., 2005). Distinct molecular interactions responsible for SNARE complex oligomerization have been reported (Littleton et al., 2001; Tokumaru et al., 2001; Kweon et al., 2002; Fdez et al., 2008), including interactions mediated by the transmembrane domains (TMDs). For example, self-interactions of the syntaxin1A TMDs have been proposed to play a scaffolding role for the subsequent formation of a

supramolecular SNARE complex at the fusion site (Lu et al., 2008), or to be implicated in mediating the transition from a hemifusion to a full fusion state (Hofmann et al., 2006).

Recent crystallographic studies of full-length SNARE complexes indicate that the TMD of VAMP2 is alpha-helical, and tightly packs against the TMD of syntaxin 1A along the N-terminal half, whilst the C-terminal parts of the TMDs steer away from each other (Stein et al., 2009). Whilst the structure likely reflects that of a *cis* SNARE complex, it nevertheless indicates differences in packing interactions between the N-terminal and C-terminal halves of the TMDs.

TMD interactions of SNARE proteins not incorporated into complexes may occur as well. For example, individual VAMP2 or syntaxin1A molecules have been reported to form TMD-mediated homodimers and heterodimers in a sequence-specific manner (Laage and Langosch, 1997; Margittai et al., 1999; Laage et al., 2000; Fleming and Engelman, 2001a; Kroch and Fleming, 2006; Tong et al., 2009). However, the relative affinity of such interactions has been controversial (Bowen et al., 2002; Roy et al., 2004), and their *in vivo* relevance remains unclear, given that all studies have been performed *in vitro*, that is, in detergent solution or in liposomes. In addition, although the critical importance of the TMD of SNAREs for membrane fusion events is recognized (Langosch et al., 2007), the precise structural and functional requirements for the TMD, especially in intact cells, are largely unknown.

In this work, we attempt to determine functionally important features of the VAMP2 TMD, and correlate TMD interactions between VAMP2 molecules to SNARE-mediated fusion activity. A bimolecular fluorescence complementation (BiFC) assay (Kerppola, 2006; Kerppola, 2008) was used to probe for interactions of SNARE

molecules in intact cells. The data show that the TMDs of VAMP2 interact, with a glycine residue in the center playing an important role. Using a toxin rescue secretion assay in neuroendocrine cells, we found that mutations which abolished TMD interactions were without effect on neurosecretion, indicating that such interactions are not relevant to the fusion activity of the v-SNARE protein. However, secretory deficits were observed with a set of mutations affecting the length of the TMD, and were more pronounced when introduced at the C-terminal half, as compared to the N-terminal half. Thus, structural length requirements at the C-terminal half of the VAMP2 TMD seem to be crucially important for bringing about SNARE-mediated neurosecretion.

Results

Dimerization of VAMP2 molecules in intact cells as visualized by BiFC.

To probe for SNARE protein interactions in intact cells, we co-expressed VAMP2 fusion proteins, each tagged at the C-terminus with complementary, nonfluorescent fragments of Venus, a temperature-insensitive GFP variant (Shyu et al., 2006; Shyu et al., 2008). Reconstitution of the fluorophore provides an indirect measure of interactions between two VAMP2 molecules covalently linked to each fragment (Fig. 1A). Neuroendocrine PC12 cells were co-transfected with the two fusion proteins, and a VAMP2-BiFC signal was observed in live cells as well as upon fixation (Fig. 1B,C). VAMP2-BiFC was detected in neuritic processes, where it overlapped with the vesicle marker synaptotagmin, as well as in a perinuclear compartment largely overlapping with a trans-Golgi marker (Fig. 1C). The BiFC signal specifically reflected VAMP2 interactions, as only occasional, weak cytosolic BiFC was observed when the two halves of Venus were employed on their own (Fig. 1C). The subcellular localization of VAMP2-BiFC matched the localization of C-terminally GFP-tagged VAMP2, as well as that of endogenous VAMP2 (Fig. S1), indicating that it was not due to aberrant localization of tagged, overexpressed proteins. In addition, tagging the C-termini of synaptotagmin did not result in BiFC (not shown), even though both tagged fragments were expressed as assessed by Western blotting (Fig. S2), suggesting that the VAMP2 BiFC signal was not merely a result of overexpressing a synaptic vesicle protein. When the C-termini of syntaxin1A molecules were tagged with Venus fragments, BiFC was observed at the plasma membrane in a non-even, patchy manner (Fig. S3), whilst BiFC of VAMP2/syntaxin1A was more homogeneously distributed across the plasma membrane

(Fig. S4). Thus, the intracellular distribution of VAMP2-BiFC likely reflects homotypic interactions between individual, non-complexed VAMP2 molecules, rather than the presence of dimeric *trans* SNARE complexes (Fig. 1D).

Dimerization of VAMP2 is mediated by the TMDs.

The sequences responsible for the interaction between VAMP2 molecules were next probed with a series of deletion mutants (Fig. 2A). VAMP2 harbours a synaptic vesicle targeting signal, and distinct mutations of this signal either enhanced its presence in the plasma membrane or in intracellular structures (Fig. S5), as previously described (Grote et al., 1995; Grote and Kelly, 1996). Deletion of the SNARE coiled-coil domain, or of the entire cytoplasmic domain of VAMP2 prevented trafficking of such mutants out of a trans-Golgi compartment (Fig. 2A,B). However, these truncated mutants still displayed BiFC (Fig. 2C,D), indicating that interactions between VAMP2 molecules detected by BiFC are mediated by the TMDs. In addition, probing BiFC between a wildtype and a TMD-only VAMP2 molecule revealed no fluorescence complementation in neuritic processes, suggesting that TMD-mediated VAMP2 interactions are not permissive for the proper targeting and trafficking of VAMP2 (Fig. 2E).

A glycine residue is crucial for TMD-mediated interactions.

A careful inspection of the sequences of the VAMP2 TMD amongst different species indicated the largely conserved presence of a glycine residue (G100) in the center of the TMD (Fig. 3A). Glycine residues in TMDs have been shown to play important structural roles in a variety of transmembrane proteins, with a high occurrence at helix

crossing points (Lemmon et al., 1994; MacKenzie et al., 1997; Burke et al., 1997; Javadpour et al., 1999; Fleming and Engelman, 2001b). We next probed for the importance of molecular volume and flexibility at this position (Fig. 3B). For this purpose, the glycine residue was replaced by amino acids of increasing molecular volume (Y > V > A > G) (Zamyatnin, 1972; Szule and Coorsen, 2004). All mutants were determined to be overexpressed to similar degrees, and to be properly localized and co-localized with synaptotagmin in neuritic processes (Fig. S6). Interestingly, whilst the G100A mutant still displayed fluorescence complementation (Fig. 3C), no complementation was observed with G100V or G100Y mutants. Lack of complementation with the G100V or G100Y mutants was not due to a lack of co-expression as assessed by Western blotting (Fig. 3D). Furthermore, a combination of G100V/wildtype VAMP2 did give BiFC (Fig. 3C), whilst a combination of G100Y/wildtype VAMP2 did not. Finally, mutating the glycine to a proline residue, reported to induce helix distortion and/or dynamically flexible hinges (Cordes et al., 2002), displayed BiFC (Fig. 3C). Together, these data indicate an important role for a glycine residue in VAMP2 TMD interactions.

TMD-mediated VAMP2 interactions are not important for neurosecretion.

We next evaluated whether the observed TMD-mediated VAMP2 interactions are important for membrane fusion events. For this purpose, neuroendocrine PC12 cells were transfected with a plasmid containing both non-tagged VAMP2 and human growth hormone (hGH) (Fdez et al., 2008). Cells were permeabilized and treated with recombinant botulinum neurotoxin type F light-chain (botF/LC), which cleaves and

inactivates VAMP2 (Fig. 4A). As expected, Ca^{2+} -dependent secretion of hGH was decreased (to 27% of control). The expression of botF/LC-resistant VAMP2 (K59R) (Schmidt and Stafford, 2005) restored secretion (102% of control) in the presence of toxin (Fig. 4B). This rescue assay was then used to measure the ability of VAMP2 TMD mutants to support exocytosis in the absence of endogenous protein. Surprisingly, none of the glycine mutants with increased molecular volume, including mutants which abolished TMD-mediated interactions as assessed by BiFC, displayed any effect on neurosecretion (Fig. 4C), whilst mutating the glycine to a proline residue slightly enhanced secretion (Fig. 4C). Finally, we also mutated a series of residues previously described to contribute to a VAMP2 TMD interaction interface as analysed *in vitro* (Laage and Langosch, 1997; Margittai et al., 1999; Laage et al., 2000; Fleming and Engelman, 2001a; Kroch and Fleming, 2006; Tong et al., 2009) (dimmut1/2/3) (Fig. 4D). These mutants were overexpressed to similar degrees as wildtype VAMP2 and properly localized (Fig. S6), still displayed BiFC (Fig. 4E), and did not show secretory deficits (Fig. 4C). Thus, TMD-mediated interactions between VAMP2 as measured by BiFC do not seem to play an important role for neurosecretion in intact cells.

The C-terminal half of the VAMP2 TMD is functionally important.

It is well established that the SNARE TMDs play an important role in bringing about membrane fusion events (Grote et al., 2000; McNew et al., 2000; Han et al., 2004; Langosch et al., 2007). To more precisely map the functionally important regions, we generated a series of N-terminal or C-terminal deletion and insertion mutants (Fig. 5A). Exogenous, non-tagged VAMP2 was expressed at ~4 times over endogenous levels, and

all mutants analysed were expressed to similar degrees (Fig. S6). We next determined the subcellular localization of all mutants as GFP-fusion proteins (Fig. 5B, Fig. S6). Deleting three residues at the N-terminus (d97-99), or three (d114-116) or five (d112-116) residues at the C-terminus resulted in VAMP2 mutants which were properly localized to neuritic processes, whilst a mutant lacking six residues (d111-116) at the C-terminus was co-localized with synaptotagmin to a lesser degree, and a mutant lacking seven residues at the C-terminus (d110-116) was retained in a perinuclear compartment (Fig. 5B, Fig. S6). Conversely, inserting three residues at the N-terminal (M96+3L) or C-terminal (I108+3L) half of the VAMP2 TMD did not alter intracellular localization, whilst inserting six residues at the N- or C-terminus of the TMD (M96+6L, I108+6L) resulted in additional punctate intracellular localization (Fig. 5B, Fig. S6). All mutants which were properly localized displayed similar predicted negative apparent free energy values for insertion of the TMD into the ER membrane, indicating that they are all likely to be properly recognized as a TMD helix and integrated into the membrane (Fig. S7).

VAMP2 TMD mutants which were properly localized were then analysed for their ability to support membrane fusion. All toxin-insensitive C-terminal truncation or insertion mutants were severely impaired in their ability to rescue secretion (Fig. 5C). In contrast, truncation or insertion mutants at the N-terminal half of the VAMP2 TMD had no or little effect (Fig. 5C). Similarly, deletion of a short region proposed to induce a kink prior to the TMD (Kweon et al., 2003) (dLK/dNLK), had no effect on the extent of neurosecretion (Fig. 5C). Altogether, the data indicate that structural length requirements, especially towards the C-terminal half of the VAMP2 TMD, are essential for SNARE-

mediated neurosecretion, whilst TMD-mediated interactions as measured here by BiFC are without functional implications.

Discussion

Recent studies suggest the importance of multiple SNARE complexes at the fusion site for successful fusion (Stewart et al., 2000; Hua and Scheller, 2001; Montecucco et al., 2005; Hofmann et al., 2006). In addition, there is evidence that multimers of syntaxin1A TMDs are essential for the formation of the fusion pore (Han et al., 2004; Lu et al., 2008). Although the critical importance of the syntaxin1A TMDs for membrane fusion events is recognized, the precise structural and functional role of the VAMP2 TMD, especially in intact cells, is not well understood.

We employed BiFC (Kerppola, 2006; Shyu et al., 2006; Kerppola, 2008; Shyu et al., 2008) to probe for SNARE protein interactions *in vivo*. Studies of this type showed that VAMP2 molecules dimerize in both a perinuclear compartment as well as in neuritic processes, and that dimerization is mediated by their TMDs. Such interactions are not sufficient to escort a truncated VAMP2 molecule, interacting with a wildtype molecule containing all necessary targeting information, out of a perinuclear compartment. As reconstitution of an intact, fluorescent GFP molecule is an irreversible event (Kerppola, 2006; Kerppola, 2008), it seems possible that complementation ‘locks’ the interaction of the TMDs in a manner preventing further exit from a trans-Golgi compartment, such that only uncomplexed, tagged full-length VAMP2 molecules would go on to their intracellular vesicular destinations.

Interestingly, BiFC between syntaxin1A molecules was observed in a non-even, patchy manner at the plasma membrane. It remains to be determined whether this signal reflects multimers of *trans* SNARE complexes (Lu et al., 2008), or clusters of SNAREs at the plasma membrane, as previously described (Lang et al., 2001; Sieber et al., 2007).

Similarly, additional studies are warranted to determine whether the rather homogenous plasma membrane BiFC signal between a syntaxin 1A and a VAMP2 molecule reflects *cis* SNARE complexes, or interactions between individual, non-complexed SNARE molecules.

The structure of the VAMP2 TMD in the membrane has been controversial. Initial computation and mutagenesis studies predicted that the TMD exists as a dimer with two helices oriented at a cross-angle of 38 degrees, with residues 99, 102, 103, 107, 110 and 111 at the dimer interface (Laage and Langosch, 1997; Laage et al., 2000; Fleming and Engelman, 2001a; Roy et al., 2004). Whilst biophysical studies on the structure of the TMD are largely confined to membrane mimetic environments *in vitro*, our studies in intact cells would indicate that these residues are not sufficient to mediate TMD interactions, and are not critical for VAMP2-mediated fusion activity.

Our data indicate an important role for a glycine residue in facilitating VAMP2 TMD interactions. Glycine is frequently found in the TMDs of membrane proteins, and has been shown to contribute to TMD dimerization of several single-pass membrane proteins (Lemmon et al., 1994; MacKenzie et al., 1997, Burke et al., 1997; Javadpour et al., 1999; Fleming and Engelman, 2001b). Replacing the glycine residue with residues of increased molecular volume abolished TMD interactions, but did not interfere with neurosecretion in our toxin rescue assay, suggesting that the TMD interactions as measured by BiFC are not necessary for the fusion activity of the v-SNARE. However, replacing the glycine residue with a helix-distorting proline residue displayed slightly enhanced neurosecretion as compared to wildtype. Thus, together with other TMD mutants which displayed deficits in secretion, the observation of both inhibitory or

enhancing effects on membrane fusion is indicative of a direct role for the VAMP2 TMD in exocytosis (Szule and Coorssen, 2004).

Mutational analysis of VAMP2 further indicated that the C-terminal residues of the TMD are functionally important. It seems likely that these residues are transiently forced into close proximity at the point of membrane fusion (Tong et al., 2009), but our BiFC analysis may not be able to resolve such interactions on the background of fluorescence from individual, non-complexed VAMP2 molecules interacting *via* their TMDs. The predicted TMD of VAMP2 is unusually large, and has been shown to be embedded in the membrane with a tilt with respect to the bilayer normal (Bowen and Brunger, 2006). Thus, the TMD-mediated interaction of VAMP2 molecules identified here by BiFC likely involves a conformation whereby glycine residues oriented toward the helix-helix interface contribute to the packing of two tilted helices, whilst additional, transient conformations close to the point of membrane fusion may exist as well.

In the present study, we used a toxin rescue assay to investigate SNARE-dependent membrane fusion. However, caveats of this assay are that it merely measures the extent of neurosecretion, rather than kinetic effects and/or fusion pore phenotypes. Thus, further investigations of the mutants described here using capacitance or amperometry approaches able to evaluate effects on fusion pore phenotypes are warranted.

In summary, we describe for the first time TMD-mediated interactions between VAMP2 molecules in intact cells using a BiFC approach. Glycine residues play a crucial role in TMD helix association, but such interactions do not seem to be required for efficient neurosecretion. Severe secretory deficits are observed when shortening or

lengthening the C-terminal, but not the N-terminal half of the TMD, suggesting that distinct structural length requirements within the VAMP2 TMD may be largely confined to the C-terminal part. In this manner, it is tempting to speculate that the conformation of the C-terminal part of the VAMP2 TMD, further modulated by the lipid environment (Tong et al., 2009; Chang et al., 2009), may regulate the formation of a hemifusion state (Chernomordik and Kozlov, 2005; Xu et al., 2005; Hofmann et al., 2006; Wong et al., 2007; Lu et al., 2008; Liu et al., 2008; Chang et al., 2009) *en route* to full membrane merger.

Materials and Methods

Plasmid constructs and site-directed mutagenesis.

For secretion assays, full-length, non-tagged rat VAMP2 (amino acids 1-116) was expressed from a pCMV-driven promoter in a vector where expression of hGH is driven from an SV40 promoter (pCMV5-VAMP2-SV40-hGH) (Fdez et al., 2008). C-terminally GFP-tagged VAMP2 was generated by subcloning full-length VAMP2 into a pGFPemd vector (Packard) using the EcoRI/BamHI sites, with a resulting linker (TDPPVAT) between the VAMP2 and the GFP sequences. GFP-tagged constructs were also generated whereby VAMP2 was subcloned into the EGFP-C1 vector (Clontech) using the HindIII/BamHI sites to generate an N-terminal GFP fusion protein. C-terminally GFP-tagged syntaxin1A was generated by subcloning full-length syntaxin1A into a pGFPemd vector (Packard) using the EcoRI/HindIII sites, with a resulting linker (KLAVPRARDPPVAT) between the syntaxin1A and the GFP sequences. N-terminally GFP-tagged syntaxin1A was a generous gift of Dr. G. Augustine.

Site-directed mutagenesis was performed using the QuickChange Site-Directed Mutagenesis Kit (Stratagene) according to manufacturer's instructions. To generate the VAMP2 BiFC constructs, a linker (SGGSGGTVGSR) was generated at the C-terminus of VAMP2 in the pCMV5-VAMP2-SV40-hGH construct using site-directed mutagenesis. The two halves of Venus (VenusN: 1-155; VenusC: 156-239) were then PCR amplified from a full-length construct, digested and cloned in-frame with the linker using the XbaI/BamHI sites.

VAMP2-VenusN was PCR amplified and subcloned into pCMV-HA (Clontech) using the EcoRI/XhoI sites to generate an N-terminally HA-tagged construct, and

VAMP2-VenusC was PCR amplified and subcloned into pCMV-myc (Clontech) using the EcoRI/XhoI sites to generate an N-terminally myc-tagged construct, respectively. To generate the syntaxin1A BiFC constructs, syntaxin1A was PCR amplified and cloned into the VAMP2 BiFC vectors using EcoRI, thereby replacing the VAMP2 sequences by the syntaxin1A sequences. To generate the synaptotagmin1 BiFC constructs, full-length synaptotagmin was PCR amplified and cloned into the syntaxin1A BiFC vectors using XbaI and BamHI, thereby replacing the syntaxin1A sequences by the synaptotagmin1 sequences. Control constructs expressing only the two individual halves of Venus were generated by deleting VAMP2 from the VAMP2 BiFC constructs by prior introduction of an EcoRI site at the C-terminus of VAMP2 using site-directed mutagenesis, followed by digestion with EcoRI and re-ligation. The VAMP2delta1-78 deletion constructs were generated by introducing an EcoRI site at position E78, followed by digestion with EcoRI and re-ligation. The VAMP2-TMD constructs were generated by introducing an EcoRI site at position W90, followed by digestion with EcoRI and re-ligation. All other mutant VAMP2 constructs were generated using site-directed mutagenesis. All constructs were verified by DNA sequencing. The identity of primers used in this study are available upon author's request.

PC12 cell culture, transfection and imaging.

PC12 cells were grown and transfected essentially as described (Fdez et al., 2008). Double-transfections were performed with each 2.4 µg of DNA using 10 µl LipofectAMINE 2000 (Invitrogen). Cells were grown for 3 days either in full media (non-differentiated) or in serum-reduced media (1%) containing 50 ng/ml NGF 2.5 S

(Invitrogen) (differentiated). Cells were examined either live, or upon fixation (Fdez et al., 2008) and mounting (ProLong-Gold antifade reagent, Invitrogen). For co-localization analysis, the following antibodies were used: rabbit polyclonal anti-synaptotagmin (p65, 1:1000) (Fdez et al., 2008), mouse monoclonal anti-VAMP2 (Cl 69.1, Synaptic Systems, 1:5000), mouse monoclonal anti-rat TGN38 (BD Biosciences, 1:800), rabbit polyclonal anti-calnexin (Stressgen, SPA860, 1:300), mouse monoclonal anti-syntaxin (CL HPC-1, SIGMA, 1:500), mouse monoclonal anti-TfR (Invitrogen, 1:300), mouse monoclonal anti-EEA1 (BD Biosciences, 1:250), mouse monoclonal anti-synaptophysin (CL SVP38, SIGMA, 1:200), mouse monoclonal anti-GM130 (BD Biosciences, 1:100) and rabbit polyclonal anti-GFP (Abcam, 1:500). Secondary antibodies included AlexaFluor594-conjugated goat anti-mouse (Invitrogen, 1:1000) and AlexaFluor594-conjugated goat anti-rabbit (Invitrogen, 1:1000).

Images were acquired on a Leica TCS-SP5 confocal microscope using a 63.0x1.40 oil UV objective (HCX PL APO CS). Images were collected using single excitation for each wavelength separately (488 nm Argon Laser line and a 500-545 nm emission band pass; 543 nm HeNe Laser line and a 556-673 nm emission band pass). 10-15 image sections of selected areas were acquired with a step size of 0.3 μm , and Z-stack images analysed and processed using Leica Applied Systems (LAS AF6000) image acquisition software. For quantification of co-localization, three independent, non-saturated z-stack images were analyzed for each condition, whereby a fixed area of interest of 36 μm^2 was chosen to determine co-localization in neuritic processes, adjusting thresholds to 28% for each channel. Co-localization rates were obtained using

Leica Applied Systems (LAS AF6000) image acquisition software. Overexpression levels were determined as previously described (Fdez et al., 2008).

For live cell imaging, cells were monitored on an Olympus microscope (Cell R IX81) using a 40x objective and an MT20 illumination system with Orca CCD camera (Hamamatsu) in a chamber at 37°C and 5% CO₂ using a Solent scientific CO₂ enrichment and temperature system.

Toxin Rescue Assays.

For toxin rescue assays, recombinantly expressed endopeptidase light-chain of botulinum neurotoxin serotype F (botF/LC) was employed. BotF/LC was expressed in BL21(DE3) E.coli as a fusion protein comprising N-terminal maltose binding protein (MBP) and C-terminal 6-his tags. The protein was purified by binding to a Ni affinity chromatography column equilibrated in lysis/binding buffer (50 mM HEPES, 200 mM NaCl, pH 7.2) and eluted with a step gradient of 20, 40, 100 and 200 mM imidazole in lysis/binding buffer. The bulk of the protein eluted in the 100 mM step. This material was pooled (40 ml), dialyzed against lysis/binding buffer (3 changes 600 ml each at 4 °C) and then frozen as aliquots (-20 °C). The protein concentration was determined from the absorbance reading at 280 nm.

The endopeptidase activity of purified botF/LC was measured against a purified recombinant substrate (VAMP2-96-GFP). Endopeptidase activity assays were performed in assay buffer (50 mM HEPES, 0.02 mM ZnCl₂, 0.1 mg/ml BSA) with 0.004 mM substrate and two different concentrations of botF/LC (11 and 53 nM) at 37 °C for 1 hour. Cleaved substrate was measured by densitometry of stained SDS-PAGE gels and

quantified against BSA standards run on the same gel. The specific activity of the preparation was 55 pmol VAMP2-96-GFP cleaved/hour/pmol enzyme.

Determination of the cleavage of endogenous VAMP2 in PC12 cells upon toxin treatment was performed as described (Fdez et al., 2008) in the presence of 150 micrograms of botF/LC. Release of hGH from toxin-treated, permeabilized PC12 cells transfected with botF-resistant VAMP2 (K59R) was measured as described (Fdez et al., 2008) in the presence of 35 μ l/well of recombinant botF/LC.

Cell extracts and immunoblotting.

Transfected PC12 cells were washed three times with wash buffer (156 mM NaCl, 5.6 mM KCl, 5.6 mM glucose, 0.2 mM EGTA, 5 mM HEPES, pH 7.4), permeabilized for 5 min in KGEP10 buffer (10 μ M digitonin, 140 mM K-glutamate, 5 mM glucose, 5 mM EGTA, 100 μ M ZnCl₂, 20 mM PIPES, pH 6.8) and incubated in KGEP10 buffer containing 35 μ l/well botF/LC for 20 min at 37 °C. Cells were subsequently washed for 10 min with wash buffer and collected in buffer containing 50 mM Tris-HCl pH 8.0, 150 mM NaCl, 10 mM EDTA, 1% Tx-100 and 1 mM PMSF.

Cell extracts were resolved on 15 % polyacrylamide gels, VAMP2 was detected with a mouse monoclonal anti-VAMP2 antibody (clone C110.1; 1:1500; Synaptic Systems), and to confirm equal amounts of protein loading, membranes were subsequently blotted with a mouse monoclonal anti-synaptophysin antibody (clone SVP38; 1:500; Sigma).

For determination of co-expression of synaptotagmin BiFC constructs, cell extracts (40 μ g) were resolved on 12.5 % SDS-PAGE gels, and endogenous, VenusN- or

VenusC-tagged synaptotagmin1 detected by a rabbit polyclonal antibody (p65, 1:1000) (Fdez et al., 2008). As the VAMP2-VenusN and VAMP2-VenusC constructs were not recognized by either anti-VAMP2 or anti-GFP antibodies on Western blots, we generated wildtype and mutant HA-VAMP2-VenusN and myc-VAMP2-VenusC constructs. Cells were co-transfected with those constructs, and extracts (40 µg) resolved on 12.5 % SDS-PAGE gels, followed by blotting with a mouse monoclonal anti-myc antibody (Sigma, 1:500) or a rabbit polyclonal anti-HA antibody (Sigma, 1:500). Anti-myc signal was detected with LumiLight Western blotting substrate (Roche), and the anti-HA signal with ECL Advance Western blotting substrate (GEHealthcare).

Acknowledgements

We thank I. Forte-Lago for technical support, and S. High for critical reading of the manuscript. This work was supported by the Spanish Ministry of Science and Innovation (grant BFU2007-63635). The laboratory of S.H. is member of the Network for Cooperative Research on Membrane Transport Proteins, cofunded by the MEC and the European Regional Development Fund (BFU2007-30688-E/BFI). S.H. is supported by a Ramón y Cajal Fellowship. E.F. is supported by a fellowship (FPI) from the Spanish MEC.

References

- Bowen, M. and Brunger, A.T.** (2006). Conformation of the synaptobrevin transmembrane domain. *Proc. Natl. Acad. Sci. USA* **103**, 8378-8383.
- Bowen, M.E., Engelman, D.M. and Brunger, A.T.** (2002). Mutational analysis of synaptobrevin transmembrane domain oligomerization. *Biochemistry* **41**, 15861-15866.
- Burke, C.L., Lemmon, M.A., Coren, B.A., Engelman, D.M. and Stern, D.F.** (1997). Dimerization of the p185neu transmembrane domain is necessary but not sufficient for transformation. *Oncogene* **14**, 687-696.
- Chang, J., Kim, S.A., Lu, X., Su, Z., Kim, S.K. and Shin, Y.K.** (2009). Fusion step-specific influence of cholesterol on SNARE-mediated membrane fusion. *Biophys. J.* **96**, 1839-1846.
- Chernomordik, L.V. and Kozlov, M.M.** (2005). Membrane hemifusion: crossing a chasm in two leaps. *Cell* **125**, 375-382.
- Chernomordik, L.V. and Kozlov, M.M.** (2008). Mechanism of membrane fusion. *Nat. Struct. Mol. Biol.* **15**, 675-683.
- Cordes, F.S., Bright, J.N. and Sansom, M.S.P.** (2002). Proline-induced distortions of transmembrane helices. *J. Mol. Biol.* **323**, 951-960.
- Fdez, E., Jowitt, T.A., Wang, M.C., Rajebhosale, M., Foster, K., Bella, J., Baldock, C., Woodman, P.G. and Hilfiker, S.** (2008). A role for soluble N-ethylmaleimide-sensitive factor attachment protein receptor complex dimerization during neurosecretion. *Mol. Biol. Cell* **19**, 3379-3389.

- Fleming, K.G. and Engelman, D.M.** (2001a). Computation and mutagenesis suggest a right-handed structure for the synaptobrevin transmembrane dimer. *Proteins* **45**, 313-317.
- Fleming, K.G. and Engelman, D.M.** (2001b). Specificity in transmembrane helix-helix interactions can define a hierarchy of stability for sequence variants. *Proc. Natl. Acad. Sci. USA* **98**, 14340-14344.
- Grote, E., Hao, J.C., Bennett, M.K. and Kelly, R.B.** (1995). A targeting signal in VAMP regulating transport to synaptic vesicles. *Cell* **81**, 581-589.
- Grote, E. and Kelly, R.B.** (1996). Endocytosis of VAMP is facilitated by a synaptic vesicle targeting signal. *J. Cell Biol.* **132**, 537-547.
- Grote, E., Baba, M., Ohsumi, Y. and Novick, P.J.** (2000). Geranylgeranylated SNAREs are dominant inhibitors of membrane fusion. *J. Cell Biol.* **151**, 453-466.
- Han, X., Wang, C.T., Bai, J., Chapman, E.R. and Jackson, M.B.** (2004). Transmembrane segments of syntaxin line the fusion pore of Ca²⁺-triggered exocytosis. *Science* **304**, 289-292.
- Hanson, P.I., Roth, R., Morisaki, H., Jahn, R. and Heuser, J.E.** (1997). Structure and conformational changes in NSF and its membrane receptor complexes visualized by quick-freeze/deep-etch electron microscopy. *Cell* **90**, 523-535.
- Hofmann, M.W., Peplowska, K., Rohde, J., Poschner, B.C., Ungermann, C. and Langosch, D.** (2006). Self-interaction of a SNARE transmembrane domain promotes the hemifusion-to-fusion transition. *J. Mol. Biol.* **364**, 1048-1060.
- Hua, Y. and Scheller, R.H.** (2001). Three SNARE complexes cooperate to mediate membrane fusion. *Proc. Natl. Acad. Sci. USA* **98**, 8065-8070.

- Jahn, R. and Scheller, R.H.** (2006). SNAREs-Engines for membrane fusion. *Nat. Rev. Mol. Cell. Biol.* **9**, 31-43.
- Jahn, R., Lang, T. and Südhof, T.C.** (2003). Membrane fusion. *Cell* **112**, 519-533.
- Javadpour, M., Eilers, M., Groesbeek, M. and Smith, S.O.** (1999). Helix packing in polytopic membrane proteins: role of glycine in transmembrane helix association. *Biophys. J.* **77**, 1609-1618.
- Kerppola, T.K.** (2008). Bimolecular fluorescence complementation (BiFC) analysis as a probe of protein interactions in living cells. *Annu. Rev. Biophys.* **37**, 465-487.
- Kerppola, T.K.** (2006). Visualization of molecular interactions by fluorescence complementation. *Nat. Rev. Mol. Cell. Biol.* **7**, 449-456.
- Kroch, A. E. and Fleming, K. G.** (2006). Alternate interfaces may mediate homomeric and heteromeric assembly in the transmembrane domains of SNARE proteins. *J. Mol. Biol.* **356**, 184-194.
- Kweon, D.H., Chen, Y., Zhang, F., Poirier, M., Kim, C.S. and Shin, Y.K.** (2002). Probing domain swapping for the neuronal SNARE complex with electron paramagnetic resonance. *Biochemistry* **41**, 5449-5452.
- Kweon, D.H., Kim, C.S. and Shin, Y.K.** (2003). Regulation of neuronal SNARE assembly by the membrane. *Nat. Struct. Biol.* **10**, 440-447.
- Laage, R. and Langosch, D.** (1997). Dimerization of the synaptic vesicle protein synaptobrevin (vesicle-associated membrane protein) II depends on specific residues within the transmembrane segment. *Eur. J. Biochem.* **249**, 540-546.

- Laage, R., Rohde, J., Brosig, B. and Langosch, D.** (2000). A conserved membrane-spanning amino acid motif drives homomeric and supports heteromeric assembly of presynaptic SNARE proteins. *J. Biol. Chem.* **275**, 17481-17487.
- Lang, T., Bruns, D., Wenzel, D., Riedel, D., Holroyd, P. Thiele, C. and Jahn, R.** (2001). SNAREs are concentrated in cholesterol-dependent clusters that define docking and fusion sites for exocytosis. *EMBO J.* **20**, 2202-2213.
- Langosch, D., Hofmann, M. and Ungermann, C.** (2007). The role of transmembrane domains in membrane fusion. *Cell. Mol. Life Sci.* **64**, 850-864.
- Lemmon, M.A., Treutlein, H.R., Adams, P.D., Brünger, A.T. and Engelman, D.M.** (1994). A dimerization motif for transmembrane alpha-helices. *Nat. Struct. Biol.* **1**, 157-163.
- Lin, R.C. and Scheller, R.H.** (1997). Structural organization of the synaptic exocytosis core complex. *Neuron* **19**, 1087-1094.
- Lin, R.C. and Scheller, R.H.** (2000). Mechanism of synaptic vesicle exocytosis. *Annu. Rev. Cell. Dev. Biol.* **16**, 19-49.
- Littleton, J.T., Bai, J., Vyas, B., Desai, R., Baltus, A.E., Garment, M.B., Carlson, S.D., Ganetzky, B. and Chapman, E.R.** (2001). Synaptotagmin mutants reveal essential functions for the C2B domain in Ca²⁺-triggered fusion and recycling of synaptic vesicles in vivo. *J. Neurosci.* **21**, 1421-1433.
- Liu, T., Wang, T., Chapman, E.R. and Weisshaar, J.C.** (2008). Productive hemifusion intermediates in fast vesicle fusion driven by neuronal SNAREs. *Biophys. J.* **94**, 1303-1314.

- Lu, X., Zhang, Y. and Shin, Y.K.** (2008). Supramolecular SNARE assembly precedes hemifusion in SNARE-mediated membrane fusion. *Nat. Struct. Mol. Biol.* **15**, 700-706.
- MacKenzie, K.R., Prestegard, J.H. and Engelman, D.M.** (1997). A transmembrane helix dimer: structure and implications. *Science* **276**, 131-133.
- Margittai, M., Otto, H. and Jahn, R.** (1999). A stable interaction between syntaxin1a and synaptobrevin 2 mediated by their transmembrane domains. *FEBS Lett.* **446**, 40-44.
- McNew, J.A., Weber, T., Parlati, F., Johnston, R.J., Melia, T.J., Sollner, T.H. and Rothman, J.E.** (2000). Close is not enough: SNARE-dependent membrane fusion requires an active mechanism that transduces force to membrane anchors. *J. Cell Biol.* **150**, 105-117.
- Montecucco, C., Schiavo, G. and Pantano, S.** (2005). SNARE complexes and neuroexocytosis: how many, how close? *Trends Biochem. Sci.* **30**, 367.
- Poirier, M.A., Xiao, W., Macosko, J.C., Chan, C., Shin, Y.K. and Bennett, M.K.** (1998). The synaptic SNARE complex is a parallel four-stranded helical bundle. *Nat. Struct. Biol.* **5**, 765-769.
- Rizo, J. and Rosenmund, C.** (2008). Synaptic vesicle fusion. *Nat. Struct. Mol. Biol.* **15**, 665-674.
- Roy, R., Laage, R. and Langosch, D.** (2004). Synaptobrevin transmembrane domain dimerization-revisited. *Biochemistry* **43**, 4964-4970.

- Schmidt, J.J. and Stafford, R.G.** (2005). Botulinum neurotoxin serotype F: identification of substrate recognition requirements and development of inhibitors with low nanomolar affinity. *Biochemistry* **44**, 4067-4073.
- Shyu, Y.J., Liu, H., Deng, X. and Hu, C.D.** (2006). Identification of new fluorescent protein fragments for bimolecular fluorescence complementation analysis under physiological conditions. *Biotechniques* **40**, 61-66.
- Shyu, Y.J., Suarez, C.D. and Hu, C.D.** (2008). Visualization of AP-1 NF-kappaB ternary complexes in living cells by using a BiFC-based FRET. *Proc. Natl. Acad. Sci. USA* **105**, 151-156.
- Sieber, J.J., Willig, K.I., Kutzner, C., Gerding-Reimers, C., Harke, B., Donnert, G., Rammner, B., Eggeling, C., Hell, S.W., Grubmuller, H. and Lang, T.** (2007). Anatomy and dynamics of a supramolecular membrane protein cluster. *Science* **317**, 1072-1076.
- Stewart, B.A., Mohtashami, M., Trimble, W.S. and Boulianne, G.L.** (2000). SNARE proteins contribute to calcium cooperativity of synaptic transmission. *Proc. Natl. Acad. Sci. USA* **97**, 13955-13960.
- Stein, A., Weber, G., Wahl, M.C. and Jahn, R.** (2009). Helical extension of the neuronal SNARE complex into the membrane. *Nature* **460**, 525-528.
- Sutton, R.B., Fasshauer, D., Jahn, R. and Brunger, A.T.** (1998). Crystal structure of a SNARE complex involved in synaptic vesicle exocytosis at 2.4Å resolution. *Nature* **395**, 347-363.
- Szule, J.A. and Coorsen, J.R.** (2004). Comment on “Transmembrane segments of syntaxin line the fusion pore of Ca²⁺-triggered exocytosis”. *Science* **306**, 813b.

- Tokumar, H., Umayahara, K., Pellegrini, L.L., Ishizuka, T., Saisu, H., Betz, H., Augustine, G.J. and Abe, T.** (2001). SNARE complex oligomerization by synaphin/complexin is essential for synaptic vesicle exocytosis. *Cell* **104**, 421-432.
- Tong, J., Borbat, P.P., Freed, J.H. and Shin, Y.K.** (2009). A scissors mechanism for stimulation of SNARE-mediated lipid mixing by cholesterol. *Proc. Natl. Acad. Sci. USA* **106**, 5141-5146.
- Ungar, D. and Hughson, F.M.** (2003). SNARE protein structure and function. *Annu. Rev. Cell. Dev. Biol.* **19**, 493-517.
- Weber, T., Zemelman, B.V., McNew, J.A., Westermann, B., Gmachl, M., Parlati, F., Sollner, T.H. and Rothman, J.E.** (1998). SNAREpins: Minimal machinery for membrane fusion. *Cell* **92**, 759-772.
- Wickner, W. and Schekman, R.** (2008). Membrane fusion. *Nat. Struct. Mol. Biol.* **15**, 658-664.
- Wong, J.L., Koppel, D.E., Cowan, A.E. and Wessel, G.M.** (2007). Membrane hemifusion is a stable intermediate of exocytosis. *Dev. Cell* **12**, 653-659.
- Xu, Y., Zhang, F., Su, Z., McNew, J.A. and Shin, Y.K.** (2005). Hemifusion in SNARE-mediated membrane fusion. *Nat. Struct. Mol. Biol.* **12**, 417-422.
- Zamyatnin, A.A.** (1972). Protein volume in solution. *Prog. Biophys. Mol. Biol.* **24**, 107-123.

Figure Legends

Fig. 1. Dimerization of VAMP2 molecules in intact cells. (A) Schematics of the BiFC VAMP2 constructs employed. (B) VAMP2 BiFC observed in live, differentiated neuroendocrine PC12 cells. (C) Upon fixation, VAMP2 BiFC was detected in a perinuclear compartment overlapping with a trans-Golgi marker (TGN38) (top), as well as in neuritic processes, where it overlapped with synaptotagmin (p65) (middle). Only occasional weak, cytosolic BiFC was observed between the two halves of Venus on their own (bottom). (D) Diagram of two possible configurations for obtaining VAMP2 BiFC. Dimerization of trans SNARE complexes may yield BiFC at membrane fusion sites (top), or dimers of VAMP2 molecules may yield BiFC at distinct intracellular locations overlapping with that of endogenous VAMP2 (bottom).

Fig. 2. VAMP2 dimerization is mediated by the TMDs. (A) Schematics of the C-terminally tagged VAMP2 deletion constructs employed. (B) Deleting the coiled-coil domain of VAMP2 ($\Delta 1-78$ -GFP), or the entire cytoplasmic domain (TMD-GFP) resulted in a solely perinuclear localization of truncated VAMP2-GFP fusion proteins. (C) Schematics of the VAMP2 BiFC truncation constructs employed. (D) Perinuclear BiFC observed with constructs lacking the coiled-coil domain of VAMP2 ($\Delta 1-78$ N/C) or the entire cytoplasmic domain (TMD-N/C). (E) BiFC between one full-length VAMP2 molecule (VAMP2-N) and a truncated molecule lacking the coiled-coil ($\Delta 1-78$ /C) or entire cytoplasmic domain (TMD-C). BiFC was only observed in a perinuclear compartment.

Fig. 3. A glycine residue within the TMD of VAMP2 is important for TMD interactions. (A) Alignment of TMD sequences of VAMP2 across species. (B) Identity of amino acid substitutions analyzed. (C) BiFC with various mutant VAMP2 TMD domain constructs. BiFC was observed with G100A mutant (top), but not with G100V or G100Y mutants. BiFC between wildtype (VAMP2-N) and G100V-mutant (G100V-C) (middle). BiFC observed with G100P mutant (bottom). (D) Cells were co-transfected with HA-VAMP2-VenusN and myc-VAMP2-VenusC, or the indicated mutant constructs, followed by SDS-PAGE and Western blotting. Similar co-expression of wildtype, G100V and G100Y mutant BiFC constructs, indicating that lack of BiFC with G100V and G100Y is not due to lack of co-expression.

Fig. 4. TMD interactions involving the glycine residue are not required for efficient neurosecretion. (A) PC12 cells were permeabilized with 10 μ M digitonin and incubated in the presence or absence of botulinum neurotoxin F light-chain (BotF/LC), followed by detection of intact VAMP2 by Western blotting. Blots were reprobbed for synaptophysin (physin) to determine equal amounts of protein loading (right). PC12 cells, transfected with a plasmid encoding for hGH as well as wildtype or botF-resistant VAMP2 (K59R) were permeabilized with 10 μ M digitonin and incubated in the presence or absence of botF/LC. Ca^{2+} -dependent hGH release was evoked by 10 μ M Ca^{2+} for 10 min, and compared to basal release (0 μ M Ca^{2+}). The amount of hGH in the medium and in the cells was determined by an enzyme-linked immunosorbent assay, and the percentage of secreted hGH, and the total amount of hGH were calculated against an hGH standard curve. The graph (right) is a representative of three independent experiments. Error bars

are only shown if larger than bar columns. (C) Ability of different point-mutated, toxin-insensitive VAMP2 constructs to support neurosecretion in the presence of BotF/LC. Cells were transfected with a plasmid encoding for hGH as well as wildtype or toxin-resistant wildtype VAMP2 (wt-r), or toxin-resistant mutant VAMP2 as indicated, permeabilized, incubated in the presence of toxin and secretion was elicited and analyzed as described above. To standardize results from repeated experiments, secretion observed in the presence of toxin-insensitive, wildtype VAMP2 (wt-r) was set to 100%, and the relative change of rescue of secretion of test plasmids in the presence of toxin normalized to this control. Values are means \pm S.E.M. (n=3). The statistical significance of differences from wildtype were analysed by a Student's t-test (*, $p < 0.05$). (D) Identity of amino acid substitutions previously reported to inhibit TMD interactions *in vitro*. (E) BiFC with various mutant VAMP2 TMD domain constructs.

Fig. 5. The C-terminal half of the VAMP2 TMD is important for SNARE-mediated neurosecretion. (A) Identity of various amino acid deletions or insertions analyzed. (B) Intracellular localization of various C-terminally tagged GFP-mutant constructs. Arrows indicate additional intracellular, punctate staining obtained with some mutants. (C) Ability of different mutated, toxin-insensitive non-tagged VAMP2 constructs to support neurosecretion in the presence of BotF/LC. Cells were transfected with a plasmid encoding for hGH as well as wildtype or toxin-resistant wildtype VAMP2 (wt-r), or toxin-resistant mutant VAMP2 as indicated, permeabilized, incubated in the presence of toxin and secretion was elicited and analyzed as described in legend to Fig. 4. To standardize results from repeated experiments, secretion observed in the presence of

toxin-insensitive, wildtype VAMP2 (wt-r) was set to 100%, and the relative change of rescue of secretion of test plasmids in the presence of toxin normalized to this control. Values are means \pm S.E.M. (n=3). The statistical significance of differences from wildtype were analysed by a Student's t-test (*, $p < 0.05$).

Figure 1

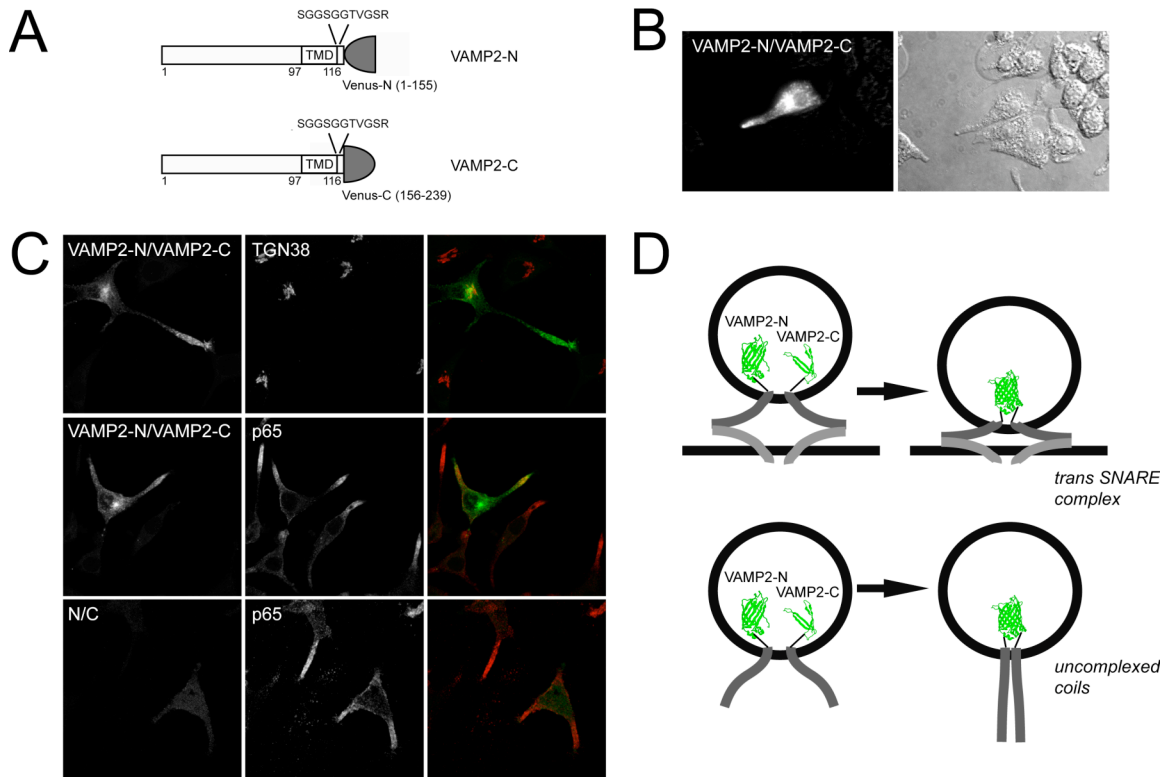


Figure 2

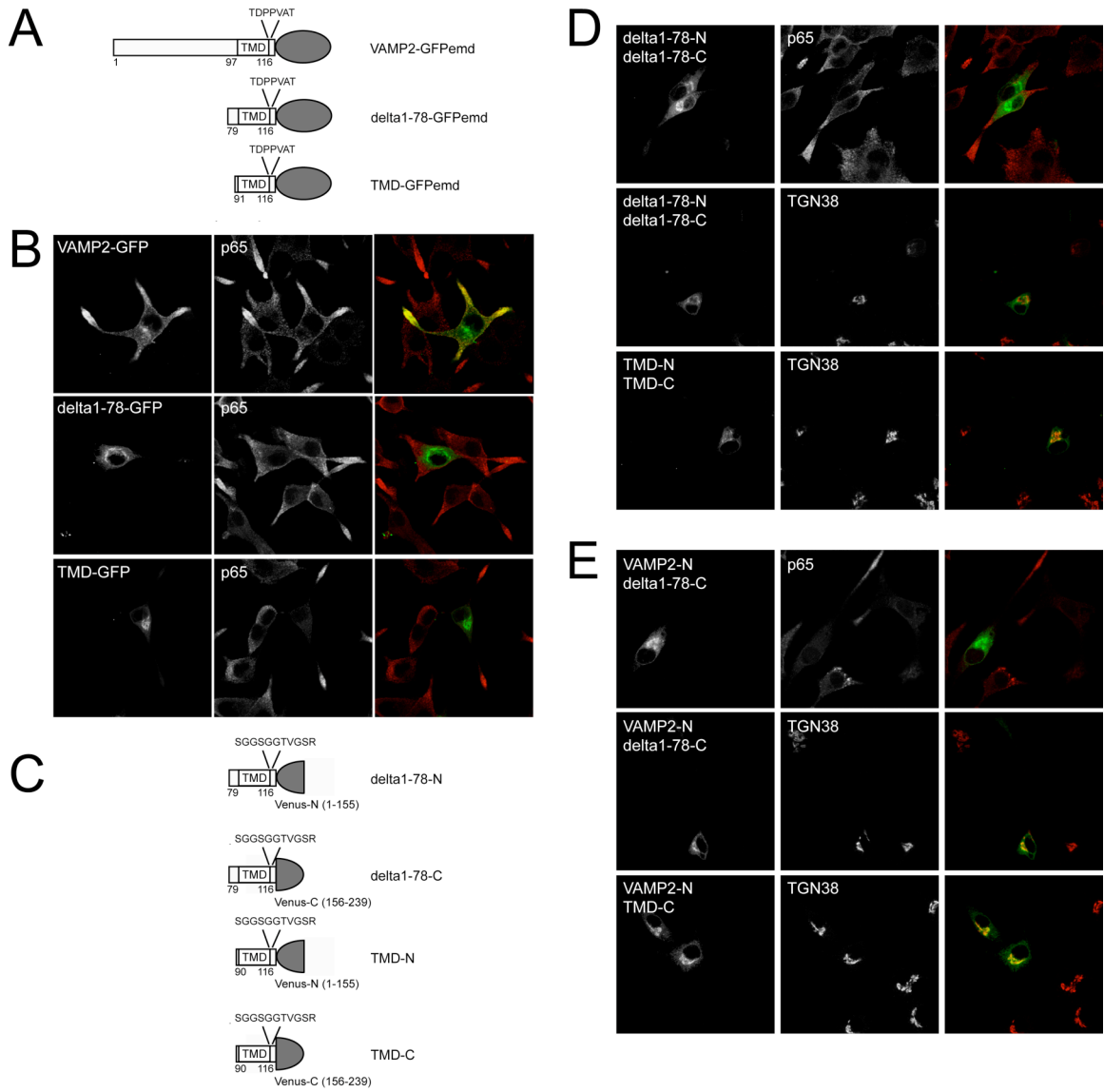


Figure 3

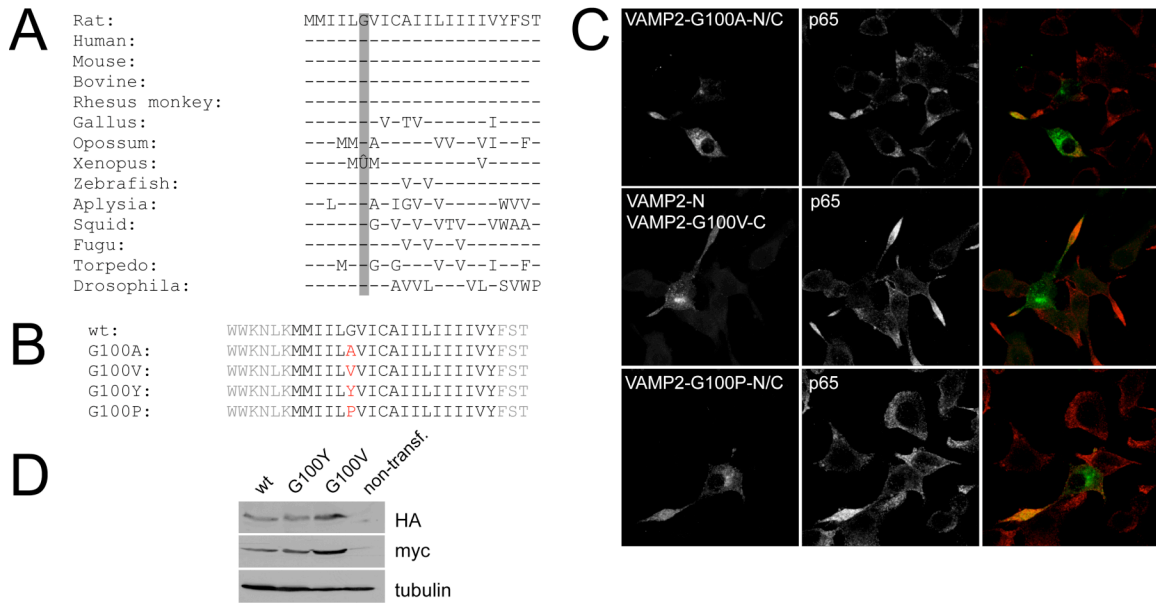


Figure 4

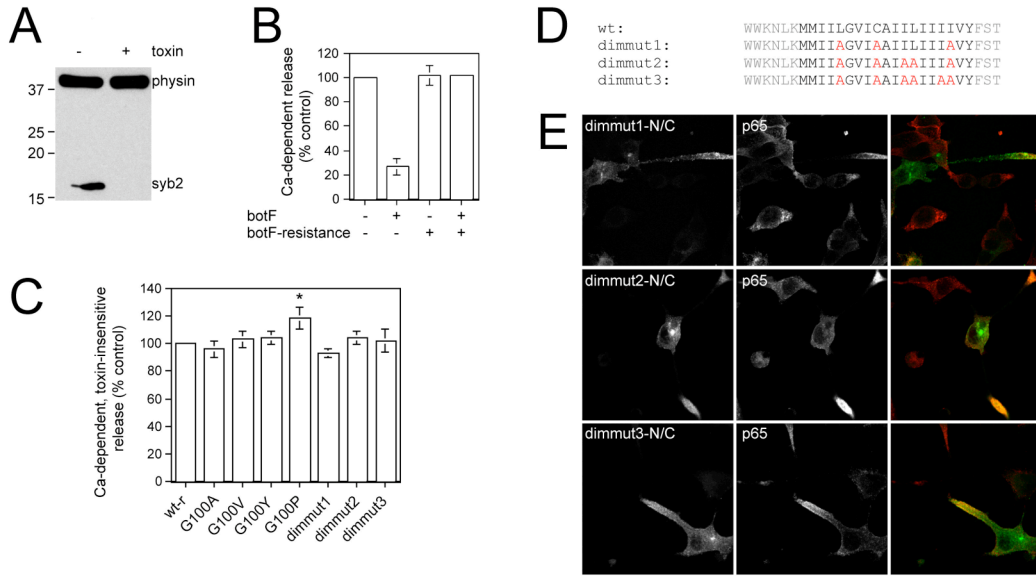


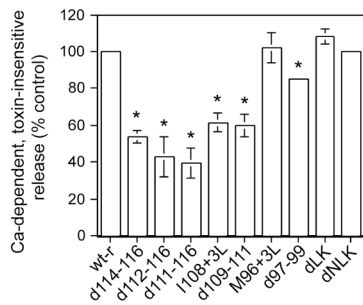
Figure 5

A

```

wt:          WWKNLKMMIILGVICAILIIIIIVYFST
d114-116:   WWKNLKMMIILGVICAILIIIIIVY---
d112-116:   WWKNLKMMIILGVICAILIIIII-----
d111-116:   WWKNLKMMIILGVICAILIIII-----
d110-116:   WWKNLKMMIILGVICAILII-----
I108+3L:    WWKNLKMMIILGVICAILIILLLIIIVYFST
I108+6L:    WWKNLKMMIILGVICAILIILLLLLIIIVYFST
d109-111:   WWKNLKMMIILGVICAILI---VYFST
M96+3L:     WWKNLKMMLLLIILGVICAILIIIIIVYFST
M96+6L:     WWKNLKMMLLLLLIILGVICAILIIIIIVYFST
d97-99:     WWKNLKMM---GVICAILIIIIIVYFST
dLK:        WWKN---MMIILGVICAILIIIIIVYFST
dNLK:       WWK---MMIILGVICAILIIIIIVYFST
    
```

C



B

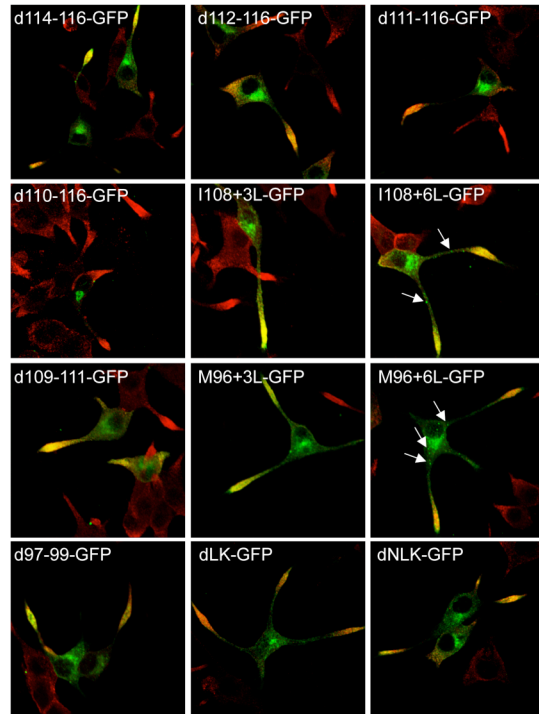


Figure S1.

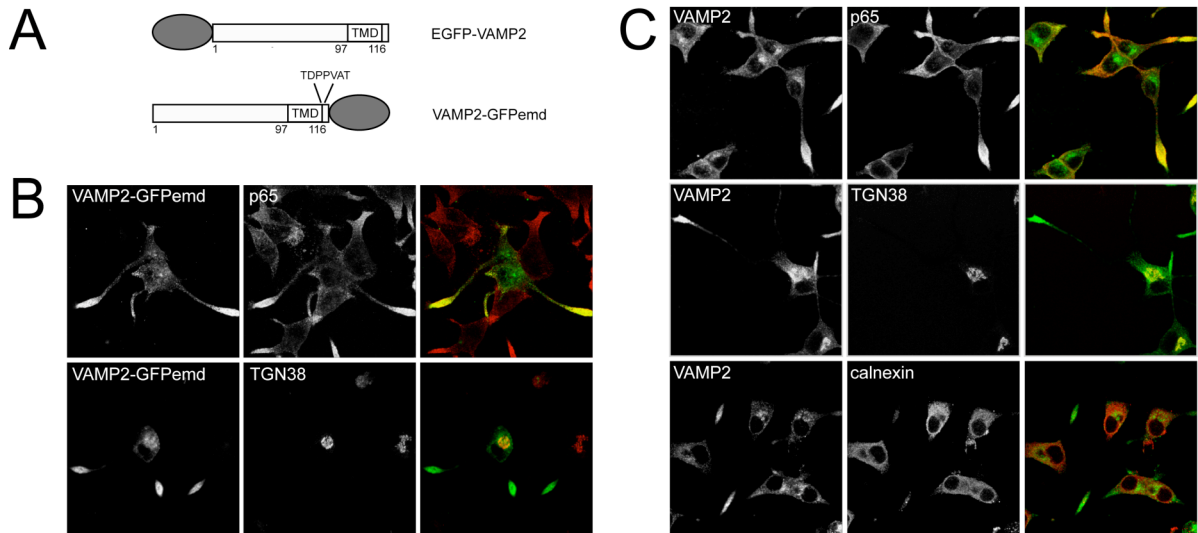


Fig. S1. Localization of endogenous VAMP2 and of C-terminally GFP-tagged VAMP2. (A) Identity of N-terminally or C-terminally GFP-tagged VAMP2 constructs. (B) C-terminally GFP-tagged VAMP2 colocalizes with synaptotagmin (p65) in neuritic processes (top), as well as with a trans-Golgi marker (TGN38) in a perinuclear compartment (bottom). The same localization was observed with an N-terminally GFP-tagged VAMP2 constructs (not shown). (C) Endogenous VAMP2 colocalizes with synaptotagmin (p65) in neuritic processes (top), with a trans-Golgi marker (TGN38) in a perinuclear compartment, and faintly with a marker for the endoplasmic reticulum (calnexin) (bottom).

Figure S2.

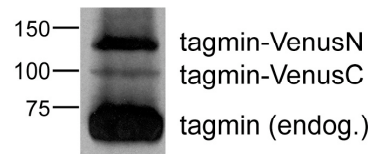


Fig. S2. Detection of synaptotagmin BiFC constructs by Western blotting from co-transfected cells. Bottom band depicts endogenous synaptotagmin levels. Whilst both tagged constructs were expressed, no BiFC signal could be detected.

Figure S3.

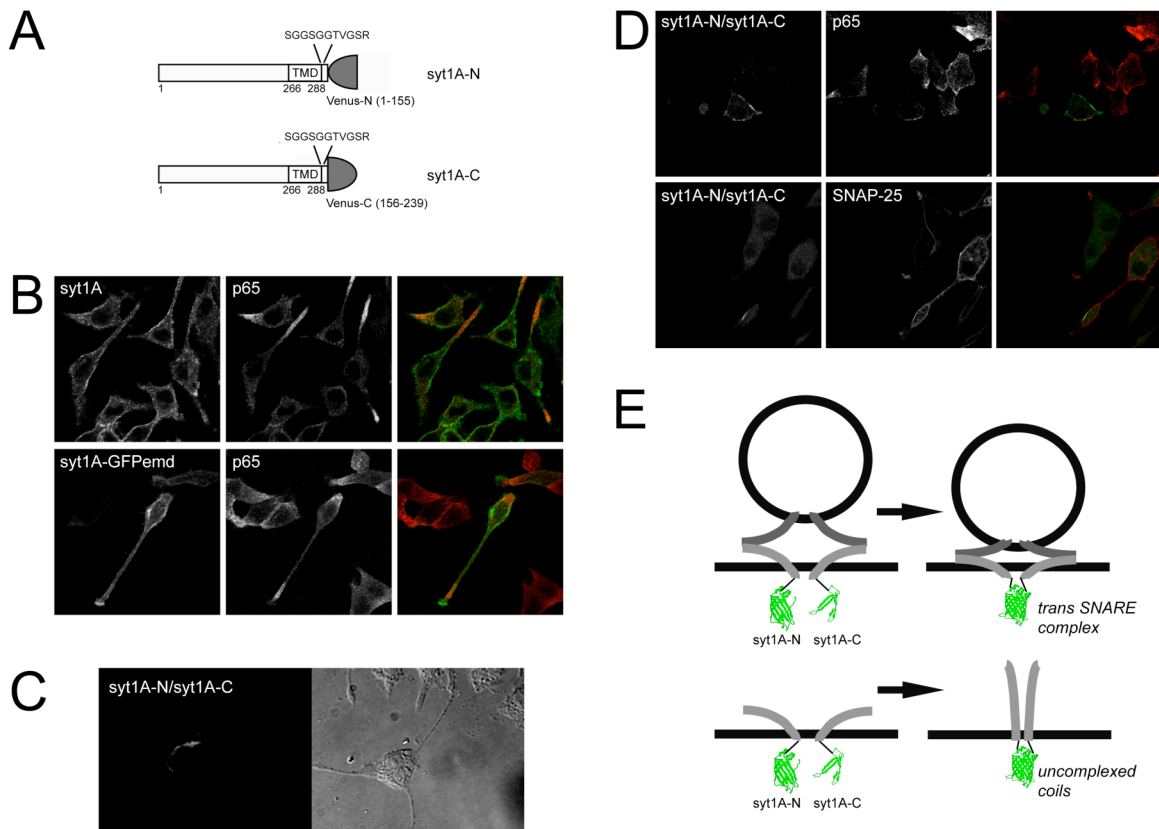


Fig. S3. Dimerization of syntaxin 1A molecules in intact cells. (A) Schematics of the BiFC syntaxin 1A constructs employed. (B) Plasma membrane localization of endogenous syntaxin 1A (top) as well as of C-terminally GFP-tagged syntaxin 1A (bottom). (C) Syntaxin 1A BiFC observed in live, differentiated neuroendocrine PC12 cells. (D) Upon fixation, syntaxin 1A BiFC was detected in a non-even, patchy manner at the plasma membrane, whilst SNAP-25 staining was largely homogeneous. In contrast to VAMP2 BiFC, syntaxin 1A BiFC was much weaker. (E) Diagram of two possible configurations for obtaining syntaxin 1A BiFC. Dimerization of trans SNARE complexes may yield BiFC at membrane fusion sites (top), or dimers of individual syntaxin 1A molecules may yield BiFC at the plasma membrane (bottom).

Figure S4.

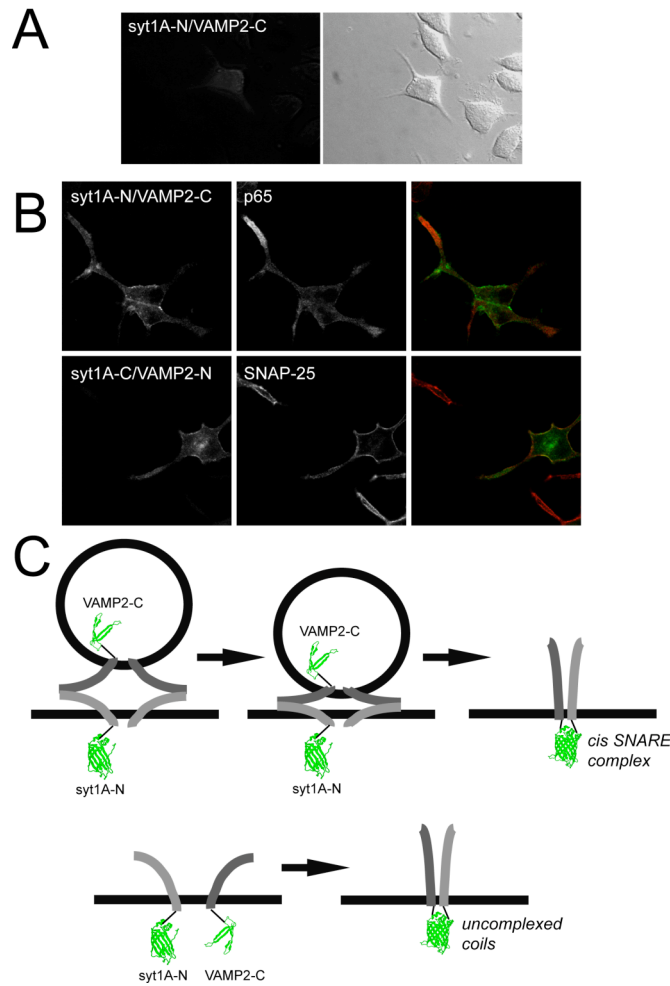


Fig. S4. Interactions between VAMP2 and syntaxin 1A molecules in intact cells. (A) Syntaxin 1A-C/VAMP2-N BiFC observed in live, differentiated neuroendocrine PC12 cells. (B) Upon fixation, syntaxin 1A/VAMP2 BiFC was detected in a rather homogeneous manner across the plasma membrane, similar to that observed with SNAP-25. In contrast to VAMP2 BiFC, syntaxin 1A/VAMP2 BiFC was much weaker. (C) Diagram of two possible configurations for obtaining syntaxin 1A/VAMP2 BiFC. Formation of cis SNARE complexes may yield BiFC at the plasma membrane (top), or individual non-complexed SNARE coils may interact at the plasma membrane (bottom).

Figure S5.

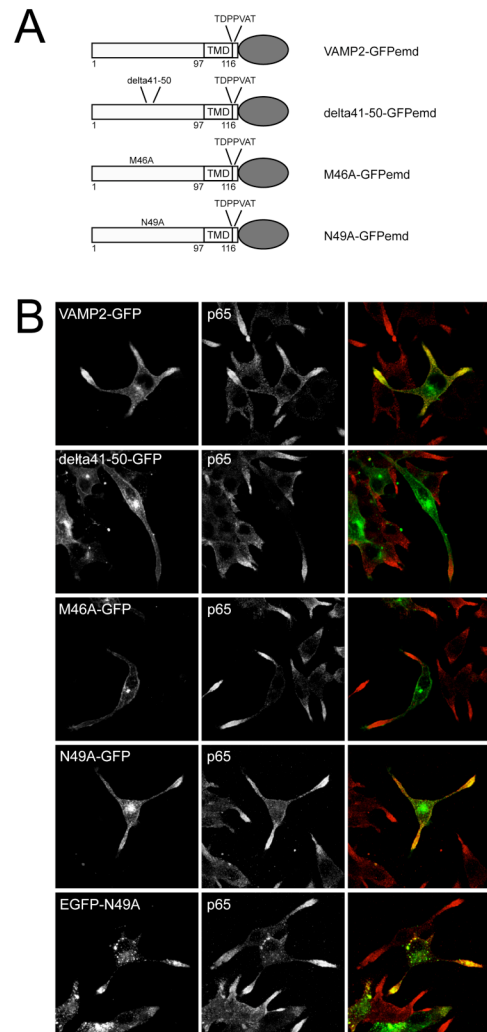


Fig. S5. Residues within VAMP2 affecting vesicular targeting. (A) Identity of C-terminally tagged mutant VAMP2 constructs analysed. (B) Subcellular localization of various C-terminally tagged mutant VAMP2 constructs. As previously described, mutating a vesicular targeting signal (delta41-50-GFP, M46A-GFP) enhances the presence of VAMP2 in the plasma membrane. Enhanced intracellular localization is observed with the N49A-GFP mutant. This is more obvious when using an N-terminally GFP-tagged construct (EGFP-N49A). Since the GFP fluorescence is quenched in an acidic environment, suggesting that the intracellular localization of the N49A-GFP mutant may include endosomal compartments, as previously described.

Figure S6.

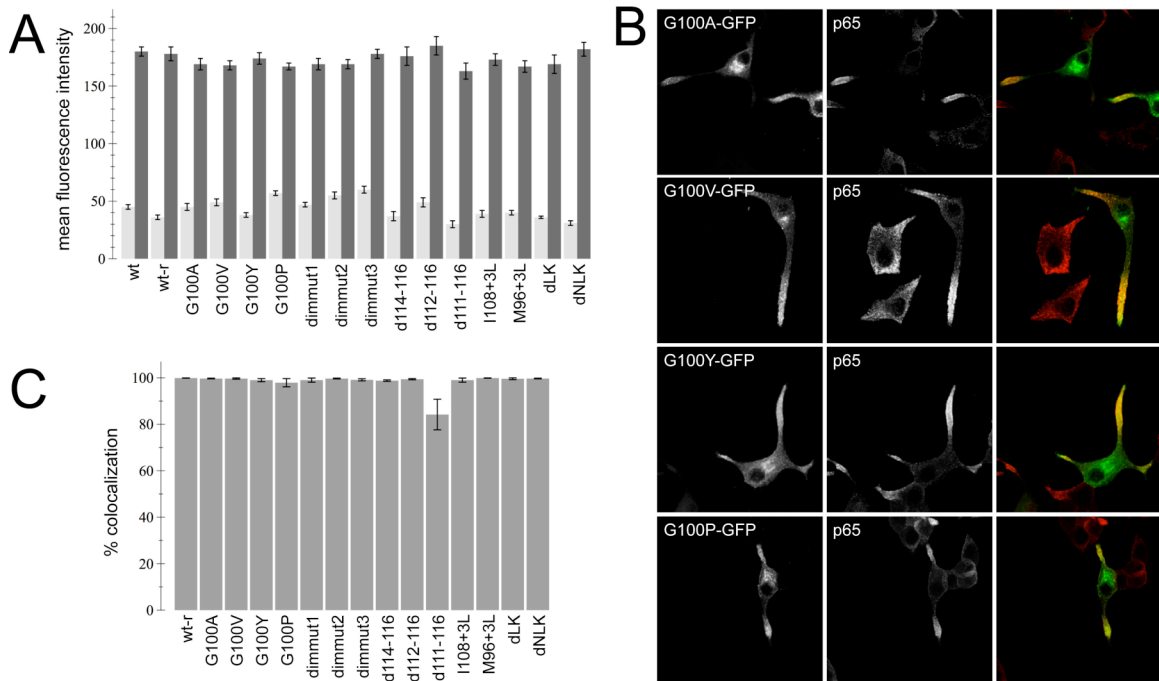


Fig. S6. Overexpression levels (A), intracellular localization (B) and colocalization (C) of mutants analysed in the present study. Mutants displayed were overexpressed to similar degrees, localized to neuritic processes as assessed by extensive overlap with a synaptic vesicle marker protein (synaptotagmin, p65), and fully co-localized with this marker protein.

Figure S7.

| CONSTRUCT | PREDICTED deltaG |
|-----------|------------------|
| wt: | -4.763 |
| G100A: | -5.087 |
| G100V: | -5.330 |
| G100Y: | -4.667 |
| G100P: | -4.093 |
| dimmut1: | -3.706 |
| dimmut2: | -2.485 |
| dimmut3: | -2.027 |
| d114-116: | -3.751 |
| d112-116: | -2.608 |
| d111-116: | -1.980 |
| I108+3L: | -6.456 |
| M96+3L: | -6.275 |
| dLK: | -4.157 |
| dNLK: | -5.087 |

Fig. S7. Prediction of corresponding apparent free energy difference, deltaG, for insertion of wildtype and mutant TMD VAMP2 sequences into the ER membrane. In principle, negative values indicate that the sequences are all predicted to be recognized as a TMD helix and integrated into the membrane. (<http://syrah.cbr.su.se/Dgpred/index.php?p=home>).

3. VESICLE POOLS AND SYNAPSES: NEW INSIGHTS INTO OLD ENIGMAS

Vesicle pools and synapsins: New insights into old enigmas

Elena Fdez and Sabine Hilfiker*

Institute of Parasitology and Biomedicine “López-Neyra”, CSIC (Spanish National Research Council), 18100 Granada, Spain (*author for correspondence; e-mail: sabine.hilfiker@ipb.csic.es)

Received 27 March 2007; Revised 14 May 2007; Accepted 14 May 2007

Published online 4 October 2007

© Springer Science+Business Media, LLC 2007

Synapsins are a multigene family of neuron-specific phosphoproteins and comprise the most abundant synaptic vesicle proteins. They have been proposed to tether synaptic vesicles to each other to maintain a reserve pool in the vicinity of the active zone. Such a role is supported by the observation that disruption of synapsin function leads to a depletion of the reserve pool of vesicles and an increase in synaptic depression. However, other functions for synapsins have been proposed as well, and there currently exists no coherent picture of how these abundant proteins modulate synaptic transmission. Here, we discuss novel insights into how synapsins may regulate neurotransmitter release.

Introduction

Synaptic transmission is initiated when an action potential triggers neurotransmitter release from a presynaptic nerve terminal (Katz, 1969). The action potential induces the opening of Ca^{2+} channels, resulting in Ca^{2+} transients which trigger synaptic vesicle exocytosis (Augustine et al., 1985). After exocytosis, synaptic vesicles are endocytosed and locally recycled to undergo another round of secretion (Ceccarelli et al., 1973; Heuser and Reese, 1973; reviewed in Südhof, 2004; Schweizer and Ryan, 2006). In addition, presynaptic nerve terminals contain many synaptic vesicles which are clustered at the active zone. Such vesicle clusters, together with local vesicle recycling events, allow nerve terminals to faithfully convert action potentials into secretory signals over a large firing range. Finally, the relationship between action potentials and release is regulated by intracellular signal transduction cascades, and can be drastically altered by the repeated use of a synapse.

Synapsins were the first synaptic vesicle proteins identified, and were discovered as major neuronal substrates for cAMP- and Ca^{2+} /calmodulin-dependent protein kinases. Biochemical studies have shown that synapsins can bind each other to form homo- and heteromultimers (Hosaka and Südhof, 1999a). In addition, synapsins bind with high affinity to synaptic vesicles as well as to cytoskeletal components such as actin. These and other data have led to a model in which synapsins, by binding to synaptic vesicles, tether vesicles to each other and/or to a presynaptic actin meshwork, thereby maintaining a reserve pool of vesicles at the presynaptic nerve terminal (reviewed in Greengard et al., 1993; Hilfiker et al., 1999). Whilst supported by a large body of experimental evidence, alternative roles for synapsins have been proposed as well, and their precise functions in exocytosis remain enigmatic (Südhof, 2004). Two reports in the present issue of Brain Cell Biology shed novel insights into their possible roles as modulators of

secretion (Tao-Cheng et al., 2007; Villanueva et al., 2007).

Synapsins and vesicle pools

A presynaptic vesicle cluster can be subdivided into distinct pools based on morphological or physiological criteria. Morphologically, a distinction is made between vesicles closely apposed to the plasma membrane (the docked vesicle pool) and those further away from the plasma membrane (the reserve pool). Physiologically, a distinction can be made based on the vesicles' ability to be released. In this manner, vesicle clusters have been subdivided into a readily releasable pool, a reserve pool and a recycling pool (Rizzoli and Betz, 2004). However, there is currently no direct correlation between morphologically and physiologically defined vesicle pools. For example, the readily releasable pool feeds from both docked as well as non-docked vesicles (Schikorski and Stevens, 2001; Rizzoli and Betz, 2004), and the recycling pool, defined as vesicles that are capable of entering the exocytic/endocytic cycle under normal conditions corresponds to around 20% of the total vesicle pool. The latter observation suggests the existence of many resting, 'reluctant' vesicles that normally do not contribute to neurotransmission

(Harata et al., 2001; Moulder and Mennerick, 2005) (Fig. 1). In addition, the size of the physiologically defined pools further depends on the transitional dynamics between them, and varies according to the type of synapse studied and the experimental paradigm employed. Thus, whilst lacking precise physiological correlates, definition of vesicle pools based on morphological criteria has yielded more straightforward information regarding proteins involved in regulating pool size and/or pool dynamics.

Synapsins exist in all organisms with a nervous system, and in vertebrates are generally encoded by three distinct genes, synapsin I, II and III, whereby alternative splicing generates further variants containing distinct C-termini (Südhof et al., 1989; Kao et al., 1998, 1999; Hosaka and Südhof, 1998) (Fig. 2). Most synapses express synapsins I and II, with levels of synapsin III much less abundant (Kao et al., 1998). At the ultrastructural level, synapsins have been shown to preferentially localize to reserve pool vesicles (De Camilli et al., 1983; Hirokawa et al., 1989; Torri-Tarelli et al., 1990; Pieribone et al., 1995; Bloom et al., 2003). Furthermore, excitatory synapses in mice deficient in all three synapsins show a selective decrease in the number of vesicles away from the plasma membrane, without an effect on the number of docked vesicles (Gitler et al., 2004). Thus, based on morphological vesicle pool criteria, synapsins

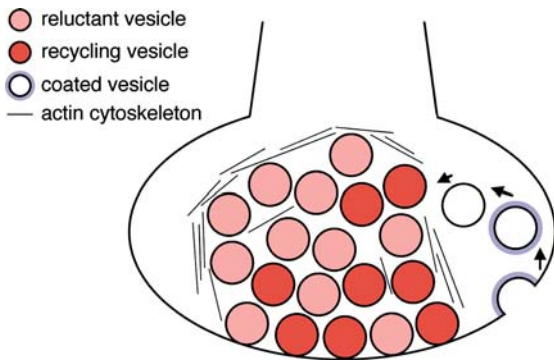


Fig. 1. Schematic representation of presynaptic vesicle pools. Morphologically, one can distinguish between a docked and a reserve pool. Physiologically defined vesicle pools include a readily releasable pool, a recycling pool and a reserve pool. Recycling pool vesicles are depicted in red, whilst 'dormant' or 'reluctant' vesicles are depicted in pink. Empty vesicles indicate newly endocytosed vesicles. Thin black lines indicate actin cytoskeleton which preferentially surrounds vesicle clusters.

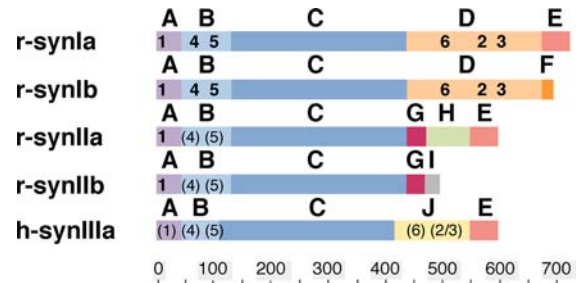


Fig. 2. Domain model of the vertebrate synapsin family, including rat synapsins Ia (r-synla) and Ib (r-synlb), rat synapsins IIa (r-synIIa) and IIb (r-synIIb) and human synapsin III (h-synIIIa). Experimentally determined phosphorylation sites (sites 1–6) are indicated in bold, with putative phosphorylation based on the presence of consensus phosphorylation sites in brackets. The distinct sites are subject to phosphorylation by the following kinases: site 1, cAMP-dependent protein kinase/Ca²⁺-calmodulin-dependent protein kinase I; sites 2/3, Ca²⁺/calmodulin-dependent protein kinase II; sites 4–6, MAP kinase; site 6, cyclin-dependent protein kinase (cdk5).

would be expected to regulate the size and/or dynamics of a reserve pool of vesicles, at least in excitatory synapses. Indeed, excitatory synapses of mice deficient in all three synapsins display an increase in the rate of synaptic depression during trains of stimuli (Gitler et al., 2004). Since stimuli used to trigger synaptic depression recruit vesicles from a physiological reserve pool, this observation correlates well with the morphological deficit of reserve pool vesicles in synapsin knockout mice. Together, these and other data suggest that synapsins tether vesicles in a reserve pool which can be mobilized during times of elevated synaptic activity.

Synapsins, phosphorylation and vesicle mobilization

How are vesicles mobilized from such a synapsin-dependent reserve pool? It seems that phosphorylation of synapsins serves as an important functional regulatory switch involved in vesicle mobilization. Synapsins are subject to phosphorylation by a variety of protein kinases. All synapsins are substrates for phosphorylation by cAMP-dependent protein kinase (PKA) and Ca^{2+} /calmodulin-dependent protein kinase I (CaM kinase I) (site 1). Furthermore, synapsins are differential targets for phosphorylation by Ca^{2+} /calmodulin-dependent protein kinase II (CaM kinase II), with synapsin I (but not synapsin II) being phosphorylated at two sites (sites 2 and 3) (Czernik et al., 1987). Finally, all synapsins are substrates for mitogen-activated protein kinase (MAP kinase) (sites 4, 5 and 6) and cyclin-dependent protein kinase (cdk5) (site 6) (Jovanovic et al., 1996; Matsubara et al., 1996) (Fig. 2). Phosphorylation results in profound changes in the biochemical properties of synapsins. Whilst a possible phosphorylation-mediated change in the ability of synapsins to multimerize remains to be determined, the phosphorylation-mediated changes in the ability of synapsins to bind to synaptic vesicles and actin are well documented. For example, phosphorylation of synapsins by PKA/CaM kinase I or by CaM kinase II drastically decreases their affinity for synaptic vesicles (Schiebler et al., 1986; Hosaka et al., 1999b; Menegon et al., 2006), whilst phosphorylation by MAP kinase has no effect on the affinity of synapsins for synaptic vesicles, but decreases their affinity for

actin (Jovanovic et al., 1996). Such *in vitro* findings are paralleled by experimental evidence *in vivo*. For example, phosphorylation at site 1 or sites 2–3, or calcium-dependent dephosphorylation at sites 4–6, leads to the reversible dissociation of synapsins from vesicle clusters and their concomitant dispersion into the axon (Chi et al., 2001, 2003; Menegon et al., 2006). The rate of synapsin dispersion precedes but parallels the rate of vesicle pool turnover, providing powerful evidence that synapsin phosphorylation comprises the mechanism underlying synaptic vesicle mobilization. In addition, vesicle mobilization seems to be dominated by distinct signalling cascades dependent on stimulation frequency. For example, phosphorylation of synapsin I by CaM kinase II seems to prevail at low stimulation frequency, whilst dephosphorylation of synapsins at the MAP kinase sites seems to prevail at high stimulation frequencies (Chi et al., 2003). A drastic decrease in the affinity of synapsin I for synaptic vesicles upon phosphorylation by CaM kinase II may be responsible for vesicle mobilization during moderate synaptic activity. On the other hand, an increase in the affinity of synapsin I for actin upon dephosphorylation of the MAP kinase sites by calcineurin may be responsible for modulating actin dynamics during high synaptic activity (Jovanovic et al., 1996; 2001). Since actin seems to be present preferentially around presynaptic vesicle clusters (Sankaranarayanan et al., 2003; Bloom et al., 2003), such dephosphorylation of the MAP kinase sites within synapsins may serve to efficiently recruit recycling vesicles back to the cluster in an actin-dependent manner, a mechanism which becomes especially important during times of high frequency activity (Bloom et al., 2003).

The study by Tom Reese's group in the current issue of *BCB* (Tao-Cheng et al., 2007) suggests that the above-mentioned model may not be entirely accurate, at least with respect to synapsin phosphorylation by CaM kinase II. Using immunogold electron microscopy in synaptic terminals from hippocampal neurons in culture, the authors find that under resting conditions, α -CaM kinase II is excluded from the synapsin-containing synaptic vesicle cluster, and instead surrounds the cluster. Co-distribution of synapsin I and CaM kinase II in neurons is only observed upon pronounced depolarization. The differential compartmentalization of synapsin and CaM kinase II under resting conditions suggests that the initial mobilization of

vesicles cannot be due to CaM kinase II-mediated synapsin phosphorylation and that such a mechanism can only act later during a stimulus train (Fig. 3). Such delayed CaM kinase II-mediated synapsin phosphorylation and concomitant vesicle mobilization may underlie the delayed and transient response enhancement phase described in hippocampal neurons (V. Jensen, SI. Walaas, O. Hvalby, personal communication). In either case, this finding suggests that vesicles may be initially recruited from the reserve pool into the readily releasable pool in a manner independent of synapsin phosphorylation. This scenario is consistent with the finding of synapsin immunoreactivity on docked vesicles (De Camilli et al., 1983; Hirokawa et al., 1989; Torri-Tarelli et al., 1990; Pieribone et al., 1995), which increases upon stimulation (Bloom et al., 2003; Tao-Cheng et al., 2007). Thus—as previously suggested (Hilfiker et al., 1998; Humeau et al., 2001)—synapsins may play an additional role in regulating neurotransmitter release, especially early in a stimulus train. Interestingly, at inhibitory synapses, synapsins preferentially regulate the size of the readily releasable pool over the reserve pool (Terada et al., 1999; Gitler et al., 2004), indicating that other vesicle tethering mechanisms must exist as well. In addition, these synapses do not contain presynaptic α -CaM kinase II (Liu and Jones, 1996). Therefore, synapsins may be continually associated with GABAergic vesicles and may affect vesicle fusion events from the readily releasable pool by an unknown mechanism.

In sum, it seems possible that synapsins may differentially contribute to the dynamics of distinct vesicle pools according to the presence and compartmentalization of a given protein kinase. Given this, future studies should determine the synapse-specific presence and/or presynaptic localization of other protein kinases that are known to influence synapsin function, such as PKA or MAP kinase. In addition, the possibility that actin filaments surrounding vesicle clusters act as scaffolds for presynaptic CaM kinase II, and possibly other protein kinases, remains an attractive but untested hypothesis.

Synapsins and vesicle integrity

An alternative function for synapsins has been proposed based on findings in synapsin I/II-deficient mice. The protein levels of several synaptic vesicle-associated proteins were reduced in extracts from mutant as compared to wild-type mice, even though mRNA levels were identical in both cases (Rosahl et al., 1995). Together with the observed decrease in vesicle number in knockout versus wild-type mice, these data could indicate that synapsins perform a role in maintaining vesicle integrity (Südhof, 2004). If this were the case, overexpression of synapsins would be expected to increase either the total number of vesicles, or the number of functional vesicles within the vesicle

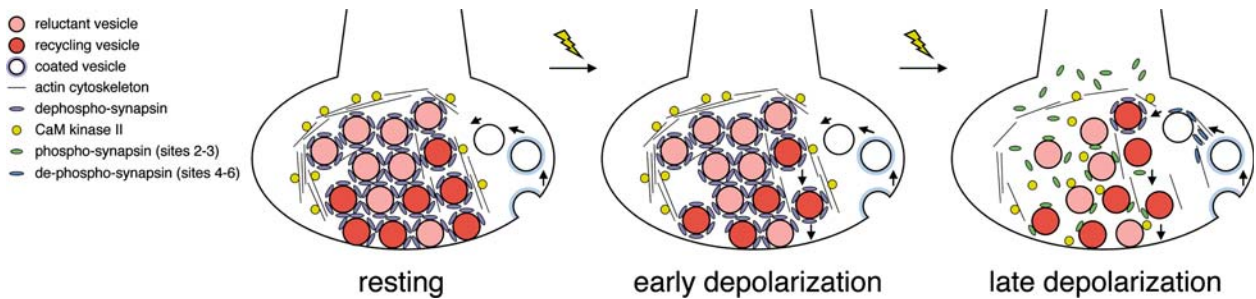


Fig. 3. Model for a delayed CaM kinase II-mediated synapsin phosphorylation. Left: before stimulation ('resting'), synaptic vesicles are clustered into a pool held together by interactions of synapsins (purple ovals) with each other or with actin filaments. CaM kinase II (yellow circles) is localized to the periphery of the vesicle cluster, possibly by interacting with the actin cytoskeleton. Early during depolarization ('early depolarization'), CaM kinase II has no access to synapsin within the cluster, and synaptic vesicles containing bound synapsin fuse with the membrane. Later during depolarization ('late depolarization') and upon vesicle recycling events, CaM kinase II can phosphorylate synapsins within the cluster. Synapsin phosphorylated by CaM kinase II (green ovals) dissociates from vesicles and can disperse into the axon. Recycled vesicles may get recruited back into the pool by their interactions with synapsins dephosphorylated at the MAP kinase sites (blue ovals). The eventual access of CaM kinase II to synapsins within the cluster may lead to an enhanced delayed response phase before vesicles are eventually depleted.

pool. Indeed, overexpression of synapsins in various cell types has been shown to increase the number of synaptic vesicles in nerve endings (Han et al., 1991; Valtorta et al., 1995; Sugiyama et al., 2000). Interestingly, synapsins may also be involved in regulating the proportion of functional vesicles. The fraction of vesicles within a synaptic vesicle cluster ('dormant' vesicles) which normally do not contribute to release have been shown to display a low release probability (Pr; Moulder and Mennerick, 2006), and synapsins seem to increase

Pr during high-frequency stimulation (Sun et al., 2006). These data suggest that synapsins decrease the number of 'dormant' vesicles, that is they increase the number of vesicles capable of entering the exo-/endocytic cycle (Fig. 4).

How could synapsins perform such a role? While several mechanisms for vesicle reluctance have been proposed (Moulder and Mennerick, 2006), reluctant or 'dormant' vesicles may comprise those with a functionally impaired complement of proteins. While the half-life of the individual

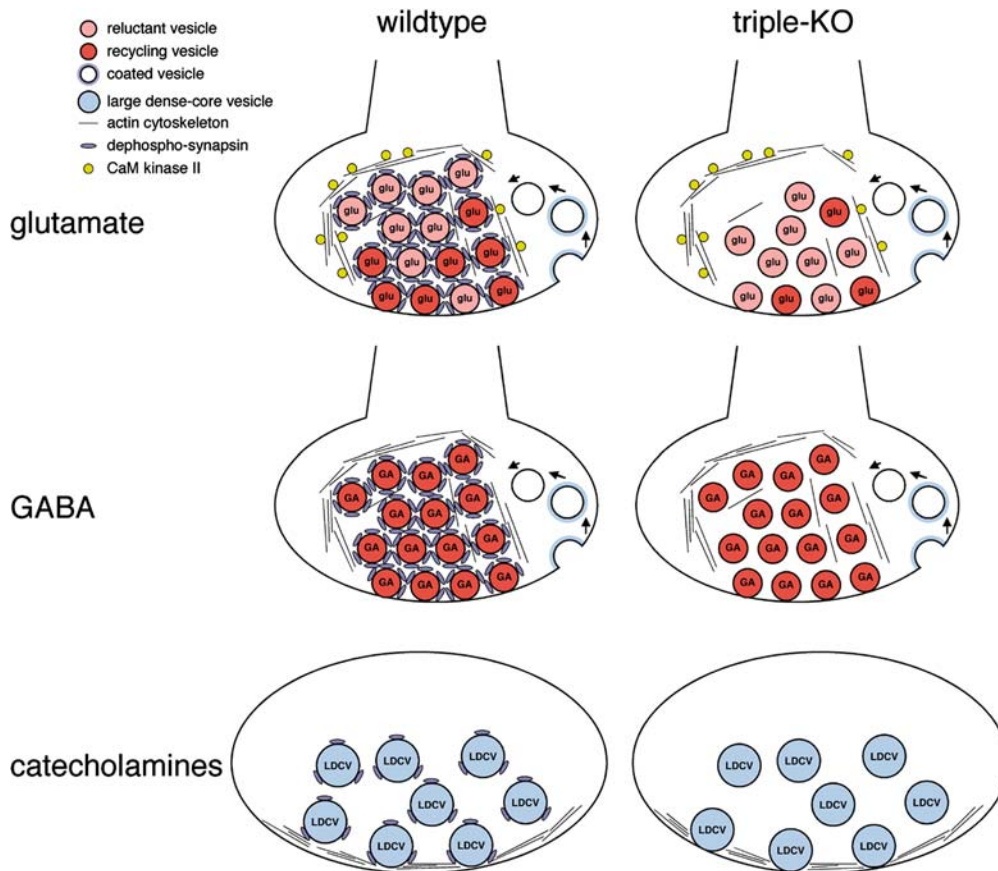


Fig. 4. Synapse-specific effects of synapsins, with wildtype synapses displayed on the left ('wildtype'), and synapsin-deficient synapses ('triple-KO') on the right. Top: in glutamatergic (glu) synapses, synapsins are involved in maintaining a cluster of vesicles, some of which are 'dormant'. CaM kinase II is present at the periphery of the cluster. The absence of synapsins leads to a depletion of vesicles away from the plasma membrane, and an increase in the number of 'dormant' vesicles. The latter effect may be due to the absence of a 'protective' function for synapsins. Middle: in GABAergic (GA) synapses, synapsins are not involved in maintaining a cluster of vesicles. These synapses do not contain CaM kinase II, indicating that synapsins may stay associated with vesicles at all times. GABAergic synapses do not contain dormant vesicles, indicating that in this case there is no need for synapsin to perform a 'protective' function. The absence of synapsins leads to no alterations in vesicle numbers, and no effects on the number of 'dormant' vesicles. However, synapsins regulate the readily releasable pool in these synapses by currently unknown mechanisms. Bottom: synapsins are associated with large dense-core vesicles (LDCV) and link vesicles to the cortical actin cytoskeleton. Upon depolarization, synapsin dissociates from LDCVs which subsequently fuse with the plasma membrane. Vesicles in the peripheral pool can freely undergo secretion. The absence of synapsins leads to increased, unhindered release from the docked pool, and no effect on the peripheral pool.

vesicle-associated proteins is rather long (Daly and Ziff, 1997), vesicles undergo many local cycles of exocytosis and endocytosis. Thus, over time proteins may become damaged and unable to fulfil their roles in vesicle fusion. If so, synapsins may protect synaptic vesicle proteins from damage, for example by physically shielding them away from the cytosol. Such a role would be analogous to the observed importance of chaperone proteins in maintaining continued presynaptic function (Fernandez-Chacon et al., 2004; Chandra et al., 2005).

Finally, synapsins may increase a functional pool of vesicles by increasing the fraction of new vesicles within a cluster. The observation that newly synthesized vesicles are preferentially released over older vesicles (Duncan et al., 2003), together with the finding that previously released vesicles tend to be preferentially released during subsequent activity (Rizzoli and Betz, 2004), may suggest that the 'active' vesicle pool is comprised of newer vesicles, while the 'dormant' vesicles may be equivalent to older vesicles. In this scenario, synapsins may regulate vesicle biogenesis rather than vesicle stability. Evidence for such a role for synapsins is currently lacking, but the localization of synapsin I to a trans-Golgi compartment in non-neuronal cells is at least consistent with this proposal (Bustos et al., 2001).

Synapsins and large dense-core vesicle exocytosis

While initially thought to be preferentially or exclusively associated with small synaptic vesicles (Navone et al., 1984), synapsins were subsequently found on large dense-core vesicles as well (Browning et al., 1987; Haycock et al., 1988). The recently described effects of synapsin depletion on cocaine-mediated dopamine release (Venton et al., 2006) further indicates that synapsins may also regulate large dense-core vesicle secretion. However, these vesicles are not organized into clusters as prominently as small synaptic vesicles, and display differential requirements for triggered exocytosis. Do synapsins then regulate large dense-core vesicle-mediated catecholamine release in a manner different from that found for small synaptic vesicle-mediated release of excitatory or inhibitory neurotransmitters?

The present study by Mark Wightman's group suggests so. The authors find that catecholamine release from chromaffin cells, as measured by amperometry, is increased in cells from synapsin-deficient mice (Villanueva et al., 2007). This increase is not due to a change in the kinetics of release or the size of individual quanta, but to an enhanced number of quanta released in response to depolarization. Enhanced secretion in the absence of synapsins is observed when release is triggered by high K^+ , but not by Ba^{2+} . Thus, synapsins seem to negatively regulate catecholamine release from a readily releasable docked pool, but not from a peripheral vesicle pool. These results are in contrast to those expected if synapsins would contribute to vesicle integrity and/or biogenesis, but such a function would also not be required in the case of large dense-core vesicles, as these do not undergo local recycling. Thus, another mechanism must account for the observed effects. Indeed, overexpression of synapsin II, the only synapsin present in chromaffin cells, leads to a pronounced decrease in K^+ -triggered catecholamine release from both synapsin-deficient as well as wild-type chromaffin cells (Villanueva et al., 2007). The latter observation suggests yet another possibility, namely that synapsins limit vesicle secretion from the docked vesicle pool for example by direct steric hindrance, or by their ability to link vesicles to the underlying actin cortical cytoskeleton (Nakata and Hirokawa, 1992) (Fig. 4). This effect would not apply to the peripheral vesicle pool, as depolarization-induced phosphorylation of synapsin (Firestone and Browning, 1992) would dissociate synapsin from large dense-core vesicles, yielding uninhibited access of these vesicles to docking sites. In this manner, signal transduction cascades impacting on synapsin function may impose additional control over catecholamine release.

The plethora of proposed mechanisms (including the ones presented here) by which synapsins regulate release from different types of synapses or cells may lead to two conclusions: (1) that we still do not understand the function of synapsins, or (2) that the function of these molecules may vary according to the model system analysed. Are mechanisms of secretion transmitter-specific? While certain essential molecules, such as SNARE proteins, clearly are required for all vesicle-membrane fusion events, irrespective of vesicle type and/or vesicle content, studying modulators of release may yield a more complex picture. Indeed,

the complement of synapsin isoforms present, together with the presence and/or compartmentalization of kinases which differentially impact upon the function of the different synapsin isoforms, and the differential dynamics of vesicle pools dependent on distinct transmitters, may result in distinct outcomes for synaptic function and plasticity over a range of stimulation frequencies. Elucidating this complexity remains an exciting avenue for further research.

Acknowledgments

Work in the laboratory is supported by a grant from the Spanish Ministry of Education and Science (MEC). SH is a Ramón y Cajal Fellow.

References

- Augustine, G. J., Charlton, M. P., and Smith, S. J. (1985). Calcium entry and transmitter release at voltage-clamped nerve terminals of squid. *J. Physiol.* *367*, 163–181.
- Bloom, O., Evergren, E., Tomilin, N., Kjaerulff, O., Low, P., Brodin, L., Pieribone, V. A., Greengard, P., and Shupliakov, O. (2003). Colocalization of synapsin and actin during synaptic vesicle recycling. *J. Cell Biol.* *161*, 737–747.
- Browning, M. D., Huang, C. K., and Greengard, P. (1987). Similarities between protein IIIa and protein IIIb, two prominent synaptic vesicle-associated phosphoproteins. *J. Neurosci.* *7*, 847–856.
- Bustos, R., Kolen, E. R., Braiterman, L., Baines, A. J., Gorelick, F. S., and Hubbard, A. L. (2001). Synapsin I is expressed in epithelial cells: Localization to a unique trans-Golgi compartment. *J. Cell Sci.* *114*, 3695–3704.
- Ceccarelli, B., Hurlbut, W. P., and Mauro, A. (1973). Turnover of transmitter and synaptic vesicles at the frog neuromuscular junction. *J. Cell Biol.* *57*, 499–524.
- Chandra, S., Gallardo, G., Fernandez-Chacón, R., Schlüter, O. M., and Südhof, T. C. (2005). Alpha-synuclein cooperates with CSPalpha in preventing neurodegeneration. *Cell* *123*, 383–396.
- Chi, P., Greengard, P., and Ryan, T. A. (2001). Synapsin dispersion and reclustering during synaptic activity. *Nat. Neurosci.* *4*, 1187–1193.
- Chi, P., Greengard, P., and Ryan, T. A. (2003). Synaptic vesicle mobilization is regulated by distinct synapsin I phosphorylation pathways at different frequencies. *Neuron* *38*, 69–78.
- Czernik, A. J., Pang, D. T., and Greengard, P. (1987). Amino acid sequences surrounding the cAMP-dependent and calcium/calmodulin-dependent phosphorylation sites in rat and bovine synapsin I. *Proc. Natl. Acad. Sci. USA* *84*, 7518–7522.
- Daly, C. and Ziff, E. B. (1997). Post-transcriptional regulation of synaptic vesicle protein expression and the developmental control of synaptic vesicle formation. *J. Neurosci.* *17*, 2365–2375.
- De Camilli, P., Harris, S. M. Jr., Huttner, W. B., and Greengard, P. (1983). Synapsin I (protein I), a nerve terminal-specific phosphoprotein. II. Its specific association with synaptic vesicles demonstrated by immunocytochemistry in agarose-embedded synaptosomes. *J. Cell Biol.* *96*, 1355–1373.
- Duncan, R. R., Greaves, J., Wiegand, U. K., Matskevich, I., Bodammer, G., Apps, D. K., Shipston, M. J., and Chow, R. H. (2003). Functional and spatial segregation of secretory vesicle pools according to vesicle age. *Nature* *422*, 176–180.
- Fernandez-Chacón, R., Wolfel, M., Nishimune, H., Tabares, L., Schmitz, F., Castellano-Munoz, M., Rosenmund, C., Montesinos, M. L., Sanes, J. R., Schneggenburger, R., and Südhof, T. C. (2004). The synaptic vesicle protein CSP alpha prevents presynaptic degeneration. *Neuron* *42*, 237–251.
- Firestone, J. and Browning, M. (1992). Synapsin II phosphorylation and catecholamine release in bovine adrenal chromaffin cells: Additive effects of histamine and nicotine. *J. Neurochem.* *58*, 441–447.
- Gitler, D., Takagishi, Y., Feng, J., Ren, Y., Rodriguez, R. M., Wetsel, W. C., Greengard, P., and Augustine, G. J. (2004). Different presynaptic roles of synapsins at excitatory and inhibitory synapses. *J. Neurosci.* *24*, 11368–11380.
- Greengard, P., Valtorta, F., Czernik, A. J., and Benfenati, F. (1993). Synaptic vesicle phosphoproteins and regulation of synaptic function. *Science* *259*, 780–785.
- Han, H. Q., Nichols, R. A., Rubin, M. R., Bähler, M., and Greengard, P. (1991). Induction of formation of presynaptic terminals in neuroblastoma cells by synapsin IIb. *Nature* *349*, 697–700.

- Harata, N., Pyle, J. L., Aravanis, A. M., Mozhayeva, M., Kavalali, E. T., and Tsien, R. W. (2001). Limited numbers of recycling vesicles in small CNS nerve terminals: implications for neural signaling and vesicular cycling. *Trends. Neurosci.* *24*, 637–643.
- Haycock, J. W., Greengard, P., and Browning, M. D. (1988). Cholinergic regulation of protein III phosphorylation in bovine adrenal chromaffin cells. *J. Neurosci.* *8*, 3233–3239.
- Heuser, J. E. and Reese, T. S. (1973). Evidence for recycling of synaptic vesicle membrane during transmitter release at the frog neuromuscular junction. *J. Cell Biol.* *57*, 315–344.
- Hilfiker, S., Schweizer, F. E., Kao, H. T., Czernik, A. J., Greengard, P., and Augustine, G. J. (1998). Two sites of action for synapsin domain E in regulating neurotransmitter release. *Nat. Neurosci.* *1*, 29–35.
- Hilfiker, S., Pieribone, V. A., Czernik, A. J., Kao, H. T., Augustine, G. J., and Greengard, P. (1999). Synapsins as regulators of neurotransmitter release. *Philos. Trans. R. Soc. Lond. B* *354*, 269–279.
- Hirokawa, N., Sobue, K., Kanda, K., Harada, A., and Yorifuji, H. (1989). The cytoskeletal architecture of the presynaptic terminal and molecular structure of synapsin I. *J. Cell Biol.* *108*, 111–126.
- Hosaka, M. and Südhof, T. C. (1998). Synapsin III, a novel synapsin with an unusual regulation by Ca^{2+} . *J. Biol. Chem.* *273*, 13371–13374.
- Hosaka, M. and Südhof, T. C. (1999). Homo- and heterodimerization of synapsins. *J. Biol. Chem.* *274*, 16747–16753.
- Hosaka, M., Hammer, R. E., and Südhof, T. C. (1999). A phospho-switch controls the dynamic association of synapsins with synaptic vesicles. *Neuron* *24*, 377–387.
- Humeau, Y., Doussau, F., Vitiello, F., Greengard, P., Benfenati, F., and Poulain, B. (2001). Synapsin controls both reserve and releasable synaptic vesicle pools during neuronal activity and short-term plasticity in *Aplysia*. *J. Neurosci.* *21*, 4195–4206.
- Jovanovic, J. N., Benfenati, F., Siow, Y. L., Sihra, T. S., Sanghera, J. S., Pelech, S. L., Greengard, P., and Czernik, A. J. (1996). Neurotrophins stimulate phosphorylation of synapsin I by MAP kinase and regulate synapsin I-actin interactions. *Proc. Natl. Acad. Sci. USA* *93*, 3679–3683.
- Jovanovic, J. N., Sihra, T. S., Nairn, A. C., Hemmings, H. C. Jr., Greengard, P., and Czernik, A. J. (2001). Opposing changes in phosphorylation of specific sites in synapsin I during Ca^{2+} -dependent glutamate release in isolated nerve terminals. *J. Neurosci.* *21*, 7944–7953.
- Katz, B. (1969). *The Release of Neural Transmitter Substances*, Liverpool Univ. Press, Liverpool.
- Kao, H. T., Porton, B., Czernik, A. J., Feng, J., Yiu, G., Häring, M., Benfenati, F., and Greengard, P. (1998). A third member of the synapsin gene family. *Proc. Natl. Acad. Sci. USA* *95*, 4667–4672.
- Kao, H. T., Porton, B., Hilfiker, S., Stefani, G., DeSalle, R., Pieribone, V. A., and Greengard, P. (1999). Molecular evolution of the synapsin gene family. *J. Exp. Zool.* *285*, 360–377.
- Liu, X. B. and Jones, E. G. (1996). Localization of alpha type II calcium calmodulin-dependent protein kinase at glutamatergic but not gamma-aminobutyric acid (GABAergic) synapses in thalamus and cerebral cortex. *Proc. Natl. Acad. Sci. USA* *93*, 7332–7336.
- Matsubara, M., Kusubata, M., Ishiguro, K., Uchida, T., Titani, K., and Taniguchi, H. (1996). Site-specific phosphorylation of synapsin I by mitogen-activated protein kinase and Cdk5 and its effects on physiological functions. *J. Biol. Chem.* *271*, 21108–21113.
- Menegon, A., Bonanomi, D., Albertinazzi, C., Lotti, F., Ferrari, G., Kao, H. T., Benfenati, F., Baldelli, P., and Valtorta, F. (2006). Protein kinase A-mediated synapsin I phosphorylation is a central modulator of Ca^{2+} -dependent synaptic activity. *J. Neurosci.* *26*, 11670–11681.
- Moulder, K. L. and Mennerick, S. (2005). Reluctant vesicles contribute to the total readily releasable pool in glutamatergic hippocampal neurons. *J. Neurosci.* *25*, 3842–3850.
- Moulder, K. L. and Mennerick, S. (2006). Synaptic vesicles: turning reluctance into action. *Neuroscientist* *12*, 11–15.
- Nakata, T. and Hirokawa, N. (1992). Organization of cortical cytoskeleton of cultured chromaffin cells and involvement in secretion as revealed by quick-freeze, deep-etching, and double-label immunoelectron microscopy. *J. Neurosci.* *12*, 2186–2197.
- Navone, F., Greengard, P., and De Camilli, P. (1984). Synapsin I in nerve terminals: selective association with small synaptic vesicles. *Science* *226*, 1209–1211.

- Pieribone, V. A., Shupliakov, O., Brodin, S., Hilfiker-Rothenfluh, S., Czernik, A. J., and Greengard, P. (1995). Distinct pools of synaptic vesicles in neurotransmitter release. *Nature* *375*, 493–497.
- Rizzoli, S. O. and Betz, W. J. (2004). The structural organization of the readily releasable pool of synaptic vesicles. *Science* *303*, 2037–2039.
- Rosahl, T. W., Spillane, E., Missler, M., Herz, J., Selig, D. K., Wolff, J. R., Hammer, R. E., Malenka, R. C., and Südhof, T. C. (1995). Essential functions of synapsins I and II in synaptic vesicle regulation. *Nature* *375*, 488–493.
- Sankaranarayanan, S., Atluri, P. P., and Ryan, T. A. (2003). Actin has a molecular scaffolding, not propulsive, role in presynaptic function. *Nat. Neurosci.* *6*, 127–135.
- Schiebler, W., Jahn, R., Doucet, J. P., Rothlein, J., and Greengard, P. (1986). Characterization of synapsin I binding to small synaptic vesicles. *J. Biol. Chem.* *261*, 8383–8390.
- Schikorski, T. and Stevens, C. F. (2001). Morphological correlates of functionally defined synaptic vesicle populations. *Nat. Neurosci.* *4*, 391–395.
- Schweizer, F. E. and Ryan, T. A. (2006). The synaptic vesicle: cycle of exocytosis and endocytosis. *Curr. Opin. Neurobiol.* *16*, 298–304.
- Südhof, T. C., Czernik, A. J., Kao, H. T., Takei, K., Johnston, P. A., Horiuchi, A., Kanazir, S. D., Wagner, M. A., Perin, M. S., de Camilli, P., and Greengard, P. (1989). Synapsins: mosaic of shared and individual domains in a family of synaptic vesicle phosphoproteins. *Science* *245*, 1474–1480.
- Südhof, T. C. (2004). The synaptic vesicle cycle. *Annu. Rev. Neurosci.* *27*, 509–547.
- Sugiyama, T., Shinoue, T., Ito, Y., Misawa, H., Tojima, T., Ito, E., and Yoshioka, T. (2000). A novel function of synapsin II in neurotransmitter release. *Mol. Brain Res.* *85*, 133–143.
- Sun, J., Bronk, P., Liu, X., Han, W., and Südhof, T. C. (2006). Synapsins regulate use-dependent synaptic plasticity in the calyx of Held by a Ca^{2+} /calmodulin-dependent pathway. *Proc. Natl. Acad. Sci. USA* *103*, 2880–2885.
- Tao-Cheng, J. H., Dosemeci, A., Winters, C. A., Reese, T. S. (2007). Changes in the distribution of calcium calmodulin-dependent protein kinase II at the presynaptic bouton after depolarization. *Brain Cell Biology*.
- Terada, S., Tsujimoto, T., Takei, Y., Takahashi, T., and Hirokawa, N. (1999). Impairment of inhibitory synaptic transmission in mice lacking synapsin I. *J. Cell Biol.* *145*, 1039–1048.
- Torri-Tarelli, F., Villa, A., Valtorta, F., De Camilli, P., and Greengard, P. (1990). Redistribution of synaptophysin and synapsin I during alpha-latrotoxin-induced release of neurotransmitter at the neuromuscular junction. *J. Cell Biol.* *110*, 449–459.
- Valtorta, F., Iezzi, N., Benfenati, F., Lu, B., Poo, M. M., and Greengard, P. (1995). Accelerated structural maturation induced by synapsin I at developing neuromuscular synapses of *Xenopus laevis*. *Eur. J. Neurosci.* *7*, 261–270.
- Venton, B. J., Seipel, A. T., Phillips, P. E. M., Wetsel, W. C., Gitler, D., Greengard, P., Augustine, G. J., and Wightman, R. M. (2006). Cocaine increases dopamine release by mobilization of a synapsin-dependent reserve pool. *J. Neurosci.* *26*, 3206–3209.
- Villanueva, M., Augustine, G. J., and Wightman, R. M. (2007). Synapsin II negatively regulates catecholamine release. *Brain Cell Biology* *35*(2/3), 125–136.

**4. SENSING THE DIFFERENCE: NEURONAL CALCIUM
SENSOR-1 AND ITS INVOLVEMENT IN VESICLE BIOGENESIS,
TRAFFICKING AND FUSION**

Chapter II

**SENSING THE DIFFERENCE: NEURONAL
CALCIUM SENSOR-1 AND ITS INVOLVEMENT IN
VESICLE BIOGENESIS, TRAFFICKING AND
FUSION**

*Elena Fdez and Sabine Hilfiker**

Institute of Parasitology and Biomedicine “Lopez-Neyra”, Consejo Superior de
Investigaciones Cientificas (CSIC), Granada, Spain.

ABSTRACT

Many aspects of brain function are regulated by Ca^{2+} signals. Temporally and spatially distinct Ca^{2+} signals are detected by a variety of proteins, including EF-hand-containing Ca^{2+} binding proteins. The neuronal Ca^{2+} sensor (NCS) protein family has emerged as a key player in modulating neuronal function and synaptic plasticity, even though the precise mechanism of action of any member of this family remains largely unknown. Neuronal calcium sensor-1 (NCS-1), also named frequenin, was originally identified in *Drosophila* in a screen for neuronal hyperexcitability mutants. Overexpression of NCS-1 has been shown to enhance evoked neurotransmitter release, paired-pulse facilitation and exocytosis in several neuronal and neuroendocrine cell types, indicating an important role for this protein in modulating synaptic efficacy. NCS-1 is an N-terminally myristoylated protein that contains four EF-hand motifs, three of which are able to bind Ca^{2+} in the submicromolar range. NCS-1 is constitutively associated with membranes even under resting Ca^{2+} conditions, suggesting that a Ca^{2+} /myristoyl switch does not operate to regulate the subcellular localization of NCS-1. Instead, binding of Ca^{2+} to NCS-1 may alternatively affect its interaction with, or modulation of, a variety of downstream binding partners. Several NCS-1-interacting proteins have been described,

* Correspondence concerning this article should be addressed to Sabine Hilfiker Institute of Parasitology and Biomedicine “Lopez-Neyra”, Consejo Superior de Investigaciones Cientificas (CSIC), Granada, Spain. sabine.hilfiker@ipb.csic.es.

including ion channels, receptors and type III phosphatidylinositol 4-kinase β (PI4K β). The latter interaction suggests that NCS-1 may enhance secretion by modulating vesicle biogenesis, vesicle trafficking and/or vesicle fusion events in a phosphoinositide-dependent manner. The present review describes our current knowledge about NCS-1 and the molecular mechanism(s) by which NCS-1 may enhance neurotransmission and synaptic plasticity.

Keywords: neuronal calcium sensor proteins, NCS, calcium, synaptic transmission, synaptic plasticity, PI4K, phosphoinositides, vesicle trafficking, dopamine

ABBREVIATIONS

| | |
|---------------------------|---|
| ARF | ADP-ribosylation factor |
| CNS | central nervous system |
| DA | dopamine |
| DLPFC | dorsolateral prefrontal cortex |
| DRIP | dopamine receptor-interacting protein |
| FAPP | four-phosphate-adaptor protein |
| GCAP | guanylate cyclase-activating protein |
| GPCR | G protein-coupled receptor |
| GRK | G protein-coupled receptor kinase |
| IL1RAPL | interleukin-1 receptor accessory protein-like protein |
| KChIP | K ⁺ -channel-interacting protein |
| NCS | neuronal Ca ²⁺ sensor |
| PI4K | phosphatidylinositol 4-kinase |
| PI4K β | type III phosphatidylinositol 4-kinase β |
| PtdIns(4)P | phosphatidylinositol 4-phosphate |
| PtdIns(4,5)P ₂ | phosphatidylinositol (4,5)-bisphosphate |
| TGN | trans-Golgi network |
| VILIP | visinin-like protein. |

1. INTRODUCTION

The cytosolic Ca²⁺ concentration in cells is tightly regulated, since changes in intracellular Ca²⁺ can regulate many different aspects of cell function. In neurons, Ca²⁺ ions regulate processes such as neurotransmission, cytoskeletal dynamics, signal transduction and gene expression. Neuronal Ca²⁺ signals can vary drastically both in their temporal as well as spatial characteristics [1]. For example, neurotransmitter release is triggered by submillisecond increases of Ca²⁺ levels within nanometers of open Ca²⁺ channels. Other Ca²⁺ signals include localized rises lasting for tens of milliseconds, spatially more extensive Ca²⁺ elevations for example in dendrites, Ca²⁺ waves propagating over a couple of seconds, or global and prolonged Ca²⁺ elevations throughout the cell. Such distinct Ca²⁺ signals are

transduced into changes of neuronal function mediated by Ca^{2+} -binding proteins, which may act either as Ca^{2+} buffers or as Ca^{2+} sensors. In either case, these proteins must be able to respond rapidly and selectively to defined Ca^{2+} signals. Such selectivity is thought to be achieved by the distinct localization of various Ca^{2+} sensing proteins as well as by their different kinetics (on-rate) and affinity towards Ca^{2+} , allowing them to transduce distinct Ca^{2+} signals into varied changes in neuronal function.

2. THE NCS FAMILY

The neuronal calcium sensor (NCS) proteins are Ca^{2+} sensors with micromolar or submicromolar affinities and change their conformation upon Ca^{2+} binding, which allows them to modulate the interaction with their targets and thus act as effector molecules to transduce Ca^{2+} signals into appropriate downstream events. Whilst it is becoming increasingly clear that the NCS proteins regulate a variety of neuronal processes [2-5], the exact functions of most NCS family members are still poorly understood.

Table 1. The NCS family of Ca^{2+} -sensor proteins.

| Protein | Class | Expression | Splice variants |
|----------------------|-------|-----------------------------|-----------------|
| NCS-1 | A | Brain, retina, non-neuronal | None |
| VILIP-1 | B | Brain, retina | None |
| VILIP-2 | B | Brain | None |
| VILIP-3 | B | Brain | None |
| Hippocalcin | B | Brain | None |
| Neurocalcin δ | B | Brain, retina | None |
| Recoverin | C | Retina | None |
| GCAP1 | D | Retina | None |
| GCAP2 | D | Retina | None |
| GCAP3 | D | Retina | None |
| KChIP1 | E | Brain | 1a, 1b |
| KChIP2 | E | Brain, cardiac myocytes | 2, 2a, 2b |
| KChIP3 | E | Brain | 3a, 3b |
| KChIP4 | E | Brain | 4a, 4b |

Abbreviations: GCAP, guanylate cyclase-activating protein; KChIP, K^+ channel-interacting protein; NCS, neuronal calcium sensor; VILIP, visinin-like protein.

The human genome encodes at least 14 genes for NCS proteins, and such diversity is further increased by the existence of splice variants (Table 1). Based on evolutionary appearance and sequence similarity, the NCS protein family has been subdivided into five subfamilies (class A-E) [2-5] (Table 1). Class A consists of NCS-1, which was originally identified as frequenin in *Drosophila* [6], and which constitutes the primordial member of the NCS family, being present in yeast. Class B includes the visinin-like proteins (VILIPs), including VILIP-1, VILIP-2, VILIP-3, neurocalcin δ and hippocalcin, and a member of this subfamily is represented in the genome of *Caenorhabditis elegans* and evolutionarily later

species. The members of classes C and D, the recoverin and the guanylate cyclase-activating proteins (GCAPs), respectively, are present in amphibia and evolutionarily subsequent species, whilst the class E proteins, the K^+ -channel-interacting proteins (KChIPs), are represented in genomes from fish onwards [5].

The different NCS class proteins also tend to differ in their expression patterns [2] (Table 1). For example, NCS-1 is widely expressed in neuronal as well as non-neuronal cells, whilst most other NCS proteins are neuron-specific. On the other hand, some NCS proteins are expressed in only a subset of neuronal cell types; for example, hippocalcin is predominantly expressed in hippocampal pyramidal neurons, whilst VILIP-3 is mostly expressed in cerebellar Purkinje cells [5]. Studies of such types have established that certain neuronal cell types express several or all of the NCS proteins, but that the overall expression pattern is unique for each protein. Thus, the NCS proteins are likely to perform distinct functions specific for each particular neuronal cell type.

| | | | | | | | | | | | | | | | | | | | | | | | | | | | | | | | | | | |
|-------------|----------------------|---------------------|---------------------|-------------|--------------|------------------------|---------|---------------|---------------|---------------|-------------|-----------|----------|---------|----------|----------|----------|----------|---------|--------|-----|-------|-------|-------|-----|----|------|----|----|-------|-------|-------|-------|-------|
| NCS-1 | ----- | ----- | ----- | ----- | MGKSNK-KLK | PEVVBEELTRKTYFTEKEVQQ | | | | | | | | | | | | | | | | | | | | | | | | | | | | |
| VILIP-1 | ----- | ----- | ----- | ----- | MGKQNS-KLA | PEVMBEDLVKSTPEFNEHELKQ | | | | | | | | | | | | | | | | | | | | | | | | | | | | |
| VILIP-2 | ----- | ----- | ----- | ----- | MGKTNS-KLA | PEVLEDLVQNTPEFSEQELKQ | | | | | | | | | | | | | | | | | | | | | | | | | | | | |
| VILIP-3 | ----- | ----- | ----- | ----- | MGKQNS-KLR | PEVLODLRENTPEFDHLELQE | | | | | | | | | | | | | | | | | | | | | | | | | | | | |
| Neurocalcin | ----- | ----- | ----- | ----- | MGKQNS-KLR | PEVMQDLRENTPEFTEHLEQE | | | | | | | | | | | | | | | | | | | | | | | | | | | | |
| Hippocalcin | ----- | ----- | ----- | ----- | MGKQNS-KLR | PEMLQDLRENTPEFSELELQE | | | | | | | | | | | | | | | | | | | | | | | | | | | | |
| Recoverin | ----- | ----- | ----- | ----- | MGNKSGALS | KEITLEELQLNTKFSSEELCS | | | | | | | | | | | | | | | | | | | | | | | | | | | | |
| GCAP-1 | ----- | ----- | ----- | ----- | MGNVMEGKS- | ---VEEL-----SSTECHQ | | | | | | | | | | | | | | | | | | | | | | | | | | | | |
| GCAP-2 | ----- | ----- | ----- | ----- | MGQEFSS- | ---WEAEAAAGEIDVAELQE | | | | | | | | | | | | | | | | | | | | | | | | | | | | |
| GCAP-3 | ----- | ----- | ----- | ----- | MGNKGS- | ---IAGDOKAVPTQETHV | | | | | | | | | | | | | | | | | | | | | | | | | | | | |
| KChIP1 | ----- | ----- | MGAVMGTFSSSLQTKQ | RRPSKDKI | EDELEMTMVCHR | PRGLEQLAEQINFTKRELQV | | | | | | | | | | | | | | | | | | | | | | | | | | | | |
| KChIP2 | ----- | ----- | MRGQGRKESLSDSRDLGDS | YDQLTDSV | DEFEFLSTVCHR | PRGLEQLQRCIKFTKRELQV | | | | | | | | | | | | | | | | | | | | | | | | | | | | |
| KChIP3 | MQPAKEVTKASDGSLLGDLG | HTPLSKKEGIKWQRPLSRQ | ALMRCCLVK | WILSSTAPQGS | DSS---- | DSELELSTVVRHQ | | | | | | | | | | | | | | | | | | | | | | | | | | | | |
| KChIP4 | ----- | ----- | ----- | MNVRV | ESISAQLEE | ASSTGDSVEDELEMAIVRHR | | | | | | | | | | | | | | | | | | | | | | | | | | | | |
| | | | | | | PEALELLEAQSKFTKRELQI | | | | | | | | | | | | | | | | | | | | | | | | | | | | |
| | | | | | | | | | | | | | | | | | | | | | | | | | | | | | | | | | | |
| NCS-1 | WYKGF | IKDCPSG | QLDAAGFO | KIYKQ | FPFPGDPTK | FATFVF | NVFDENK | DGRIEFSEPIQAL | SVTSRGT | LDEKLRWAPKLYD | LDNDGY | ITRNEMLD | IVDAIY | | | | | | | | | | | | | | | | | | | | | |
| VILIP-1 | WYKGF | LKDCPSG | RLLNLEEFQ | QLYVK | FFPYGDASK | FAQHAF | RTFDK | NGDGTID | DFREFICAL | SITSRGS | FBQKLNWAF | NMYD | LDGDG | KITRLEM | LEITIAIY | | | | | | | | | | | | | | | | | | | |
| VILIP-2 | WYKGF | LKDCPSG | LINLEEFQ | QLYIK | FFPYGDASK | FAQHAF | RTFDK | NGDGTID | DFREFICAL | SVTSRGS | FBQKLNWAF | NMYD | LDGDG | RITRLEM | LEITIAIY | | | | | | | | | | | | | | | | | | | |
| VILIP-3 | WYKGF | LKDCPTG | HLTVDEFK | KIYAN | FFPYGDASK | FAEHVF | RTFDN | GDGTID | DFREFI | IAL | SVTSRGL | BQKLNWAF | SMYD | LDNGY | ISRSEM | LEIVQAIY | | | | | | | | | | | | | | | | | | |
| Neurocalcin | WYKGF | LKDCPSG | HLNLEEFK | KIYAN | FFPYGDASK | FAEHVF | RTFDN | GDGTID | DFREFI | IAL | SVTSRGL | BQKLNWAF | SMYD | LDNGY | ISRSEM | LEIVQAIY | | | | | | | | | | | | | | | | | | |
| Hippocalcin | WYKGF | LKDCPTG | HLNLEEFK | KIYAN | FFPYGDASK | FAEHVF | RTFDN | GDGTID | DFREFI | IAL | SVTSRGL | BQKLNWAF | SMYD | LDNGY | ISRSEM | LEIVQAIY | | | | | | | | | | | | | | | | | | |
| Recoverin | WYQSF | LKDCPTG | RITQQQFO | SIYAK | FFFDIDPK | AMVAQHVF | RSPDN | LDGTL | DFKPYVIAL | HMITAG | TNQLKLEWAF | NFSLV | VMGNT | ISKN | NEVLEIV | MAIF | | | | | | | | | | | | | | | | | | |
| GCAP-1 | WYKFK | WTECP | SQQLTYEYFR | QFQGL | KNLSP | SASQVVEQMF | ETFDN | KDGYI | DFMEYVAGL | SLVLR | KGKVEQKLR | NWFKLYD | VPCNG | CDIR | DELLT | ITIQAIR | | | | | | | | | | | | | | | | | | |
| GCAP-2 | WYKFK | VMECP | SGTLFMHEFK | R-FFK | VTDDE | EASQVVEGFM | RAFDN | KDNTI | DFLEYVAAL | NLVL | RGTLEH | KLWTFKIYD | KDNGC | DIR | LELLN | IVEGIIY | | | | | | | | | | | | | | | | | | |
| GCAP-3 | WYRTF | MEYPS | GLQTLHEFK | TLLGL | QGLN | KANKHIDQVY | NTFD | TNKD | GFVDFLEFIAAV | NLIMQ | EKMEQKLR | NWFKLYD | ADGNS | TDKN | LELLDM | FMAVQ | | | | | | | | | | | | | | | | | | |
| KChIP1 | LYRGF | KNECP | SGVNNEDTFK | QIYAQ | FFPHGD | ASTYAHYLF | NAFDT | TQTS | SVKFEFVIAL | SILLR | GTVHEKLR | WTFNLYD | INKDG | YITKE | EMMD | IVKAIY | | | | | | | | | | | | | | | | | | |
| KChIP2 | LYRGF | KNECP | SGIVNNEENFK | QIYSQ | FFPHQ | SDSSTYATFLF | NAFDT | NH | DGSSVSEDFVAGL | SV | ILRGT | VDRLNWAF | NLYD | INKD | GCTI | TRKEM | LDIMKSIY | | | | | | | | | | | | | | | | | |
| KChIP3 | LYRGF | KNECP | TLGVDIEDTFK | LIYAQ | FFPHQ | SDATYAHYLF | NAFD | AD | NGALHFEFVVG | SILLR | GTVHEKLR | NWAFNLYD | INKD | GYIT | KEEML | AIMKSIY | | | | | | | | | | | | | | | | | | |
| KChIP4 | LYRGF | KNECP | SGVNNEDTFK | EIYSQ | FFPHQ | SDSSTYAHYLF | NAFD | TDH | NGAVSEDFIKGL | SILLR | GTVQEKLNWAF | NLYD | INKD | GYIT | KEEML | DIMKAIY | | | | | | | | | | | | | | | | | | |
| | | | | | | | | | | | | | | | | | | | | | | | | | | | | | | | | | | |
| NCS-1 | QMVGN | IVELP | EEEN---TP | EKR | VDRI | FAMDK | NADGKLT | LQEFQ | EGSKAD | PSIVQALS | YDGLV | ----- | ----- | ----- | ----- | ----- | | | | | | | | | | | | | | | | | | |
| VILIP-1 | KMVG | TVM | MKNE | EDG--LTP | ER | VDKIF | SKMDK | NDQIT | LDEFK | EAAK | SDPSIV | LLQC | DIQK | ----- | ----- | ----- | | | | | | | | | | | | | | | | | | |
| VILIP-2 | KMVG | TVM | MKNE | EDG--LTP | QR | VDKIF | SKMD | NDQIT | LEEFK | EAAK | SDPSIV | LLQC | DMQK | ----- | ----- | ----- | | | | | | | | | | | | | | | | | | |
| VILIP-3 | KMV | SSVM | KMP | EDES---TP | EKR | TDKIF | RQMD | TNNDGKLS | LEEF | IRGAK | SDPSIV | RLQC | DPSSASQF | ----- | ----- | ----- | | | | | | | | | | | | | | | | | | |
| Neurocalcin | KMV | SSVM | KMP | EDES---TP | EKR | TEKIF | RQMD | TNNDGKLS | LEEF | IRGAK | SDPSIV | RLQC | DPSSASQF | ----- | ----- | ----- | | | | | | | | | | | | | | | | | | |
| Hippocalcin | KMV | SSVM | KMP | EDES---TP | EKR | TEKIF | RQMD | TNNDGKLS | LEEF | IRGAK | SDPSIV | RLQC | DPSSASQF | ----- | ----- | ----- | | | | | | | | | | | | | | | | | | |
| Recoverin | KMIT | PEDV | KLLP | DDDE--NTP | EKR | AEKI | WKYFG | KNDKLT | EKEF | IEG | TLANKE | ILRLIQF | EPQK | V | KEK | MKNA | | | | | | | | | | | | | | | | | | |
| GCAP-1 | AMN | PCSD | TTMT | ADEF--- | --- | TD | VFSK | LDV | NDGELS | LEEF | IEG | VQKQ | MLD | TLTR | SLD | TRV | RRLLQ | NGEQDEEG | ADEAAE | AAG--- | | | | | | | | | | | | | | |
| GCAP-2 | QLK | KACR | RELQ | TEQGLLTP | EEV | VDRI | FLE | LDV | DENGDGELS | LN | EFV | EGARR | DKW | MKLM | Q | DMNP | SSW | LAQ | RRKSAMF | --- | | | | | | | | | | | | | | |
| GCAP-3 | ALN | QQTLS | -----P | EEF | INL | V | HKID | IN | NDGELT | LEEF | IN | MAK | QD | LL | EVYK | SF | DN | SVL | RVIC | NC | GKQ | P | DME | TD | SSK | SP | KAGL | GK | V | K | M | K | | |
| KChIP1 | DMG | KY | TY | PVLR | ED---TP | RQ | HVD | V | FKMD | KNDG | IVT | LDEF | IE | SCQ | ED | DN | IM | RS | LOL | FQ | NVM | ----- | ----- | ----- | | | | | | | | | | |
| KChIP2 | DMG | KY | TY | PALRE | ---AP | RE | HV | BS | FK | M | DR | ND | GVV | TE | EF | IE | SC | Q | ED | DN | IM | RS | M | Q | L | F | EN | V | I | ----- | ----- | ----- | | |
| KChIP3 | DMG | RH | TY | P | LLRED | ---AP | AE | H | V | RF | FK | M | DR | ND | GVV | TE | EF | IE | SC | Q | ED | DN | IM | RS | M | Q | L | F | EN | V | I | ----- | ----- | ----- |
| KChIP4 | DMG | K | CT | Y | PVLR | ED---AP | RQ | H | V | ET | FK | M | DR | ND | GVV | TE | EF | IE | SC | Q | ED | DN | IM | RS | M | Q | L | F | EN | V | I | ----- | ----- | ----- |

Figure 1. Alignment of human NCS protein sequences. Amino acid sequence alignment of human NCS proteins illustrates high overall sequence homology. Amino acids highlighted in blue are identical, whilst amino acids highlighted in grey are similar to those of human NCS-1, respectively. The database accession numbers for the sequences are as follows: NCS-1 (P62166), VILIP-1 (NP_003376), VILIP-2 (Q5TG97), VILIP-3 (P62748), Neurocalcin (P61601), Hippocalcin (NP_002134), Recoverin (P35243),

GCAP-1 (P43080), GCAP-2 (Q9UMX6), GCAP-3 (O95843), KChIP1 (NP_055407), KChIP2 (Q9HD11), KChIP3 (Q9Y2W7) and KChIP4 (Q9H2A4).

A major impediment in trying to study the individual roles of the different NCS proteins has been their high sequence similarity (Figure 1). NCS proteins are all of similar size, possess around 50% or more of sequence identity with each other, have N-terminal myristoylation consensus sequences (except KChIPs 2-4), and show high-affinity Ca^{2+} binding *in vitro* not far above basal Ca^{2+} concentrations (100 nM). In addition, all members of the family possess four EF-hand motifs (Figure 1). Generally, EF hands are comprised of 29-residue helix-loop-helix motifs, with 12 residues forming a Ca^{2+} -binding loop [7]. However, only three (or two in the case of recoverin and KChIP1) are able to bind Ca^{2+} . In all of the proteins, the first EF-hand is predicted to be unable to bind Ca^{2+} due to the presence of a conserved cysteine-proline substitution in the Ca^{2+} -binding loop (Figure 1). Instead, EF-1 seems to be involved in interactions with the myristoyl group in the Ca^{2+} -free forms, or possibly interactions with binding partners in the Ca^{2+} -bound forms of the proteins, respectively.

The high sequence similarity amongst NCS proteins raises important issues of apparent functional redundancy. For example, whilst multiple NCS proteins may interact with the same protein partner(s) when assayed *in vitro*, the affinity of such interactions may vary significantly, and moreover, specificity *in vivo* may be achieved by the distinct cellular and subcellular localizations of the different NCS proteins and/or their protein targets. Therefore, *in vitro* interaction studies, or cellular overexpression studies to elucidate the function(s) and molecular mode(s) of action of individual NCS proteins, have to be interpreted with great care. In the present chapter, we will describe current knowledge about the cellular functions and possible molecular mechanism(s) of action of NCS-1.

3. CELLULAR AND SUBCELLULAR LOCALIZATION OF NCS-1

Localization studies of NCS-1 have been generally hampered by the compromised specificity of the antibodies used. For example, only few of the affinity-purified anti-NCS-1 antibodies currently available have been tested for their cross-reactivity with other members of the NCS family by Western blotting. However, where anti-NCS-1 antibodies have been immunodepleted against other NCS protein species, the localization data obtained have been reliable [8]. In addition, *in situ* hybridization studies to detect NCS-1 mRNA have clearly established that NCS-1 gene expression is pan-neuronal [9]. Whilst initially thought to be neuron-specific [10], NCS-1 has subsequently been shown to be expressed in most non-neuronal tissues as well, even though at reduced levels [11]. Thus, its expression was found in glands, kidney, skin, heart, breast, uterus, pancreas, colon and prostate [11]. Similarly, NCS-1 expression has been found in neuroendocrine cells [12] as well as in several mammalian tissue culture cell lines, such as COS-7 [13], MDCK [14], HEK-293 [15], AtT-20 [16], 3T3L1 [17] and HL-60 cells [18], respectively. Together, these findings suggest that NCS-1 may perform more general, rather than solely neuron-specific functions.

The subcellular distribution of NCS-1 has been investigated by various techniques. Subcellular fractionation assays using rat brain material suggest that NCS-1 is broadly distributed, being partially cytosolic and partially associated with the membranes of the trans-Golgi network (TGN) and the endoplasmic reticulum [19]. Immunocytochemical and electron-microscopic histochemistry techniques also indicate that endogenous NCS-1 displays perinuclear staining and is associated with the TGN [8,13,19-21]. Various studies indicate the presence of NCS-1 in both pre- and postsynaptic compartments [8,21-24], and small amounts have also been detected on vesicular structures and at the plasma membrane [19,25]. Whilst initially suggested to be localized to small synaptic-like microvesicles in neuroendocrine PC12 cells [12,26,27], subsequent studies clearly established that only minute amounts of NCS-1 colocalize with small synaptic-like microvesicles [19]. In addition, NCS-1 does not co-localize with large dense-core vesicles in PC12 cells (Figure 2) or in chromaffin cells [20]. Thus, the co-localization of NCS-1 with synaptophysin in differentiated PC12 cells [26], but its virtual absence from highly-purified small synaptic vesicle preparations of rat brain [19] may indicate the presence of NCS-1 on immature transport organelles (containing synaptophysin), rather than on mature vesicles (see also below).

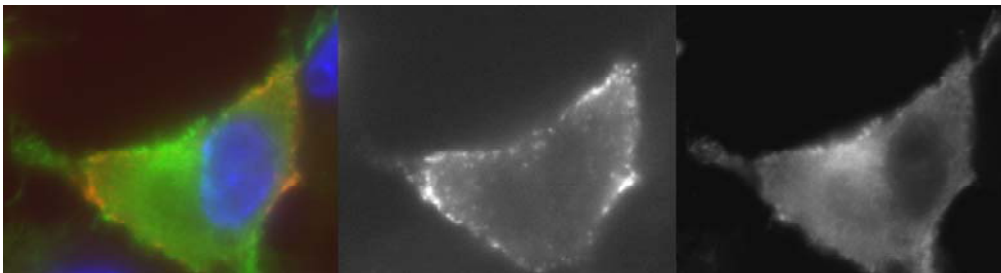


Figure 2. Localization of NCS-1 in transfected PC12 cells. Non-differentiated PC12 cells were co-transfected with constructs encoding for NCS-1 and human growth hormone (hGH), which is packaged into large dense-core vesicles. The localization of NCS-1 and hGH was assessed by double-immunocytochemistry using anti-NCS-1 chicken polyclonal antibodies at a dilution to preferentially visualize NCS-1-overexpressing cells, and anti-hGH rabbit polyclonal antibodies to visualize hGH [31]. Cells were fixed and analysed as described [31]. hGH (red) is mainly localized to large dense-core vesicles situated in the cell periphery, whilst overexpressed NCS-1 (green) is partially cytosolic and partially localized to the nuclear periphery, typical of TGN staining.

Finally, localization studies of NCS-1 performed upon overexpression of the protein have to be interpreted with care, as dependent on the expression levels, perinuclear staining is also increasingly accompanied with staining at and/or close to the plasma membrane [28-31]. This may indicate that, dependent on the level of overexpression, intracellular membrane binding sites become saturated, and that the protein starts to associate with other membranes in a non-specific manner. In sum, studies of endogenous NCS-1 localization suggest a broad distribution, with NCS-1 being present in cell bodies as well as pre- and postsynaptic

compartments, and being partially cytosolic and partially associated with membranes of the TGN, and possibly with TGN-derived transport vesicles.

4. MYRISTOYLATION AND SUBCELLULAR TARGETING OF NCS-1

Controlling the intracellular localization of NCS-1 is important for its ability to appropriately respond to differing Ca^{2+} signals, and thus for its function in regulating neuronal events. How is the specific membrane association of NCS-1 achieved? With the exception of KChIPs 2-4 [32,33], all NCS proteins are N-terminally myristoylated. Myristoyl tails are 14 carbon acyl chains added to the N-termini of proteins, which then act as membrane anchors [34]. This modification is determined by a vaguely-defined 17-residue motif at the extreme N-terminus of proteins [35]. Myristoylation can be required, but must not necessarily be sufficient for membrane anchoring [36], and other protein features, such as regions rich in basic residues, can mediate further membrane attraction [37]. Also, myristoylation does not always serve a constitutive membrane anchoring function. The fatty acid can switch between folding back to a domain of the acylated protein, and extending to the outside again, both controlled by the binding of Ca^{2+} . Such a Ca^{2+} /myristoyl switch mechanism for reversible membrane association has been described in detail for some NCS proteins, such as recoverin [34]. If Ca^{2+} is low, recoverin cradles its myristoyl group in a hydrophobic pocket created by the N-terminus of the protein. The binding of two Ca^{2+} ions by cytosolic recoverin leads to a large conformational change, which is followed by the extrusion of the myristoyl group previously buried within the hydrophobic pocket [38,39]. This results in translocation and myristoyl-dependent association of Ca^{2+} -bound recoverin to intracellular membranes [34,40]. Further, basic residues in the N-terminal domain electrostatically interact with the negatively charged phospholipid headgroups at the membrane surface, and such electrostatic interaction may contribute to the overall energetics of membrane binding [41]. Importantly, the Ca^{2+} -induced rotation of two domains of the protein exposes many hydrophobic residues that otherwise contact the myristoyl group in the Ca^{2+} -free state. The generation of such a hydrophobic crevice may generate a potential binding site in recoverin for its target protein, rhodopsin kinase.

Whilst hippocalcin [25,30], neurocalcin δ [42,43], VILIP-1 and VILIP-3 [44,45] all seem to possess a Ca^{2+} /myristoyl switch mechanism for reversible membrane association, such mechanism does not apply for NCS-1. In contrast, biochemical studies suggest that the myristoyl group of NCS-1 is exposed even in the absence of Ca^{2+} [46,47]. Further, analysis of full-length NCS-1 fused to GFP in live cells [25], or endogenous NCS-1 in fixed cells [8,21] indicates that NCS-1 is associated with TGN membranes even under basal or lowered Ca^{2+} concentrations, or if all Ca^{2+} -binding EF-hands are mutated. Intriguingly, intracellular increases in Ca^{2+} can evoke the translocation of cytosolic NCS-1 to membranes [19], suggesting that a (small) portion of cytosolic NCS-1 may be recruited to membranes via a mechanism different from the Ca^{2+} /myristoyl switch. However, in all cases, membrane association requires N-terminal myristoylation.

What are the determinants for the absence of a Ca^{2+} /myristoyl switch in certain NCS proteins, such as NCS-1, KChIP1, GCAP1 and GCAP2? Structural comparisons between NCS proteins have not provided immediate clues as to the basis of this difference (see also below), and for example the features within the sequence of recoverin that determine the Ca^{2+} /myristoyl switch mechanism, such as the inactivated first EF-hand and the hydrophobic residues that cradle the myristoyl group in the Ca^{2+} -free form, are highly conserved across all NCS proteins [48]. An elegant recent study has used sequence and structural comparison between NCS proteins in an attempt to identify candidate residues that determine the absence of a Ca^{2+} /myristoyl switch mechanism for NCS-1 [48]. These studies indicate that the N-terminus and first EF-hand domain determine the inability of NCS-1 to sequester the myristoyl group in the Ca^{2+} -free state. Specifically, two acid (E14 and E15) and two basic residues (R18 and K19) within a key motif (EELTRK) are part of an α -helix in the crystal structure of NCS-1 which joins the myristoyl tail to EF-hand 1. These residues undergo hydrogen-bond interactions which could stabilize the helix in a rigid conformation to keep the N-terminus of NCS-1 in an open conformation, with the myristoyl group exposed [48] (Figure 3). Indeed, mutagenesis studies indicate that these residues are sufficient to lock the myristoyl group in an open conformation. Interestingly, these residues are not conserved in NCS-1 from lower species, including *S. cerevisiae* (Figure 4), and the fission yeast homologue of NCS-1 does seem to undergo a Ca^{2+} /myristoyl switch mechanism [49], suggesting that the ancestral form of the protein may have displayed a switch mechanism, which may have been lost in NCS-1 from higher organisms.

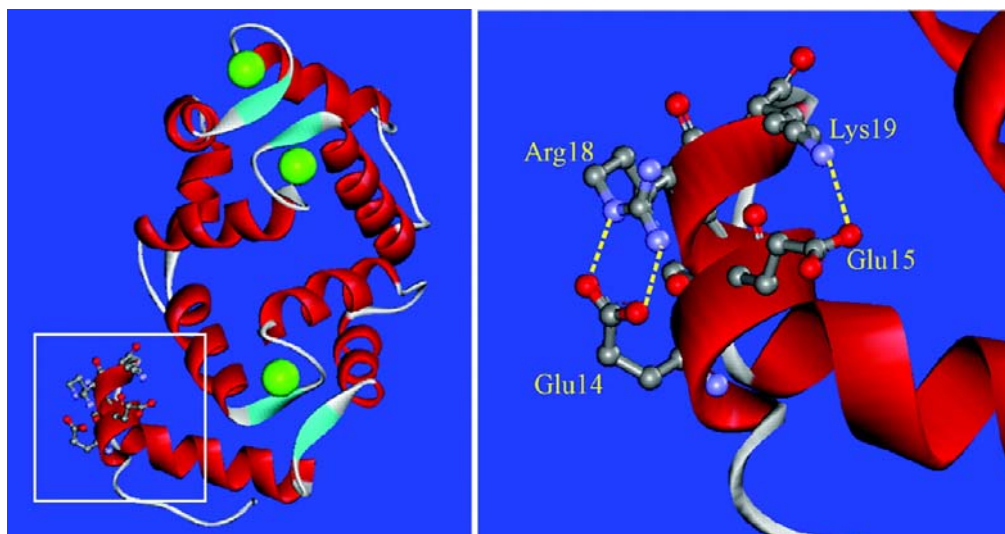


Figure 3. Structure of NCS-1 indicating residues that may determine the absence of a Ca^{2+} /myristoyl switch mechanism. *Left*, ribbon representation of the crystal structure of human NCS-1, with alpha helices in red, loop regions in light blue, and the three bound Ca^{2+} ions represented by green balls. Residues Glu14, Glu15, Arg18 and Lys19 are shown as ball-and-stick representation in the boxed region. *Right*, expansion of the boxed region showing the hydrogen-bonding interactions between the indicated residues. Reproduced from *J. Biol. Chem.* (2004) 279, 14347-14354 by copyright permission of the Journal of Biological Chemistry.

Since the myristoyl anchor is not sufficient to confer specificity of the association of myristoylated proteins with distinct intracellular membranes, additional targeting features have to exist. To determine such features, a minimal myristoylation motif derived from hippocalcin (amino acid residues 1-14) was fused to GFP. This protein construct was targeted to the TGN and to the plasma membrane when overexpressed in cells, suggesting that the N-terminal residues contain all the intrinsic targeting information necessary for proper intracellular localization [30]. Further, basic residues at positions 3, 7 and 9 were found to be essential for the efficient targeting of this motif to the TGN and the plasma membrane, and mutation of all three amino acids to non-charged residues led to the association of the motif with distinct intracellular organelles [30]. Unfortunately, this approach was not performed with the N-terminal residues of NCS-1, and indeed basic residues at positions 3, 7 and 9 are not fully conserved across NCS-1 from different species (Figure 4). In addition, other NCS proteins that are targeted to the TGN and the plasma membrane, such as VILIP-1, do not contain basic residues at all three positions (see Figure 1). Finally, VILIP-3, which does possess the three basic residues predicted to be important for proper targeting, displays calcium-independent Golgi localization, and shows a slight membrane association even in its non-myristoylated form [45]. Together, these data suggest that whilst residues at the extreme N-terminus clearly are important for proper intracellular localization of NCS proteins, additional protein-dependent localization mechanisms, or lipid preferences together with differences in the lipid composition of individual membranes [50], may aid in the distinct localization of various NCS proteins, and thus their ability to sense different Ca²⁺ signals.

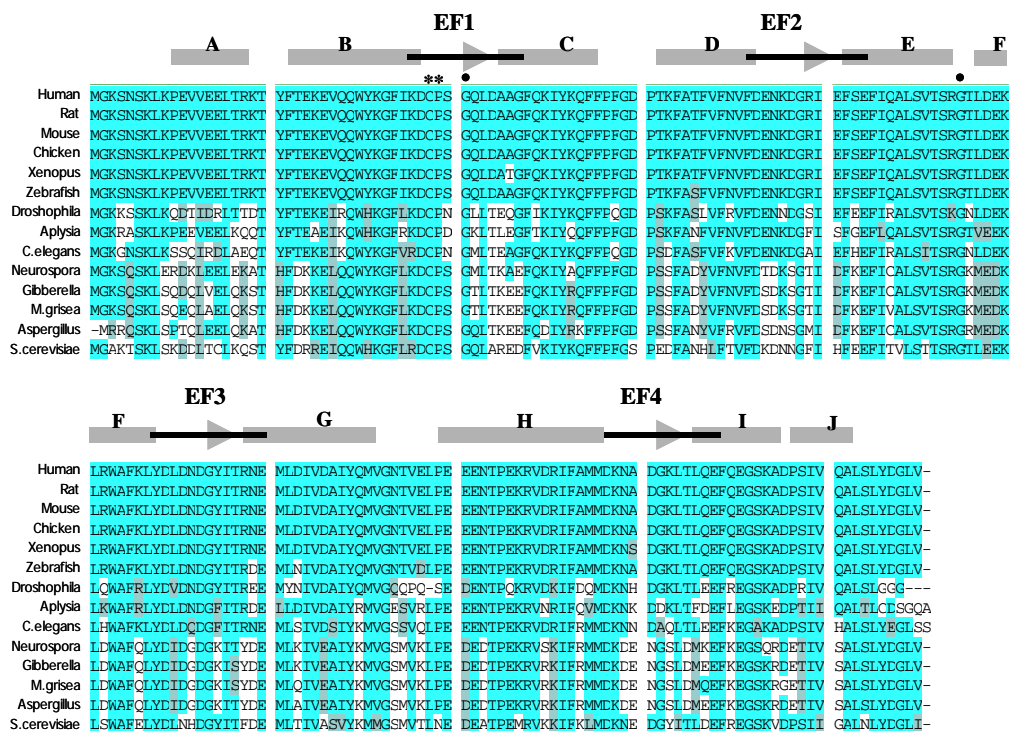


Figure 4. Alignment of NCS-1 proteins from different species. Amino acid sequence alignment of NCS-1 proteins illustrates high overall sequence homology across species. Amino acids highlighted in blue are identical, whilst amino acids highlighted in grey are similar to those of human NCS-1, respectively. The secondary structural elements (alpha helices A to J, with helix J corresponding to the C-terminal helix mentioned in the text, and β -sheets indicated by arrows) are shown in gray, with the four EF hands labeled EF1 to EF4. The consensus sequence for the 29-residue EF-hand motif is indicated by black lines. The conserved cysteine-proline substitution in EF-1 is indicated by asterisks, and the two rotational glycine residues by black dots, respectively. The database accession numbers for the sequences are as follows: human (P62166), rat (P62168), mouse (Q8BNY6), chicken (P62167), Xenopus (Q6GQJ0), Zebrafish (Q53A16), Drosophila (P37236), Aplysia (Q16981), *C. elegans* (P36608), Neurospora (EAA28220), Gibberella (EAA77148), *M. grisea* (Q52FT6), Aspergillus (Q4WLA4) and *S. cerevisiae* (Q06389).

In general, all members of the NCS family display high-affinity Ca^{2+} binding and cooperativity of Ca^{2+} binding *in vitro*. For example, Ca^{2+} binding to NCS-1 is half-maximal below 1 μM free Ca^{2+} and co-operative, with a Hill coefficient of approximately 2 [51]. Thus, NCS-1, as well as other NCS proteins, are able to transduce very small changes in intracellular Ca^{2+} concentrations in a range that would activate only a small proportion of calmodulin, and a fraction of the NCS proteins are likely active under basal conditions. In such a manner, the presence or absence of a Ca^{2+} /myristoyl switch mechanism, together with the targeting of different NCS proteins to distinct intracellular domains, allows for spatial and temporal control of Ca^{2+} sensing. For example, NCS proteins such as hippocalcin, neurocalcin δ and VILIP-1, which possess a Ca^{2+} /myristoyl switch mechanism, will require slow, prolonged and global Ca^{2+} elevation to translocate from the cytosol to their respective intracellular membrane compartments. In contrast, membrane-associated NCS-1 will be able to respond to brief, rapid and local Ca^{2+} transients mainly close to the TGN.

5. STRUCTURAL FEATURES OF NCS-1: THE HYDROPHOBIC CREVICE

The structures of several NCS proteins, including unmyristoylated, Ca^{2+} -bound human and yeast NCS-1 [13,46], unmyristoylated Ca^{2+} -bound GCAP-2 [52], unmyristoylated Ca^{2+} -bound neurocalcin δ [53] and unmyristoylated Ca^{2+} -bound KChIP1 complexed with the N-terminus of distinct K^+ channels [54,55], have been solved by different techniques such as X-ray crystallography or NMR. Recoverin has been most extensively characterized by such means, with structures of the protein available in its myristoylated, Ca^{2+} -free form [56,57], its myristoylated, Ca^{2+} -bound form [39] and in intermediate forms [58,59] thought to reflect a transient structure following the binding of the first Ca^{2+} ion. Such studies have shown that Ca^{2+} -free recoverin exists in a compact structure, with the myristoyl group buried within a hydrophobic pocket formed by residues from EF-1 and additional hydrophobic residues contributed by other helices [56]. In addition, recoverin was found to possess two distinct domains, with EF-1 and EF-2 intimately interacting to form the N-terminal domain, EF-3 and EF-4 forming the C-terminal domain, and a U-shaped linker between these domains positioning the four EF-hands in a compact tandem array. Importantly, comparison of the Ca^{2+} -free with the Ca^{2+} -bound forms of myristoylated recoverin demonstrated extensive

conformational changes upon Ca^{2+} binding as a result of rotation of the backbone at two glycine residues [39]. On the one hand, rotation at Gly 42, located in the loop between the helices of EF-1, was found to expose the myristoyl group towards the aqueous solution and to expose a hydrophobic surface potentially able to interact with target proteins. On the other hand, rotation at Gly 96, in the U-shaped linker between the two domains, further leads to differences in helix interactions between EF-2 and EF-3 which account for the cooperativity of Ca^{2+} binding, whilst minor structural changes occur in the very C-terminal domain [39].

These structural studies of recoverin have yielded great insights into the molecular mechanics of the Ca^{2+} /myristoyl switch mechanism, and superposition of the main chain structures have revealed large overall similarities in the structural fold of the different NCS proteins, including NCS-1 [13,52,53]. However, many of the hydrophobic residues that clamp the myristoyl group in the Ca^{2+} -free state of recoverin are conserved between all NCS family members, and thus cannot be used to predict the presence or absence of a Ca^{2+} /myristoyl switch mechanism. Similarly, upon Ca^{2+} binding, the structures of NCS proteins all reveal a hydrophobic surface, formed by highly conserved residues from the N-terminal as well as C-terminal domains (Figure 5). This solvent-exposed hydrophobic crevice has been suggested to serve as a possible binding site for downstream protein targets. Indeed, mutagenesis studies for some NCS proteins have revealed that distinct residues within the crevice are important for downstream target regulation [60-62]. However, the high sequence conservation of these residues amongst members of the NCS family indicates that whilst they may contribute to target interactions, they are not determinants of the specificity of such interactions, and alternative roles for the crevice, for example in mediating dimerization of NCS proteins, have been proposed as well [52,53,57,63].

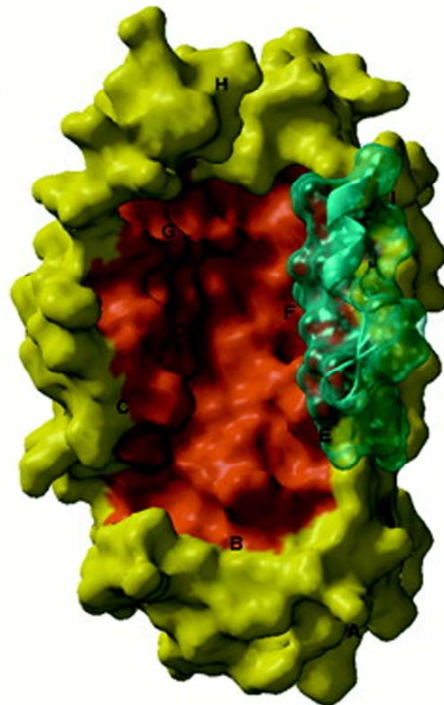


Figure 5. Molecular surface structure of human NCS-1. Molecular surface structure of human NCS-1, viewed down the large hydrophobic crevice (red). The secondary structural elements are labeled (A-J), and the C-terminal helix J is displayed in cyan. Reproduced from *J. Biol. Chem.* (2001) 276, 11949-11955 by copyright permission of the Journal of Biological Chemistry.

There also exist profound differences in the structural details of NCS proteins which may underlie their distinct functional roles. For example, the very N-terminus shows virtually no sequence similarity between NCS-1 and recoverin, neurocalcin δ , the GCAPs or the KChIPs (see Figure 1), and structural studies reveal the existence of an N-terminal helix of variable length and orientation in the different NCS proteins [52,56]. Importantly, the extreme C-terminus, also relatively variable in primary sequence between different NCS proteins, is comprised of an additional C-terminal helix. This helix interacts with helices of EF-3 and EF-4 in recoverin and GCAP-2 in a manner similar to the interaction of calmodulin with its helical target peptides [64], and thus has been proposed to enhance the specificity of NCS proteins by blocking their adventitious binding to calmodulin targets. Interestingly, the C-terminal helix in KChIP1 has been proposed to interact with the N-terminus of the K⁺ channel Kv4.2, suggesting that this helix may directly be involved in target interactions [55]. Similarly, the extreme C-terminus of NCS-1 has been shown to be essential for its interaction with one specific downstream target [65], and introduction of a peptide derived from the very C-terminus of NCS-1 into presynaptic terminals can abolish a certain type of facilitation [66]. Therefore, the relative structural positioning of the C-terminal helix may affect the shape of the hydrophobic crevice and thus aid in determining the specificity by which different NCS proteins, including NCS-1, associate with their target proteins (Figure 5).

Structural studies on NCS-1 have determined additional features unique to this protein as well. For example, the C-terminal helix in human, non-myristoylated, Ca²⁺-bound NCS-1 is positioned in such a manner that it exposes a much larger hydrophobic patch than the one for example seen in recoverin or neurocalcin δ [13]. However, the hydrophobic crevice of the yeast counterpart of NCS-1 is less than half the size of that of human NCS-1 [46], mainly because of the relative position of the C-terminal helix with respect to the rest of the protein structure. The functional significance of this (especially with respect to differences in the function of yeast versus mammalian NCS-1) remains unknown. In addition, the myristoyl group of NCS-1 is solvent-exposed in the absence of Ca²⁺, in agreement with the observation that myristoylated NCS-1 is membrane-associated even in the absence of Ca²⁺. Instead, the myristoyl group of NCS-1 seems to be involved in conferring some degree of cooperativity in Ca²⁺ binding [46,67]. Thus, Ca²⁺-induced structural changes in NCS-1 are predicted to increase its propensity to interact with membranes by means independent of the N-myristoyl group.

In conclusion, the most prominent structural effect produced by Ca²⁺ binding to different NCS proteins seems to involve ‘flipping out’ of the myristoyl group (for NCS proteins which contain a Ca²⁺/myristoyl switch mechanism), and in all cases exposure of a hydrophobic crevice in the protein. This crevice, in conjunction with the relative orientation of the C-terminal helix, may confer specificity to accommodate distinct downstream protein targets. However, additional structural studies with myristoylated NCS proteins will be necessary to more rigorously determine the structural impact of the myristoyl group on the proteins in the presence and absence of Ca²⁺. Ultimately, the structures of individual NCS proteins bound to

their respective target proteins will need to be determined to fully understand the selectivity and mechanism of action of distinct NCS proteins.

6. PHYSIOLOGICAL IMPORTANCE OF NCS-1: A MODULATOR OF SYNAPTIC EFFICACY

Whilst structure-function, localization and protein interaction studies may give a confusing picture as to the exact role(s) of the distinct NCS proteins in the nervous system, genetic manipulations of individual NCS proteins have clearly demonstrated their physiological importance in regulating distinct neuronal functions. NCS-1 was originally discovered in *Drosophila*, and its overexpression was shown to cause a frequency-dependent facilitation of neurotransmitter release at the neuromuscular junction [6]. Subsequently, overexpression of NCS-1 in *Xenopus* was found to enhance both spontaneous and evoked transmission at the neuromuscular junction [68]. In addition, direct loading of NCS-1 into the presynaptic nerve terminal at the calyx of Held synapse mimicked activity-dependent facilitation of P/Q-type Ca^{2+} currents during repetitive stimulation, whilst a C-terminal peptide derived from NCS-1 abolished such facilitation [66]. The latter result suggests that the C-terminal fragment of NCS-1 may interfere with a direct or indirect interaction of NCS-1 with P/Q-type Ca^{2+} channels, even though such an interaction has yet to be described.

In general, the above-mentioned facilitating effects of NCS-1 may have been indirect, caused for example by effects on channels or Ca^{2+} regulatory processes. However, a recent study at hippocampal neurons in culture has clearly shown that overexpression of NCS-1 in glutamatergic synapses more directly and specifically facilitates evoked transmission to paired pulses, thereby increasing the reliability of postsynaptic activation [69]. Calcium currents were unaffected in these cells, and there was no effect of NCS-1 on basal transmission. In addition, down-regulation of native NCS-1 (but presumably a series of additional proteins as well) was accompanied by a reduction in facilitation, suggesting that normal facilitation may also be produced by the action of native, endogenous NCS-1 [69]. These data suggest that NCS-1 may act as a Ca^{2+} -binding target modulating secretion to mediate facilitation at some synapses, and in addition basal release at other synapses, by regulating the underlying molecular process(es) in different ways [70]. Finally, a role for NCS-1 in associative learning and memory has been suggested by disruption of its expression in *C. elegans* [71], and the description of NCS-1 loss-of-function genetics in mice is greatly awaited. Together, the currently available studies clearly establish an important role for NCS-1 in enhancing synaptic transmission in different model systems. Thus, elucidating the mechanism(s) by which NCS-1 performs its potentiating role(s) has since become a major focus of investigation.

7. MECHANISM OF NCS-1 ACTION

How does NCS-1 work to facilitate transmitter release? Conceptually, NCS-1 may enhance transmitter release in a variety of ways [70,72], such as by increasing the number of functional synaptic contacts. Alternatively, NCS-1 may increase the number of vesicles per synaptic contact. This may mobilize additional vesicles to docking sites to increase the size of the readily releasable vesicle pool. NCS-1 may act to 'prime' docked vesicles, making them more available for release by increasing the probability of release. Such an effect may be mediated by an NCS-1-dependent change in the lipid or protein composition of the vesicle and/or plasma membrane, thereby affecting the efficiency with which a vesicle fuses upon Ca^{2+} influx. Finally, NCS-1 may directly affect the fusion machinery to increase the sensitivity of secretion to a local increase in Ca^{2+} elevation as intracellular residual Ca^{2+} builds up, or may enhance secretion indirectly, for example by increasing the amount and/or activity of presynaptic channels and/or postsynaptic receptors.

Evidence supporting several of these possible mechanistic explanations for the NCS-1-mediated enhancement of transmission have been accumulating. For example, overexpression of NCS-1 in *Xenopus* neuromuscular synapses in culture has been found to increase the number and size of synaptic contacts [73]. Similarly, overexpression of NCS-1 in the NG108-myocyte co-culture model led to enhanced synapse formation, probably due to an increase in the number of cholinergic synaptic vesicles [28]. In an anterior pituitary cell line, NCS-1 overexpression was found to increase the storage pool of adrenocorticotrophin, indicating that NCS-1 may act to increase the number of regulated secretory vesicles in this cell line [16]. Overexpression of NCS-1 in PC12 or chromaffin cells was found to enhance release [12,20,27,31], either by increasing the number of vesicles available for release or by increasing the fusion-competence of individual vesicles. Indeed, a recent study of insulin secretion by pancreatic β cells suggested that NCS-1 increases exocytosis by promoting the priming of secretory granules for release and increasing the number of granules in the readily releasable pool [74]. Finally, a series of studies suggested that NCS-1 can increase the surface expression of presynaptic Ca^{2+} channels and regulate postsynaptic receptor trafficking (see below). So how does NCS-1 work? Whilst only careful *in vivo* experiments (together with quantitative electron microscopy to evaluate changes in the number of vesicles) will be able to tease apart some of these possibilities, additional clues as to the mechanism of NCS-1 action have come from studying NCS-1-protein interactions.

8. NCS-1 AND ITS INTERACTING PARTNERS: MULTIFUNCTIONAL OR PROMISCUOUS?

The high sequence similarity amongst different NCS proteins has not only hampered the determination of their exact cellular and subcellular localizations, but also the determination of their interactions with specific downstream targets. For example, even though only 21% homologous to calmodulin, NCS-1 can substitute for calmodulin in activating several Ca^{2+} /calmodulin-dependent enzymes, such as the protein phosphatase calcineurin or cyclic

nucleotide phosphodiesterase, both *in vitro* and *in vivo* [75]. Similarly, recoverin, but also several other NCS family members including NCS-1, can inhibit the phosphorylation of rhodopsin by G protein-coupled receptor kinase 1 (GRK1; also known as rhodopsin kinase) [76-79]. In addition, several NCS proteins including NCS-1 can attenuate the GRK2-mediated phosphorylation of distinct receptors [80,81] (see also below). These data support the hypothesis that NCS proteins may be direct regulators of G protein-coupled receptor (GPCR) signaling [82], by interacting with different subtypes of GRKs to regulate the desensitization of different receptors. In this manner, NCS proteins may exert calcium sensitivity on the signaling properties of GPCRs. However, this would not ensure specificity, and indeed the ubiquitous calcium sensor calmodulin has been shown to regulate the activity of GRKs as well [83,84]. It seems possible that the apparent promiscuity of some of these described interactions *in vitro* is due to the high sequence similarity amongst these EF-hand-containing proteins, and is not necessarily reflecting a multifunctional nature of individual NCS proteins in regulating multiple downstream events. Specificity *in vivo* may then be achieved by the detailed subcellular localization of individual NCS proteins and individual GRKs. A detailed analysis of identified NCS-target protein interactions, using a more complete array of different NCS proteins, together with detailed subcellular localization studies are necessary to clearly establish which NCS-target protein interactions are likely to be relevant *in vivo*.

Finally, other described NCS-1-protein interactions, such as with distinct K⁺ channels [15,85], could similarly be due to the high sequence similarity between NCS-1 and KChIPs, rather than representing a specific, high-affinity interaction of mechanistic importance to explain the facilitating effects of NCS-1 in synaptic transmission. In addition to those currently described, additional specific binding partners for NCS-1 likely exist [47], although their exact nature remains to be determined. Below we discuss the relevance of two well-established NCS-1 interactions in more detail.

9. THE NCS-1-DISEASE CONNECTION

Abnormal activity of the dopamine (DA) system has been implicated in several psychiatric and neurological illnesses, such as schizophrenia, bipolar disorder, or attention deficit hyperactivity disorder [86], even though the precise sites of dopamine dysfunction in these disorders are currently unknown. In the CNS, DA modulates neuronal excitability by regulating ligand- and voltage-gated ion channels. The actions of DA are mediated by a family of seven-transmembrane G-protein-coupled receptors (GPCRs), D1-D5 receptors, which display unique properties with respect to their effects on downstream signaling cascades. Receptor desensitization, characterized by a decline in receptor responsiveness to agonist, represents a critical adaptation mechanism that protects against receptor overstimulation. The desensitization of activated GPCRs is mediated by the phosphorylation of residues within the intracellular domains of receptors and is mediated both by second messenger-dependent kinases and by GRKs, followed by receptor internalization. In addition, the intracellular activity of the individual DA receptor subtypes are regulated by the actions of a cohort of cytoskeletal, adaptor and signaling proteins called dopamine receptor-

interacting proteins (DRIPs). DRIPs seem to regulate most stages of the life-cycle of a DA receptor, including biosynthesis, trafficking to the plasma membrane, and internalization [86]. The recent discovery that the levels of NCS-1 are upregulated in patients with schizophrenia or bipolar disorders [87], and that NCS-1 expression shows cell-specific changes in brains of schizophrenics [88], together with the identification of NCS-1 as a DRIP for the D2 receptor [80] suggests the possibility that defects in Ca^{2+} homeostasis (mediated by NCS-1) might contribute to abnormalities in the brain DA system in several neurological diseases [89].

NCS-1 was identified as a DRIP for the D2 receptor in a screen of a brain cDNA library using the very C-terminal tail of the D2 receptor. The D2 receptor-interacting region in NCS-1 was mapped to the N-terminal 71 residues, and the interaction was shown to occur in a Ca^{2+} -independent manner [80]. When expressed in mammalian cells, NCS-1 attenuated the DA-induced D2 receptor internalization by a mechanism which involved a reduction in D2 receptor phosphorylation. NCS-1 exerted its effect on D2 receptor signaling through an interaction with GRK2, a kinase also associated with the D2 receptor. The effect of NCS-1 in inhibiting GRK2-dependent desensitization of D2 receptors was Ca^{2+} -dependent [80]. The difference in the Ca^{2+} dependency between the NCS-1/D2 receptor interaction and the NCS-1/GRK2 interaction suggests the presence of two distinct complexes, and the possibility that NCS-1 and GRK2 may compete for binding to the D2 receptor. In this scenario, elevated levels of NCS-1, combined with abnormalities in Ca^{2+} homeostasis, may potentiate signaling through the D2 receptor by preventing GRK2-mediated D2 receptor internalization (Figure 6). However, the reported (albeit weak) inhibition of GRK2-mediated M2 muscarinic receptor phosphorylation by VILIP-1 and neurocalcin δ [81] leaves open the possibility that the observed effects on D2 receptor internalization are mediated by an NCS protein distinct from NCS-1, and further experiments will be necessary to determine the exact nature of the NCS protein involved.

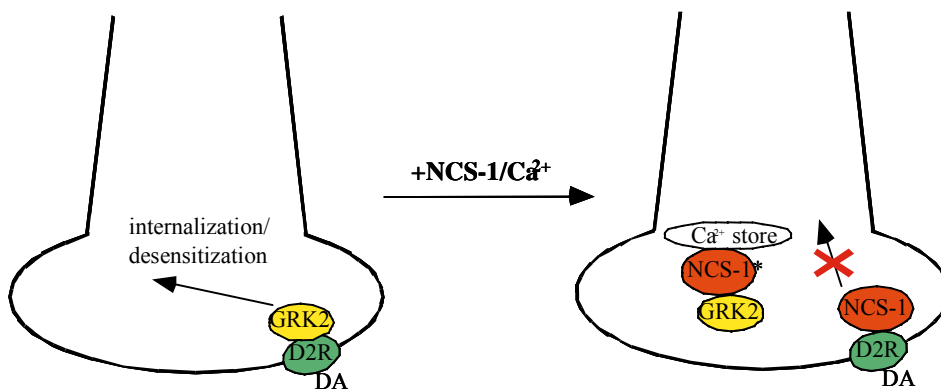


Figure 6. Model for the role of NCS-1 in D2 receptor signaling. The interaction between the dopamine (DA) D2 receptor (D2R) and GRK2 results in desensitization of the receptor via internalization, either pre- and/or postsynaptically (left). NCS-1 interacts with the D2 receptor in a Ca^{2+} -independent manner, presumably at the plasma membrane. In contrast, the interaction between NCS-1 and GRK2 seems to be Ca^{2+} -dependent (indicated by NCS-1*) [80]. Thus, Ca^{2+} -bound NCS-1 may recruit GRK2, thereby

inhibiting GRK2 to interact with the D2 receptor (right). Such NCS-1/GRK2 interaction may occur on intracellular organelles and may be promoted by Ca^{2+} release from intracellular stores (e.g. Golgi) or by Ca^{2+} entry across the plasma membrane. In either case, abnormal Ca^{2+} homeostasis and/or an increase in the levels of NCS-1 would result in the potentiation of signaling through the D2 receptor.

In either case, how may an increase in NCS-1 levels in the dorsolateral prefrontal cortex (DLPFC) relate to schizophrenia? Dysfunction in the DLPFC is largely responsible for the debilitating deficits in working memory-dependent executive functions observed in schizophrenic patients [86]. NCS-1 inhibits the desensitization of the D2 receptor, and thus enhances the influence of D2 receptors on cell activity [80]. This is expected to result in a depressive effect on excitatory transmission and thus a decreased activation of this cortical area, an outcome which would explain the efficacy of D2 receptor antagonists in treating symptoms of schizophrenia [86]. Additional experiments will be needed to establish a conclusive link between NCS-1, D2 receptors and neurological illnesses such as schizophrenia or bipolar disorder.

NCS-1 has also recently been described as an interacting protein of interleukin-1 receptor accessory protein-like protein (IL1RAPL) [65]. Mutations in IL1RAPL are responsible for a form of X-linked mental retardation [90]. Yeast two-hybrid analysis suggested that the 16 C-terminal residues of NCS-1 (but not of hippocalcin or calmodulin) interact with ILRAPL, and *in vivo* experiments further established that this interaction occurs in a Ca^{2+} -independent manner [65]. Finally, overexpression of IL1RAPL was found to inhibit secretion from neuroendocrine cells, suggesting a role for this protein in regulating neurotransmitter release. The implication of a gene product involved in mental retardation, in addition to its role in the regulation of synaptic transmission is similar to that found for α GDI (GDP dissociation inhibitor) [91,92]. This protein is a regulator of Rab3 activities, proteins that participate in synaptic vesicle fusion [93]. Further studies will be necessary to determine whether genes such as IL1RAPL that are involved in mental retardation act by regulating novel aspects of synaptic activity (e.g. mediated by NCS-1), the dysfunction of which may result in an impairment of the development of cognitive functions.

10. THE NCS-1-TRAFFICKING CONNECTION

Important insight into the possible mechanism of action of NCS-1 has come from studies performed in yeast. Frequenin, the orthologue of NCS-1 and the only NCS family member identified in *S. cerevisiae*, was found to interact with PIK1, one of the two non-redundant phosphatidylinositol 4-kinases (PI4Ks) in yeast [94]. Binding was found to be of high-affinity, and purification of the frequenin-PIK1 complex revealed a 1:1 stoichiometry [95]. Mapping experiments suggested that frequenin binds to a hydrophobic domain within PIK1, but unfortunately the corresponding interacting domain within frequenin was not determined in these studies [95,96]. The binding of frequenin to PIK1, while Ca^{2+} -independent, enhanced the activity of PIK1 by 3-fold [94], indicating that frequenin may act as a regulator of PIK1 activity. Importantly, overexpression of PIK1 was found to suppress the lethality of frequenin-mutant cells, indicating that PIK1 is the sole essential target for frequenin in yeast cells [94]. PIK1 is localized to the cytoplasm and to *trans*-Golgi membranes, and a mutation

in PIK1 causes an accumulation of Golgi structures and a concomitant defect in Golgi-to-cell-surface and Golgi-to-vacuole trafficking [97,98]. Thus, at least in yeast, frequenin acts to modulate the activity of PIK1 and thereby regulates intracellular membrane trafficking events.

Evidence for a similar role of NCS-1 in mammalian cells has been accumulating as well. For example, expression of human NCS-1 in *S. cerevisiae* (but not of recoverin or KChIP2) can rescue the inviability of frequenin-mutant cells, suggesting that the function of NCS-1 in mammals may closely resemble that of frequenin in yeast [96]. Furthermore, endogenous mammalian NCS-1 seems to interact with PI4K β (the PIK1 homologue) in neuronal and non-neuronal cells [14,19,20,29], stimulate the activity of PI4K β *in vitro* [29,99], and colocalize with PI4K β on the TGN [13].

PI4Ks are responsible for the synthesis of phosphatidylinositol 4-phosphate (PtdIns(4)P), the precursor of phosphatidylinositol (4,5)-bisphosphate (PtdIns(4,5)P₂). On the one hand, the ability of NCS-1 to enhance agonist-evoked secretion could be attributed to its activation of PI4K β , leading to the upregulation of Ins(1,4,5)P₃ receptor signalling and Ca²⁺ mobilization [31,100]. On the other hand, both PtdIns(4)P and PtdIns(4,5)P₂ are known to play important roles in several membrane trafficking steps, including vesicle budding from the TGN, exocytosis and endocytosis. In sum, the data suggest that PI4K β constitutes an *in vivo* downstream target of NCS-1, and indicate that the NCS-1-mediated modulation of phosphoinositide levels may regulate intracellular membrane trafficking events. If indeed the case, alterations in the number and/or fusion ability of vesicles, mediated by changes in membrane phosphoinositide composition, may underlie the observed facilitating effects of NCS-1 on synaptic transmission *in vivo*.

11. PHOSPHOINOSITIDES AND MEMBRANE TRAFFICKING

Phosphoinositides have emerged as important regulators of a variety of membrane trafficking processes. For example, *de novo* synthesis of PtdIns(4,5)P₂ has been shown to be important for an ATP-dependent priming step preceding the Ca⁺-dependent fusion of regulated secretory vesicles. PtdIns(4,5)P₂ also plays a positive role in regulating clathrin-mediated endocytosis from the plasma membrane and in regulating an actin-based vesicle motility mechanism [101]. In addition, PtdIns(4)P and PtdIns(4,5)P₂ are necessary for the exit of transport carriers from the TGN.

The TGN is a major sorting station within the cell, in which distinct vesicle populations, destined for various locations, are formed. A key aspect of this process is the formation of protein complexes that recognize sorting signals on the cytosolic portion of cargo proteins and make a coat that is necessary to collect cargo and form transport intermediates [102]. Sorting signals are recognized only on certain membrane surfaces, and the mechanisms that determine where cytosolic coats form on membranes are poorly understood. However, recent data strengthen the hypothesis that phosphoinositides [103] determine the membrane locations where coat proteins may assemble [104]. In this scenario, dual interactions of distinct coat proteins with specific phosphoinositides as well as with additional protein

binding sites (such as small GTPases) control their efficient and specific recruitment to membranes [105].

In mammals, the Golgi complex contains three PI4Ks, with PI4K β being recruited to the Golgi complex in response to ADP-ribosylation factor (ARF; a small GTPase) activation [106]. Recent studies have identified two effectors of PtdIns(4)P, FAPP1 and FAPP2 (four-phosphate-adaptor proteins 1 and 2), which interact with both PtdIns(4)P and ARF and which control the generation of constitutive post-Golgi vesicle carriers [107]. Thus, an ARF-dependent recruitment of PI4K β , followed by the production of PtdIns(4)P and the consecutive recruitment of FAPPs may generate distinct TGN membrane domains from which constitutive TGN-derived carriers emerge [104,105,108,109].

How does NCS-1 fit into this picture? A recent study suggests that NCS-1 is able to recruit ARF1 to the TGN in a Ca²⁺-dependent manner [110]. Whilst both NCS-1 and ARF1 can activate PI4K β in isolation, an antagonistic mode of action was uncovered when both proteins were present in combination with PI4K β . These data suggest that activation of PI4K β can proceed in the presence of ARF1 or NCS-1 alone, but not if both effectors are present simultaneously, and further indicate that ARF1-NCS-1 may form a mutually exclusive complex in preference to binding to PI4K β . Thus, the inhibitory interaction between the ARF1 and NCS-1 pathways may function to prevent the simultaneous activation of PI4K β by both effectors, and thereby may assist in the generation of segregated trafficking domains at the TGN [110]. However, clearly additional work is necessary to corroborate these findings.

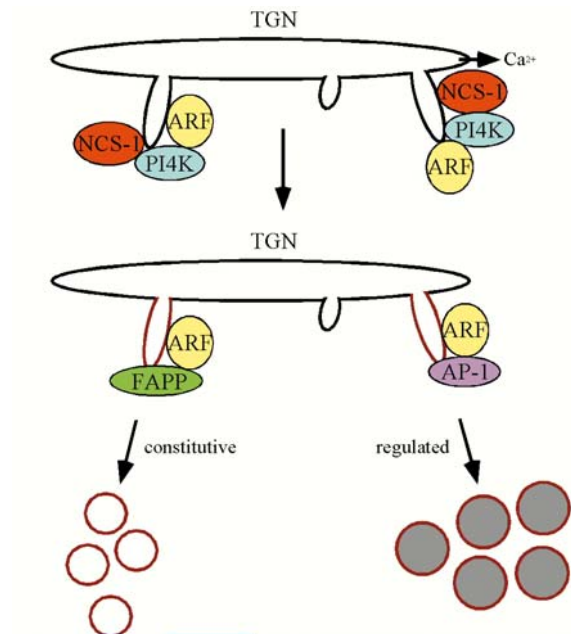


Figure 7. Model for the role of NCS-1 in vesicle trafficking out of the TGN. NCS-1 (with or without ARF), possibly upon Ca^{2+} release from the TGN, can recruit PI4K β (PI4K) to the TGN. This results in the production of PtdIns(4)P (red lines) at defined domains of the TGN, followed by the ARF-mediated and PtdIns(4)P-dependent recruitment of distinct coat proteins (FAPPs for the generation of constitutive post-Golgi vesicle carriers, and AP-1 for the generation of regulated vesicle carriers, respectively). An increase in constitutive vesicle carriers is followed by a concomitant increase in the levels of PtdIns(4,5)P₂ at the plasma membrane (blue lines), which seems to affect the size of a readily releasable vesicle pool. On the other hand, an increase in regulated secretory vesicle carriers (e.g. large dense-core vesicles) may be reflected in a concomitant increase in the actual number of vesicles available for release.

An alternative mechanism of NCS-1 function may involve the possibility that NCS-1 (with or without ARF1) helps in the recruitment and/or maintenance of PI4K β at the Golgi complex (Figure 7). This will further enhance the production of PtdIns(4)P and thus the recruitment of FAPP coat proteins, leading to an increase in the generation of constitutive post-Golgi transport vesicles. The fusion of these constitutive vesicles containing elevated levels of PtdIns(4)P with the plasma membrane, followed by conversion to PtdIns(4,5)P₂, would lead to an increase in the levels of PtdIns(4,5)P₂ at the plasma membrane. Indeed, plasmalemmal PtdIns(4,5)P₂ levels have been shown to increase the size of the readily releasable vesicle pool [111], an effect which is similar to that observed when NCS-1 is overexpressed in certain cell systems. On the other hand, the NCS-1-mediated enhanced production of PtdIns(4)P at the Golgi may result in the increased generation of transport carriers destined for the regulated secretory pathway [72], which could be more directly reflected in the number of secretory vesicles available for release and/or their ability to fuse with the plasma membrane [112], again an effect observed or proposed for the action of NCS-1 in enhancing neurotransmission.

Whatever the exact mechanism, an NCS-1-mediated effect on trafficking out of the Golgi complex adds an additional layer of Ca^{2+} -dependent regulation. Indeed, the Golgi can act as a Ca^{2+} store [113], and local Ca^{2+} release has been shown to be important for traffic from a pre-Golgi compartment to the Golgi complex [114] and within the Golgi complex [115]. Thus, NCS-1 may act as a Ca^{2+} sensor with a specific role in post-Golgi membrane traffic.

CONCLUSIONS

Whilst far from being understood at a molecular level, current data suggest that NCS-1 may potentiate secretion from a variety of cell types by enhancing the trafficking of TGN-derived transport carriers in a PI4K β -specific manner. In addition, the established role of NCS-1 in D2 receptor desensitization, together with the finding that it can interact with various receptors and/or channels either directly and/or indirectly, suggest additional roles for NCS-1 in regulating a variety of neuronal functions. Whether the latter effects are indirect and due to alterations in membrane trafficking, or whether NCS-1 stays bound to carrier vesicles and performs additional roles by stabilizing and/or regulating the activity of a defined subset of proteins on these vesicles remains to be determined. In either case, NCS-1 is an important molecule which may constitute a major regulatory site for modification of

synaptic properties and comprise an important target for understanding and treating neurological illnesses such as schizophrenia or bipolar disorder.

ACKNOWLEDGEMENTS

Work in our laboratory is supported by a grant from the Spanish Ministry of Education and Science. To whom correspondence should be addressed: sabine.hilfiker@ipb.csic.es.

REFERENCES

- [1] Augustine, G.J., Santamaria, F. and Tanaka, K. 2003, *Neuron*, 40, 331.
- [2] Braunewell, K.-H. and Gundelfinger, E.D. 1999, *Cell Tissue Res.*, 295, 1.
- [3] Burgoyne, R.D. and Weiss, J.L. 2001, *Biochem. J.*, 353, 1.
- [4] Burgoyne, R.D. 2004, *Biochim. Biophys. Acta*, 1742, 59.
- [5] Burgoyne, R.D., O'Callaghan, D.W., Hasdemir, B., Haynes, L.P. and Tepikin, A.V. 2004, *Trends Neurosci.*, 27, 203.
- [6] Pongs, O., Lindemeier, J., Zhu, X.R., Theil, T., Engelkamp, D., Krah-Jentgens, I., Lambrecht, H.-G., Koch, K.W., Schwemer, J., Rivosecchi, R., Mallart, A., Galceran, J., Canal, I., Barbas, J.A. and Ferrús, A. 1993, *Neuron*, 11, 15.
- [7] Moncreif, N.D., Kretsinger, R. H. and Goodman, M. 1990, *J. Mol. Evol.*, 30, 522.
- [8] Martone, M.E., Edelman, V.M., Ellisman, M.H. and Nef, P. 1999, *Cell Tissue Res.*, 295, 395.
- [9] Paterlini, M., Revilla, V., Grant, A.L. and Wisden, W. 2000, *Neuroscience*, 99, 205.
- [10] Olafsson, P., Soares, H.D., Herzog, K.-H., Wang, T., Morgan, J.I. and Lu, B. 1997, *Mol. Brain Res.*, 44, 73.
- [11] Gierke, P., Zhao, C., Brackmann, M., Linke, B., Heinemann, U. and Braunewell, K.-H. 2004, *Biochem. Biophys. Res. Commun.*, 323, 38.
- [12] McFerran, B.W., Graham, M.E. and Burgoyne, R.D. 1998, *J. Biol. Chem.*, 273, 22768.
- [13] Bourne, Y., Dannenberg, J., Pollmann, V., Marchot, P. and Pongs, O. 2001, *J. Biol. Chem.*, 276, 11949.
- [14] Weisz, O.A., Gibson, G.A., Leung, S.-M., Roder, J. and Jeromin, A. 2000, *J. Biol. Chem.*, 275, 24341.
- [15] Guo, W., Malin, S.A., Johns, D.C., Jeromin, A. and Nerbonne, J.M. 2002, *J. Biol. Chem.*, 277, 26436.
- [16] Guild, S.B., Murray, A.T., Wilson, M.L., Wiegand, U.K., Apps, D.K., Jin, Y., Rindler, M., Roder, J. and Jeromin, A. 2001, *Mol. Cell. Endocrinol.*, 184, 51.
- [17] Mora, S., Durham, P.L., Smith, J.R., Russo, A.F., Jeromin, A. and Pessin, J.E. 2002, *J. Biol. Chem.*, 277, 27494.

- [18] Brochetta, C., Perrotta, M.G., Jeromin, A., Romano, M., Vita, F., Soranzo, M.R., Borelli, V., Roder, J. and Zabucchi, G. 2003, *Inflammation*, 27, 361.
- [19] Taverna, E., Francolini, M., Jeromin, A., Hilfiker, S., Roder, J. and Rosa, P. 2002, *J. Cell Sci.*, 115, 3909.
- [20] Pan, C.-Y., Jeromin, A., Lundstrom, K., Yoo, S.H., Roder, J. and Fox, A.P. 2002, *J. Neurosci.*, 22, 2427.
- [21] Negyessy, L. and Goldman-Rakic, P.S. 2005, *J. Comp. Neurol.*, 488, 464.
- [22] Jinno, S., Jeromin, A., Roder, J. and Kosaka, T. 2002, *Neuroscience*, 113, 449.
- [23] Wilkinson, B.L., Jeromin, A., Roder, J. and Hyson, R.L. 2003, *Neuroscience*, 117, 957.
- [24] Bergmann, M., Grabs, D., Roder, J., Rager, G. and Jeromin, A. 2002, *J. Comp. Neurol.*, 449, 231.
- [25] O'Callaghan, D.W., Ivings, L., Weiss, J.L., Ashby, M.C., Tepikin, A.V. and Burgoyne, R.D. 2002, *J. Biol. Chem.*, 277, 14227.
- [26] Scalettar, B.A., Rosa, P., Taverna, E., Francolini, M., Tsuboi, T., Terakawa, S., Koizumi, S., Roder, J. and Jeromin, A. 2002, *J. Cell Sci.*, 115, 2399.
- [27] Koizumi, S., Rosa, P., Willars, G.B., Challiss, A.J., Taverna, E., Francolini, M., Bootman, M.D., Lipp, P., Inoue, K., Roder, J. and Jeromin, A. 2002, *J. Biol. Chem.*, 277, 30315.
- [28] Chen, X.-L., Zhong, Z.-G., Yokoyama, S., Bark, C., Meister, B., Berggren, P.-O., Roder, J., Higashida, H. and Jeromin, A. 2001, *J. Physiol.*, 532, 649.
- [29] Zhao, W., Varnai, P., Tuymetova, G., Balla, A., Toth, Z.E., Oker-Blom, C., Roder, J., Jeromin, A. and Balla, T. 2001, *J. Biol. Chem.*, 276, 40183.
- [30] O'Callaghan, D.W. and Burgoyne, R.D. 2003, *J. Cell Sci.*, 116, 4833.
- [31] Rajebhosale, M., Greenwood, S., Vidugiriene, J., Jeromin, A. and Hilfiker, S. 2003, *J. Biol. Chem.*, 278, 6075.
- [32] An, W.F., Bowlby, M.R., Betty, M., Cao, J., Ling, H.P., Mendoza, G., Hinson, J.W., Mattsson, K.I., Strassle, B.W., Trimmer, J.S. and Rhodes, K.J. 2000, *Nature*, 403, 553.
- [33] Holmqvist, M.H., Cao, J., Hernandez-Pineda, R., Jacobson, M.D., Carroll, K.I., Sung, M. A., Betty, M., Ge, P., Gilbride, K.J., Brown, M.E., Jurman, M.E., Lawson, D., Silos-Santiago, I., Xie, Y., Covarrubias, M., Rhodes, K.J., Distefano, P.S. and An, W.F. 2002, *Proc. Natl. Acad. Sci. USA*, 99, 1035.
- [34] Zozulya, S. and Stryer, L. 1992, *Proc. Natl. Acad. Sci. USA*, 89, 11569.
- [35] Maurer-Stroh, S., Eisenhaber, B. and Eisenhaber, F. 2002, *J. Mol. Biol.*, 317, 523.
- [36] Resh, M.D. 1994, *Cell*, 76, 411.
- [37] Resh, M.D. 1999, *Biochim. Biophys. Acta*, 1451, 1.
- [38] Tanaka, T., Ames, J.B., Harvey, T.S., Stryer, L. and Ikura, M. 1995, *Nature*, 376, 444.
- [39] Ames, J.B., Ishima, R., Tanaka, T., Gordon, J.I., Stryer, L. and Ikura, M. 1997, *Nature*, 389, 198.
- [40] Dizhoor, A.M., Chen, C.K., Olshevskaya, E., Sinelnikova, V.V., Phillipov, P. and Hurley, J.B. 1993, *Science*, 259, 829.
- [41] Valentine, K.G., Mesleh, M.F., Opella, S.J., Ikura, M. and Ames, J.B. 2003, *Biochemistry*, 42, 6333.
- [42] Ladant, D. 1995, *J. Biol. Chem.*, 270, 3179.

- [43] Ivings, L., Pennington, S.R., Jenkins, R., Weiss, J.L. and Burgoyne, R.D. 2002, *Biochem. J.*, 363, 599.
- [44] Spilker, C., Dresbach, T. and Braunewell, K.-H. 2002, *J. Neurosci.*, 22, 7331.
- [45] Spilker, C. and Braunewell, K.-H. 2003, *Mol. Cell. Neurosci.*, 24, 766.
- [46] Ames, J.B., Hendricks, K.B., Strahl, T., Huttner, I.G., Hamasaki, N. and Thorner, J. 2000, *Biochemistry*, 39, 12149.
- [47] McFerran, B.W., Weiss, J.L. and Burgoyne, R.D. 1999, *J. Biol. Chem.*, 274, 30258.
- [48] O'Callaghan, D.W. and Burgoyne, R.D. 2004, *J. Biol. Chem.*, 279, 14347.
- [49] Hamasaki-Katagiri, N., Molchanova, T., Takeda, K. and Ames, J.B. 2004, *J. Biol. Chem.*, 279, 12744.
- [50] Senin, I.I., Hoepfner-Heitmann, D., Polkovnikova, O.O., Churumova, V.A., Tikhomirova, N.K., Philippov, P.P. and Koch, K.-W. 2004, *J. Biol. Chem.*, 279, 48647.
- [51] Cox, J.A., Drussel, I., Comte, M., Nef, S., Nef, P., Lenz, S.E. and Gundelfinger, E.D. 1994, *J. Biol. Chem.*, 269, 32807.
- [52] Ames, J.B., Dizhoor, A.M., Ikura, M., Palczewski, K. and Stryer, L. 1999, *J. Biol. Chem.*, 274, 19329.
- [53] Vijay-Kumar, S. and Kumar, V.D. 1999, *Nat. Struct. Biol.*, 6, 80.
- [54] Scannevin, R.H., Wang, K.-W., Jow, F., Megules, J., Kospco, D.C., Edris, W., Carroll, K.C., Lu, Q., Xu, W., Xu, Z., Katz, A.H., Olland, S., Lin, L., Taylor, M., Stahl M., Malakian, K., Somers, W., Mosyak, L., Bowlby, M., Chanda, P. and Rhodes, K.J. 2004, *Neuron*, 41, 587.
- [55] Zhou, W., Qian, Y., Kunjilwar, K., Pfaffinger, P.J. and Choe, S. 2004, *Neuron*, 41, 573.
- [56] Tanaka, T., Ames, J.B., Harvey, T.S., Stryer, L. and Ikura, M. 1995, *Nature*, 376, 444.
- [57] Flaherty, K.M., Zoulyya, S., Stryer, L. and McKay, D.B. 1993, *Cell*, 75, 709.
- [58] Ames, J.B., Hamashima, N. and Molchanova, T. 2002, *Biochemistry*, 41, 5776.
- [59] Weiergraber, O.H., Senin, I.I., Philippov, P.P., Granzin, J. and Koch, K.-W. 2003, *J. Biol. Chem.*, 278, 22972.
- [60] Olshevskaya, E.V., Boikov, S., Ermilov, A., Krylov, D., Hurlay, J.B. and Dizhoor, A.M. 1999, *J. Biol. Chem.*, 274, 10823.
- [61] Tachibanaki, S., Nanda, K., Sasaki, K., Ozaki, K. and Kawamura, S. 2000, *J. Biol. Chem.*, 275, 3313.
- [62] Ermilov, A.N., Olshevskaya, E.V., Dizhoor, A.M. 2001, *J. Biol. Chem.*, 276, 48143.
- [63] Hwang, J.-Y., Schlesinger, R. and Koch, K.-W. 2004, *Eur. J. Biochem.*, 271, 3785.
- [64] Ikura, M., Clore, G.M., Gronenborn, A.M., Zhu, G., Klee, C.B. and Bax, A. 1992, *Science*, 256, 632.
- [65] Bahi, N., Friocourt, G., Carrie, A., Graham, M.E., Weiss, J.L., Chafey, P., Fauchereau, F., Burgoyne, R.D. and Chelly, J. 2003, *Hum. Mol. Genet.*, 12, 1415.
- [66] Tsujimoto, T., Jeromin, A., Saitoh, N., Roder, J.C. and Takahashi, T. 2002, *Science*, 295, 2276.
- [67] Jeromin, A., Muralidhar, D., Parameswaran, M.N., Roder, J., Fairwell, T., Scarlata, S., Dowal, L., Mustafá, S.M., Chary, K.V.R. and Sharma, Y. 2004, *J. Biol. Chem.*, 279, 27158.
- [68] Olafsson, P., Wang, T. and Lu, B. 1995, *Proc. Natl. Acad. Sci. USA*, 92, 8001.

-
- [69] Sippy, T., Cruz-Martin, A., Jeromin, A. and Schweizer, F.E. 2003, *Nat. Neurosci.*, *6*, 1031.
- [70] Zucker, R.S. 2003, *Nat. Neurosci.*, *6*, 1006.
- [71] Gomez, M., De Castro, E., Guarin, E., Sasakura, H., Kuhara, A., Mori, I., Bartfai, T., Bargmann, C.I. and Nef, P. 2001, *Neuron*, *30*, 241.
- [72] Hilfiker, S. 2003, *Biochem. Soc. Trans.*, *31*, 828.
- [73] Wang, C.-Y., Yang, F., He, X., Chow, A., Du, J., Russell, J.T. and Lu, B. 2001, *Neuron*, *32*, 99.
- [74] Gromada, J., Bark, C., Smidt, K., Efanov, A.M., Janson, J., Mandic, S.A., Webb, D.-L., Zhang, W., Meister, B., Jeromin, A. and Berggren, P.-O. 2005, *Proc. Natl. Acad. Sci. USA*, *102*, 10303.
- [75] Schaad, N.C., De Castro, E., Nef, S., Hegi, S., Hinrichsen, R., Martone, M.E., Ellisman, M.H., Sikkink, R., Rusnak, F., Sygush, J. and Nef, P. 1996, *Proc. Natl. Acad. Sci. USA*, *93*, 9253.
- [76] Calvert, P.D., Klenchin, V.A. and Bownds, M.D. 1995, *J. Biol. Chem.*, *270*, 24127.
- [77] Chen, C.K., Ingelese, J., Lefkowitz, R.J. and Hurley, J.B. 1995, *J. Biol. Chem.*, *270*, 18060.
- [78] De Castro, E., Nef, S., Fiumelli, H., Lenz, S.E., Kawamura, S. and Nef, P. 1995, *Biochem. Biophys. Res. Commun.*, *216*, 133.
- [79] Faurobert, E., Chen, C.-K., Hurley, J.B. and Teng, D. H.-F. 1996, *J. Biol. Chem.*, *271*, 10256.
- [80] Kabbani, N., Negyessy, L., Lin, R., Goldman-Rakic, P. and Levenson, R. 2002, *J. Neurosci.*, *22*, 8476.
- [81] Kato, M., Watanabe, Y., Iino, S., Takaoka, Y., Kobayashi, S., Haga, T. and Hidaka, H. 1998, *Biochem. J.*, *331*, 871.
- [82] Iacovelli, L., Sallese, M., Mariggio, S., and De Blasi, A. 1999, *FASEB J.*, *13*, 1.
- [83] Chuang, T.-T., Paolucci, L. and De Blasi, A. 1996, *J. Biol. Chem.*, *271*, 28691.
- [84] Pronin, A.N., Satpaev, D.K., Slepak, V.Z. and Benovic, J.L. 1997, *J. Biol. Chem.*, *272*, 18273.
- [85] Nakamura, T.Y., Pountney, D.J., Ozaita, A., Nandi, S., Ueda, S., Rudy, B. and Coetzee, W.A. 2001, *Proc. Natl. Acad. Sci. USA*, *98*, 12808.
- [86] Bergson, C., Levenson, R., Goldman-Rakic, P.S. and Lidow, M.S. 2003, *Trends Pharmacol. Sci.*, *24*, 486.
- [87] Koh, P.O., Undie, A.S., Kabbani, N., Levenson, R., Goldman-Rakic, P.S. and Lidow, M.S. 2003, *Proc. Natl. Acad. Sci. USA*, *100*, 313.
- [88] Bernstein, A.M., 2002, *NeuroReport*, *13*, 393.
- [89] Carlsson, A., Waters, N., Holm-Waters, S., Tedroff, J., Nilsson, M. and Carlsson, M.L. 2001, *Annu. Rev. Pharmacol. Toxicol.*, *41*, 237.
- [90] Carrie, A., Jun, L., Bienvenu, T., Vinet, M.C., McDonell, N., Couvert, P. Zemni, R., Cardona, A., Van Buggenhout, G., Frints, S., Hamel, B., Moraine, C., Ropers, H.H., Strom, T., Howell, G.R., Whittaker, A., Ross, M.T., Kahn, A., Fryns, J.P., Beldjord, C., Marynen, P. and Chelly, J. 1999, *Nat. Genet.*, *23*, 25.

- [91] D'Adamo, P., Menegon, A., Lo Nigro, C., Grasso, M., Gulisano, M., Tamanini, F., Bienvenu, T., Gedeon, A.K., Oostra, B., Wu, S.K., Tandon, A., Valtorta, F., Balch, W.E., Chelly, J. and Toniolo, D. 1998, *Nat. Genet.*, *19*, 134.
- [92] Bienvenu, T., des Portes, V., Saint Martin, A., McDonell, N., Billuart, P., Carrie, A., Vinet, M.C., Couvert, B., Toniolo, D., Ropers, H.H., Moraine, C., van Bokhoven, H., Fryns, J.P., Kahn, A., Beldjord, C. and Chelly, J. 1998, *Hum. Mol. Genet.*, *7*, 1311.
- [93] Geppert, M. and Sudhof, T.C. 1998, *Ann. Rev. Neurosci.*, *21*, 75.
- [94] Hendricks, K.B., Wang, B.Q., Schieders, E.A. and Thorner, J. 1999, *Nat. Cell Biol.*, *1*, 234.
- [95] Huttner, I.G., Strahl, T., Osawa, M., King, D.S., Ames, J.B. and Thorner, J. 2003, *J. Biol. Chem.*, *278*, 4862.
- [96] Strahl, T., Grafelmann, B., Dannenberg, J., Thorner, J. and Pongs, O. 2003, *J. Biol. Chem.*, *278*, 49589.
- [97] Walch-Solimena, C. and Novick, P. 1999, *Nat. Cell Biol.*, *1*, 523.
- [98] Audhya, A., Foti, M. and Emr, S.D. 2000, *Mol. Biol. Cell*, *11*, 2673.
- [99] Zheng, Q., Bobich, J.A., Vidugiriene, J., McFadden, S.C., Thomas, F., Roder, J. and Jeromin, A. 2005, *J. Neurochem.*, *92*, 442.
- [100] Kapp-Barnea, Y., Melnikov, S., Shefler, I., Jeromin, A. and Sagi-Eisenberg, R. 2003, *J. Immunol.*, *171*, 5320.
- [101] Martin, T.F.J. 2001, *Curr. Opin. Cell Biol.*, *13*, 493.
- [102] Robinson, M.S. 2004, *Trends Cell Biol.*, *14*, 167.
- [103] Downes, C.P., Gray, A. and Lucocq, J.M. 2005, *Trends Cell Biol.*, *15*, 259.
- [104] De Matteis, M.A. and Godi, A. 2004, *Nat. Cell Biol.*, *6*, 487.
- [105] Itoh, T. and De Camilli, P. 2004, *Nature*, *429*, 141.
- [106] Godi, A., Pertile, P., Meyers, R., Marra, P., Di Tullio, G., Iurisci, C., Luini, A., Corda, D. and De Matteis, M.A. 1999, *Nat. Cell Biol.*, *1*, 280.
- [107] Godi, A., Di Campli, A., Konstantakopoulos, A., Di Tullio, G., Alessi, D.R., Kular, G.S., Daniele, T., Marra, P., Lucocq, J.M. and De Matteis, M.A. 2004, *Nat. Cell Biol.*, *6*, 393.
- [108] Shin, H.-W. and Nakayama, K. 2004, *Trends Biochem. Sci.*, *29*, 513.
- [109] Roth, M. 2004, *Nat. Cell Biol.*, *6*, 384.
- [110] Haynes, L.P., Thomas, G.M.H. and Burgoyne, R.D. 2005, *J. Biol. Chem.*, *280*, 6047.
- [111] Milosevic, I., Sorensen, J.B., Lang, T., Krauss, M., Nagy, G., Haucke, V., Jahn, R. and Neher, E. 2005, *J. Neurosci.*, *25*, 2557.
- [112] Gong, L.-W., Di Paolo, G., Diaz, E., Cestra, G., Diaz, M.-E., Lindau, M., De Camilli, P. and Toomre, D. 2005, *Proc. Natl. Acad. Sci. USA*, *102*, 5204.
- [113] Pinton, P., Pozzan, T. and Rizzuto, R. 1998, *EMBO J.*, *17*, 5298.
- [114] Chen, J.-L., Ahluwalia, J.P. and Stamnes, M. 2002, *J. Biol. Chem.*, *277*, 35682.
- [115] Porat, A. and Elazar, Z. 2000, *J. Biol. Chem.*, *275*, 29233.

ANNEXES

VI. ANNEXES:

1. ANNEX I: Detection of endogenous SNARE complexes in PC12 cells.

Previous studies have reported the existence of distinct SDS-resistant SNARE complexes, which may indicate possible multimerization and/or distinctly folded states [79, 249, 330]. In PC12 cell extracts, two defined high-molecular weight species of SDS-resistant SNARE complexes (100 kDa and 230 kDa) have been described [331]. In this study, detection of these two complexes depended on the antibody used, and on whether the blotting membrane was heat-treated or not [331].

When we attempted to reproduce these results, we mainly observed one high molecular weight SDS-resistant SNARE complex of approximately 220kDa. This band was only detectable when we used an anti-syntaxin antibody (HPC-1), but not when using an anti-VAMP2 or an anti-SNAP25 antibody (Figure 27A). Occasionally, we could observe two distinct bands of around 220kDa and 100kDa (Figure 27B1), and additional bands between 60 kDa and 220 kDa were obtained when the membranes were heat-treated, as previously described [331] (Figure 27B2). In addition, SDS-resistant SNARE complexes of all distinct sizes could be disrupted by previously boiling the sample at 95°C before electrophoretic separation [246, 331] (Figure 27B).

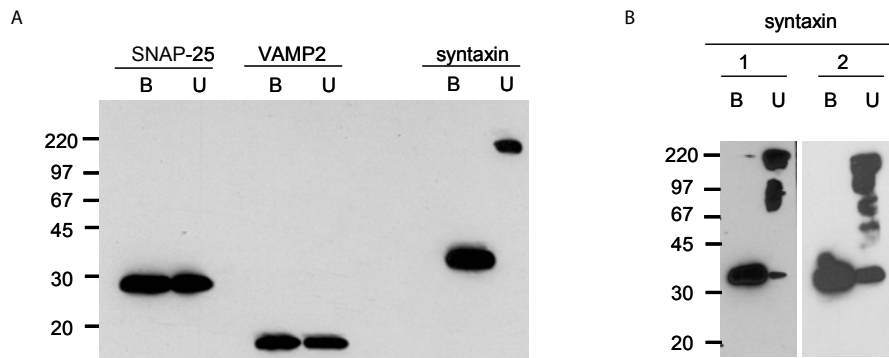


Figure 27. Detection of endogenous SDS-resistant SNARE complexes in PC12 cell extracts. A) 40 μ g of total protein extracts were boiled at 95°C (B) or unboiled (U) and subsequently run on 15% SDS-PAGE gels, followed by Western blotting with specific antibodies against the three neuronal SNAREs, VAMP2 (12 kDa), syntaxin1A (35 kDa) and SNAP-25 (25 kDa). B) In some experiments, two distinct SDS-resistant SNARE complexes were detected. Upon heat-treatment of the membranes (3 minutes at 95°C), additional bands could be detected. Numbers on the left indicate molecular weight markers (kDa).

In addition, it has been suggested that the relative levels of the 100 kDa and 220 kDa SDS-resistant SNARE complexes can be altered upon conditions which promote neurosecretion [331]. Indeed, stimulating cells with a high K^+ buffer (equivalent to our secretion buffer) decreased the relative amount of the 220 kDa complex, as compared to cells treated with physiological saline (Figure 28). This change was visible in membrane fractions, whilst no SDS-resistant complexes could be observed in vesicle fractions (Figure 28).

However, at least in our hands, we observed a considerable inter-experimental variability in both ratio and relative amount of those complexes. In addition, since the functional relevance of those biochemically identified, distinct SDS-resistant SNARE complexes remains unclear, we did not further pursue these experiments.

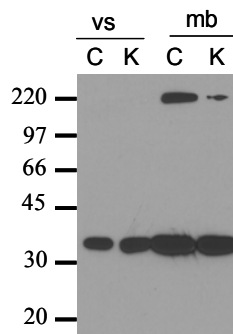


Figure 28. Effect of K^+ stimulation on amount of SDS-resistant SNARE complexes. Vesicle and membrane fractions from control (C) and cells stimulated for 10 minutes with secretion buffer (K) were run on 15% SDS-PAGE gels, followed by Western blotting and detection with an anti-syntaxin antibody.

Materials and Methods.

PC12 cell extracts were obtained essentially as described [332]. SNARE proteins were detected on nitrocellulose membranes using specific mouse monoclonal antibodies against syntaxin1A (HPC-1, 1:1000 Abcam), VAMP2 (cl69.1, 1:1000, Synaptic Systems) or SNAP-25 (1:1000, Chemicon).

Vesicle and membrane fractions were obtained by passing the cells seven times through a cell homogenizer (Isobiotec, 6 micron ball) in a buffer containing 0.25 M sucrose, 4 mM HEPES, pH 7.2, 1 mM $MgCl_2$ and 1 mM PMSF. After homogenization, the sample was centrifuged at 13.000 rpm for 20 minutes at 4°C. The soluble fraction containing vesicles was subjected to BCA assays for protein concentration determination (approximately 2 mg/ml). The membrane pellet was directly diluted in an equal volume of SDS sample buffer.

2. ANNEX II: Detection of overexpressed GFP-tagged VAMP2 proteins.

We performed an extensive amount of control experiments to exclude that the inhibitory effects of our VAMP2 mutants on neurosecretion were due to secondary effects, such as a decreased incorporation into SNARE complexes in cells. The approach of one such control experiment was to detect the amounts of N-terminally or C-terminally GFP-tagged wildtype or mutant VAMP2 molecules incorporated into SNARE complexes in transfected cells.

For this purpose, we initially tagged wildtype VAMP2 molecules at either the N-terminus or C-terminus with GFP, expressed them in PC12 cells, and detected their incorporation into SNARE complexes by SDS-PAGE and immunoblotting. Again, incorporation of tagged VAMP2 molecules into SDS-resistant complexes (in the absence of boiling) could not be observed with either anti-VAMP2 antibodies (Figure 29). Surprisingly, in boiled samples, only C-terminally tagged VAMP2 could be detected with both antibodies in cell extracts, whilst in the absence of boiling, only the monoclonal anti-VAMP2 antibody was able to detect C-terminally tagged VAMP2 (Figure 29). Since the monoclonal anti-VAMP2 antibody was raised against residues 2-17, it is possible that this epitope is not fully available when VAMP2 is tagged at the N-terminus with GFP. However, the results of the polyclonal anti-VAMP2 antibody are hard to explain, given that this antibody is particularly good at recognizing the C-terminus of VAMP2, and thus should recognize an N-terminally GFP-tagged VAMP2 molecule. Thus, conformational constraints may account for those observations.

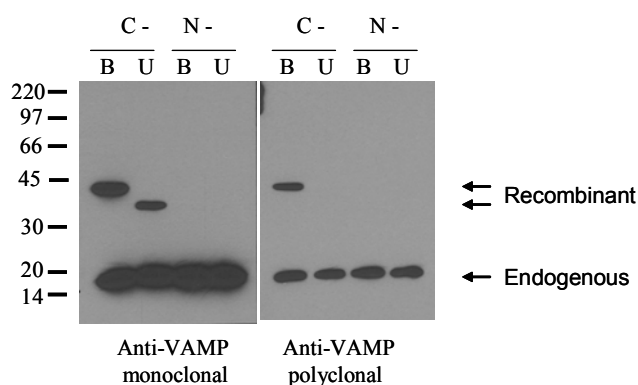


Figure 29. Detection of GFP-tagged VAMP2 protein by Western blotting. 40 μ g of total protein extract from transfected PC12 cells was run on 15% SDS-PAGE gels, followed by Western blotting with two different anti-VAMP2 antibodies: a mouse monoclonal (Cl69.1, Synaptic Systems, 1:1000) or a rabbit polyclonal (Synaptic Systems, 1:1000). No band of the predicted molecular weight of GFP-VAMP2 was observed when VAMP2 was GFP-tagged at the N-terminal end (N-). When VAMP2 was GFP-tagged at the C-terminal end (C-), a band of the predicted molecular weight could be detected with both monoclonal and polyclonal anti-VAMP2 antibodies in boiled samples (B). When the sample was not subjected to boiling (U), a distinct band could be detected with the monoclonal, but not polyclonal anti-VAMP2 antibody. SDS-resistant SNARE complexes (in the absence of boiling) were non-detectable in all cases. Numbers on the left indicate molecular weight markers (kDa).

We next probed whether N-terminally or C-terminally GFP-tagged VAMP2 was detectable by anti-GFP antibodies (Figure 30). C-terminally GFP-tagged VAMP2 was only detectable in non-boiled samples, and no SDS-resistant complexes could be observed. In contrast, N-terminally tagged VAMP2 was detectable in boiled samples, and the two distinct, SDS-resistant SNARE complexes were detectable in non-boiled samples (Figure 30).

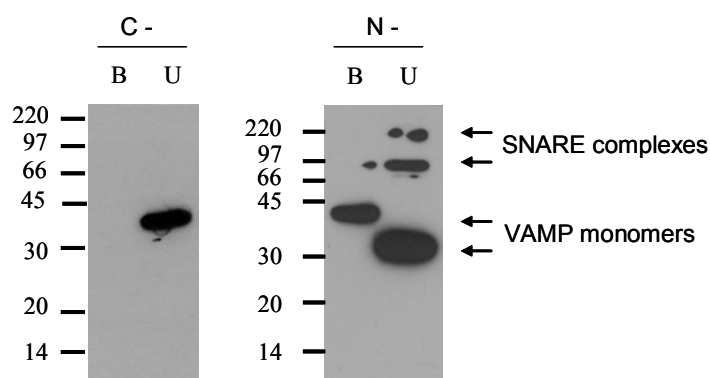


Figure 30. Detection of GFP-tagged VAMP2-containing SNARE complexes. 40 μ g of total protein extract from transfected PC12 cells was boiled (B) or not boiled (U) and run on 15% SDS-PAGE gels followed by Western blotting with an anti-GFP antibody (Abcam, 1:5000). VAMP2 was tagged with GFP at either the N-terminus (N-) or C-terminus (C-). Numbers on the left indicate molecular markers (kDa).

Finally, using N-terminally GFP-tagged VAMP2 constructs, we attempted to determine whether wildtype and mutant VAMP2 would incorporate with similar efficiency into native SNARE complexes. However, as described in Annex I, there was considerable inter-experimental variability in the detection of the two distinct high-molecular weight SDS-resistant SNARE complexes (see Figure 31 as example), and this approach was abandoned, as it did not yield any useful conclusive evidence.

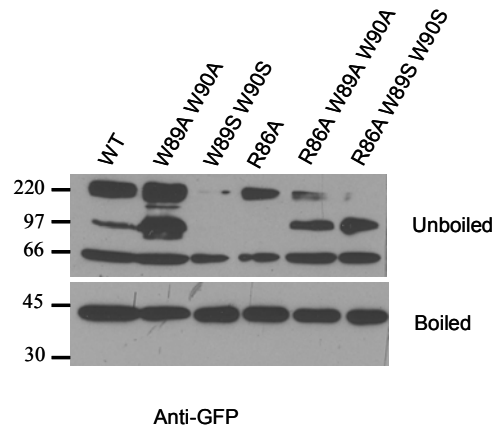


Figure 31. Detection of SDS-resistant SNARE complexes incorporating N-terminally GFP-tagged wildtype or mutant VAMP2 molecules. 40 μ g of total protein extract from transfected PC12 cells were run on 15% SDS-PAGE gels, followed by Western blotting with a rabbit polyclonal anti-GFP antibody (Abcam, 1:5000).

3. ANNEX III: Determination of tryptophan solvent accessibility in inherent tryptophan fluorescence experiments.

A classical experiment to study solvent accessibility of tryptophan residues involves the use of solvent quenchers like iodide or caesium ions [333]. Therefore, we determined the solvent accessibility of wildtype and W89AW90A-mutant VAMP2 by analyzing changes in tryptophan fluorescence with increasing KI concentrations. The results indicate that both tryptophans are solvent accessible in the SNARE complex dimer, as no significant change in the slope of the Stern-Vollmer plot was observed upon SNARE complex monomerization by addition of 1 M NaCl (Figure 32). Whilst further assays using a penetrating quencher such as acrylamide may be required to observe different solvent accessibilities of the tryptophans in SNARE complex dimers as compared to monomers, the data are in agreement with a lack of shift of the peak tryptophan fluorescence of SNARE complex dimers upon increasing salt concentrations, and thus would indicate that both tryptophans are solvent-exposed in the SNARE complex dimer [332].

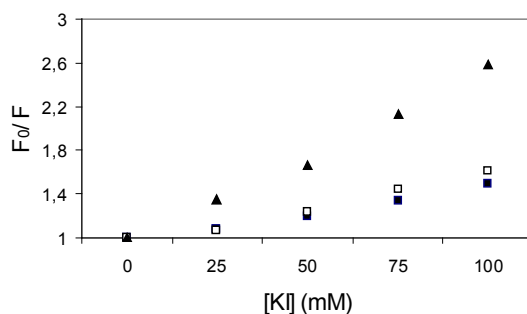


Figure 32. Stern-Vollmer plot depicting changes in fluorescence intensities of free tryptophan (▲), SNARE complex dimers (□) and SNARE complex monomers (■) with increasing KI concentrations. The slope of SNARE complex dimers and monomers is approximately 37% and 30% that of free tryptophan, respectively.

Materials and Methods.

SNARE complex dimers and monomers were obtained as described [332]. Tryptophan fluorescence was detected by excitation at 280 nm, obtaining a maximum emission peak at approximately 350 nm. A solution of 5M KI was used for quenching studies, whereby small amounts (0-3 μ l) were added to a final volume of 120 μ l of sample containing SNARE complex dimers or monomers (50 μ g/ml).

4. ANNEX IV: Peptidergic approach to interfere with SNARE complex dimerization *in vitro*.

If SNARE complex dimers are important for neurosecretion *in vivo*, disrupting such dimers with peptides should result in secretory deficits. Therefore, we also attempted to use a peptidergic approach. For this purpose, we designed a peptide covering the residues in rat VAMP2 (amino acids 77-94) involved in SNARE complex dimerization (FET SAA KLK RKY WWK NLK-amide), a mutant peptide where the W89 and W90 residues were mutated to alanines (FET SAA KLK RKY AAK NLK-amide), and a scrambled peptide, containing the same amino acid composition as the active peptide and the same predicted secondary structure, but a distinct primary sequence (FKA ASL RTW KEW YKK LNK-amide). The peptides were amidated at the C-terminus to minimize their degradation *in vivo*. A similar peptide (amino acids 77-90) had been previously reported to inhibit neurosecretion in cells [160].

We first tested whether the active, but not mutant or scrambled peptides, would be able to interfere with SNARE complex dimer formation *in vitro*. For this purpose, we used VAMP2 coils tagged for FRET experiments *in vitro* [332]. We assembled SNARE complex dimers *in vitro*, followed by their disruption into monomers with high salt, and subsequently studied the ability of active and mutant peptides to interfere with reformation of dimers upon dilution of the samples into low salt conditions. No significant changes in FRET signals were observed in the presence of active, mutant or scrambled peptides (at 1 mM final concentration), suggesting that the peptide mimicking the VAMP2 dimerization interface is not able to compete for SNARE complex dimer formation *in vitro* (Figure 33).

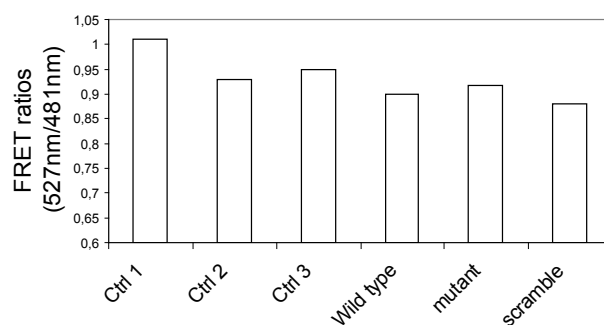


Figure 33. Peptides mimicking the membrane-proximal region of VAMP2 do not interfere with dimerization of SNARE complex monomers. FRET ratios (emission ratio 527/481 nm) from SNARE complex dimers in 50 mM NaCl (Ctrl 1), SNARE complex dimers in 150 mM NaCl (Ctrl 2), SNARE complex monomers after dilution into 150 mM NaCl (Ctrl 3), SNARE complex monomers after dilution into 150 mM NaCl in the presence of 1 mM wild type peptide, SNARE complex monomers after dilution into 150 mM NaCl in the presence of 1 mM mutant peptide, and SNARE complex monomers after dilution into 150 mM NaCl in the presence of 1 mM scrambled peptide.

Whilst the VAMP2 peptide may not be able to compete for dimerization of preformed SNARE complex monomers, it may be able to interfere with dimerization when added to SNARE coils, which subsequently form complex dimers. Thus, we added active and scrambled peptides along with SNARE coils, followed by overnight incubation of samples to allow for complex formation. Fluorescent protein precipitates were obtained when the three SNARE coils (FRET-VAMP2, SNAP-25 and syntaxin1A) were assembled in the presence of 1 mM wildtype peptide, but not with scrambled peptide. In addition, no fluorescent protein precipitates were obtained when FRET-VAMP2 coils were incubated on their own with wildtype peptide. These data indicate that precipitation is somehow specific for the active peptide, and only occurs in the presence of all three SNARE coils (forming SNARE complex monomers/dimers). Further experiments may be warranted to establish how the active peptide leads to SNARE complex oligomerization/aggregation *in vitro*.

Materials and Methods.

Recombinant, FRET-tagged SNARE complex dimers containing VAMP-CFP, VAMP-Venus, SNAP-25 and syntaxin1A coils were purified as described [332]. Dimers (0.11 mg/ml) were then disrupted into monomers by addition of 850 mM NaCl. SNARE complex monomers were diluted into low salt (150 mM NaCl) to allow reformation of dimers in the presence or absence of 1 mM wild type, mutant or scrambled peptides, respectively.

5. ANNEX V: Measuring cooperativity of SNARE-dependent neurosecretion.

Previous studies have shown that multiple SNARE complexes are necessary to bring about an individual membrane fusion event [240, 242, 243]. For example, in PC12 cells, three (or at least three) SNARE complexes seem to cooperatively mediate vesicle fusion [243]. As another means to obtain evidence for the importance of SNARE complex dimers in neurosecretion, we aimed to determine whether interfering with such dimers would change SNARE-mediated cooperativity. Two approaches were considered; a) to overexpress wildtype and mutant VAMP2 in cells on the background of endogenous VAMP2, followed by such cooperativity studies, or b) to overexpress toxin-insensitive, wildtype or mutant VAMP2, followed by cooperativity studies in the presence of neurotoxin.

In the first instance, we aimed to reproduce previous studies demonstrating that SNAREs act in a cooperative manner [10, 243]. This involved transfecting PC12 cells with constructs encoding for wildtype or mutant VAMP2 and hGH as a secretion reporter as described [332], followed by measuring a concentration-dependent inhibition of exocytosis in cracked PC12 cells by soluble, cytosolic VAMP2 coils [243]. As expected, release from cracked PC12 cells was dependent on cytosol, MgATP and CaCl₂ (Figure 34A).

We next aimed to determine the concentration-dependent inhibitory effect of adding cytosolic VAMP2 coils to cracked PC12 cells. Again, in agreement with previous studies [243], we observed for example a roughly 40% of inhibition of release in the presence of 3 μ M VAMP2 coils (Figure 34B). However, whilst generally reproducible, we found that extremely large amounts and concentrations (up to 60 μ M) of VAMP2 coils were required to obtain proper cooperativity curves, and as a consequence abandoned these studies.

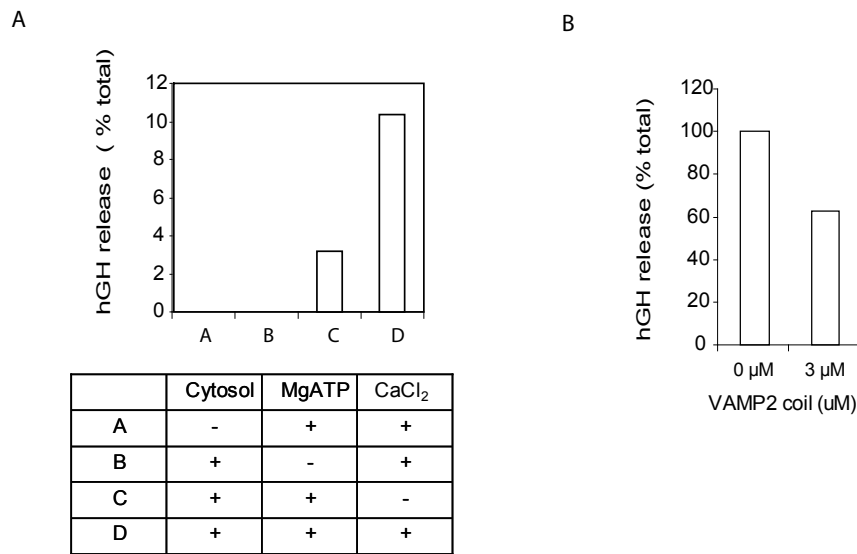


Figure 34. VAMP2 cooperativity assay. A) hGH release was dependent on the presence of cytosol (A) and MgATP (B), and spontaneous and evoked release were measured in the absence (C) or presence (D) of CaCl₂, respectively. Data were normalized against secretion determined in the absence of cytosol. B) Decrease of hGH release after addition of 3 μ M VAMP2 coil. Data were normalized against spontaneous release value, and secretion in the absence of VAMP2 coils was set to 100%.

Materials and Methods.

PC12 cells were grown and transfected as described [332]. The cracked PC12 cell assay was essentially performed as described [243]. 10⁶ cells were collected and homogenized (Isobiotec, 6 micron ball) in buffer containing 50 mM HEPES, pH 7.2, 105 mM K-Glutamate, 20 mM K-acetate and 2 mM EGTA. Priming reactions were done for 15 minutes at 30°C in the presence or absence (as indicated) of 1 mg/ml cytosol, 2 mM MgATP and VAMP2 coils. Recombinant VAMP2 coils were purified as described [332]. Triggering of secretion was done in the presence of 1 μ M free CaCl₂ for 2 minutes at 30°C. Reactions were stopped by incubation on ice for 3 minutes. Release of hGH was measured as total percentage in supernatants by ELISA, as described [332].

6. ANNEX VI: Additional insights into detecting VAMP2 interactions by bimolecular fluorescence complementation approaches.

We have determined, using a bimolecular fluorescence complementation (BiFC) approach, that VAMP2 molecules dimerize through their TMDs in intact cells. This interaction was found to occur in neuritic processes as well as in a perinuclear compartment, where it partially overlapped with a trans-Golgi marker (Fdez et al., under review), as well as with a cis-Golgi marker (GM130) and a trans-Golgi-endosomal marker (TfR) (Figure 35). Such localization matched endogenous VAMP2 localization, as well as GFP-tagged, overexpressed VAMP2 localization (Fdez et al., under review), indicating that it was not due to overexpressing a tagged VAMP2 molecule.

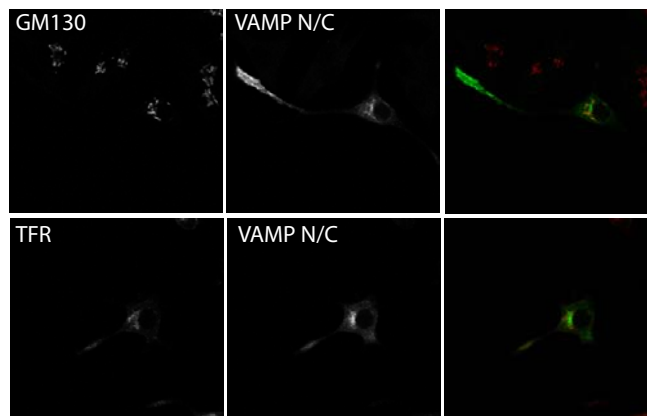


Figure 36. Partial colocalization of VAMP2 BiFC signal (VAMP N/C) in differentiated PC12 cells with GM130 (Transduction Labs, 1:100) and TfR (Zymed, 1:100) in a perinuclear compartment.

Given that VAMP2 interactions as detected by BiFC were also observed in a perinuclear compartment, it seems likely that they reflect homotypic interactions between individual, non-complexed VAMP2 molecules, rather than the presence of dimeric *trans* SNARE complexes. In agreement with this, the VAMP2 triple mutant (R86AW89AW90A) defective in SNARE complex dimer stability *in vitro*

[332] still displayed a BiFC signal *in vivo* similar to wildtype VAMP2 in both non-differentiated and differentiated PC12 cells (Figure 37).

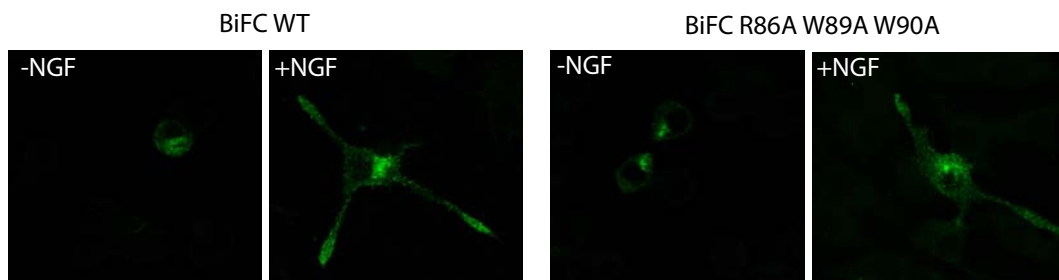


Figure 37. A VAMP2 triple mutant defective in SNARE complex dimerization *in vitro* still displays a BiFC signal in both non-differentiated (-NGF) and differentiated (+NGF) PC12 cells.

Upon determining that the TMD was responsible for the interaction between VAMP2 molecules in intact cells as detected by BiFC (Fdez et al., under review), we subjected the TMD to extensive mutational analysis to pinpoint residue(s) important for this interaction. The most crude approach towards elucidating sequence requirements (versus mere length requirements) involved replacing the TMD by a polyalanine sequence (VAMPpoly) (Figure 38). However, VAMPpoly, when tagged either at the N-terminus or C-terminus with GFP, was mainly cytosolic, with only occasional punctate structures detectable. These data suggest that VAMPpoly is not properly targetted to vesicular membranes upon synthesis.

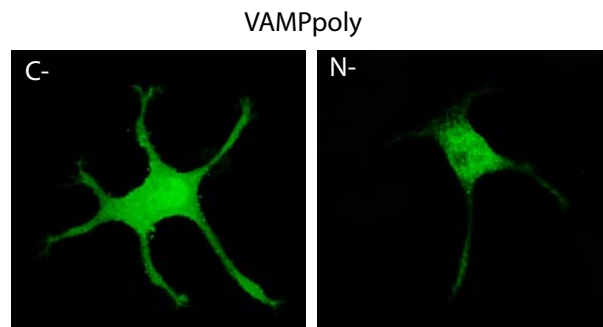


Figure 38. Replacing the TMD of VAMP2 by a polyalanine segment (VAMPpoly) leads to mislocalization. Cytosolic, and occasional punctate localization of either N- or C- terminally GFP-tagged VAMPpoly molecules.

When we assessed the VAMPpoly in our BiFC approach, we observed a strong, punctate BiFC signal in cell bodies and neurites in the absence of a strong cytosolic signal (Figure 39). However, we were unable to observe colocalization with an extensive set of markers for distinct intracellular compartments (Figure 39).

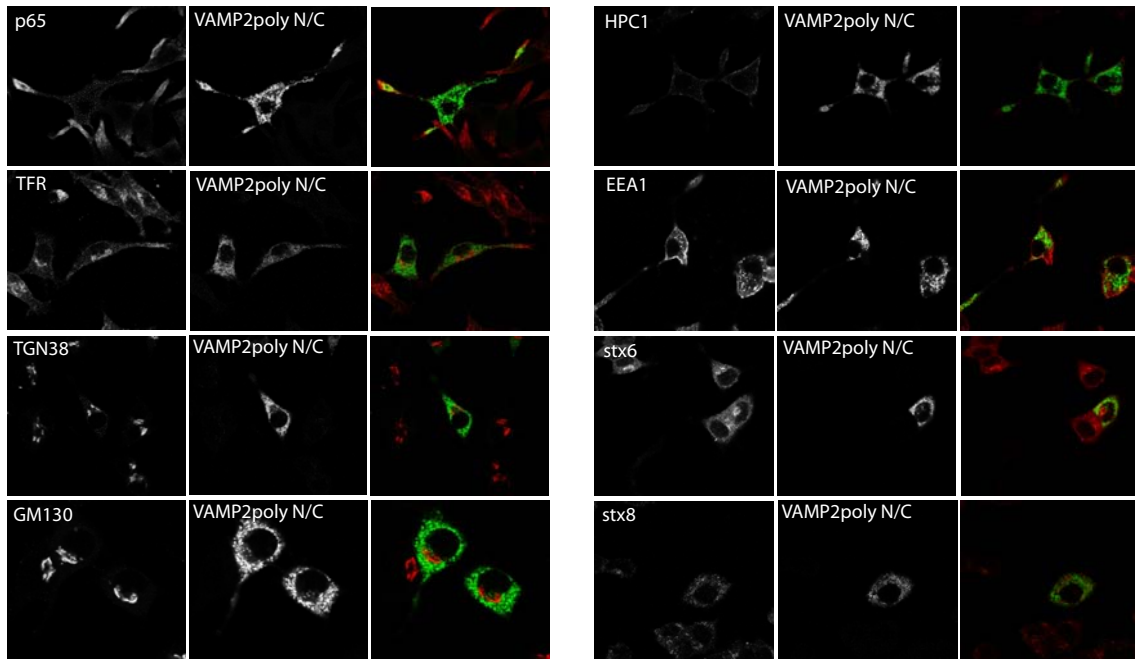


Figure 39. Localization of VAMP2poly BiFC signal (VAMP2poly N/C) in PC12 cells. No colocalization was observed with Golgi or endosomal markers such as GM130 (Transduction Labs, 1:100), TFR (Zymed, 1:100), syntaxin6 (Synaptic Systems, 1:500), syntaxin8 (Synaptic Systems, 1:500), EEA1 (Transduction Labs, 1:300) or TGN38 (1:800). Similarly, no colocalization was detectable with the synaptic vesicle marker synaptotagmin (p65, 1:1000) or the plasma membrane-localized t-SNARE syntaxin1A (HPC1, 1:1000).

These data suggest that the VAMP2poly BiFC signal may reflect protein aggregates. Indeed, polyalanine segments have been previously reported to aggregate in hydrophobic environments [334], and a similar result was obtained when we used a set of BiFC constructs which only contained the polyalanine segment, in the absence of the VAMP2 sequence (data not shown).

In addition, it is surprising that GFP-tagged VAMP2poly was largely cytosolic, whilst VAMP2poly BiFC displayed punctate fluorescence. As the two halves of the GFP moieties in the BiFC approach are usually unstructured, and only adopt a defined structure upon close molecular contact, it is possible that BiFC-tagged proteins are generally less soluble than fully GFP-tagged proteins,

which could explain the present findings, and point to the importance of carefully controlling BiFC-type studies.

In a set of subsequent experiments, we determined that a glycine residue (G100) was crucial for TMD-mediated interactions between VAMP2 molecules as detected by BiFC (Fdez et al., under review). Replacing this residue by amino acids with increasing molecular volume (such as valine or tyrosine) abolished the BiFC signal. To exclude that the lack of a BiFC signal with these mutants was due to a lack of co-expression, we aimed to detect BiFC-tagged VAMP2 molecules by Western blotting with distinct anti-VAMP2 or anti-GFP antibodies. However, we could not detect BiFC-tagged proteins with any of the antibodies used (Figure 40), and had to tag BiFC constructs with a myc- and an HA-tag to show co-expression (Fdez et al., under review). Such lack of detection may indicate conformational issues of tagged VAMP2.

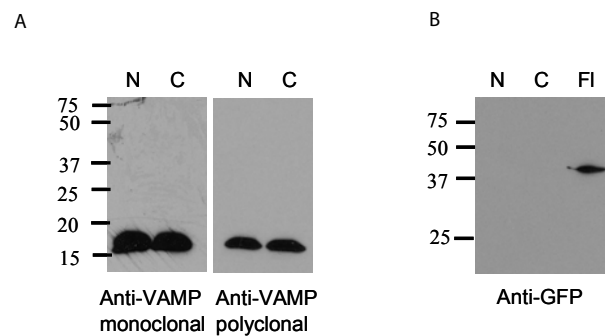


Figure 40. Detection of BiFC-tagged VAMP2 proteins. 40 μ g of total protein extract from transfected PC12 cells was boiled at 95°C for 5 minutes and run on 15% SDS-PAGE gels, followed by Western blotting with different antibodies. A) pcmv/VAMP-VenusN (N) and pcmv/VAMP-VenusC (C) transfected PC12 cell extracts were probed with two different anti-VAMP2 antibodies: a mouse monoclonal anti-VAMP2 (Cl69.1, Synaptic Systems, 1:1000) and a rabbit polyclonal anti-VAMP2 (Synaptic Systems, 1:1000). We could only detect endogenous VAMP2. B) The same extracts as in A) were probed with a rabbit polyclonal anti-GFP antibody (Abcam, 1:1000). As a positive control, we used the VAMP-polyalanine-full length venus (FI). An additional rabbit polyclonal anti-GFP antibody (FitzGerald, 1:1000) also failed to detect BiFC proteins (data not shown).

Materials and Methods.

Immunofluorescence and image acquisition was done essentially as described (Fdez, et al. 2009, under review). TfR and GM130 antibodies were kindly provided by Dr. Philip Woodman.

The TMD replacement of VAMP2 by an artificial polyalanine segment was done by flanking the TMD sequence by two silent SacII sites at positions M95 and Y113, introduced by site-directed mutagenesis. The TMD was then removed and replaced by polyalanine oligo-adaptors. Polyalanine BiFC control constructs were generated by removing VAMP2 residues (1-90) after introduction of a silent EcoRI site by site-directed mutagenesis in pcmv-VAMPpoly BiFC constructs.

7. ANNEX VII: Primer sequences.

Sequencing primers:

| Name | Sequence |
|---------------|----------------------------|
| pEGFP_N5' | GGTAGGCGTGACGGTGGGAG |
| pEGFP_N3' | CGTCGCCGTCCAGCTCGACCAG |
| pEGFP-C5' | ATGGTCCTGCTGGAGTTCGTG |
| PEGFP-C3' | CATTTTATGTTTCAGGTTTCAGGGG |
| pCMV-seq5' | GCAAATGGGCGGTAGGCCGTGTA |
| pCMV-seq3' | TTATTAGGACAAGGCTGGTGGG |
| PGEX 5'seq | CTGGCAAGCCACGTTTGGTG |
| PGEX 3'seq | GGAGCTGCATGTGTCAGAGG |
| Sv40seq5' | CTAACTCCGCCCATCCCGCCCCTAAC |
| Pcmv-HA-seq5' | GCCTTTACTTCTAGGCCTGTAC |
| Pcmv-HA-seq3' | GCATTCTAGTTGTGGTTTGTCC |

Site-directed mutagenesis primers:

| Name | Sequence |
|------------------------|--------------------------------------|
| VAMP R86A W89S W90S 5' | GCAGCCAAGCTCAAGGCAAATACAGCTCTAAAAAC |
| VAMP R86A W89S W90S 3' | GTTTTTAGAGCTGTATTTTGCCTTGAGCTTGGCTGC |
| VAMP R86E W89S W90S 5' | GCAGCCAAGCTCAAGGAGAAATACAGCTCTAAAAAC |
| VAMP R86E W89S W90S 3' | GTTTTTAGAGCTGTATTTCTCCTTGAGCTTGGCTGC |
| VAMP R86AW89A W90A 5' | GCAGCCAAGCTCAAGGCAAATACGCGGCAAAAAAC |
| VAMP R86AW89A W90A 3' | GTTTTTTGCCGCGTATTTTGCCTTGAGCTTGGCTGC |
| VAMP R86EW89A W90A 5' | GCAGCCAAGCTCAAGGAGAAATACGCGGCAAAAAAC |
| VAMP R86E W89A W90A 3' | GTTTTTTGCCGCGTATTTCTCCTTGAGCTTGGCTGC |
| VAMP R56G 5' | GACAAGGTCCTGGAGGGGGACCAGAATCG |
| VAMP R56G 3' | CGATAGCTTCTGGTCCCCCTCCAGGAGGTC |
| VAMP W89A 5' | CTCAAGCGCAAATACGCATGGAAAAAAG |

| | |
|---------------------------|---|
| VAMP W89A 3′ | CTTGAGGTTTTTCCATGCGTATTTGCGAG |
| VAMP R86E 5′ | GCAGCCAAGCTCAAGGAGAAATACTGGTGGAAA |
| VAMP R86E 3′ | TTCCACCAGTATTTCTCCTTGAGCTTGGCTGC |
| VAMP R86A 5′ | GCAGCCAAGCTCAAGGCAAATACTGGTGGAAA |
| VAMP R86A 3′ | TTCCACCAGTATTTTGCCCTTGAGCTTGGCTGC |
| Vamp W90A 5′ | CAAGGAGAAATACTGGGCGAAAAACCTCAAGATG |
| Vamp W90A 3′ | CATCTTGAGGTTTTTCGCCAGTATTTCTCCTTG |
| Vamp W89A W90A 5′ | CTCAAGCGCAAATACGCGGCAAAAAACCTCAAGATG |
| Vamp W89A W90A 3′ | CATCTTGAGGTTTTTTGCCGCGTATTTGCGCTTGAG |
| Vamp L99A 5′ | CAAGATGATGATCATCGCAGGAGTGATTGCGCC |
| Vamp L99A 3′ | GGCGCAAATCACTCCTGCGATGATCATCATCTTG |
| VAMP C103A L99A 5′ | CATCGCAGGAGTGATTGCCGCCATCATCCTCATC |
| VAMP C103A L99A 3′ | GATGAGGATGATGGCGGCAATCACTCCTGCGATG |
| VAMP I111A | CATCCTCATCATCATCGCAGTTTACTTCAGCAC |
| C103A L99A 5′ | |
| VAMP I111A | GTGCTGAAGTAAACTGCGATGATGATGAGGATG |
| C103A L99A 3′ | |
| FRET Xho_intr5′ | GGAAAAACCTCAAGATGATGCTCGAGGGTGGTTCCGGCGGC AGTCT |
| FRET Xho_intr3′ | AGACTGCCGCCGGAACCACCCTCGAGCATCATCTTGAGGTTT TTCC |
| FRET Prelinker 5′ | GGAAAAACCTCAAGATGATGGGTGGTTCCCTCAAGCTTATTC ATCGTG |
| FRET Prelinker 3′ | CACGATGAATAAGCTTGAGGGAACCACCCATCATCTTGAGG TTTTTCC |
| FRET Linker 5′ | CAAGATGATGGGTGGTTCCGGCGGCAGTCTCAAGCTTATTCA TCGTG |
| FRET Linker 3′ | CACGATGAATAAGCTTGAGACTGCCGCCGGAACCACCCATC ATCTTG |
| FRET control Prelinker 5′ | GTGGTGGTGGTGGAAATTCTAGGAGGTTCTATGTCCGCTACCG CTGCCAC |
| FRET control Prelinker 3′ | GTGGCAGCGGTAGCCGACATAGAACCTCCTAGAATTCCACC ACCACCAC |
| FRET control Linker 5′ | GTGGAATTCTAGGAGGTTCTGGAGGTTCAATGTCCGCTACCG CTGCCAC |
| FRET control Linker 3′ | GTGGCAGCGGTAGCCGACATTGAACCTCCAGAACCTCCTAG AATTCCAC |
| BiFC Prelinker 5′ | CATCGTTTTACTTCAGCACTTCAGGAGGAAGTGGTTCTAGAGG CGTCCAAGTC |
| BiFC Prelinker 3′ | GACTTGGACGCCTCTAGAACCCTCCTCCTGAAGTGCTGAA |

GTAAACGAT
 BiFC Linker 5' CACTTCAGGAGGAAGTGGTGGTACAGGCGGATCTAGAGGCG
 TCCAAGTC
 BiFC Linker 3' GACTTGGACGCCTCTAGATCCGCCTGTACCACCACTTCCTCC
 TGAAGTG
 BiFC Eco Intro 5' CGTTTACTTCAGCACGAATTCAGGAGGAAGTGG
 BiFC Eco Intro 3' CCACTTCCTCCTGAATTCGTGCTGAAGTAAACG
 W90 Eco Intro 5' GCGCAAATACTGGTGAATTCATGAAAAACCTCAAGATG
 W90 Eco Intro 3' CATCTTGAGGTTTTTCATGAATTCACCAGTATTTGCGC
 W90 Hind Intro 5' CGCAAATACTGGTGGAAAGCTTGGAAAAACCTCAAG
 W90 Hind Intro 3' CTTGAGGTTTTTCCAAGCTTCCACCAGTATTTGCG
 Vamp Q76V 5' CAGGCAGGGGCCTCCGTGTTTGAAACAAGTGCAG
 Vamp Q76V 3' CTGCACTTGTTTCAAACACGGAGGCCCTGCCTG
 Vamp Q76V F77W 5' GCAGGGGCCTCCGTGTGGGAAACAAGTGCAGCC
 Vamp Q76V F77W 3' GGCTGCACTTGTTTCCCACACGGAGGCCCTGC
 Vamp M46A 5' GATGAGGTGGTGGACATCGCGAGGGTGAATGTGGACAAG
 Vamp M46A 3' CTTGTCCACATTCACCCTCGCGATGTCCACCACCTCATC
 T79 Eco Intro 5' GGCCTCCCAGTTTGAAGAATTCATGACAAGTGCAGCCAAGC
 T79 Eco Intro 3' GCTTGGCTGCACTTGTCATGAATTCTTCAAACCTGGGAGGCC
 Vamp K59R 5' CCTGGAGCGAGACCAGAGGCTATCGGAACTGGATG
 Vamp K59R 3' CATCCAGTTCGATAGCCTCTGGTCTCGCTCCAGG
 VampN49A_5' GTGGACATCATGAGGGTGGCTGTGGACAAGGTCCTGG
 VampN49A_3' CCAGGACCTTGTCCACAGCCACCCTCATGATGTCCAC
 VampI108+6L_5' CATCCTCATCCTGCTGCTGCTCCTCCTCATCATCATCGTTTAC
 TTC
 VampI108+6L_3' GAAGTAAACGATGATGATGAGGAGGAGCAGCAGCAGGATG
 AGATG
 Vamp del 41-44_5' CCAGGCCCAGGTGGATATCTGAGGGTGAATGTGGACAAG
 Vamp del 41-44_3' CTTGTCCACATTCACCCTCAGATATCCACCTGGGCCTGG
 Vamp Del 45-50_5' GACCCAGGCCCAGGTGGATGACAAGGTCCTGGAGCGAG
 Vamp Del 45-50_3' CTCGCTCCAGGACCTTGTTCATCCACCTGGGCCTGGGTC
 Vamp (R56G) K59R 5' CCTGGAGGGGGACCAGAGGCTATCGGAACTGGATG
 Vamp (R56G) K59R 3' CATCCAGTTCGATAGCCTCTGGTCCCCCTCCAGG
 Delta108-110_5' GATTTGCGCCATCATCCTCATCGTTTACTTCAGCAC
 Delta108-110_3' GTGCTGAAGTAAACGATGAGGATGATGGCGCAAATC
 M96+3L_5' GAAAAACCTCAAGATGATGCTGCTGCTGATCATCTTGGGAGT
 GATTTG
 M96+3L_3' CAAATCACTCCCAAGATGATCAGCAGCAGCATCATCTTGAG
 GTTTTTC
 M96+6L_5' GATGATGCTGCTGCTGCTGCTGCTGCTGATCATCTTGGGAGTG

| | |
|----------------------|--|
| M96+6L_3' | CACTCCCAAGATGATCAGCAGCAGCAGCAGCAGCATCATC |
| Del 97-99_5' | GAAAAACCTCAAGATGATGGGAGTGATTTGCGCCATC |
| Del 97-99_3' | GATGGCGCAAATCACTCCCATCATCTTGAGGTTTTTC |
| G100P_5' | GATGATGATCATCTTGCCAGTGATTTGCGCCATC |
| G100P_3' | GATGGCGCAAATCACTGGCAAGATGATCATCATC |
| G100A_5' | GATGATGATCATCTTGCCCGTGATTTGCGCCATC |
| G100A_3' | GATGGCGCAAATCACGGCCAAGATGATCATCATC |
| G100Y5' | GATGATCATCTTGTACGTGATTTGCGCC |
| G100Y3' | GGCGCAAATCACGTACAAGATGATCATC |
| G100V5' | GATGATGATCATCTTGTTGGTGGTGATTTGCGCCATC |
| G100V3' | GATGGCGCAAATCACCAAGATGATCATCATC |
| I106A L107A 5' | GTGATTGCCGCCATCGCAGCCATCATCATCGCAG |
| I106A L107A 3' | CTGCGATGATGATGGCTGCGATGGCGGCAATCAC |
| I110A 5' | CATCGCAGCCATCATCGCCGAGTTTACTTCAGC |
| I110A 3' | GCTGAAGTAACTGCGGCGATGATGGCTGCGATG |
| SacII introM95_5' | GGAAAAACCTCAAGATGGCCGCGGATGATCATCTTGGGAG |
| SacII introM95_3' | CTCCAAGATGATCATCCGCGGCCATCTTGAGGTTTTTCC |
| SacII introY113_5' | CATCATCATCGTTTACCCGCGGCATTCAGCACTTCAGGAG |
| SacII introY113_3' | CTCCTGAAGTGCTGAATGCCGCGGGTAAACGATGATGATG |
| SacII Y113_5' GFPemd | CATCATCATCGTTTACCCGCGGCATTCAGCACTACGGATC |
| SacII Y113_3' GFPemd | GATCCGTAGTGCTGAATGCCGCGGGTAAACGATGATGATG |
| EcoRintropolyala_5' | CAAGCGCAAATACTGGTGAATTCATGAAAAACCTCAAGATG |
| EcoRintropolyala_3' | GC GCCATCTTGAGGTTTTTTCATGAATTCACCAGTATTTGCGCTTG |

Subcloning primers:

| | |
|------------------------|----------------------------------|
| CFP (Venus) HindIII_5' | ATAAAAGCTTGTGAGCAAGGGC |
| CFP (Venus) HindIII_3' | ATAAAAGCTTTTACTTGTACAGCTC |
| Venus-Eco5' | ATTTGAATTCATGGTGAGCAAGG |
| Venus-Eco3' | TAAAGAATTCCTTGTACAGCTCGTC |
| VenusN_Xba5' | TAAATCTAGAATGGTGAGCAAGGGCGAG |
| VenusN_BamH3' | ATTTGGATCCTTAGGCGGTGATATAGACGTTG |
| venus C_Xba5' | TAAATCTAGAGACAAGCAGAAGAACGGC |
| VenusC_BamH3' | ATTTGGATCCTTACTTGTACAGCTCGTCCATG |
| SNAP_Eco5' | ATTTGAATTCTAGTGGTGGATGAAC |
| SNAP_Eco3' | TAAACTCGAGACCACTTCCCAGCATCTTTG |
| Taxin_Eco 5' | CAGCGAATTCATGAAGGACCGAACCCAGG |
| Taxin_Eco 3' | CCTGAATTCCTCCAAAGATGCCCCCGATGG |

| | |
|---------------------|---|
| TAXIN Eco 5' | ATTTGAATTCTAATGAAGGACCGAACCCAGG |
| TAXIN Xho 3' | AAATCTCGAGTTATCCAAAGATGCCCCCGAT |
| VAMP Eco 5' | ATTTGAATTCTAATGTTCGGCTACCGCT |
| VAMP Xho 3' | ATTCCTCGAGTTAAGTGCTGAAGTAAACG |
| BiMC_Taxin_Eco 5' | ATTTGAATTCATGAAGGACCGAACCCAGG |
| BiMC_Taxin_Eco 3' | AAATGAATTCCTCCAAAGATGCCCCCGATGG |
| VenusN_EcoR5' | CAGCGAATTCATGGTGAGCAAGGGCGAGG |
| VenusN_EcoR3' | GCCTGAATTCTGCTGCTTGTTCGGCCATGAT |
| Tagmin_Xba5' | CGGATCTAGAATGGTGAGTGCCAGTCATCC |
| Tagmin_BamH3' | CTCAGGATCCCTTCTTGACAGCCAGCATGG |
| VenusC_Eco 5' | CAGCGAATTCATGAAGAACGGCATCAAGGTG |
| VenusC_Eco 3' | CAGCGAATTCGCTTGTACAGCTCGTCCATG |
| VenusN_Xho3' | GTACCTCGAGTTACTGCTTGTTCGGCCATGATATAG |
| VenusC_Xho3' | GGTACCTCGAGTTACTTGTACAGCTCGTCCATGC |
| SacII_Polyalanine5' | P- GGCCGCTGCTGCTGCGGCTGCGGCCGCTGCGGCTGCTGCG GCCGC |
| SacII_Polyalanine3' | P- GGCCGCAGCAGCCGCAGCGGCCGCAGCCGCAGCAGCAGC GGCCGC |

DISCUSSION

VII. DISCUSSION:

1. Structure of SNARE complex oligomers in solution:

In the present study, we show that recombinant cytosolic neuronal SNARE complexes oligomerize *in vitro*. We used a range of biochemical and biophysical techniques which all support this conclusion. Using analytical ultracentrifugation and light scattering, we found that SNARE complexes form dimers in solution. These dimers were found to form with micromolar affinity, and to be disrupted into monomers by the addition of 1 M NaCl. Whilst in agreement with some studies [100, 140, 149], the data contradict with a previous study using analytical ultracentrifugation, which reported a monomer-trimer equilibrium of SNARE complexes in solution [147]. However, given the fact that this determination was protein concentration-dependent, and that 10-50 times more protein was used as compared to in our studies, it seems possible that their experimental setup was not sufficiently sensitive. Alternatively, it may be that a mixture of oligomeric species exist in solution. However, our hydrodynamic data suggest the presence of a very homogeneous population of SNARE complex dimers, even though by MALLS, a small amount of higher order oligomeric species could be detected at times.

We used hydrodynamic bead modelling, transmission electron microscopy and SAXS (small angle X-ray scattering) to determine the overall global solution structure of the SNARE complex dimer. All three approaches revealed an open, two-winged structure in which both monomers interact with an obtuse angle of approximately 130°. Since SNARE complexes form sequentially from the N- to the C-terminus [68], a functionally relevant dimer should involve C-terminal SNARE complex regions that lie close to the point of membrane fusion. Indeed, using FRET *in vitro*, we could determine that the two SNARE complexes interact in a parallel fashion, with the C-termini of both monomers adjacent to each other in the dimer.

The open configuration of the SNARE complex dimer as determined in solution differs from all lattice interactions observed in the SNARE complex crystal structure [148]. In fact, when we analysed the ten most probable lattice

dimer interactions in the crystal structure, we observed three distinct parallel crystallographic dimers, with one involving a C-terminal residue of VAMP2 (W89). However, the SNARE monomers within this putative dimer displayed a closed conformation quite distinct from the open, wing-shaped solution structure identified in the present study. Furthermore, we performed hydrodynamic bead modelling of all putative crystallographic dimers, and found that they all were very different from the experimental hydrodynamic data of the SNARE complex dimer in solution. Therefore, interactions observed in crystal lattices have to be interpreted with caution and may not be observed in physiological contexts [335].

Whilst our studies employed the cytosolic SNARE coils devoid of the TMDs, other studies to determine the oligomeric nature of SNARE complexes have been performed with full-length SNAREs upon detergent solubilization. For example, initial studies indicated the presence of distinct oligomeric high-molecular mass SNARE complex species by SDS-PAGE [336]. However, whilst we could detect the two described SDS-resistant complexes in PC12 cells, we did not further pursue these experiments due to high interexperimental variability of the presence of one versus the other complex, at least in our hands (Annex I).

On the other hand, star-shaped oligomers of SNARE complexes have been described upon detergent solubilization and isolation of native SNAREs [260]. These star-shaped structures were mostly composed of three to four complexes emanating from the center, and were also observed when full-length, purified SNAREs were assembled into complexes, indicating that they form in the absence of auxiliary proteins [260]. These complexes are likely formed by interactions mediated by the TMDs, as a recent crystal structure of full-length SNARE complexes revealed a very similar, star-shaped configuration whereby four SNARE complexes interact via their TMDs [260]. However, it is difficult to imagine how such TMD-mediated oligomers may be accommodated close to the point of membrane fusion, and it is likely that other configurations may exist as well, especially in an intact cell context.

SNARE complex dimerization may affect its interaction with reported regulatory proteins such as complexins or synaptotagmin I [149, 293]. Conversely, interaction of SNARE complexes with regulatory proteins may regulate the extent of dimerization. Using size exclusion chromatography, we found no effect of recombinant, full-length complexin I, which was capable of

binding to SNARE complex dimers, and did not seem to interfere with dimer formation. Complexin I bound stoichiometrically to the SNARE complex dimer, as judged by the shift of its apparent molecular weight. In contrast, we could not detect binding of the recombinant, soluble C2AB fragment of synaptotagmin I to SNARE complexes dimers or monomers in solution, neither in the presence nor absence of Ca^{2+} . This lack of co-migration in size exclusion chromatography has been previously observed [337], which may indicate a low affinity-interaction in solution, in the absence of phospholipids. Alternatively, our recombinant synaptotagmin protein may not be fully functional, which would also result in a lack of interaction with SNARE complexes. Finally, since a recent study indicates that synaptotagmin I binds to the complexin-bound SNARE complex, we may have missed such interactions, as we did not perform those studies in the presence of complexin I.

Several bivalent cation binding sites have been described in the crystal structure of the SNARE complex [65, 148, 149], and the Ca^{2+} cooperativity of membrane fusion may be, at least in part, imparted by the SNARE complex itself. Therefore, we aimed to address whether SNARE complex dimerization is subject to regulation by Ca^{2+} . Whilst the presence of Ca^{2+} induced a discrete molecular weight shift of the SNARE complex dimer (data not shown), such behaviour was likely due to column packing issues. Future studies, for example using analytical ultracentrifugation, may yield insight into the possible role of Ca^{2+} in SNARE complex oligomerization.

In sum, our studies indicate that SNARE complexes, devoid of TMDs, form defined dimers in solution, whilst it is clear that in the presence of the TMDs, embedded in their respective lipid context, and in a trans SNARE complex configuration, additional interactions may occur as well.

2. Mapping of the dimer interface.

We aimed to determine which residues may be involved in forming the SNARE complex dimer interface. Since W89 and W90 within VAMP2 are located towards the C-terminal end of the SNARE complex, and are the only tryptophans within the cytosolic SNARE complex, we initially employed tryptophan fluorescence quenching experiments. When dimers were converted to monomers by addition of increasing salt, we observed a decrease in the intrinsic tryptophan fluorescence, indicating that W89 and W90 of VAMP2 participate in SNARE complex dimerization. However, the peak fluorescence emission wavelength remained unchanged at all salt concentrations, which, together with other data (see Annex III), indicate that both tryptophan residues occupy hydrophilic environments. These data are difficult to explain in molecular terms, but may indicate that fluorescence decrease upon monomerization results from the release of rotational constraints imposed upon at least one of the tryptophan residues within the dimer.

To get further evidence for the involvement of the tryptophans in dimer interactions, we used a combination of mutational analysis and sedimentation equilibrium assays. The results indicate that mutating both residues decreases dimer stability to increasing salt without fully abolishing dimer interactions. Mutating another residue within VAMP2 (R86) further decreased dimer stability, but again was not sufficient to fully disrupt dimers under physiological salt conditions. Thus, additional residues must contribute to the dimer interface as well, which may be contributed by VAMP2, SNAP-25 and/or syntaxin1A. Due to the extensive amount of work in purifying distinct mutant proteins for such studies, we have not mapped the dimerization interface by a mutational approach in more detail.

SNARE complex dimers formed with a triple-mutant VAMP2 (R86A,W89A,W90A), which display reduced stability, still bound to complexin I with the same efficiency as wildtype dimers. This is consistent with the reported complexin binding interface on SNARE complexes, which is distinct from the dimerization interface [65]. We used full-length complexin I containing the N-terminal sequence, which has recently been suggested to directly or indirectly interact with the membrane-proximal part (specifically residues W89 and W90) of

VAMP2, [296] to activate evoked fusion. It has been proposed that this action may enhance the force transfer of SNARE complexes onto the fusing membranes. Thus, one could imagine that SNARE complex dimerization, involving W89 and W90 residues of VAMP2, may modulate binding of the N-terminal region of complexin I. However, differences in the affinity of complexin binding to wildtype and mutant SNARE complex dimers may not have been apparent in the context of strong binding of the central domain of complexin, and additional studies, e.g. using the N-terminal region of complexin on its own, will be necessary to further evaluate this possibility.

3. Effects of VAMP2 dimerization mutants on secretion:

To test for the functional significance of SNARE complex dimers *in vivo*, we used two different approaches in transfected neuroendocrine PC12 cells. Using a toxin rescue assay, we found that VAMP2 mutations which impaired SNARE complex dimerization *in vitro* were deficient in supporting secretion *in vivo*. On the other hand, overexpression of these VAMP2 mutants, in the context of endogenous protein, displayed a dominant-negative effect on neurosecretion. Importantly, the extent by which the respective mutants interfered with secretion *in vivo* paralleled dimer stability as assessed *in vitro*.

This correlation does not formally prove that the mechanism by which these mutants impair neurosecretion is due to a decrease in SNARE complex dimerization, and other scenarios remain possible as well. For example, our data are in agreement with a recent study using VAMP2-deficient neurons [296]. Whilst expression of wildtype VAMP2 was found to rescue the loss of neurotransmission in knockout neurons, a W89AW90A mutant displayed a twofold decrease in fast evoked fusion, with the remainder being largely asynchronous release. Interestingly, this study also reported an increase in miniature frequency, indicating enhanced spontaneous membrane fusion events [296]. Whilst we did not find significant differences in release under physiological saline conditions, our assay system was not optimized to detect differences in such spontaneous fusion events, and further studies will be needed to evaluate this possibility. Future experiments may involve the use of sucrose, known to deplete

the readily-releasable pool, in cells expressing wildtype or mutant VAMP2 constructs. In either case, the phenotype of the W89AW90A VAMP2 mutant was proposed to involve complexin binding, since it phenocopied the complexin loss-of-function phenotype. However, as in our case, no definite formal proof for a causal relationship has been presented, and further studies are necessary to establish for example binding between the VAMP2 membrane-proximal domain and the N-terminal sequence of complexin.

The membrane-proximal part of VAMP2 has alternatively been suggested to be embedded in the membrane, with W89 and W90 facing the hydrophobic part of the bilayer, thereby preventing VAMP2 from assembling into the SNARE complex [286, 288]. However, when we mutated W89 and W90 to hydrophilic serines, which would impede membrane association, we did not find enhanced secretion, as would be expected based on this model, but an inhibition of exocytosis.

Yet another model has been proposed to suggest that the membrane-proximal part of VAMP2 interacts with calmodulin [160, 161]. Calmodulin is a ubiquitous Ca^{2+} sensor, suggested to participate in the late triggering step of neurosecretion [338], and has been reported to bind to the C-terminal motif of VAMP2 (residues 77-90) in a Ca^{2+} dependent manner. The consensus calmodulin binding motif involves specific hydrophobic residues at position 1-5-8-14, and an overall electrostatic charge of +2 to +6 [339]. W90 is at position 14 of this motif, and a mutation to alanine would not be tolerated. However, we found that a single W90A VAMP2 mutation had no effect on secretion, either in the presence or absence of endogenous VAMP2. In addition, the overall net charge of this motif in the case of VAMP2 is +3, and abolishing charge requirements were not found to affect neurosecretion (K83AK87A; data not shown). Again, our data are in agreement with recent studies, which show that whilst expressing W89AW90A mutant VAMP2 in a knockout background displays severe secretory deficits, no effects are seen when expressing K85AR86A or R86AK87A mutants [296]. Finally, we were not able to detect binding of purified VAMP2 to calmodulin-agarose as previously described [160, 161] (data not shown), and thus our combined data would indicate that calmodulin binding to the membrane-proximal region of VAMP2 is not relevant for VAMP2 function in intact cells.

In sum, whilst we cannot fully exclude compound effects, our combined data would indicate that the secretory effects of the VAMP2 mutants are, at least in part, due to interfering with SNARE complex dimer stability *in vivo*.

4. Visualization of SNARE protein interactions by BiFC *in vivo*:

As another approach towards obtaining evidence for SNARE complex oligomers in intact cells, we employed BiFC [340-343]. VAMP2 molecules were found to dimerize through their TMDs in intact cells as well as upon fixation. This feature impeded further determination of SNARE complex oligomers by BiFC, but allowed us to dissect the sequence requirements within the TMD of VAMP2 required for interactions, the relevance of such TMD interactions, and in general, the sequence requirements within the TMD of VAMP2 important for neurosecretion in intact cells. We also used BiFC of syntaxin1A molecules, which was observed in a non-even, patchy manner at the plasma membrane. Such signal may reflect clusters of t-SNAREs at the plasma membrane and/or multimers of trans SNARE complexes before membrane fusion. A combination of imaging studies in the presence of toxins (which would cleave non-assembled syntaxin1A, but not syntaxin1A incorporated into SNARE complexes, which is resistant to toxin cleavage) may be necessary to further reveal the molecular identity of such BiFC signal. In addition, immunogold electron microscopy (using an anti-GFP antibody) may yield further insights into where, with respect to vesicles and plasma membrane, the BiFC signal is occurring. Similarly, additional studies would be required to further establish whether the rather homogeneous, plasma membrane BiFC signal between VAMP2 and syntaxin1A reflects cis SNARE complexes, or interactions between those molecules in a non-complexed manner. However, given that we had previously analysed VAMP2 in great detail, for the present study we also focused on dissecting the molecular determinants responsible for BiFC between VAMP2 molecules.

5. Characterization of VAMP2 TMD-mediated dimerization:

The TMDs of VAMP2 have been reported to dimerize in the presence of detergent or upon reconstitution into liposomes [252-255, 257, 258, 260]. Our BiFC signal also supports the idea that VAMP2 TMDs interact in intact cells. However, whilst the *in vitro* studies have suggested that a set of residues within the TMD are involved in dimerization, our studies indicate that these residues are neither required for interactions (as measured by BiFC) nor neurosecretion in intact cells. Thus, studies in artificial membranes have to be generally interpreted with caution.

We observed that the VAMP2 TMD harbours a highly conserved glycine residue (G100). Glycines frequently occur in the TMDs of membrane proteins [344]. The presence of glycine is usually accompanied by a preponderance of beta-branched residues like isoleucine and valine, and is generally associated with structural roles in TMD helices [345]. One such structural role for glycine seems to involve TMD dimerization of single-pass, as well as polytopic membrane proteins through specific packing interactions [346-348]. The lack of side chain in glycine residues is thought to mediate the closest contact point between two α -helices through van der Waals interactions [346]. Interestingly, bulky hydrophobic residues like valine appear to pack well against the molecular notch formed by glycine residues in the opposing helix, favouring helix crossing angles. Similarly, glycines themselves appear to pack well against glycines in the opposing helix, creating the closest approach of helix-helix packing [346]. To test for the possible role of glycine VAMP2 TMD interactions due to helix packing issues, we replaced VAMP2 G100 with residues of increasing molecular volume (Y > V > A > G). We found that mutating the glycine to another small residue like alanine still allowed VAMP2 TMD interactions as measured by BiFC. In fact, glycine, alanine and proline are the most common residues found at helix-helix crossing points [346]. In contrast, mutating the glycine to two different bulky residues (valine and tyrosine) fully abolished TMD dimerization. Interestingly, a combination of WT and G100V still allowed dimerization, whereas WT and G100Y did not. Together, our data indicate that a glycine residue within the TMD of VAMP2 plays a crucial role for TMD-mediated interactions as assessed by BiFC.

The manner in which the VAMP2 TMD is embedded into the membrane has been somewhat controversial. The predicted TMD is unusually large, and it is likely that it is embedded into the membrane with a tilt with respect to the bilayer normal [286, 290]. If so, two TMD helices likely are packing against each other with rather large, open helix crossing angle. Interestingly, such open, scissor-like conformation has recently been observed *in vitro* [257] in the absence of cholesterol. In artificial membranes containing physiological cholesterol levels, the two TMD helices were suggested to lie against each other in a closed, parallel fashion [257]. It is hard to imagine how such suggested conformational change might be relevant, given the fact that cholesterol levels in vesicular membranes do not undergo drastic fluctuations within the time frame of vesicle fusion events. However, these studies nevertheless indicate that distinct TMD interactions can occur dependent on the lipid composition of artificial membranes. In our intact cell system, we would suggest that the TMD-mediated dimerization involves a conformation whereby glycine residues form a molecular notch, contributing to the helix-helix packing of two tilted helices. Interestingly, the syntaxin1A TMD also contains a glycine residue, and further mutational analysis may be warranted to characterize a possible role for the glycine residue in the syntaxin1A TMD for self-interactions.

To test for the importance of TMD-mediated VAMP2 interactions in neurosecretion, we used a toxin rescue assay. In this case, we used recombinant BoNT/F-LC and a toxin-resistant VAMP2 mutant (K59R). This novel toxin rescue system was developed because of the ease of purifying BoNT/F-LC, as compared to the BoNT/B-LC preparation (data not shown). Surprisingly, none of the glycine mutants were defective in supporting neurosecretion, indicating that the TMD-mediated interactions do not seem to play an important role in neurosecretion in intact cells.

Glycine residues have also been reported to induce a certain destabilization of α -helicity of a TMD in membrane environments by deforming the helix or acting as a “hinge” [349]. Interestingly, glycine residues are common in TMDs of viral fusion proteins, and a model for viral fusion proposes that the bending of the TMD around this flexible hinge, perhaps induced by forces acting from elsewhere in the molecule, may destabilize the hemifusion diaphragm and thus driving fusion pore formation (Figure 41) [274].

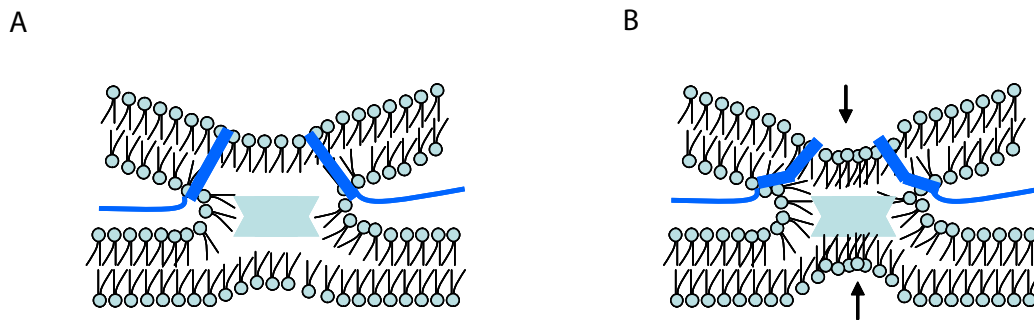


Figure 41. Model for the participation of a TMD glycine residue in fusion. A) Rigid TMD is embedded in the membrane. B) Same example as A, but with TMD containing a bend around a glycine hinge. This could result in compression (increasing negative curvature) in the inner leaflet (down pointing arrow) and expansion of the outer leaflet (up pointing arrow) of the hemifusion diaphragm, thus forcing the lipids into a more stable fusion pore rearrangement.

Based on this viral model, one could speculate how in the case of VAMP2, the bending force might come from SNARE complex formation [332]. To test this possibility, we replaced the G100 of VAMP2 with a proline residue, which mimics this putative “hinge” [350]. The G100P mutant still displayed BiFC, and resulted in a slight enhancement of neurosecretion, suggesting that a hinge in the TMD may indeed be favorable for bringing about membrane fusion events. However, such hinge does not seem to be necessary, as a mutant lacking the glycine residue still was capable of bringing about neurosecretion (data not shown).

6. N- and C-terminal regions of VAMP2 TMD differentially affect neurosecretion:

Whilst previous evidence indicates that the TMDs of SNAREs are important for membrane fusion events (see review [262]), a precise characterization of the functionally important regions has been lacking. We generated a series of deletion and insertion mutants along the VAMP2 TMD sequence and studied their ability to support neurosecretion using our toxin rescue assay. Interestingly, we found that deletions or insertions at the N-terminal region had no or little effect on neurosecretion, whilst mutating the C-terminal end of the TMD profoundly impaired neurosecretion. These data indicate that structural and length requirements of this C-terminal region are functionally important. This finding is in agreement with structural studies of the TMD in the presence of cholesterol, where the C-terminal regions of the TMD were reported to be forced into close proximity, possibly favouring membrane fusion [257]. It will be interesting to further address effects of lipid environments on such structural constraints of the VAMP2 TMD. In addition, since our toxin rescue assay only measures the extent of full fusion, without being able to differentiate kinetic effects, additional studies (such as amperometry or capacitance measurements) may be warranted to characterize the effects of our mutants on fusion pore phenotypes. In sum, our data provide the first detailed mutational analysis of VAMP2 with respect to membrane fusion, indicating structurally distinct regions within the TMD differentially required for membrane merger.

CONCLUSIONS

VIII. CONCLUSIONS:

- 1- SNARE complexes form defined dimers *in vitro*.
- 2- SNARE complex dimers display a two-winged, open structure whereby the individual monomers interact towards their C-termini.
- 3- At least three residues (R86, W89 and W90) within the C-terminal region of VAMP2 are involved in SNARE complex dimerization *in vitro*.
- 4- VAMP2 mutants that reduce the stability of SNARE complex dimers *in vitro* are unable to support neurosecretion *in vivo*.
- 5- VAMP2 mutants that reduce the stability of SNARE complex dimers *in vitro* cause dominant-negative secretory effects *in vivo*.
- 6- VAMP2 displays BiFC *in vivo*, with a subcellular localization identical to that of endogenous VAMP2 *in vivo*.
- 7- VAMP2 TMD-TMD interactions, as revealed by BiFC, involve a central glycine residue (G100) *in vivo*.
- 8- VAMP2 TMD-mediated interactions are not crucial for neurosecretion *in vivo*.
- 9- The C-terminal part of the TMD of VAMP2 is functionally important for neurosecretion *in vivo*.

REFERENCES

IX. REFERENCES:

1. Bennett, M.K. and R.H. Scheller, *A molecular description of synaptic vesicle membrane trafficking*. Annu Rev Biochem, 1994. **63**: p. 63-100.
2. Rothman, J.E., *Mechanisms of intracellular protein transport*. Nature, 1994. **372**(6501): p. 55-63.
3. Bonifacino, J.S. and B.S. Glick, *The mechanisms of vesicle budding and fusion*. Cell, 2004. **116**(2): p. 153-66.
4. Pfeffer, S.R., *Unsolved mysteries in membrane traffic*. Annu Rev Biochem, 2007. **76**: p. 629-45.
5. Bennett, M.K., *SNAREs and the specificity of transport vesicle targeting*. Curr Opin Cell Biol, 1995. **7**(4): p. 581-6.
6. Jahn, R. and R.H. Scheller, *SNAREs--engines for membrane fusion*. Nat Rev Mol Cell Biol, 2006. **7**(9): p. 631-43.
7. Hermann, G.J., et al., *Mitochondrial fusion in yeast requires the transmembrane GTPase Fzo1p*. J Cell Biol, 1998. **143**(2): p. 359-73.
8. Sesaki, H. and R.E. Jensen, *UGO1 encodes an outer membrane protein required for mitochondrial fusion*. J Cell Biol, 2001. **152**(6): p. 1123-34.
9. Titorenko, V.I. and R.A. Rachubinski, *Dynamics of peroxisome assembly and function*. Trends Cell Biol, 2001. **11**(1): p. 22-29.
10. Scales, S.J., et al., *SNAREs contribute to the specificity of membrane fusion*. Neuron, 2000. **26**(2): p. 457-64.
11. Fasshauer, D., et al., *Mixed and non-cognate SNARE complexes. Characterization of assembly and biophysical properties*. J Biol Chem, 1999. **274**(22): p. 15440-6.
12. Yang, B., et al., *SNARE interactions are not selective. Implications for membrane fusion specificity*. J Biol Chem, 1999. **274**(9): p. 5649-53.
13. Fukuda, R., et al., *Functional architecture of an intracellular membrane t-SNARE*. Nature, 2000. **407**(6801): p. 198-202.
14. McNew, J.A., et al., *Compartmental specificity of cellular membrane fusion encoded in SNARE proteins*. Nature, 2000. **407**(6801): p. 153-9.

15. Parlati, F., et al., *Topological restriction of SNARE-dependent membrane fusion*. Nature, 2000. **407**(6801): p. 194-8.
16. Parlati, F., et al., *Distinct SNARE complexes mediating membrane fusion in Golgi transport based on combinatorial specificity*. Proc Natl Acad Sci U S A, 2002. **99**(8): p. 5424-9.
17. Brandhorst, D., et al., *Homotypic fusion of early endosomes: SNAREs do not determine fusion specificity*. Proc Natl Acad Sci U S A, 2006. **103**(8): p. 2701-6.
18. Borisovska, M., et al., *v-SNAREs control exocytosis of vesicles from priming to fusion*. Embo J, 2005. **24**(12): p. 2114-26.
19. Sorensen, J.B., et al., *Differential control of the releasable vesicle pools by SNAP-25 splice variants and SNAP-23*. Cell, 2003. **114**(1): p. 75-86.
20. Antonin, W., et al., *A SNARE complex mediating fusion of late endosomes defines conserved properties of SNARE structure and function*. Embo J, 2000. **19**(23): p. 6453-64.
21. Wang, C.C., et al., *A role of VAMP8/endobrevin in regulated exocytosis of pancreatic acinar cells*. Dev Cell, 2004. **7**(3): p. 359-71.
22. Pfeffer, S.R., *Transport-vesicle targeting: tethers before SNAREs*. Nat Cell Biol, 1999. **1**(1): p. E17-22.
23. Pfeffer, S.R., *Rab GTPases: specifying and deciphering organelle identity and function*. Trends Cell Biol, 2001. **11**(12): p. 487-91.
24. Vale, R.D., *AAA proteins. Lords of the ring*. J Cell Biol, 2000. **150**(1): p. F13-9.
25. Chen, Y.A. and R.H. Scheller, *SNARE-mediated membrane fusion*. Nat Rev Mol Cell Biol, 2001. **2**(2): p. 98-106.
26. Szule, J.A. and J.R. Coorsen, *Revisiting the role of SNAREs in exocytosis and membrane fusion*. Biochim Biophys Acta, 2003. **1641**(2-3): p. 121-35.
27. Melkikh, A.V. and V.D. Seleznev, *Models of active transport of neurotransmitters in synaptic vesicles*. J Theor Biol, 2007. **248**(2): p. 350-3.
28. Rizzoli, S.O. and W.J. Betz, *The structural organization of the readily releasable pool of synaptic vesicles*. Science, 2004. **303**(5666): p. 2037-9.
29. Rizzoli, S.O. and W.J. Betz, *Synaptic vesicle pools*. Nat Rev Neurosci, 2005. **6**(1): p. 57-69.

30. Schikorski, T. and C.F. Stevens, *Morphological correlates of functionally defined synaptic vesicle populations*. Nat Neurosci, 2001. **4**(4): p. 391-5.
31. Katz, B., *The release of neural transmitter substances.*, in *Liverpool Univ Press*. 1969: Liverpool, UK. p. .
32. Augustine, G.J., M.P. Charlton, and S.J. Smith, *Calcium entry and transmitter release at voltage-clamped nerve terminals of squid*. J Physiol, 1985. **367**: p. 163-81.
33. Katz, B. and R. Miledi, *The timing of calcium action during neuromuscular transmission*. J Physiol, 1967. **189**(3): p. 535-44.
34. Li, C., et al., *Ca(2+)-dependent and -independent activities of neural and non-neural synaptotagmins*. Nature, 1995. **375**(6532): p. 594-9.
35. Martin, T.F., *Tuning exocytosis for speed: fast and slow modes*. Biochim Biophys Acta, 2003. **1641**(2-3): p. 157-65.
36. Llinas, R., et al., *Intraterminal injection of synapsin I or calcium/calmodulin-dependent protein kinase II alters neurotransmitter release at the squid giant synapse*. Proc Natl Acad Sci U S A, 1985. **82**(9): p. 3035-9.
37. Ryan, T.A., et al., *Synaptic vesicle recycling in synapsin I knock-out mice*. J Cell Biol, 1996. **134**(5): p. 1219-27.
38. Chi, P., P. Greengard, and T.A. Ryan, *Synapsin dispersion and recluster during synaptic activity*. Nat Neurosci, 2001. **4**(12): p. 1187-93.
39. Kraszewski, K., et al., *Mobility of synaptic vesicles in nerve endings monitored by recovery from photobleaching of synaptic vesicle-associated fluorescence*. J Neurosci, 1996. **16**(19): p. 5905-13.
40. Czernik, A.J., D.T. Pang, and P. Greengard, *Amino acid sequences surrounding the cAMP-dependent and calcium/calmodulin-dependent phosphorylation sites in rat and bovine synapsin I*. Proc Natl Acad Sci U S A, 1987. **84**(21): p. 7518-22.
41. Jovanovic, J.N., et al., *Neurotrophins stimulate phosphorylation of synapsin I by MAP kinase and regulate synapsin I-actin interactions*. Proc Natl Acad Sci U S A, 1996. **93**(8): p. 3679-83.

42. Matsubara, M., et al., *Site-specific phosphorylation of synapsin I by mitogen-activated protein kinase and Cdk5 and its effects on physiological functions*. J Biol Chem, 1996. **271**(35): p. 21108-13.
43. Menegon, A., et al., *Protein kinase A-mediated synapsin I phosphorylation is a central modulator of Ca²⁺-dependent synaptic activity*. J Neurosci, 2006. **26**(45): p. 11670-81.
44. Baumert, M., et al., *Synaptobrevin: an integral membrane protein of 18,000 daltons present in small synaptic vesicles of rat brain*. Embo J, 1989. **8**(2): p. 379-84.
45. Bennett, M.K., N. Calakos, and R.H. Scheller, *Syntaxin: a synaptic protein implicated in docking of synaptic vesicles at presynaptic active zones*. Science, 1992. **257**(5067): p. 255-9.
46. Oyler, G.A., et al., *The identification of a novel synaptosomal-associated protein, SNAP-25, differentially expressed by neuronal subpopulations*. J Cell Biol, 1989. **109**(6 Pt 1): p. 3039-52.
47. Trimble, W.S., D.M. Cowan, and R.H. Scheller, *VAMP-1: a synaptic vesicle-associated integral membrane protein*. Proc Natl Acad Sci U S A, 1988. **85**(12): p. 4538-42.
48. Sollner, T., et al., *A protein assembly-disassembly pathway in vitro that may correspond to sequential steps of synaptic vesicle docking, activation, and fusion*. Cell, 1993. **75**(3): p. 409-18.
49. Geppert, M. and T.C. Sudhof, *RAB3 and synaptotagmin: the yin and yang of synaptic membrane fusion*. Annu Rev Neurosci, 1998. **21**: p. 75-95.
50. McMahon, H.T., et al., *Complexins: cytosolic proteins that regulate SNAP receptor function*. Cell, 1995. **83**(1): p. 111-9.
51. Fujita, Y., et al., *Tomosyn: a syntaxin-1-binding protein that forms a novel complex in the neurotransmitter release process*. Neuron, 1998. **20**(5): p. 905-15.
52. Betz, A., et al., *Munc13-1 is a presynaptic phorbol ester receptor that enhances neurotransmitter release*. Neuron, 1998. **21**(1): p. 123-36.
53. Ilardi, J.M., S. Mochida, and Z.H. Sheng, *Snapiin: a SNARE-associated protein implicated in synaptic transmission*. Nat Neurosci, 1999. **2**(2): p. 119-24.

54. Lao, G., et al., *Syntaxin-1 clamp that controls SNARE assembly*. *Neuron*, 2000. **25**(1): p. 191-201.
55. Tang, J., et al., *A complexin/syntaxin 1 switch controls fast synaptic vesicle exocytosis*. *Cell*, 2006. **126**(6): p. 1175-87.
56. Lang, T., et al., *SNAREs are concentrated in cholesterol-dependent clusters that define docking and fusion sites for exocytosis*. *Embo J*, 2001. **20**(9): p. 2202-13.
57. Sieber, J.J., et al., *Anatomy and dynamics of a supramolecular membrane protein cluster*. *Science*, 2007. **317**(5841): p. 1072-6.
58. Fiebig, K.M., et al., *Folding intermediates of SNARE complex assembly*. *Nat Struct Biol*, 1999. **6**(2): p. 117-23.
59. Fasshauer, D. and M. Margittai, *A transient N-terminal interaction of SNAP-25 and syntaxin nucleates SNARE assembly*. *J Biol Chem*, 2004. **279**(9): p. 7613-21.
60. Nicholson, K.L., et al., *Regulation of SNARE complex assembly by an N-terminal domain of the t-SNARE Sso1p*. *Nat Struct Biol*, 1998. **5**(9): p. 793-802.
61. Chen, Y.A., S.J. Scales, and R.H. Scheller, *Sequential SNARE assembly underlies priming and triggering of exocytosis*. *Neuron*, 2001. **30**(1): p. 161-70.
62. Xu, T., et al., *Multiple kinetic components of exocytosis distinguished by neurotoxin sensitivity*. *Nat Neurosci*, 1998. **1**(3): p. 192-200.
63. Xu, T., et al., *Inhibition of SNARE complex assembly differentially affects kinetic components of exocytosis*. *Cell*, 1999. **99**(7): p. 713-22.
64. Zhang, Y., et al., *A partially zipped SNARE complex stabilized by the membrane*. *J Biol Chem*, 2005. **280**(16): p. 15595-600.
65. Chen, X., et al., *Three-dimensional structure of the complexin/SNARE complex*. *Neuron*, 2002. **33**(3): p. 397-409.
66. Hanson, P.I., J.E. Heuser, and R. Jahn, *Neurotransmitter release - four years of SNARE complexes*. *Curr Opin Neurobiol*, 1997. **7**(3): p. 310-5.
67. Hay, J.C. and R.H. Scheller, *SNAREs and NSF in targeted membrane fusion*. *Curr Opin Cell Biol*, 1997. **9**(4): p. 505-12.

68. Sorensen, J.B., et al., *Sequential N- to C-terminal SNARE complex assembly drives priming and fusion of secretory vesicles*. *Embo J*, 2006. **25**(5): p. 955-66.
69. Sorensen, J.B., et al., *The SNARE protein SNAP-25 is linked to fast calcium triggering of exocytosis*. *Proc Natl Acad Sci U S A*, 2002. **99**(3): p. 1627-32.
70. Sakaba, T., et al., *Distinct kinetic changes in neurotransmitter release after SNARE protein cleavage*. *Science*, 2005. **309**(5733): p. 491-4.
71. Fernandez-Chacon, R., et al., *Synaptotagmin I functions as a calcium regulator of release probability*. *Nature*, 2001. **410**(6824): p. 41-9.
72. Perin, M.S., et al., *Phospholipid binding by a synaptic vesicle protein homologous to the regulatory region of protein kinase C*. *Nature*, 1990. **345**(6272): p. 260-3.
73. Ishizuka, T., et al., *Synaphin: a protein associated with the docking/fusion complex in presynaptic terminals*. *Biochem Biophys Res Commun*, 1995. **213**(3): p. 1107-14.
74. Yoon, T.Y., et al., *Complexin and Ca²⁺ stimulate SNARE-mediated membrane fusion*. *Nat Struct Mol Biol*, 2008. **15**(7): p. 707-13.
75. Giraud, C.G., et al., *A clamping mechanism involved in SNARE-dependent exocytosis*. *Science*, 2006. **313**(5787): p. 676-80.
76. Melia, T.J., Jr., *Putting the clamps on membrane fusion: how complexin sets the stage for calcium-mediated exocytosis*. *FEBS Lett*, 2007. **581**(11): p. 2131-9.
77. Schaub, J.R., et al., *Hemifusion arrest by complexin is relieved by Ca²⁺-synaptotagmin I*. *Nat Struct Mol Biol*, 2006. **13**(8): p. 748-50.
78. Sudhof, T.C. and J.E. Rothman, *Membrane fusion: grappling with SNARE and SM proteins*. *Science*, 2009. **323**(5913): p. 474-7.
79. Otto, H., P.I. Hanson, and R. Jahn, *Assembly and disassembly of a ternary complex of synaptobrevin, syntaxin, and SNAP-25 in the membrane of synaptic vesicles*. *Proc Natl Acad Sci U S A*, 1997. **94**(12): p. 6197-201.
80. Malhotra, V., et al., *Role of an N-ethylmaleimide-sensitive transport component in promoting fusion of transport vesicles with cisternae of the Golgi stack*. *Cell*, 1988. **54**(2): p. 221-7.

81. Whiteheart, S.W., et al., *Soluble N-ethylmaleimide-sensitive fusion attachment proteins (SNAPs) bind to a multi-SNAP receptor complex in Golgi membranes*. J Biol Chem, 1992. **267**(17): p. 12239-43.
82. Whiteheart, S.W., et al., *SNAP family of NSF attachment proteins includes a brain-specific isoform*. Nature, 1993. **362**(6418): p. 353-5.
83. Hanson, P.I., et al., *The N-ethylmaleimide-sensitive fusion protein and alpha-SNAP induce a conformational change in syntaxin*. J Biol Chem, 1995. **270**(28): p. 16955-61.
84. Hanson, P.I., et al., *Structure and conformational changes in NSF and its membrane receptor complexes visualized by quick-freeze/deep-etch electron microscopy*. Cell, 1997. **90**(3): p. 523-35.
85. Banerjee, A., et al., *N-Ethylmaleimide-sensitive factor acts at a prefusion ATP-dependent step in Ca²⁺-activated exocytosis*. J Biol Chem, 1996. **271**(34): p. 20223-6.
86. Haas, A., *NSF--fusion and beyond*. Trends Cell Biol, 1998. **8**(12): p. 471-3.
87. Haas, A. and W. Wickner, *Homotypic vacuole fusion requires Sec17p (yeast alpha-SNAP) and Sec18p (yeast NSF)*. Embo J, 1996. **15**(13): p. 3296-305.
88. Mayer, A., W. Wickner, and A. Haas, *Sec18p (NSF)-driven release of Sec17p (alpha-SNAP) can precede docking and fusion of yeast vacuoles*. Cell, 1996. **85**(1): p. 83-94.
89. Hanson, P.I. and S.W. Whiteheart, *AAA+ proteins: have engine, will work*. Nat Rev Mol Cell Biol, 2005. **6**(7): p. 519-29.
90. Marz, K.E., J.M. Lauer, and P.I. Hanson, *Defining the SNARE complex binding surface of alpha-SNAP: implications for SNARE complex disassembly*. J Biol Chem, 2003. **278**(29): p. 27000-8.
91. Scales, S.J., B.Y. Yoo, and R.H. Scheller, *The ionic layer is required for efficient dissociation of the SNARE complex by alpha-SNAP and NSF*. Proc Natl Acad Sci U S A, 2001. **98**(25): p. 14262-7.
92. Grote, E., C.M. Carr, and P.J. Novick, *Ordering the final events in yeast exocytosis*. J Cell Biol, 2000. **151**(2): p. 439-52.

93. Ungermann, C. and D. Langosch, *Functions of SNAREs in intracellular membrane fusion and lipid bilayer mixing*. J Cell Sci, 2005. **118**(Pt 17): p. 3819-28.
94. Sudhof, T.C., et al., *A synaptic vesicle membrane protein is conserved from mammals to Drosophila*. Neuron, 1989. **2**(5): p. 1475-81.
95. Han, X., et al., *Transmembrane segments of syntaxin line the fusion pore of Ca²⁺-triggered exocytosis*. Science, 2004. **304**(5668): p. 289-92.
96. Hess, D.T., et al., *The 25 kDa synaptosomal-associated protein SNAP-25 is the major methionine-rich polypeptide in rapid axonal transport and a major substrate for palmitoylation in adult CNS*. J Neurosci, 1992. **12**(12): p. 4634-41.
97. Hazzard, J., T.C. Sudhof, and J. Rizo, *NMR analysis of the structure of synaptobrevin and of its interaction with syntaxin*. J Biomol NMR, 1999. **14**(3): p. 203-7.
98. Dulubova, I., et al., *A conformational switch in syntaxin during exocytosis: role of munc18*. Embo J, 1999. **18**(16): p. 4372-82.
99. Fasshauer, D., et al., *Structural changes are associated with soluble N-ethylmaleimide-sensitive fusion protein attachment protein receptor complex formation*. J Biol Chem, 1997. **272**(44): p. 28036-41.
100. Fasshauer, D., et al., *A structural change occurs upon binding of syntaxin to SNAP-25*. J Biol Chem, 1997. **272**(7): p. 4582-90.
101. Margittai, M., et al., *The Habc domain and the SNARE core complex are connected by a highly flexible linker*. Biochemistry, 2003. **42**(14): p. 4009-14.
102. Fernandez, I., et al., *Three-dimensional structure of an evolutionarily conserved N-terminal domain of syntaxin 1A*. Cell, 1998. **94**(6): p. 841-9.
103. Lerman, J.C., et al., *Structural analysis of the neuronal SNARE protein syntaxin-1A*. Biochemistry, 2000. **39**(29): p. 8470-9.
104. Misura, K.M., R.H. Scheller, and W.I. Weis, *Three-dimensional structure of the neuronal-Sec1-syntaxin 1a complex*. Nature, 2000. **404**(6776): p. 355-62.
105. Yang, B., et al., *nSec1 binds a closed conformation of syntaxin1A*. J Cell Biol, 2000. **148**(2): p. 247-52.

106. Margittai, M., et al., *Single-molecule fluorescence resonance energy transfer reveals a dynamic equilibrium between closed and open conformations of syntaxin 1*. Proc Natl Acad Sci U S A, 2003. **100**(26): p. 15516-21.
107. Burkhardt, P., et al., *Munc18a controls SNARE assembly through its interaction with the syntaxin N-peptide*. Embo J, 2008. **27**(7): p. 923-33.
108. Dulubova, I., et al., *Munc18-1 binds directly to the neuronal SNARE complex*. Proc Natl Acad Sci U S A, 2007. **104**(8): p. 2697-702.
109. Roth, A.F., et al., *Global analysis of protein palmitoylation in yeast*. Cell, 2006. **125**(5): p. 1003-13.
110. Hepp, R., J.P. Cabaniols, and P.A. Roche, *Differential phosphorylation of SNAP-25 in vivo by protein kinase C and protein kinase A*. FEBS Lett, 2002. **532**(1-2): p. 52-6.
111. Hepp, R., et al., *Phosphorylation of SNAP-23 regulates exocytosis from mast cells*. J Biol Chem, 2005. **280**(8): p. 6610-20.
112. Gerst, J.E., *SNARE regulators: matchmakers and matchbreakers*. Biochim Biophys Acta, 2003. **1641**(2-3): p. 99-110.
113. Gerst, J.E., *SNAREs and SNARE regulators in membrane fusion and exocytosis*. Cell Mol Life Sci, 1999. **55**(5): p. 707-34.
114. Lin, R.C. and R.H. Scheller, *Mechanisms of synaptic vesicle exocytosis*. Annu Rev Cell Dev Biol, 2000. **16**: p. 19-49.
115. Turner, K.M., R.D. Burgoyne, and A. Morgan, *Protein phosphorylation and the regulation of synaptic membrane traffic*. Trends Neurosci, 1999. **22**(10): p. 459-64.
116. Snyder, D.A., M.L. Kelly, and D.J. Woodbury, *SNARE complex regulation by phosphorylation*. Cell Biochem Biophys, 2006. **45**(1): p. 111-23.
117. Veit, M., *Palmitoylation of the 25-kDa synaptosomal protein (SNAP-25) in vitro occurs in the absence of an enzyme, but is stimulated by binding to syntaxin*. Biochem J, 2000. **345 Pt 1**: p. 145-51.
118. Lane, S.R. and Y. Liu, *Characterization of the palmitoylation domain of SNAP-25*. J Neurochem, 1997. **69**(5): p. 1864-9.
119. Vogel, K. and P.A. Roche, *SNAP-23 and SNAP-25 are palmitoylated in vivo*. Biochem Biophys Res Commun, 1999. **258**(2): p. 407-10.

120. Valdez-Taubas, J. and H. Pelham, *Swf1-dependent palmitoylation of the SNARE Tlg1 prevents its ubiquitination and degradation*. *Embo J*, 2005. **24**(14): p. 2524-32.
121. Gonzalo, S., W.K. Greentree, and M.E. Linder, *SNAP-25 is targeted to the plasma membrane through a novel membrane-binding domain*. *J Biol Chem*, 1999. **274**(30): p. 21313-8.
122. Koticha, D.K., et al., *Role of the cysteine-rich domain of the t-SNARE component, SYNDET, in membrane binding and subcellular localization*. *J Biol Chem*, 1999. **274**(13): p. 9053-60.
123. Kasai, K. and K. Akagawa, *Roles of the cytoplasmic and transmembrane domains of syntaxins in intracellular localization and trafficking*. *J Cell Sci*, 2001. **114**(Pt 17): p. 3115-24.
124. Watson, R.T. and J.E. Pessin, *Transmembrane domain length determines intracellular membrane compartment localization of syntaxins 3, 4, and 5*. *Am J Physiol Cell Physiol*, 2001. **281**(1): p. C215-23.
125. Salaun, C., et al., *Plasma membrane targeting of exocytic SNARE proteins*. *Biochim Biophys Acta*, 2004. **1693**(2): p. 81-9.
126. Grote, E., et al., *A targeting signal in VAMP regulating transport to synaptic vesicles*. *Cell*, 1995. **81**(4): p. 581-9.
127. Grote, E. and R.B. Kelly, *Endocytosis of VAMP is facilitated by a synaptic vesicle targeting signal*. *J Cell Biol*, 1996. **132**(4): p. 537-47.
128. Dittman, J.S. and J.M. Kaplan, *Factors regulating the abundance and localization of synaptobrevin in the plasma membrane*. *Proc Natl Acad Sci U S A*, 2006. **103**(30): p. 11399-404.
129. Taubenblatt, P., et al., *VAMP (synaptobrevin) is present in the plasma membrane of nerve terminals*. *J Cell Sci*, 1999. **112** (Pt 20): p. 3559-67.
130. Fernandez-Alfonso, T., R. Kwan, and T.A. Ryan, *Synaptic vesicles interchange their membrane proteins with a large surface reservoir during recycling*. *Neuron*, 2006. **51**(2): p. 179-86.
131. Koh, S., et al., *Immunoelectron microscopic localization of the HPC-1 antigen in rat cerebellum*. *J Neurocytol*, 1993. **22**(11): p. 995-1005.
132. Kretschmar, S., W. Volkandt, and H. Zimmermann, *Colocalization on the same synaptic vesicles of syntaxin and SNAP-25 with synaptic vesicle*

- proteins: a re-evaluation of functional models required?* Neurosci Res, 1996. **26**(2): p. 141-8.
133. Mitchell, S.J. and T.A. Ryan, *Syntaxin-1A is excluded from recycling synaptic vesicles at nerve terminals*. J Neurosci, 2004. **24**(20): p. 4884-8.
 134. Walch-Solimena, C., et al., *The t-SNAREs syntaxin 1 and SNAP-25 are present on organelles that participate in synaptic vesicle recycling*. J Cell Biol, 1995. **128**(4): p. 637-45.
 135. Chen, Y.A., et al., *SNARE complex formation is triggered by Ca²⁺ and drives membrane fusion*. Cell, 1999. **97**(2): p. 165-74.
 136. Poirier, M.A., et al., *Protease resistance of syntaxin.SNAP-25.VAMP complexes. Implications for assembly and structure*. J Biol Chem, 1998. **273**(18): p. 11370-7.
 137. Hayashi, T., et al., *Disassembly of the reconstituted synaptic vesicle membrane fusion complex in vitro*. Embo J, 1995. **14**(10): p. 2317-25.
 138. Rice, L.M. and A.T. Brunger, *Crystal structure of the vesicular transport protein Sec17: implications for SNAP function in SNARE complex disassembly*. Mol Cell, 1999. **4**(1): p. 85-95.
 139. Zhang, F., et al., *The four-helix bundle of the neuronal target membrane SNARE complex is neither disordered in the middle nor uncoiled at the C-terminal region*. J Biol Chem, 2002. **277**(27): p. 24294-8.
 140. Margittai, M., et al., *Homo- and heterooligomeric SNARE complexes studied by site-directed spin labeling*. J Biol Chem, 2001. **276**(16): p. 13169-77.
 141. Xiao, W., et al., *The neuronal t-SNARE complex is a parallel four-helix bundle*. Nat Struct Biol, 2001. **8**(4): p. 308-11.
 142. Bowen, M.E., et al., *Single molecule observation of liposome-bilayer fusion thermally induced by soluble N-ethyl maleimide sensitive-factor attachment protein receptors (SNAREs)*. Biophys J, 2004. **87**(5): p. 3569-84.
 143. Liu, T., et al., *SNARE-driven, 25-millisecond vesicle fusion in vitro*. Biophys J, 2005. **89**(4): p. 2458-72.
 144. Woodbury, D.J. and K. Rognlien, *The t-SNARE syntaxin is sufficient for spontaneous fusion of synaptic vesicles to planar membranes*. Cell Biol Int, 2000. **24**(11): p. 809-18.

145. Washbourne, P., et al., *Genetic ablation of the t-SNARE SNAP-25 distinguishes mechanisms of neuroexocytosis*. Nat Neurosci, 2002. **5**(1): p. 19-26.
146. Rice, L.M., P. Brennwald, and A.T. Brunger, *Formation of a yeast SNARE complex is accompanied by significant structural changes*. FEBS Lett, 1997. **415**(1): p. 49-55.
147. Fasshauer, D., et al., *Identification of a minimal core of the synaptic SNARE complex sufficient for reversible assembly and disassembly*. Biochemistry, 1998. **37**(29): p. 10354-62.
148. Sutton, R.B., et al., *Crystal structure of a SNARE complex involved in synaptic exocytosis at 2.4 Å resolution*. Nature, 1998. **395**(6700): p. 347-53.
149. Ernst, J.A. and A.T. Brunger, *High resolution structure, stability, and synaptotagmin binding of a truncated neuronal SNARE complex*. J Biol Chem, 2003. **278**(10): p. 8630-6.
150. Fasshauer, D., et al., *Conserved structural features of the synaptic fusion complex: SNARE proteins reclassified as Q- and R-SNAREs*. Proc Natl Acad Sci U S A, 1998. **95**(26): p. 15781-6.
151. Bock, J.B., et al., *A genomic perspective on membrane compartment organization*. Nature, 2001. **409**(6822): p. 839-41.
152. Bock, J.B. and R.H. Scheller, *SNARE proteins mediate lipid bilayer fusion*. Proc Natl Acad Sci U S A, 1999. **96**(22): p. 12227-9.
153. Graf, C.T., et al., *Identification of functionally interacting SNAREs by using complementary substitutions in the conserved '0' layer*. Mol Biol Cell, 2005. **16**(5): p. 2263-74.
154. Katz, L. and P. Brennwald, *Testing the 3Q:1R "rule": mutational analysis of the ionic "zero" layer in the yeast exocytic SNARE complex reveals no requirement for arginine*. Mol Biol Cell, 2000. **11**(11): p. 3849-58.
155. Ossig, R., et al., *Exocytosis requires asymmetry in the central layer of the SNARE complex*. Embo J, 2000. **19**(22): p. 6000-10.
156. Hay, J.C., *SNARE complex structure and function*. Exp Cell Res, 2001. **271**(1): p. 10-21.
157. Wei, S., et al., *Exocytotic mechanism studied by truncated and zero layer mutants of the C-terminus of SNAP-25*. Embo J, 2000. **19**(6): p. 1279-89.

158. Deak, F., et al., *Structural determinants of synaptobrevin 2 function in synaptic vesicle fusion*. J Neurosci, 2006. **26**(25): p. 6668-76.
159. Lauer, J.M., et al., *SNARE complex zero layer residues are not critical for N-ethylmaleimide-sensitive factor-mediated disassembly*. J Biol Chem, 2006. **281**(21): p. 14823-32.
160. Quetglas, S., et al., *Calmodulin and lipid binding to synaptobrevin regulates calcium-dependent exocytosis*. Embo J, 2002. **21**(15): p. 3970-9.
161. Quetglas, S., et al., *Ca²⁺-dependent regulation of synaptic SNARE complex assembly via a calmodulin- and phospholipid-binding domain of synaptobrevin*. Proc Natl Acad Sci U S A, 2000. **97**(17): p. 9695-700.
162. Antonin, W., et al., *Crystal structure of the endosomal SNARE complex reveals common structural principles of all SNAREs*. Nat Struct Biol, 2002. **9**(2): p. 107-11.
163. Zwilling, D., et al., *Early endosomal SNAREs form a structurally conserved SNARE complex and fuse liposomes with multiple topologies*. Embo J, 2007. **26**(1): p. 9-18.
164. Strop, P., et al., *The structure of the yeast plasma membrane SNARE complex reveals destabilizing water-filled cavities*. J Biol Chem, 2008. **283**(2): p. 1113-9.
165. Jahn, R. and T.C. Sudhof, *Membrane fusion and exocytosis*. Annu Rev Biochem, 1999. **68**: p. 863-911.
166. Weber, T., et al., *SNAREpins: minimal machinery for membrane fusion*. Cell, 1998. **92**(6): p. 759-72.
167. Lin, R.C. and R.H. Scheller, *Structural organization of the synaptic exocytosis core complex*. Neuron, 1997. **19**(5): p. 1087-94.
168. Jahn, R., T. Lang, and T.C. Sudhof, *Membrane fusion*. Cell, 2003. **112**(4): p. 519-33.
169. Bai, J. and R.E. Pagano, *Measurement of spontaneous transfer and transbilayer movement of BODIPY-labeled lipids in lipid vesicles*. Biochemistry, 1997. **36**(29): p. 8840-8.
170. Parlati, F., et al., *Rapid and efficient fusion of phospholipid vesicles by the alpha-helical core of a SNARE complex in the absence of an N-terminal regulatory domain*. Proc Natl Acad Sci U S A, 1999. **96**(22): p. 12565-70.

171. Langosch, D., et al., *Peptide mimics of SNARE transmembrane segments drive membrane fusion depending on their conformational plasticity*. J Mol Biol, 2001. **311**(4): p. 709-21.
172. Xu, Y., et al., *Hemifusion in SNARE-mediated membrane fusion*. Nat Struct Mol Biol, 2005. **12**(5): p. 417-22.
173. Earp, L.J., et al., *The many mechanisms of viral membrane fusion proteins*. Curr Top Microbiol Immunol, 2005. **285**: p. 25-66.
174. Chernomordik, L.V. and M.M. Kozlov, *Protein-lipid interplay in fusion and fission of biological membranes*. Annu Rev Biochem, 2003. **72**: p. 175-207.
175. Giraud, C.G., et al., *SNAREs can promote complete fusion and hemifusion as alternative outcomes*. J Cell Biol, 2005. **170**(2): p. 249-60.
176. Lu, X., et al., *Membrane fusion induced by neuronal SNAREs transits through hemifusion*. J Biol Chem, 2005. **280**(34): p. 30538-41.
177. Chernomordik, L.V., et al., *Lysolipids reversibly inhibit Ca(2+)-, GTP- and pH-dependent fusion of biological membranes*. FEBS Lett, 1993. **318**(1): p. 71-6.
178. Grote, E., et al., *Geranylgeranylated SNAREs are dominant inhibitors of membrane fusion*. J Cell Biol, 2000. **151**(2): p. 453-66.
179. Markin, V.S., M.M. Kozlov, and V.L. Borovjagin, *On the theory of membrane fusion. The stalk mechanism*. Gen Physiol Biophys, 1984. **3**(5): p. 361-77.
180. Kiessling, V. and L.K. Tamm, *Measuring distances in supported bilayers by fluorescence interference-contrast microscopy: polymer supports and SNARE proteins*. Biophys J, 2003. **84**(1): p. 408-18.
181. Knecht, V. and H. Grubmuller, *Mechanical coupling via the membrane fusion SNARE protein syntaxin 1A: a molecular dynamics study*. Biophys J, 2003. **84**(3): p. 1527-47.
182. Chernomordik, L., M.M. Kozlov, and J. Zimmerberg, *Lipids in biological membrane fusion*. J Membr Biol, 1995. **146**(1): p. 1-14.
183. Israelachvili, J.N., S. Marcelja, and R.G. Horn, *Physical principles of membrane organization*. Q Rev Biophys, 1980. **13**(2): p. 121-200.
184. Zimmerberg, J., S.S. Vogel, and L.V. Chernomordik, *Mechanisms of membrane fusion*. Annu Rev Biophys Biomol Struct, 1993. **22**: p. 433-66.

185. Peters, C., et al., *Trans-complex formation by proteolipid channels in the terminal phase of membrane fusion*. Nature, 2001. **409**(6820): p. 581-8.
186. Cohen, F.S. and G.B. Melikyan, *The energetics of membrane fusion from binding, through hemifusion, pore formation, and pore enlargement*. J Membr Biol, 2004. **199**(1): p. 1-14.
187. Sorensen, J.B., *Formation, stabilisation and fusion of the readily releasable pool of secretory vesicles*. Pflugers Arch, 2004. **448**(4): p. 347-62.
188. De Blas, G.A., et al., *Dynamics of SNARE assembly and disassembly during sperm acrosomal exocytosis*. PLoS Biol, 2005. **3**(10): p. e323.
189. Foran, P., C.C. Shone, and J.O. Dolly, *Differences in the protease activities of tetanus and botulinum B toxins revealed by the cleavage of vesicle-associated membrane protein and various sized fragments*. Biochemistry, 1994. **33**(51): p. 15365-74.
190. Hua, S.Y. and M.P. Charlton, *Activity-dependent changes in partial VAMP complexes during neurotransmitter release*. Nat Neurosci, 1999. **2**(12): p. 1078-83.
191. Bai, J. and E.R. Chapman, *The C2 domains of synaptotagmin--partners in exocytosis*. Trends Biochem Sci, 2004. **29**(3): p. 143-51.
192. Breidenbach, M.A. and A.T. Brunger, *New insights into clostridial neurotoxin-SNARE interactions*. Trends Mol Med, 2005. **11**(8): p. 377-81.
193. Chaddock, J.A. and P.M. Marks, *Clostridial neurotoxins: structure-function led design of new therapeutics*. Cell Mol Life Sci, 2006. **63**(5): p. 540-51.
194. Davletov, B., M. Bajohrs, and T. Binz, *Beyond BOTOX: advantages and limitations of individual botulinum neurotoxins*. Trends Neurosci, 2005. **28**(8): p. 446-52.
195. Grumelli, C., et al., *Internalization and mechanism of action of clostridial toxins in neurons*. Neurotoxicology, 2005. **26**(5): p. 761-7.
196. Dolly, J.O., et al., *Botulinum neurotoxin and dendrotoxin as probes for studies on transmitter release*. J Physiol (Paris), 1984. **79**(4): p. 280-303.
197. Humeau, Y., et al., *How botulinum and tetanus neurotoxins block neurotransmitter release*. Biochimie, 2000. **82**(5): p. 427-46.

198. Wein, L.M. and Y. Liu, *Analyzing a bioterror attack on the food supply: the case of botulinum toxin in milk*. Proc Natl Acad Sci U S A, 2005. **102**(28): p. 9984-9.
199. Lacy, D.B., et al., *Crystal structure of botulinum neurotoxin type A and implications for toxicity*. Nat Struct Biol, 1998. **5**(10): p. 898-902.
200. Lalli, G., et al., *The journey of tetanus and botulinum neurotoxins in neurons*. Trends Microbiol, 2003. **11**(9): p. 431-7.
201. Benecke, R., et al., *Tetanus toxin induced actions on spinal Renshaw cells and Ia-inhibitory interneurons during development of local tetanus in the cat*. Exp Brain Res, 1977. **27**(3-4): p. 271-86.
202. Mellanby, J. and J. Green, *How does tetanus toxin act?* Neuroscience, 1981. **6**(3): p. 281-300.
203. Wellhoner, N.H., *Tetanus neurotoxin*. Rev Physiol Biochem Pharmacol, 1982. **93**: p. 1-68.
204. Schiavo, G., et al., *Tetanus toxin is a zinc protein and its inhibition of neurotransmitter release and protease activity depend on zinc*. Embo J, 1992. **11**(10): p. 3577-83.
205. Charles, P.D., *Botulinum neurotoxin serotype A: a clinical update on non-cosmetic uses*. Am J Health Syst Pharm, 2004. **61**(22 Suppl 6): p. S11-23.
206. Foran, P., et al., *Botulinum neurotoxin C1 cleaves both syntaxin and SNAP-25 in intact and permeabilized chromaffin cells: correlation with its blockade of catecholamine release*. Biochemistry, 1996. **35**(8): p. 2630-6.
207. Schiavo, G., M. Matteoli, and C. Montecucco, *Neurotoxins affecting neuroexocytosis*. Physiol Rev, 2000. **80**(2): p. 717-66.
208. Schoch, S., et al., *SNARE function analyzed in synaptobrevin/VAMP knockout mice*. Science, 2001. **294**(5544): p. 1117-22.
209. McMahon, H.T., et al., *Cellubrevin is a ubiquitous tetanus-toxin substrate homologous to a putative synaptic vesicle fusion protein*. Nature, 1993. **364**(6435): p. 346-9.
210. Deak, F., et al., *Synaptobrevin is essential for fast synaptic-vesicle endocytosis*. Nat Cell Biol, 2004. **6**(11): p. 1102-8.
211. Wu, M.N. and H.J. Bellen, *Genetic dissection of synaptic transmission in Drosophila*. Curr Opin Neurobiol, 1997. **7**(5): p. 624-30.

212. Nonet, M.L., et al., *Synaptic transmission deficits in Caenorhabditis elegans synaptobrevin mutants*. J Neurosci, 1998. **18**(1): p. 70-80.
213. Hess, E.J., K.A. Collins, and M.C. Wilson, *Mouse model of hyperkinesis implicates SNAP-25 in behavioral regulation*. J Neurosci, 1996. **16**(9): p. 3104-11.
214. Hess, E.J., *The Use of Transgenes and Mutations in the Mouse to Study the Genetic Basis of Locomotor Hyperactivity*. Methods, 1996. **10**(3): p. 374-83.
215. Fujiwara, T., et al., *Analysis of knock-out mice to determine the role of HPC-1/syntaxin 1A in expressing synaptic plasticity*. J Neurosci, 2006. **26**(21): p. 5767-76.
216. Schulze, K.L., et al., *Genetic and electrophysiological studies of Drosophila syntaxin-1A demonstrate its role in nonneuronal secretion and neurotransmission*. Cell, 1995. **80**(2): p. 311-20.
217. Brodie, K., et al., *Syntaxin and synaptobrevin function downstream of vesicle docking in Drosophila*. Neuron, 1995. **15**(3): p. 663-73.
218. Littleton, J.T., et al., *Temperature-sensitive paralytic mutations demonstrate that synaptic exocytosis requires SNARE complex assembly and disassembly*. Neuron, 1998. **21**(2): p. 401-13.
219. Ogawa, H., et al., *Functional properties of the unc-64 gene encoding a Caenorhabditis elegans syntaxin*. J Biol Chem, 1998. **273**(4): p. 2192-8.
220. Saifee, O., L. Wei, and M.L. Nonet, *The Caenorhabditis elegans unc-64 locus encodes a syntaxin that interacts genetically with synaptobrevin*. Mol Biol Cell, 1998. **9**(6): p. 1235-52.
221. Bennett, M.K. and R.H. Scheller, *The molecular machinery for secretion is conserved from yeast to neurons*. Proc Natl Acad Sci U S A, 1993. **90**(7): p. 2559-63.
222. Hu, C., et al., *Fusion of cells by flipped SNAREs*. Science, 2003. **300**(5626): p. 1745-9.
223. Pobbati, A.V., A. Stein, and D. Fasshauer, *N- to C-terminal SNARE complex assembly promotes rapid membrane fusion*. Science, 2006. **313**(5787): p. 673-6.

224. Schuette, C.G., et al., *Determinants of liposome fusion mediated by synaptic SNARE proteins*. Proc Natl Acad Sci U S A, 2004. **101**(9): p. 2858-63.
225. von Gersdorff, H. and G. Matthews, *Dynamics of synaptic vesicle fusion and membrane retrieval in synaptic terminals*. Nature, 1994. **367**(6465): p. 735-9.
226. Wolfel, M. and R. Schneggenburger, *Presynaptic capacitance measurements and Ca²⁺ uncaging reveal submillisecond exocytosis kinetics and characterize the Ca²⁺ sensitivity of vesicle pool depletion at a fast CNS synapse*. J Neurosci, 2003. **23**(18): p. 7059-68.
227. Takamori, S., et al., *Molecular anatomy of a trafficking organelle*. Cell, 2006. **127**(4): p. 831-46.
228. Malinin, V.S. and B.R. Lentz, *Energetics of vesicle fusion intermediates: comparison of calculations with observed effects of osmotic and curvature stresses*. Biophys J, 2004. **86**(5): p. 2951-64.
229. Weinreb, G. and B.R. Lentz, *Analysis of membrane fusion as a two-state sequential process: evaluation of the stalk model*. Biophys J, 2007. **92**(11): p. 4012-29.
230. Dennison, S.M., et al., *Neuronal SNAREs do not trigger fusion between synthetic membranes but do promote PEG-mediated membrane fusion*. Biophys J, 2006. **90**(5): p. 1661-75.
231. Brunger, A.T., et al., *Single-molecule studies of the neuronal SNARE fusion machinery*. Annu Rev Biochem, 2009. **78**: p. 903-28.
232. Fix, M., et al., *Imaging single membrane fusion events mediated by SNARE proteins*. Proc Natl Acad Sci U S A, 2004. **101**(19): p. 7311-6.
233. Chen, X., et al., *Are neuronal SNARE proteins Ca²⁺ sensors?* J Mol Biol, 2005. **347**(1): p. 145-58.
234. McNew, J.A., et al., *Close is not enough: SNARE-dependent membrane fusion requires an active mechanism that transduces force to membrane anchors*. J Cell Biol, 2000. **150**(1): p. 105-17.
235. Melia, T.J., et al., *Regulation of membrane fusion by the membrane-proximal coil of the t-SNARE during zippering of SNAREpins*. J Cell Biol, 2002. **158**(5): p. 929-40.

236. McNew, J.A., et al., *The length of the flexible SNAREpin juxtamembrane region is a critical determinant of SNARE-dependent fusion*. Mol Cell, 1999. **4**(3): p. 415-21.
237. Gonelle-Gispert, C., et al., *SNAP-25a and -25b isoforms are both expressed in insulin-secreting cells and can function in insulin secretion*. Biochem J, 1999. **339** (Pt 1): p. 159-65.
238. Washbourne, P., et al., *Botulinum neurotoxin E-insensitive mutants of SNAP-25 fail to bind VAMP but support exocytosis*. J Neurochem, 1999. **73**(6): p. 2424-33.
239. Montecucco, C., G. Schiavo, and S. Pantano, *SNARE complexes and neuroexocytosis: how many, how close?* Trends Biochem Sci, 2005. **30**(7): p. 367-72.
240. Cull-Candy, S.G., H. Lundh, and S. Thesleff, *Effects of botulinum toxin on neuromuscular transmission in the rat*. J Physiol, 1976. **260**(1): p. 177-203.
241. Bevan, S. and L.M. Wendon, *A study of the action of tetanus toxin at rat soleus neuromuscular junctions*. J Physiol, 1984. **348**: p. 1-17.
242. Stewart, B.A., et al., *SNARE proteins contribute to calcium cooperativity of synaptic transmission*. Proc Natl Acad Sci U S A, 2000. **97**(25): p. 13955-60.
243. Hua, Y. and R.H. Scheller, *Three SNARE complexes cooperate to mediate membrane fusion*. Proc Natl Acad Sci U S A, 2001. **98**(14): p. 8065-70.
244. Keller, J.E., F. Cai, and E.A. Neale, *Uptake of botulinum neurotoxin into cultured neurons*. Biochemistry, 2004. **43**(2): p. 526-32.
245. Keller, J.E. and E.A. Neale, *The role of the synaptic protein snap-25 in the potency of botulinum neurotoxin type A*. J Biol Chem, 2001. **276**(16): p. 13476-82.
246. Hayashi, T., et al., *Synaptic vesicle membrane fusion complex: action of clostridial neurotoxins on assembly*. Embo J, 1994. **13**(21): p. 5051-61.
247. Kweon, D.H., et al., *Probing domain swapping for the neuronal SNARE complex with electron paramagnetic resonance*. Biochemistry, 2002. **41**(17): p. 5449-52.

248. Littleton, J.T., et al., *synaptotagmin mutants reveal essential functions for the C2B domain in Ca²⁺-triggered fusion and recycling of synaptic vesicles in vivo*. J Neurosci, 2001. **21**(5): p. 1421-33.
249. Tokumaru, H., et al., *SNARE complex oligomerization by synaphin/complexin is essential for synaptic vesicle exocytosis*. Cell, 2001. **104**(3): p. 421-32.
250. Lu, X., Y. Zhang, and Y.K. Shin, *Supramolecular SNARE assembly precedes hemifusion in SNARE-mediated membrane fusion*. Nat Struct Mol Biol, 2008. **15**(7): p. 700-6.
251. Hofmann, M.W., et al., *Self-interaction of a SNARE transmembrane domain promotes the hemifusion-to-fusion transition*. J Mol Biol, 2006. **364**(5): p. 1048-60.
252. Fleming, K.G. and D.M. Engelman, *Computation and mutagenesis suggest a right-handed structure for the synaptobrevin transmembrane dimer*. Proteins, 2001. **45**(4): p. 313-7.
253. Kroch, A.E. and K.G. Fleming, *Alternate interfaces may mediate homomeric and heteromeric assembly in the transmembrane domains of SNARE proteins*. J Mol Biol, 2006. **357**(1): p. 184-94.
254. Laage, R. and D. Langosch, *Dimerization of the synaptic vesicle protein synaptobrevin (vesicle-associated membrane protein) II depends on specific residues within the transmembrane segment*. Eur J Biochem, 1997. **249**(2): p. 540-6.
255. Laage, R., et al., *A conserved membrane-spanning amino acid motif drives homomeric and supports heteromeric assembly of presynaptic SNARE proteins*. J Biol Chem, 2000. **275**(23): p. 17481-7.
256. Margittai, M., H. Otto, and R. Jahn, *A stable interaction between syntaxin 1a and synaptobrevin 2 mediated by their transmembrane domains*. FEBS Lett, 1999. **446**(1): p. 40-4.
257. Tong, J., et al., *A scissors mechanism for stimulation of SNARE-mediated lipid mixing by cholesterol*. Proc Natl Acad Sci U S A, 2009. **106**(13): p. 5141-6.
258. Bowen, M.E., D.M. Engelman, and A.T. Brunger, *Mutational analysis of synaptobrevin transmembrane domain oligomerization*. Biochemistry, 2002. **41**(52): p. 15861-6.

259. Roy, R., R. Laage, and D. Langosch, *Synaptobrevin transmembrane domain dimerization-revisited*. *Biochemistry*, 2004. **43**(17): p. 4964-70.
260. Rickman, C., et al., *Self-assembly of SNARE fusion proteins into star-shaped oligomers*. *Biochem J*, 2005. **388**(Pt 1): p. 75-9.
261. Stein, A., et al., *Helical extension of the neuronal SNARE complex into the membrane*. *Nature*, 2009. **460**(7254): p. 525-8.
262. Langosch, D., M. Hofmann, and C. Ungermann, *The role of transmembrane domains in membrane fusion*. *Cell Mol Life Sci*, 2007. **64**(7-8): p. 850-64.
263. Martens, S. and H.T. McMahon, *Mechanisms of membrane fusion: disparate players and common principles*. *Nat Rev Mol Cell Biol*, 2008. **9**(7): p. 543-56.
264. Sollner, T.H., *Intracellular and viral membrane fusion: a uniting mechanism*. *Curr Opin Cell Biol*, 2004. **16**(4): p. 429-35.
265. Kielian, M. and F.A. Rey, *Virus membrane-fusion proteins: more than one way to make a hairpin*. *Nat Rev Microbiol*, 2006. **4**(1): p. 67-76.
266. de Lima, M.C., et al., *Target cell membrane sialic acid modulates both binding and fusion activity of influenza virus*. *Biochim Biophys Acta*, 1995. **1236**(2): p. 323-30.
267. Sattentau, Q.J. and R.A. Weiss, *The CD4 antigen: physiological ligand and HIV receptor*. *Cell*, 1988. **52**(5): p. 631-3.
268. Colman, P.M. and M.C. Lawrence, *The structural biology of type I viral membrane fusion*. *Nat Rev Mol Cell Biol*, 2003. **4**(4): p. 309-19.
269. Kemble, G.W., T. Danieli, and J.M. White, *Lipid-anchored influenza hemagglutinin promotes hemifusion, not complete fusion*. *Cell*, 1994. **76**(2): p. 383-91.
270. Melikyan, G.B., et al., *A point mutation in the transmembrane domain of the hemagglutinin of influenza virus stabilizes a hemifusion intermediate that can transit to fusion*. *Mol Biol Cell*, 2000. **11**(11): p. 3765-75.
271. Razinkov, V.I., G.B. Melikyan, and F.S. Cohen, *Hemifusion between cells expressing hemagglutinin of influenza virus and planar membranes can precede the formation of fusion pores that subsequently fully enlarge*. *Biophys J*, 1999. **77**(6): p. 3144-51.

272. Langosch, D., B. Brosig, and R. Pipkorn, *Peptide mimics of the vesicular stomatitis virus G-protein transmembrane segment drive membrane fusion in vitro*. J Biol Chem, 2001. **276**(34): p. 32016-21.
273. Dennison, S.M., et al., *VSV transmembrane domain (TMD) peptide promotes PEG-mediated fusion of liposomes in a conformationally sensitive fashion*. Biochemistry, 2002. **41**(50): p. 14925-34.
274. Cleverley, D.Z. and J. Lenard, *The transmembrane domain in viral fusion: essential role for a conserved glycine residue in vesicular stomatitis virus G protein*. Proc Natl Acad Sci U S A, 1998. **95**(7): p. 3425-30.
275. Rohde, J., et al., *The transmembrane domain of Vam3 affects the composition of cis- and trans-SNARE complexes to promote homotypic vacuole fusion*. J Biol Chem, 2003. **278**(3): p. 1656-62.
276. Danieli, T., et al., *Membrane fusion mediated by the influenza virus hemagglutinin requires the concerted action of at least three hemagglutinin trimers*. J Cell Biol, 1996. **133**(3): p. 559-69.
277. Markovic, I., et al., *Membrane fusion mediated by baculovirus gp64 involves assembly of stable gp64 trimers into multiprotein aggregates*. J Cell Biol, 1998. **143**(5): p. 1155-66.
278. Calakos, N. and R.H. Scheller, *Vesicle-associated membrane protein and synaptophysin are associated on the synaptic vesicle*. J Biol Chem, 1994. **269**(40): p. 24534-7.
279. Edelman, L., et al., *Synaptobrevin binding to synaptophysin: a potential mechanism for controlling the exocytotic fusion machine*. Embo J, 1995. **14**(2): p. 224-31.
280. Washbourne, P., G. Schiavo, and C. Montecucco, *Vesicle-associated membrane protein-2 (synaptobrevin-2) forms a complex with synaptophysin*. Biochem J, 1995. **305 (Pt 3)**: p. 721-4.
281. Pennuto, M., et al., *Fluorescence resonance energy transfer detection of synaptophysin I and vesicle-associated membrane protein 2 interactions during exocytosis from single live synapses*. Mol Biol Cell, 2002. **13**(8): p. 2706-17.
282. Wang, Y., et al., *Functional analysis of conserved structural elements in yeast syntaxin Vam3p*. J Biol Chem, 2001. **276**(30): p. 28598-605.

283. Kim, C.S., D.H. Kweon, and Y.K. Shin, *Membrane topologies of neuronal SNARE folding intermediates*. *Biochemistry*, 2002. **41**(36): p. 10928-33.
284. Kweon, D.H., C.S. Kim, and Y.K. Shin, *Insertion of the membrane-proximal region of the neuronal SNARE coiled coil into the membrane*. *J Biol Chem*, 2003. **278**(14): p. 12367-73.
285. Weimbs, T., et al., *A model for structural similarity between different SNARE complexes based on sequence relationships*. *Trends Cell Biol*, 1998. **8**(7): p. 260-2.
286. Kweon, D.H., C.S. Kim, and Y.K. Shin, *Regulation of neuronal SNARE assembly by the membrane*. *Nat Struct Biol*, 2003. **10**(6): p. 440-7.
287. Gonen, T., et al., *Lipid-protein interactions in double-layered two-dimensional AQP0 crystals*. *Nature*, 2005. **438**(7068): p. 633-8.
288. Hu, K., et al., *Vesicular restriction of synaptobrevin suggests a role for calcium in membrane fusion*. *Nature*, 2002. **415**(6872): p. 646-50.
289. De Haro, L., et al., *Calmodulin-dependent regulation of a lipid binding domain in the v-SNARE synaptobrevin and its role in vesicular fusion*. *Biol Cell*, 2003. **95**(7): p. 459-64.
290. Bowen, M. and A.T. Brunger, *Conformation of the synaptobrevin transmembrane domain*. *Proc Natl Acad Sci U S A*, 2006. **103**(22): p. 8378-83.
291. Han, X., et al., *Interaction of mutant influenza virus hemagglutinin fusion peptides with lipid bilayers: probing the role of hydrophobic residue size in the central region of the fusion peptide*. *Biochemistry*, 1999. **38**(45): p. 15052-9.
292. Epand, R.F., et al., *Membrane orientation of the SIV fusion peptide determines its effect on bilayer stability and ability to promote membrane fusion*. *Biochem Biophys Res Commun*, 1994. **205**(3): p. 1938-43.
293. Pabst, S., et al., *Selective interaction of complexin with the neuronal SNARE complex. Determination of the binding regions*. *J Biol Chem*, 2000. **275**(26): p. 19808-18.
294. Reim, K., et al., *Complexins regulate a late step in Ca²⁺-dependent neurotransmitter release*. *Cell*, 2001. **104**(1): p. 71-81.
295. Xue, M., et al., *Distinct domains of complexin I differentially regulate neurotransmitter release*. *Nat Struct Mol Biol*, 2007. **14**(10): p. 949-58.

296. Maximov, A., et al., *Complexin controls the force transfer from SNARE complexes to membranes in fusion*. Science, 2009. **323**(5913): p. 516-21.
297. Giraudo, C.G., et al., *Alternative zippering as an on-off switch for SNARE-mediated fusion*. Science, 2009. **323**(5913): p. 512-6.
298. Li, C., B.A. Davletov, and T.C. Sudhof, *Distinct Ca²⁺ and Sr²⁺ binding properties of synaptotagmins. Definition of candidate Ca²⁺ sensors for the fast and slow components of neurotransmitter release*. J Biol Chem, 1995. **270**(42): p. 24898-902.
299. Perin, M.S., et al., *Domain structure of synaptotagmin (p65)*. J Biol Chem, 1991. **266**(1): p. 623-9.
300. Bai, J., W.C. Tucker, and E.R. Chapman, *PIP₂ increases the speed of response of synaptotagmin and steers its membrane-penetration activity toward the plasma membrane*. Nat Struct Mol Biol, 2004. **11**(1): p. 36-44.
301. Brose, N., et al., *Synaptotagmin: a calcium sensor on the synaptic vesicle surface*. Science, 1992. **256**(5059): p. 1021-5.
302. Chapman, E.R. and R. Jahn, *Calcium-dependent interaction of the cytoplasmic region of synaptotagmin with membranes. Autonomous function of a single C2-homologous domain*. J Biol Chem, 1994. **269**(8): p. 5735-41.
303. Davletov, B., et al., *Phosphorylation of synaptotagmin I by casein kinase II*. J Biol Chem, 1993. **268**(9): p. 6816-22.
304. Fernandez, I., et al., *Three-dimensional structure of the synaptotagmin I C2B-domain: synaptotagmin I as a phospholipid binding machine*. Neuron, 2001. **32**(6): p. 1057-69.
305. Sutton, R.B., et al., *Structure of the first C2 domain of synaptotagmin I: a novel Ca²⁺/phospholipid-binding fold*. Cell, 1995. **80**(6): p. 929-38.
306. Desai, R.C., et al., *The C2B domain of synaptotagmin is a Ca(2+)-sensing module essential for exocytosis*. J Cell Biol, 2000. **150**(5): p. 1125-36.
307. Chapman, E.R., et al., *A novel function for the second C2 domain of synaptotagmin. Ca²⁺-triggered dimerization*. J Biol Chem, 1996. **271**(10): p. 5844-9.
308. Zhang, X., J. Rizo, and T.C. Sudhof, *Mechanism of phospholipid binding by the C2A-domain of synaptotagmin I*. Biochemistry, 1998. **37**(36): p. 12395-403.

309. Bai, J., et al., *Membrane-embedded synaptotagmin penetrates cis or trans target membranes and clusters via a novel mechanism*. J Biol Chem, 2000. **275**(33): p. 25427-35.
310. Chapman, E.R. and A.F. Davis, *Direct interaction of a Ca²⁺-binding loop of synaptotagmin with lipid bilayers*. J Biol Chem, 1998. **273**(22): p. 13995-4001.
311. Davis, A.F., et al., *Kinetics of synaptotagmin responses to Ca²⁺ and assembly with the core SNARE complex onto membranes*. Neuron, 1999. **24**(2): p. 363-76.
312. Davletov, B.A. and T.C. Sudhof, *A single C2 domain from synaptotagmin I is sufficient for high affinity Ca²⁺/phospholipid binding*. J Biol Chem, 1993. **268**(35): p. 26386-90.
313. Rhee, J.S., et al., *Augmenting neurotransmitter release by enhancing the apparent Ca²⁺ affinity of synaptotagmin I*. Proc Natl Acad Sci U S A, 2005. **102**(51): p. 18664-9.
314. Fernandez-Chacon, R., et al., *Structure/function analysis of Ca²⁺ binding to the C2A domain of synaptotagmin I*. J Neurosci, 2002. **22**(19): p. 8438-46.
315. Bai, J., et al., *Fusion pore dynamics are regulated by synaptotagmin*t-SNARE interactions*. Neuron, 2004. **41**(6): p. 929-42.
316. Martens, S., M.M. Kozlov, and H.T. McMahon, *How synaptotagmin promotes membrane fusion*. Science, 2007. **316**(5828): p. 1205-8.
317. Dai, H., et al., *A quaternary SNARE-synaptotagmin-Ca²⁺-phospholipid complex in neurotransmitter release*. J Mol Biol, 2007. **367**(3): p. 848-63.
318. Tokumaru, H., C. Shimizu-Okabe, and T. Abe, *Direct interaction of SNARE complex binding protein synaphin/complexin with calcium sensor synaptotagmin I*. Brain Cell Biol, 2008. **36**(5-6): p. 173-89.
319. Rohrbough, J. and K. Broadie, *Lipid regulation of the synaptic vesicle cycle*. Nat Rev Neurosci, 2005. **6**(2): p. 139-50.
320. Davletov, B., E. Connell, and F. Darios, *Regulation of SNARE fusion machinery by fatty acids*. Cell Mol Life Sci, 2007. **64**(13): p. 1597-608.
321. Latham, C.F., et al., *Molecular dissection of the Munc18c/syntaxin4 interaction: implications for regulation of membrane trafficking*. Traffic, 2006. **7**(10): p. 1408-19.

322. Chernomordik, L.V., J. Zimmerberg, and M.M. Kozlov, *Membranes of the world unite!* J Cell Biol, 2006. **175**(2): p. 201-7.
323. Brash, A.R., *Arachidonic acid as a bioactive molecule.* J Clin Invest, 2001. **107**(11): p. 1339-45.
324. Darios, F. and B. Davletov, *Omega-3 and omega-6 fatty acids stimulate cell membrane expansion by acting on syntaxin 3.* Nature, 2006. **440**(7085): p. 813-7.
325. Rickman, C. and B. Davletov, *Arachidonic acid allows SNARE complex formation in the presence of Munc18.* Chem Biol, 2005. **12**(5): p. 545-53.
326. Connell, E., et al., *Mechanism of arachidonic acid action on syntaxin-Munc18.* EMBO Rep, 2007. **8**(4): p. 414-9.
327. Jeon, H.J., et al., *Dopamine release in PC12 cells is mediated by Ca(2+)-dependent production of ceramide via sphingomyelin pathway.* J Neurochem, 2005. **95**(3): p. 811-20.
328. Rohrbough, J., et al., *Ceramidase regulates synaptic vesicle exocytosis and trafficking.* J Neurosci, 2004. **24**(36): p. 7789-803.
329. Darios, F., et al., *Sphingosine facilitates SNARE complex assembly and activates synaptic vesicle exocytosis.* Neuron, 2009. **62**(5): p. 683-94.
330. Brunger, A.T., *Structure of proteins involved in synaptic vesicle fusion in neurons.* Annu Rev Biophys Biomol Struct, 2001. **30**: p. 157-71.
331. Kubista, H., H. Edelbauer, and S. Boehm, *Evidence for structural and functional diversity among SDS-resistant SNARE complexes in neuroendocrine cells.* J Cell Sci, 2004. **117**(Pt 6): p. 955-66.
332. Fdez, E., et al., *A role for soluble N-ethylmaleimide-sensitive factor attachment protein receptor complex dimerization during neurosecretion.* Mol Biol Cell, 2008. **19**(8): p. 3379-89.
333. Schenkel, J., et al., *Fluorescence studies on the role of tryptophan in heterogeneous nuclear ribonucleoprotein particles of HeLa cells.* Biochem J, 1989. **263**(1): p. 279-83.
334. Soto, P., A. Baumketner, and J.E. Shea, *Aggregation of polyalanine in a hydrophobic environment.* J Chem Phys, 2006. **124**(13): p. 134904.
335. Vestergaard, B., et al., *The SAXS solution structure of RF1 differs from its crystal structure and is similar to its ribosome bound cryo-EM structure.* Mol Cell, 2005. **20**(6): p. 929-38.

336. Lawrence, G.W. and J.O. Dolly, *Multiple forms of SNARE complexes in exocytosis from chromaffin cells: effects of Ca(2+), MgATP and botulinum toxin type A*. J Cell Sci, 2002. **115**(Pt 3): p. 667-73.
337. Bowen, M.E., et al., *Single-molecule studies of synaptotagmin and complexin binding to the SNARE complex*. Biophys J, 2005. **89**(1): p. 690-702.
338. Chen, Y.A., et al., *Calmodulin and protein kinase C increase Ca(2+)-stimulated secretion by modulating membrane-attached exocytic machinery*. J Biol Chem, 1999. **274**(37): p. 26469-76.
339. Rhoads, A.R. and F. Friedberg, *Sequence motifs for calmodulin recognition*. Faseb J, 1997. **11**(5): p. 331-40.
340. Hu, C.D., Y. Chinenov, and T.K. Kerppola, *Visualization of interactions among bZIP and Rel family proteins in living cells using bimolecular fluorescence complementation*. Mol Cell, 2002. **9**(4): p. 789-98.
341. Hu, C.D., A.V. Grinberg, and T.K. Kerppola, *Visualization of protein interactions in living cells using bimolecular fluorescence complementation (BiFC) analysis*. Curr Protoc Cell Biol, 2006. **Chapter 21**: p. Unit 21 3.
342. Kerppola, T.K., *Visualization of molecular interactions by fluorescence complementation*. Nat Rev Mol Cell Biol, 2006. **7**(6): p. 449-56.
343. Kerppola, T.K., *Bimolecular fluorescence complementation: visualization of molecular interactions in living cells*. Methods Cell Biol, 2008. **85**: p. 431-70.
344. Landolt-Marticorena, C., et al., *Non-random distribution of amino acids in the transmembrane segments of human type I single span membrane proteins*. J Mol Biol, 1993. **229**(3): p. 602-8.
345. Li, S.C. and C.M. Deber, *Glycine and beta-branched residues support and modulate peptide helicity in membrane environments*. FEBS Lett, 1992. **311**(3): p. 217-20.
346. Javadpour, M.M., et al., *Helix packing in polytopic membrane proteins: role of glycine in transmembrane helix association*. Biophys J, 1999. **77**(3): p. 1609-18.
347. Lemmon, M.A. and D.M. Engelman, *Specificity and promiscuity in membrane helix interactions*. FEBS Lett, 1994. **346**(1): p. 17-20.

348. MacKenzie, K.R., J.H. Prestegard, and D.M. Engelman, *A transmembrane helix dimer: structure and implications*. Science, 1997. **276**(5309): p. 131-3.
349. Li, S.C. and C.M. Deber, *A measure of helical propensity for amino acids in membrane environments*. Nat Struct Biol, 1994. **1**(6): p. 368-73.
350. Reiersen, H. and A.R. Rees, *The hunchback and its neighbours: proline as an environmental modulator*. Trends Biochem Sci, 2001. **26**(11): p. 679-84.

